2006-07-26

Structure-Activity Studies of Glycosphingolipids as Antigens of Natural Killer T Cells

Randal Donald Goff
Brigham Young University - Provo

STRUCTURE-ACTIVITY STUDIES OF GLYCOSPHINGOLIPIDS AS ANTIGENS OF NATURAL KILLER T CELLS

by

Randal D. Goff

A dissertation submitted to the faculty of

Brigham Young University

in partial fulfillment of the requirements for the degree of

Doctor of Philosophy

Department of Chemistry and Biochemistry

Brigham Young University

December 2006

BRIGHAM YOUNG UNIVERSITY

GRADUATE COMMITTEE APPROVAL

of a dissertation submitted by

Randal D. Goff

This dissertation has been read by each member of the following graduate committee and by majority vote has been found to be satisfactory.

Date	Paul B. Savage, Chair
Date	Merritt B. Andrus
Date	Steven A. Fleming
Date	Matt A. Peterson
Date	Barry M. Willardson

BRIGHAM YOUNG UNIVERSITY

As chair of the candidate's graduate committee, I have read the dissertation of Randal D. Goff in its final form and have found that (1) its format, citations, and bibliographical style are consistent and acceptable and fulfill university and department style requirements; (2) its illustrative materials including figures, tables, and charts are in place; and (3) the final manuscript is satisfactory to the graduate committee and is ready for submission to the university library.

Date

Paul B. Savage
Chair, Graduate Committee

Accepted for the Department

David V. Dearden
Graduate Coordinator

Accepted for the College

Earl M. Wooley
Dean, College of Physical and Mathematical Sciences

ABSTRACT

STRUCTURE-ACTIVITY STUDIES OF GLYCOSPHINGOLIPIDS

AS ANTIGENS OF NATURAL KILLER T CELLS

Randal D. Goff

Department of Chemistry and Biochemistry

Doctor of Philosophy

Glycosphingolipids (GSLs), composed of a polar saccharide head and a lipophilic ceramide tail, are ubiquitous components of the plasma membrane of eukaryotic cells. They serve in many regulatory capacities and have antigenic properties towards natural killer T (NKT) cells of the innate immune system. Critical to the recognition of glycosylceramides by NKT cells are antigen presenting cells (APC), such as dendritic cells, which are responsible for binding, processing, and delivery of ligands to these lymphocytes. This event is mediated by CD1d, a major histocompatibility complex-like protein expressed on the surface of APCs, which binds GSL antigens by the ceramide moiety and presents the polar group to the T cell receptors of CD1d-restricted cells. The subsequent immune response involves NKT cell proliferation and emission of numerous cytokines, such as interferon-γ (IFN-γ) and interleukin-4 (IL-4), resulting in the

stimulation of the innate and adaptive immune systems through maturation of APCs, activation of T cells, and secretion of antibodies by B cells.

To understand the structure-activity relationship between GSLs and NKT cell activity and the requirements for intracellular processing of antigens, analogs of the model compound αGalCer (KRN-7000) have been synthesized. These include fluorophore-appended 6"-amino-α-galactosylceramides and *N*-alkenoyl GSLs, such as PBS-57, a potent αGalCer surrogate useful in NKT cell stimulation studies. A nonantigenic β-*C*-galactosylceramide has also been prepared as an inhibitor of these innate lymphocytes.

To probe the potential for using NKT cells to bias the immune system between the proinflammatory T_H1 response or the immunomodulatory T_H2 mode, versions of αGalCer with shortened ceramides have been created. One of these truncated analogs, PBS-25, has successfully been cocrystallized with CD1d and the binary complex structure solved by X-ray crystallography.

Synthetic glycosphingolipids derived from *Novosphingobium capsulatum* and *Sphingomonas paucimobilis* have also been made. In assays with classical Vα14i/Vα24i NKT cell lines, these Gram-negative bacterial antigens were recognized directly and specifically by host immune systems through CD1d-restriction, unlike GSL-deficient microbes (e.g., *Salmonella typhimurium*). A search for other GSL-bearing alpha-proteobacteria led to the discovery of another natural glycosphingolipid, an *N*-alkenoylphytosphingoid-α-galactoside, isolated from the outer membrane of *Ehrlichia muris*.

ACKNOWLEDGMENTS

As with all meaningful endeavors in life, this body of work is the result of a successful collaboration between several individuals with a common goal. I primarily wish to thank Dr. Paul B. Savage for his guidance, council, and funding. His insight into my potential and patience with my inexperience has helped me mature as a scientist and gain confidence in my abilities. I also thank Dr. Xiaoti Zhou for his assistance in becoming familiarized with synthetic lab work during the initial stages of this project and working with me on the synthesis of *N*-appended GSLs (Chapter 2). Ms. Gao Ying and I worked together on the creation of several compounds, including the truncated (Chapter 3), unsaturated (Chapter 4), and *Sphingomonas* GSLs (Chapter 6); she making the glycosyl donors and I making the ceramide acceptors. Ms. Yang Liu and I shared a similar opportunity to create a scaled-up quantity of compound PBS-57 (**4-3**) for the National Institutes of Health. Dr. Ning Yin was very helpful in this partnership by providing advice and helping to synthesize some of the bacterial compounds (Chapter 6). Drs. R. Todd Bronson, Uale Taotafa, and Bangwei Ding also dispensed needed help and guidance in honing laboratory techniques.

Our collaborators in the immunological community, Professors Luc Teyton at The Scripps Research Institute and Albert Bendelac at the University of Chicago, were invaluable for their roles in understanding the underlying function of these compounds in

the context of the innate and adaptive immune systems. Drs. Jochen Mattner, Dapeng Zhou, and Yuval Sagiv from the Bendelac Group were responsible for many of the in vivo and in vitro activity studies of our GSLs (Chapters 3 and 4) and were instrumental in the discovery of the role of iGb3 in NKT cell maturation (Chapter 1) and how bacterial glycosphingolipids interact with NKT cells (Chapters 6 and 7). Drs. Carlos Cantu III and Nicholas Schrantz from the Teyton Group did many of the cytokine release profiles and other structure-activity assays cited in this work. I also thank Drs. Dirk M. Zajonc and Ian A. Wilson at Scripps for their involvement in solving the crystal structure of CD1d complexed with PBS-25 (**3-3b**; Chapter 3), Professor Samuel Strober at Stanford University for the evaluation of β-*C*-glycoside **5-3**, and Professor David Walker at the University of Texas Medical Branch for the gift of *Ehrlichia muris* (Chapter 7)

From the academic community at Brigham Young University, I praise the members of my graduate committee and those in the organic area faculty for their willingness to give of their time and talents for my betterment. To Drs. Du Li and Bruce J. Jackson, I also give thanks for their assistance in obtaining NMR and MS data, respectively, for characterizing the many compounds that needed to be synthesized for this project.

On a personal note, I am very grateful for the love and support of my family and friends for helping me to realize my goal of achieving a graduate degree. My parents, Cecil and Beverly Goff, instilled in me the value of an education and hard work at an early age. My children, Logan, Hannah, Heather, and Rachel, have been the inspiration to push myself outside of my comfort zone. And lastly, to my sweet wife Autumn I express my profound love and gratitude. I was able to perform this work because of her support, encouragement, and patience. I am a better person because of her.

TABLE OF CONTENTS

Abstract v

Acknowledgments vii

List of Abbreviatons xii

CHAPTER 1. THE ROLE OF GLYCOSPHINGOLIPIDS AS CD1d-RESTRICTED ANTIGENS OF NATURAL KILLER T CELLS

1.1 Adaptive Immunity 1

1.1.1 B Cells and T Cells 2

1.1.2 Antigen Presenting Cells and T Cell Receptors 3

1.2 CD1d-Restricted Immune Response 7

1.2.1 MHC-Like CD1 Receptors 7

1.2.2 CD1d-Dependent Natural Killer T Cells 10

1.2.3 Cellular Trafficking of CD1d and Antigen Presentation to NKT Cells 12

1.3 Glycosphingolipids as NKT Cell Antigens 16

1.3.1 Exogenous Antigens 16

1.3.1.1 Glycosphingolipids 17

1.3.1.2 α-Galactosylceramide 17

1.3.2 Endogenous Antigens 20

1.4 References 23

CHAPTER 2. PREPARATION OF *N*-APPENDED 6”-AMINO-α-GALACTOSYL-CERAMIDES AND THEIR STIMULATORY EFFECTS ON NKT CELLS

2.1 Introduction 29

2.2 Results and Discussion 34

2.3 Conclusions 43

2.4 Experimental Section 44

2.5 References 58

CHAPTER 3. STRUCTURE-ACTIVITY RELATIONSHIP STUDIES OF TRUNCATED GLYCOSPHINGOLIPIDS ON NKT CELL CYTOKINE RELEASE PROFILES

3.1 Introduction 60

3.2 Results and Discussion 70

3.3 Conclusions 87

3.4 Experimental Section 89

3.5 References 114

CHAPTER 4. STRUCTURE-ACTIVITY RELATIONSHIP STUDIES OF *N*-ALKENOYL GLYCOSPHINGOLIPIDS AND NKT CELL ACTIVITY

4.1 Introduction 118

4.2 Results and Discussion 122

4.3 Conclusions 136

4.4 Experimental Section 137

4.5 References 157

CHAPTER 5. PREPARATION OF A β-*C*-GLYCOSPHINGOLIPID FOR SUPPRESSION OF NKT CELL ACTIVITY

5.1 Introduction 159

5.2 Results and Discussion 163

5.3 Conclusions 172

5.4 Experimental Section 173

5.5 References 189

CHAPTER 6. PREPARATION OF GLYCOSPHINGOLIPIDS FROM *SPHINGOMONAS* ALPHA-PROTEOBACTERIA AND THEIR NKT CELL-STIMULATORY ACTIVITY

6.1 Introduction 192

6.2 Results and Discussion 201

6.3 Conclusions 212

6.4 Experimental Section 214

6.5 References 229

CHAPTER 7. ISOLATION AND CHARACTERIZATION OF A GLYCOSPHINGO-LIPID FROM THE ALPHA-PROTEOBACTERIUM *EHRLICHIA MURIS*

7.1 Introduction 234

7.2 Results and Discussion 237

7.3 Conclusions 253

7.4 Experimental Section 254

7.5 References 259

APPENDIX. ^{1}H AND ^{13}C NMR SPECTRA OF FINAL COMPOUNDS 262

LIST OF ABBREVIATIONS

Ab	Antibody
APC	Antigen presenting cell
BCR	B cell receptor
BMDC	Bone marrow-derived dendritic cell
CD	Cluster of Differentiation
CHO	Chinese hamster ovary
CTL	Cytotoxic T cell
DC	Dendritic cell
DN	Double negative
EAE	Experimental autoimmune encephalomyelitis
EDCI	*N*-Ethyl-*N*'-(3-dimethylaminopropyl)carbodiimide HCl
ELISA	Enzyme-linked immunosorbent assay
ESI-MS	Electrospray ionization mass spectrometry
FAB-MS	Fast atom bombardment mass spectrometry
HBTU	*O*-(Benzotriazol-1-yl)-*N*,*N*,*N*',*N*'-tetramethyluronium hexafluorophosphate
HWE	Horner-Wadsworth-Emmons
GSL	Glycosphingolipid
GMM	Glucose monomycolate
IFN-γ	Interferon-γ
Ig	Immunoglobulin
IL	Interleukin
KO	Knockout

LAM	Lipoarabinomannan
LPS	Lipopolysaccharide
LTP	Lipid transfer protein
MHC	Major histocompatibility complex
MOG	Myelin oligodendrocyte glycoprotein
NBD	7-Nitrobenzo-2-oxa-1,3-diazole
NBDGJ	*N*-butyldeoxygalactonojirimycin
NHS	*N*-Hydroxysuccinimide
NK Cell	Natural killer cell
NKT Cell	Natural killer T cell
NOD	Non-obese diabetic
NPC1	Neimann-Pick type C1 protein
PBC	Primary biliary cirrhosis
PBL	Peripheral blood lymphocyte
PBS	Phosphate-buffered saline
PIM	Phosphotidylinositolmannoside
PUFA	Polyunsaturated fatty acid
SAR	Structure-activity relationship
TCR	T cell receptor
T_H	T helper cell
TLR	Toll-like receptor

CHAPTER 1.

THE ROLE OF GLYCOSPHINGOLIPIDS AS CD1d-RESTRICTED ANTIGENS OF NATURAL KILLER T CELLS

1.1 Adaptive Immunity

The immune system may be divided into two categories of functionality: innate and adaptive immunity. The innate segment of this system is general, always active, and is composed of a wide variety of mechanisms. These include the actions of antimicrobial peptides, chemical defenses, enzymes, phagocytes, and physical barriers (e.g., skin, mucous membranes).[1] While innate immunity is of paramount importance as an initial and rapid mode of protection for the host organism, reliance is also placed on the adaptive ability of the immune system to provide specific coverage of those bodies it cannot recognize or is inherently ineffective against. The degree of specificity of the innate system components is dictated by the genes that encode them. Since the number of genes in an organism is finite, this immune mechanism cannot identify and control all potential invaders. It has been estimated that the variety of different innate immune receptors involved in antigen recognition is in the hundreds, while those of the adaptive system are on the order of 10^{14} and 10^{18} for B cell and T cell receptors, respectively.[2] Thus, adaptive immunity is a necessary function to identify and neutralize the myriad of nonnative cells that escape the notice of the inbred system.

The power of adaptive immunity is in its ability to be activated through binding of a seemingly limitless number of antigens. Naïve lymphocytes circulate the body and encounter structures that they identify as originating from a foreign source, such as

bacteria, viruses, parasites, unfamiliar blood cells, or potentially any exogenous molecule. Binding to the receptors of these lymphocytes causes them to proliferate and mature into either an effector cell, capable of responding to the invading bodies, or a memory cell that will recognize the specific antigenic structure for future immunological activity (Figure 1.1). These memory cells have a much longer lifespan than a typical cell,

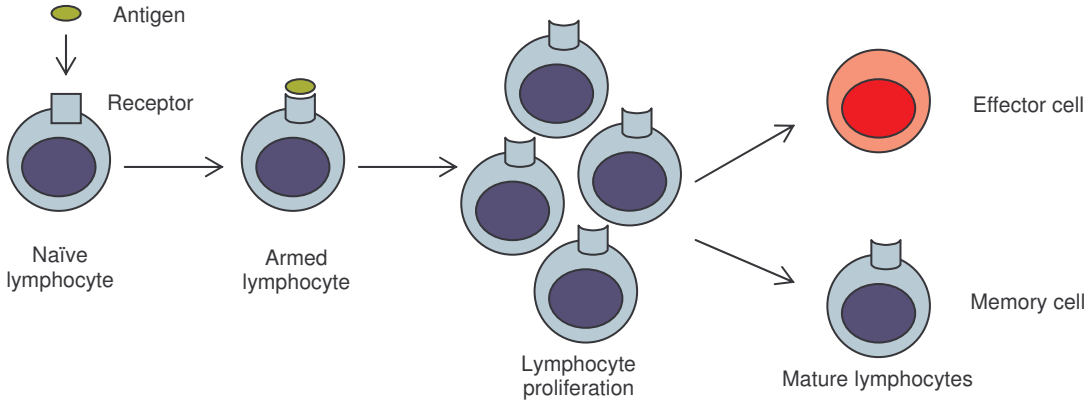

Figure 1.1. Antigenic Activation of Lymphocytes.[1]

inducing the ability to avoid illness or tissue damage attributable to that specific structure over the lifetime of the host.[1] Antigen mutation will require binding and memorization by other naïve cells, however, if the changes are different enough not to be identified by existing memory lymphocytes.

1.1.1 B Cells and T Cells

Adaptive immunity can be divided further to humoral (body fluid-based) and cell-mediated immune response mechanisms. Both systems utilize bone marrow-derived lymphocytes to identify, eradicate, and remember antigens but they mature in different parts of the immune system. Humoral B cells are readied in the bone marrow and are relegated to patrolling the lymph and circulatory systems. Once binding and identification of cognate antigen occurs via a B cell receptor (BCR), often referred to as immunoglobulin (Ig), antibodies (secreted Ig) are released into the plasma. Binding to

foreign bodies often results, which may inactivate the structure or serve as an identifying tag for innate phagocytes to engulf and eliminate the invaders.[3] Genetic or somatic permutations in the amino acid sequence of the N-terminal, or variant component of Ig, allow the estimated 10^{14} different types of BCRs to exist, with each B cell containing one type of receptor.

Analagous to this structure is the T cell receptor (TCR), a membrane-bound glycoprotein used for antigen binding by the cell-mediated immunity system. Immature T cells contain TCRs composed of a constant pre-T_α domain and a β chain. After maturation in the thymus, the pre-T_α component is replaced with an α chain that, along with the β segment, contains N-terminal variable regions.[4] The large number of possible TCRs arises from recombination of the V, J, and D_β gene loci that encode for the V_α and V_β heterodimer segments.[5] A subpopulation of T cells in the lymph system (<5%) and intestinal tract (15%) exists that display a less variable γ/δ TCR. These lymphocytes, which do not undergo thymic processing, are believed to aid in the defense of mucosal surfaces, like those found in the bowels.[6] Like B lymphocytes, T cells may consist of a diverse population due to the variable nature of the heterodimer.

1.1.2 Antigen Presenting Cells and T Cell Receptors

Although TCRs are necessary for antigen recognition, they do not possess the ability to directly identify foreign structures. The assistance of secondary cells is required to display these exogenous molecules so they can be recognized by T cells, a necessity for subsequent immune activity. Typical TCRs recognize antigen presented by the major histocompatibility complex (MHC), of which the class I type is possessed by virtually all nucleated cells. Endogenous cells can use MHC I to display self proteins when they are

in distress, such as during a viral invasion or development of tumor-like behavior. This binary complex signals the cell for elimination by effector T lymphocytes (Figure 1.2).[7]

In a similar but more exclusive process, MHC class II proteins are used to signal lymphocytes for proliferation and eradication of exogenous cells. The group of endogenous bodies known as antigen-presenting cells (APCs), which possess MHC II, are required to bind, process, and deliver antigenic compounds to the TCR. APCs, consisting of dendritic cells, monocytes, macrophages, and B lymphocytes, engulf pathogens and foreign structures preparatory to TCR presentation. Once these items, typically proteins, are digested and processed in early endosomes, they are bound to MHC II proteins and displayed on the cellular membrane (Figure 1.2).[1] Constrained exogenous fragments are available for recognition by the proper TCR. Only a correct ternary complex will induce the immune response, so the TCR must recognize both the restricted antigen and the cognate MHC II protein.

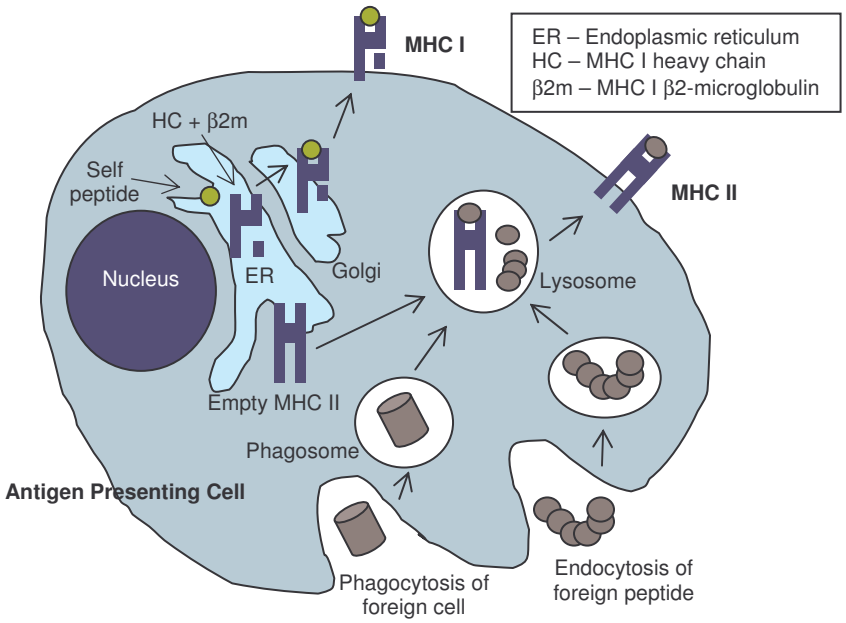

Figure 1.2. Intracellular Trafficking of MHC Molecules.[10]

Dendritic cells (DCs) make up the most significant population of APCs. They have been traced to originate from stem cells in bone marrow and are programmed to primarily

circulate through boundary-type tissues, such as skin and mucosal membranes, but also blood and the lymph system to scavenge and identify pathogens. Once foreign structures are identified by these immature cells and are internalized by phagocytosis, DCs migrate to the lymph system. These now mature DCs cannot further internalize other antigens but rather present the MHC-bound peptides to a subset of T cells, which in turn may activate B lymphocytes. The released antibodies and effector T cells are induced to travel to the site of infection and neutralize the invaders. The potency of dendritic cells lies in their unique ability to activate naïve T lymphocytes and initiate the adaptive immune response. Besides this, the diverse population of DCs in various stages of maturity expresses a wide variety of surface receptors, other than MHC II, and secretes numerous types of chemical signals that ultimately dictate the type of adaptive immune response that will be given.[8]

The interaction of TCRs with MHC-antigen complexes is not especially strong – it has been estimated that 8000 TCRs must be bound to initiate immune activity – so helper molecules are present on T cell membranes to strengthen the interaction with APCs via signal transduction enhancement. During thymic processing T cells contain both CD4 and CD8 assistant molecules, one of which is usually lost upon maturation. The $CD8^+$ subdivision can recognize type I MHC-bound antigens, therefore this type of cell is designated as a cytotoxic T lymphocyte (CTL) because it can identify and engulf distressed endogenous cells. $CD4^+$ cells are involved in recognizing type II MHC antigens, a requirement for proliferation and further adaptive immune behavior. Thus, these cells are termed T helper (T_H) lymphocytes (Figure 1.3).[1,4]

Besides displaying direct antimicrobial behavior, T cells can secrete chemical signals called cytokines. These specialized proteins are involved in recruitment of CTLs and T_H cells, macrophages, and innate natural killer cells, promoting proinflammatory behavior, and even suppression of the immune system once infection has been eliminated. In fighting disease, the main cytokines released are interleukin-2 (IL-2), which directs CTLs to activate, and interferon-γ (IFN-γ) that can stimulate macrophage involvement.[9] Another T_H-secreted cytokine, IL-4, can be used to enlist B cells to take action. Communication between an antigen-presenting B cell to its armed T_H cell compliment via the TCR will induce IL-4 signaling between the two lymphocytes, thus instructing the B cell to proliferate and express antibody, an important aid in eliminating exogenous material (Figure 1.3).[3]

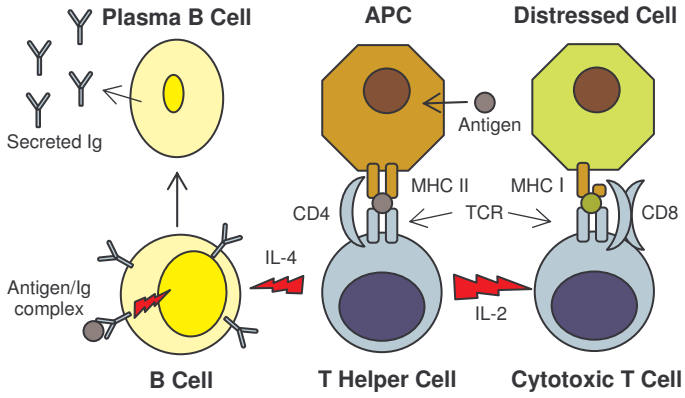

Figure 1.3. Interaction within Adaptive Immunity.[1]

While innate and adaptive mechanisms of the immune system have their own specialized functions, it is important to remember that both components do not exist independently of each other. Typically, the adaptive system is only activated once it is signaled by the innate system for assistance. One example would be the need of T cells to be costimulated with the necessary MHC II-peptide cognate as well as the membrane-bound CD80 and CD86 molecules of APCs, compounds which are expressed only upon inducement of a Toll-like receptor (TLR), a component of innate immunity.[2] Conversely, a T_H cell that secretes IL-2 cytokine can recruit natural killer (NK) cells, a component of

the innate system, to fight infection. NK cells can also be directed to destroy compromised host cells that have been coated with IgG antibodies, products of B lymphocytes.[4]

1.2 CD1d-Restricted Immune Response

1.2.1 MHC-Like CD1 Receptors

Until recently, the focus of antigen-mediated immune reactions in mammals has been placed solely on the presentation of exogenous peptide fragments to T lymphocytes via the major histocompatibility complex. Studies of a monoclonal antibody specific for a human antigen led to the identification of the CD1 (cluster of differentiation 1) family of genes (CD1A-E) that encode for five different proteins (CD1a-e).[10] Although similar in function to MHC, the CD1 proteins are not encoded by polymorphic genes and are encoded on a chromosome different from that of MHC. CD1 is divided into two groups based on the amino acid sequence in the α1 and α2 domains: CD1a,b,c,e in Group 1 and CD1d in Group 2. Though the full extent of this protein group existing in mammals is not known, identification of CD1 in humans, mice, rats, rabbits, guinea pigs, sheep, cows, and rhesus macaques demonstrate that these receptors may be conserved throughout the family (Figure 1.4).[10]

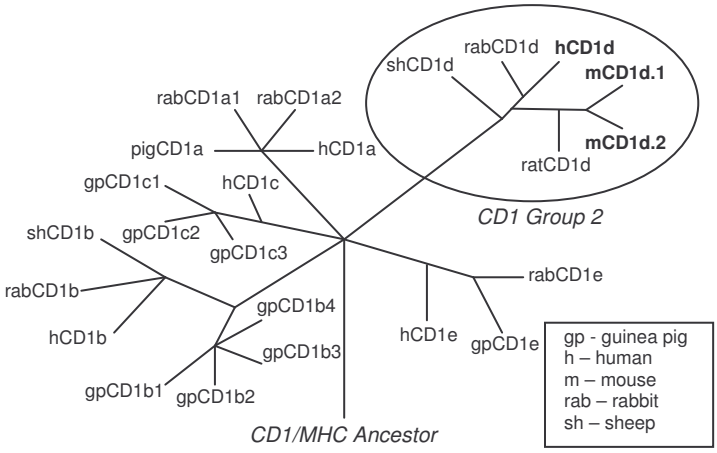

Figure 1.4. Family Tree of CD1 Proteins.[10]

CD1 proteins have a conserved tertiary structure and share some physical characteristics with MHC. CD1 molecules are typically associated with β2-microglobulin, a component of MHC type-I protein. Crystal structures of CD1a, CD1b, and CD1d[11] have demonstrated this noncovalent pairing at the α3 domain, which seems to be necessary for cell-surface expression as cells deficient in β2-microglobulin lack the ability to display CD1.[12] Perhaps more significant is the similarity in antigen binding grooves. The grooves are bounded by α-helical domains (α1 and α2) with a β-pleated sheet forming the floor (Figure 1.5). Unlike the MHC proteins that contain residues capable of hydrogen bonding in their binding clefts, CD1 proteins are lined with

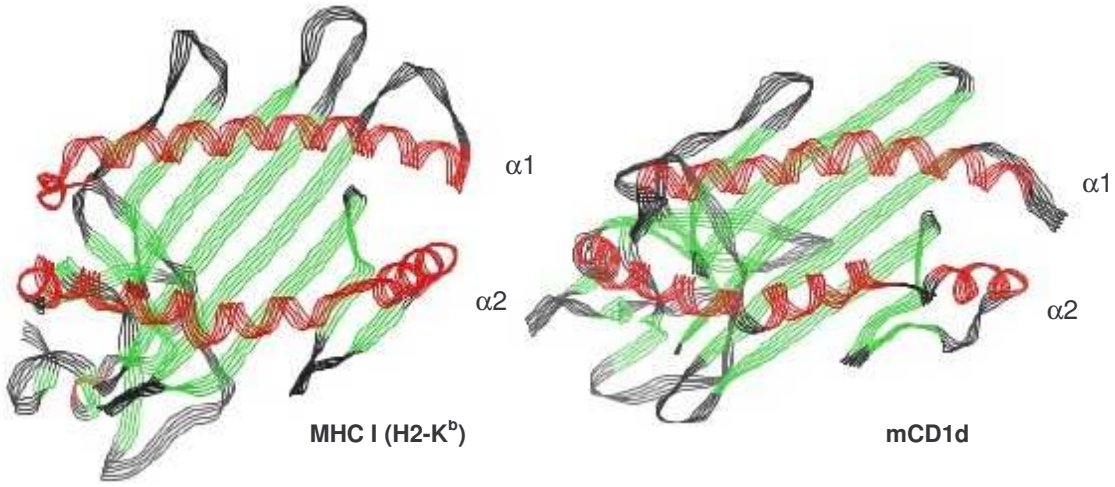

Figure 1.5. Comparison of a Human MHC I Protein and Murine CD1d.

predominantly hydrophobic amino acids.[10] This suggests that natural antigens of CD1 contain a lipid segment. There are some differences in the structures of the binding domains between CD1a, b, and d, such as the number of internal channels and overall volume, which indicate that each CD1 member may be designed to hold a specific class of lipid-containing antigen.

Research on CD1-restricted T cells has indicated that microbial lipids, especially those from mycobacteria, can stimulate adaptive immune activity. This represents a potential change in the exclusive MHC II-protein paradigm where it was previously thought that lipid stimulation (e.g., Toll-like Receptor 4 binding to lipopolysaccharide) was an exclusive purview of innate immunity.[1] In 1994, Brenner and coworkers demonstrated that mycolic acid isolated from *Mycobacterium tuberculosis* stimulated the proliferation of T cells from a DN1 hybridoma via restriction to CD1b but not with CD1c.[13] Along with this discovery came findings that mycobacterial lipoarabinomannan (LAM),[14] phosphotidylinositolmannoside (PIM_2, PIM_6)[14] and glucose monomycolate (GMM)[15] stimulated IFN-γ production and proliferation of certain T cell lines through CD1b binding and subsequent presentation (Figure 1.6). Since then, other *M. tuberculosis* lipids have been identified as T cell antigens through restriction of CD1a (didehydroxymycobactin lipoprotein)[16] and CD1c (mannosyl-β-1-phosphodolichol).[17]

Self-antigens have also been found to stimulate T cell proliferation via CD1 molecules. Ubiquitous phosphorylated cellular compounds like phosphotidylinositol have been found to be antigenic with human CD1b as well as the ganglioside GM2.[11c] Sulfatide, the major lipid component of mammalian brain tissue, has been successfully presented to and recognized by T cell receptors using CD1a, b, and c (Figure 1.6).[11a,18]

An interesting feature of this pathway is that the T cell receptors used to identify these glycolipid-APC complexes using CD1a-c cannot be differentiated from those that bind peptide-MHC II cognates. They possess the same ability to diversify through α and β chain shuffling as conventional receptors. Additionally, T cells lacking in the nuclear machinery to create the β TCR subunit that were transfected with genes from TCR^+ cells

were ultimately able to recognize glycolipid antigens presented to them by CD1-bearing antigen presenting cells.[19]

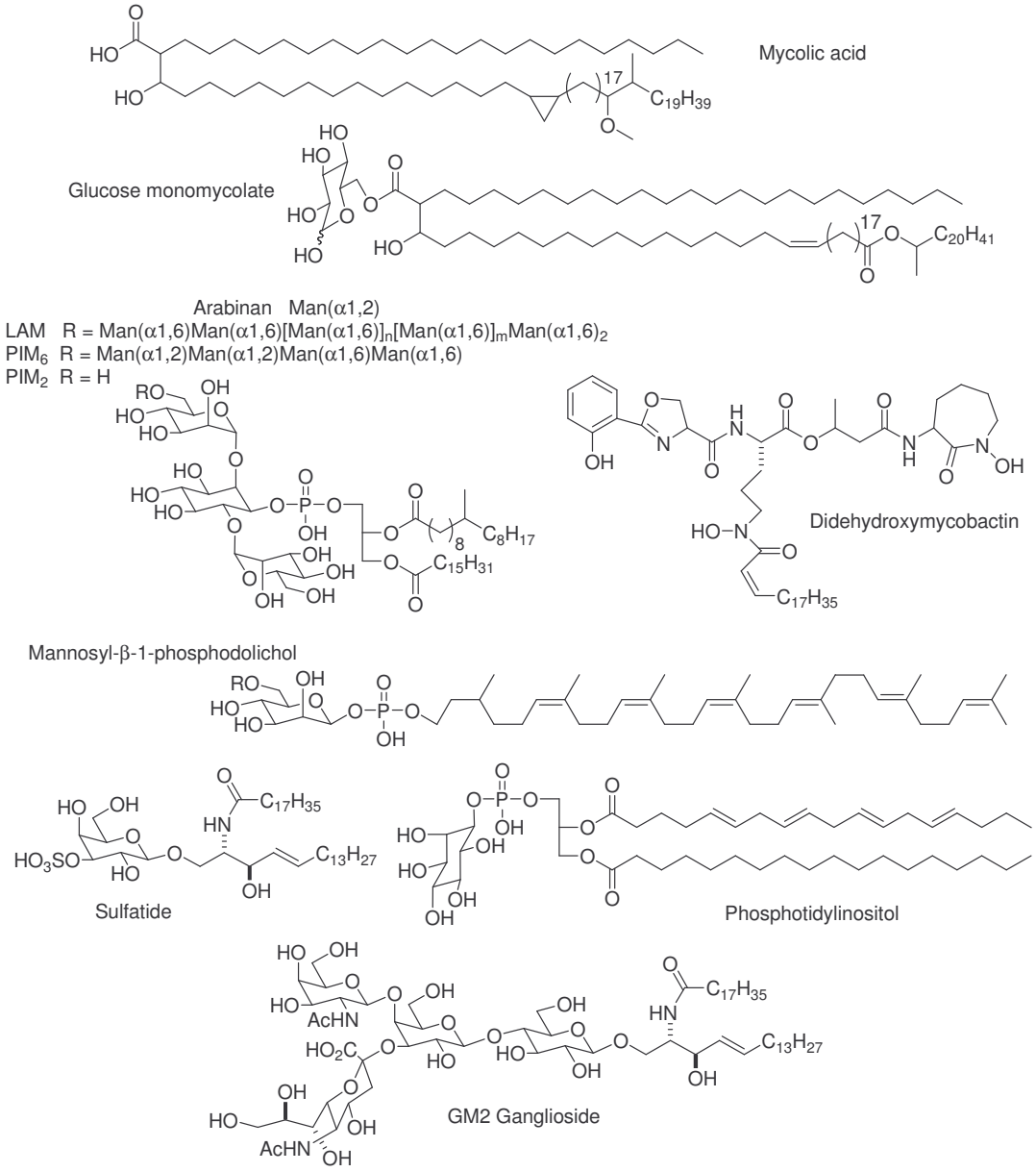

Figure 1.6. Exogenous and Endogenous Antigens of the CD1 Family.

1.2.2 CD1d-Dependent Natural Killer T Cells

Lipid compounds bound by the CD1d isoform are presented to the immune system in a fashion different from CD1a-c ligands. A group of lymphocytes termed natural killer T (NKT) cells, rather than typical T cells, are involved in binding CD1d-restricted antigens

and initiating a response. This class of lymphocyte is considered to be unusual by virtue of its T cell receptor. Unlike typical T cells, NKT cells do not display receptors that are ultravariable, either through recombinatorial or somatic means. Though there are subpopulations of NKT cells with slightly different TCRs, the majority in humans display the invariant Vα24-Jα18/Vβ11 arrangement, also termed Vα24i. In mice, whose TCR homology is almost identical to humans, the Vα14-Jα18/Vβ8 (Vα14i) type is the major form (Figure 1.7).[20]

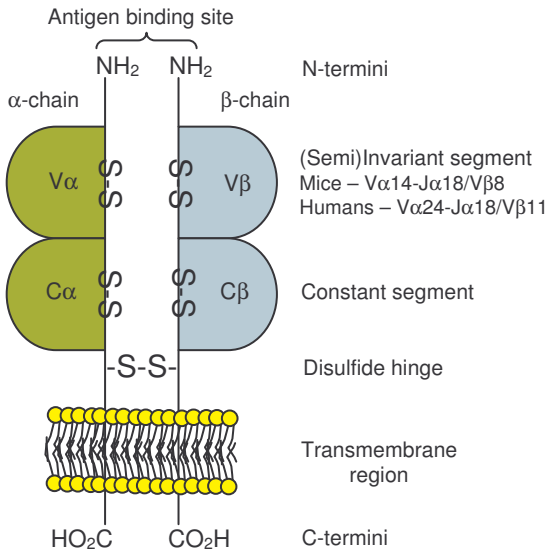

Figure 1.7. A Typical NKT Cell Receptor.

NKT cells are considered to be part of the innate immune system rather than being lumped together with adaptable T cells due to their semi-invariant nature, which imbues them with a type of natural memory even though they may not have been exposed to foreign antigen.[21] Although they are limited in scope due to their smaller assortment of receptors, the exact population of these lymphocytes is not known. They have been found to be difficult to classify due to the presence or absence of several different receptors and/or associate molecules. The natural killer cell protein NK1.1 present on most NKT cells, from which they are named, is not found in the whole population though these lymphocytes share the same phenotype as natural killer cells. Groups have been identified that express CD4 or CD8 proteins or are double negative for both. Also, not all $NK1.1^+$ T cells are CD1d dependent. Therefore, implementation of a name to accurately

describe this class of lymphocytes has been problematic.[22] To better distinguish the whole population of "classical" NKT cells, which are those that require antigen presentation by CD1d to stimulate an immune response, the technique of staining NKT cells with fluorophore-labeled tetramers of CD1d that have been loaded with an antigenic glycolipid is routinely done.[23]

Although NKT cells are limited in the scope of expressed TCRs, identify antigen solely through CD1d restriction, and make up a small population of circulating lymphocytes (<1% outside the liver),[10] their contribution to the immune system is phenomenal. Upon activation, Vα14i or Vα24i cells produce a large amount of cytokines in a few hours. Both T_H1- (IFN-γ, IL-2) and T_H2-types (IL-4) can be produced with varying ratios. When a T_H1-type profile is released, the immune system can be directed down a proinflammatory pathway to fight a microbial infection or cause antitumor behavior. Converse to this, promotion of a T_H2 mode can suppress immunity after infection has been cleared or when autoimmunity problems are present.[24] The exact reason as to how this bias occurs is still not precisely known but will be discussed in further detail in Chapter 3. Another significant finding is that NKT cells are necessary for clearing a host organism of certain types of bacterial infection.[25]

1.2.3 Cellular Trafficking of CD1d and Antigen Presentation to NKT Cells

Like type I and II MHC proteins, CD1d is assembled in the endoplasmic reticulum where both glycosylation and β2-microglobulin association occurs. After processing in the Golgi apparatus it is shuttled to the plasma membrane, secured by the α3 tail segment. The tyrosine-rich tail allows for endocytosis via adaptor protein 2 (and 3 for mCD1d only), which aid in the delivery of CD1d to sorting endosomes and lysosomes to

be loaded with antigen (Figure 1.8).[10] The tail section seems to be a necessary structure for ultimate stimulation of NKT cells. Tail-deleted CD1d (CD1-TD) proteins cannot be trafficked through lysosomes, resulting in the inability to load antigen and thus fail to stimulate the Vα14i or Vα24i cell type.[26] Additionally, the ability of antigen presenting cells to recycle CD1d back into late endosomes, which is necessary for future antigen loading, is abrogated. This is thought to be detrimental to both activating immature NKT cells in the thymus with natural (self) antigen and with foreign compounds in the lymph system to prompt proliferation.[27]

Once internalized by the cell, lipid-based NKT cell antigens may require processing to become recognizable by the natural killer TCR before being shuttled to a CD1d molecule for loading. Evidence has been seen that mycobacterial-derived glycolipid antigens of CD1b often require lysosomal editing for them to be loadable.[28] One example is the trimming of the lengthy glycan of lipoarabinomannan to become recognizable by $\alpha\beta^+$ TCRs via CD1b restriction.[14] Akin to this is processing of certain lipid-containing oligosaccharides for NKT cell stimulation. Prigozy et al. established that glycolipids with certain glycosidic linkages will not induce NKT cell activity without glycan truncation, presumably due to lack of recognition by the TCR.[29] In an APC-free assay with direct CD1d loading of digalactosyl lipids, connected by an α(1,2), α(1,3), or α(1,6) linkage, only the Galα(1,6)Gal analog could cause IL-2 production when introduced to an NKT cell hybridoma, however all three were antigenic when $CD1d^+$ APCs were used. Furthermore, when either lysosomotropic inhibitors or a specific inhibitor of α-galactosidase A, deoxygalactonojirimycin, were introduced the same effect was seen, indicating that for some glycolipids lysosomal processing must first occur for

the polar head group to be antigenic for TCRs.[29] Thus, after cellular entry it is likely that glycolipid antigens are trafficked to the lysosome to await any needed editing before loading onto CD1d (Figure 1.8).

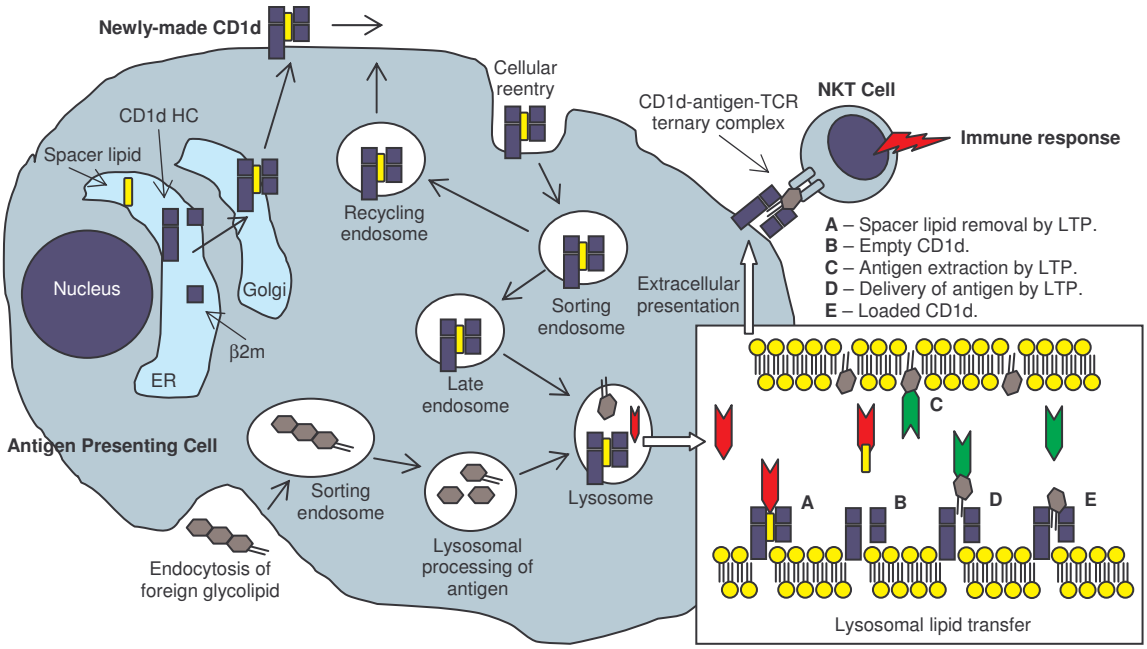

Figure 1.8. CD1 Cellular Trafficking and Antigen Presentation to NKT Cells.[10,32]

Due to the hydrophilic environment of the cell it is necessary for lipid antigens to be aided during transport to the CD1d binding pocket. Some kind of lipid transport protein (LTP) would decrease the energy needed for a hydrophobic molecule to traverse an aqueous setting. It is also possible that a lipid spacer in the binding groove of CD1d may need to be removed before antigen insertion.[30] A group of proteins responsible for regulation of lipid metabolism in endosomes, the saposins,[31] appear to perform this function. Late endosomal or lysosomal CD1d is approached by saposin or a related LTP (e.g., GM2 activator protein) and its bound lipid is removed. A different LTP molecule removes the antigenic lipid from the lysosomal membrane and presents it to CD1d. Interaction of the antigen with LTP appears to occur through the polar head group,[32] which is the component that is clear of the CD1 binding cleft.[30] The exchange of one

antigen to another is based on the relative affinities of the lipid tail by CD1d and the polar head by the LTP. This relationship may be what determines the range of antigens available for binding by CD1d and subsequent NKT cell presentation (Figure 1.8).[32]

Once LTP-mediated binding of antigen occurs to CD1d, the protein-glycolipid complex is shuttled from the lysosome to the cellular membrane. Depending on the nature of the antigen, self or foreign, the matured dendritic cell may travel to the lymph system, the spleen, or other organs to activate fully developed NKT cells. Some DCs may be localized to the thymus and be involved in the maturation of NKT cells.[27] When an armed DC encounters a developed NKT cell in peripheral tissues, the TCR binds the CD1d-restricted antigen, presumably by the polar head group and possibly with a portion of the receptor protein. Recognition of this cognate occurs and the appropriate immune response is given, a large part of which is secretion of T_H1-type IFN-γ and T_H2-type IL-4 cytokines (Figure 1.9). IFN-γ is used to activate NK cells along with macrophages and IL-4 will summon B cells to make IgE and IgG antibodies.

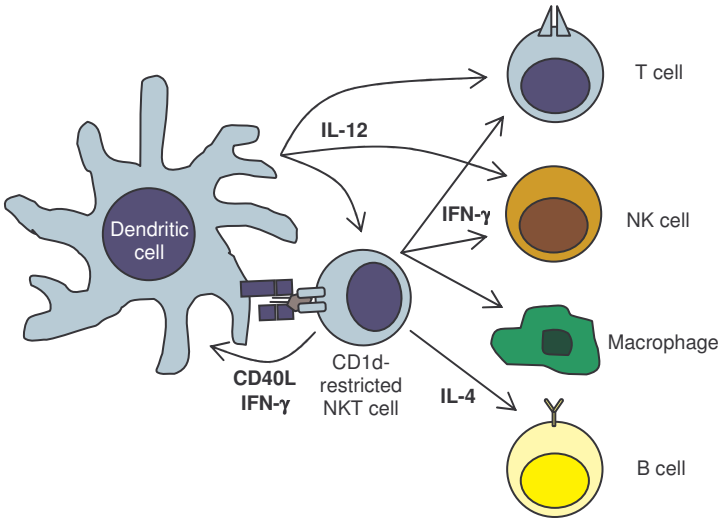

Figure 1.9. Overall Effects of NKT Cell Stimulation.[10]

Upregulation of CD40L by the NKT cell can occur, which promotes immature DCs to mature, produce adhesion molecules, and secrete IL-12 cytokine. Like IFN-γ, IL-12 is used to recruit NK cells and will also alert cytotoxic T cells (Figure 1.9). NKT cell proliferation can be effected for a heightened response as well. Indeed, the stimulatory

effect via CD1d-restriction is a good example of innate and adaptive immunity being unified to fight host infection.[1,10]

1.3 Glycosphingolipids as NKT Cell Antigens

1.3.1 Exogenous Antigens

As was previously mentioned, mycobacterial lipids have been identified as antigens of the adaptive immune system when they are bound to CD1a, CD1b, and CD1c.[13-17] The commonality between all these ligands is their extremely long lipid tail section, some with methyl branching and/or unsaturation. The presence of such structures seems to be necessary for CD1 binding as all these isoforms have deep hydrophobic acceptor pockets. A second shared feature is a polar head group, typically made up of a saccharide, a linker phosphate moiety, and an amide or ester bond. In the case of the CD1a antigen didehyroxymycobactin the sugar/phosphate combination is replaced by a lysine peptide.[16]

In 1995, α-monogalactosylceramides, a group of compounds isolated from the sea sponge *Agelas mauritianus*,[33] were identified as antagonists to murine tumors.[34] A set of B16 melanoma-bearing mice had longer survival rates and increased lymphocyte profiles after a glycolipid dose of 100 μg/kg. Koezuka and coworkers found that these ligands, termed agelasphins, were not directly cytotoxic, yet displayed antitumor behavior through stimulation of the immune system (Figure 1.10).

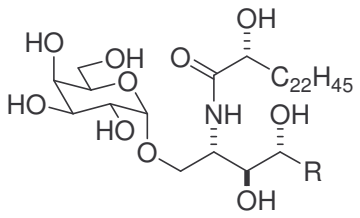

Agelasphin-7a R = $(CH2)_{11}CH_3$
Agelasphin-9a R = $(CH2)_{12}CH_3$
Agelasphin-9b R = $(CH2)_{11}CH(CH_3)_2$
Agelasphin-11 R = $(CH2)_{11}CH(CH_3)C_2H_5$

Figure 1.10. Antigenic Agelasphins.[33a]

1.3.1.1 Glycosphingolipids

These glycosylceramides belong to a larger family of compounds termed glycosphingolipids. These are compounds found ubiquitously in the plasma membranes of eukaryotic cells. Besides being identified as cellular antigens, they also function as cell surface receptors, immunomodulating agents, regulators of cell growth, aid in cell-type-specific adhesion processes, and are required for the proper functioning of the nervous system.[35] Many of these compounds, such as the gangliosides, sphingomyelin, and sulfatide make up a large portion of brain lipids and the coating of myelin sheaths in nerves.

Glycosphingolipids (GSLs) are typically composed of two distinct portions: a ceramide tail consisting of a fatty acid and sphingoid (long chain) base, and a saccharide head. The ceramide forms a glycosidic bond between the primary hydroxide of the sphingoid and the anomeric carbon of the sugar. In mammals, GSLs use the unsaturated sphingoid known as sphingosine and include one of a number of different endogenous fatty acids, such as palmitic (hexadecanoic), arachidic (eicosanoic), and cerotic (hexacosanoic) acid. The glycosidic bond in mammalian GSLs is also typically beta. The compounds isolated from marine sponges instead had phytosphingosine and most had α-anomeric saccharide linkages.[33,34]

1.3.1.2 α-Galactosylceramide

Studies on antitumor activity of GSLs by the Pharmaceutical Research Laboratory of Kirin Brewery led to the discovery of the antigenic model compound KRN-7000, often called αGalCer or αGC (Figure 1.11). Making structural variants on the original agelasphins led Koezuka and coworkers to some conclusions as to how the structure of

GSLs could affect antitumor behavior in murine models.[36] The ceramide portion seems to play an important role in overall activity; the optimal being those containing natural phytosphingosine ((2*S*, 3*S*, 4*R*)-2-amino-1,3,4-octadecanetriol) as the sphingoid and an amide composed of a tetracosanoyl chain or longer. The C3 hydroxyl group in the *S* configuration was required for the compound to be functional, with the C4 hydroxyl group giving added potency. The saccharide portion was found to be stimulatory when in pyranosyl rather than furanosyl form and the glycosidic linkage needed to be alpha.[37] The type of sugar also was found to be important as α-galactosides routinely had higher activities than glucosyl analogs.[38,39]

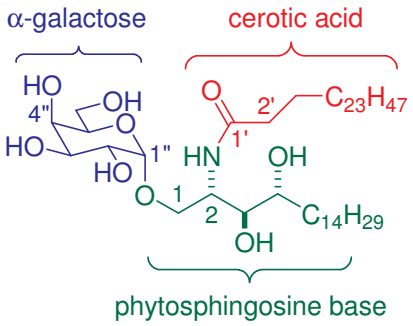

Figure 1.11. αGalCer (KRN-7000).

αGalCer was established as the first known NKT cell antigen when the connection was made between the structures of CD1b and CD1d and the discovery of the antigenic properties of CD1b-restricted mycobacterial lipids. Since it was known that αGalCer could cause a heightened immune response against melanomas and its overall structure is not dissimilar to glycolipids from mycobacteria, it was examined for NKT cell stimulation in the presence of dendritic cells. Using the Vα14i type of murine NKT cells, aliquots of DCs pulsated with various synthetic glycosylceramides at 100 ng/mL per dose were administered and the uptake of radiolabeled thymidine measured to determine the amount of NKT cell proliferation.[39]

An interesting finding from this and a similar experiment is that different subpopulations of NKT cells may react differently to the same GSL antigen. Kawano et al. used the Vα14i group and found almost no proliferation of these cells using α-

mannosylceramide.[39] When a Vα19-Jα26 transgenic set was used in knockout mice with deleted TCRs, α-mannosylceramide performed significantly better than other glycosyl ligands at causing thymidine uptake and release of IL-4 and IFN-γ.[40] This finding is significant in that it may demonstrate that different populations of these semi-invariant lymphocytes may serve different functions in bridging the innate and adaptive immune systems by virtue of the ligands that they can bind.

αGalCer has been deemed as a model compound for the study of NKT cell-mediated immunity. Research into its use as an antitumor agent has shown its potential for cancer therapy. Beside finding prolonged lifespans in B16 melanoma- and EL-4 lymphoma-bearing mice,[36,41] Koezuka and coworkers demonstrated the following:

1) The potency of αGalCer was greater than that of mitomycin C, a common chemotherapeutic agent.[41]

2) αGalCer was effective at inhibiting colon26 adenocarcinoma cells that had developed from colorectal liver metastasis.[42]

3) Metastasized EL-4[43] and B16[44] hepatic tumors are strongly antagonized by αGalCer.

These favorable results led to a Phase I clinical trial using αGalCer in otherwise healthy patients with various solid tumors (e.g., melanoma, kidney carcoma, breast mass).[45] Dose levels from 50-4800 μg/m^2 given to 24 tumor-bearing men and women induced significant quantities of T_H1-type cytokines within 2 h after administration with an overall increase in NKT cell population, initially much lower than in healthy controls. Ultimately a clinical response was not witnessed even though a significant amount of antitumor signal was given via NKT cell activation, thus this protocol was not used in a

Phase II study. A significant autoimmune response has also been achieved using αGalCer. Research groups have presented evidence that αGalCer treatment can prolong the life of insulin-producing pancreatic islets in non-obese diabetic mice as well as stave off the onset of murine multiple sclerosis in susceptible individuals due to the heightened release of T_H2 cytokines.[46]

1.3.2 Endogenous Antigens

Although αGalCer is a potent ligand, it is likely not an antigen natural to mammals due to its plant-based phytosphingosine and α-glycoside components. Yet this general structure of a polar saccharide group combined with a hydrophobic tail is seen as antigenic throughout the CD1 family. This would give credence to the idea that a host ligand would share this archetypal structure.

One of the significant aspects of adaptive immunity is native immune cell recognition of other self cells, meaning that cells reactive to foreign antigens should be able to identify host cells and not react to them. For this to happen, positive selection in the thymus occurs so lymphocytes can be "educated" as to which type of cells to avoid and which type to confront. For typical T cells, which are $CD4^+CD8^+$ double positive at this stage, this is accomplished by the recognition of a self-peptide/MHC complex presented by a dendritic cell. Those that cannot bind or recognize the complex undergo apoptosis through withholding of maturation signals and those that strongly bind are also eliminated via negative selection due to the potential of autoreactivity in peripheral systems. Only those that bind with moderate avidity are allowed to survive.[1] Like these adaptive cells, innate NKT cells mature in the thymus but there is also evidence of them developing in the liver and bone marrow.[10] Apparently, NKT cells originate from the

same immature $CD4^+CD8^+$ double positive thymocytes as regular T cells. Once a self antigen is shared by a CD1d-bearing cortical lymphocyte, which is also $CD4^+CD8^+$ double positive, differentiation into NKT cell morphology occurs with formation of an invariant α TCR chain (Figure 1.12).[47,48] When CD1d is inhibited in the thymus, NKT cells cannot be formed and immune deficiency results.[10]

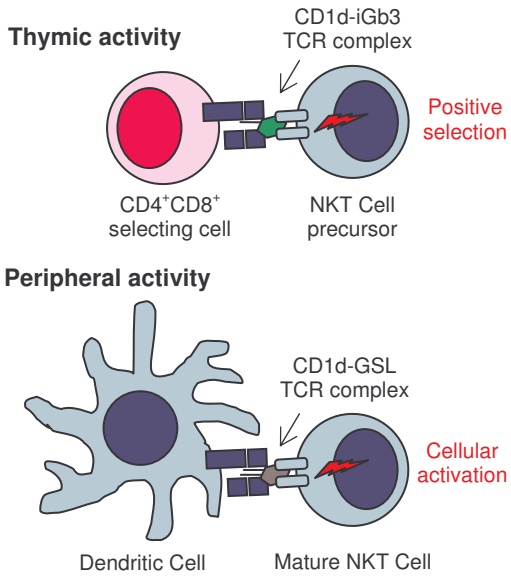

Figure 1.12. Endogenous and Exogenous Activation of NKT Cells.[48]

A significant concern to researchers is the exact type of self ligand needed to form NKT cells. It was shown that αGalCer was likely not to be this ligand due to a decrease in NKT cells in murine fetal thymi upon introduction of this ligand; most likely from negative selection.[49] It is more probable that the native compound is isoglobotrihexosylceramide (iGb3), the synthase gene of which is native to mice and humans. In the catabolic pathway of GSLs in mice and humans, enzyme deficiencies lead to diseases due to buildup of noneliminatory metabolites. One example of this is Sandhoff disease, a breakdown of nerve cells in the central nervous system due to lack of β-hexosaminidase A and B (Figure 1.13). In mice lacking the B enzyme ($Hexb^{-/-}$), it was found that the NKT Vα14i population was severely diminished, but not the normal level of T, B, or NK cells nor the expression of CD1d receptor.[51]

Through various experiments it has been established that iGb3 is indeed the candidate for natural selection of thymic NKT cells. Using various α-digalactosylceramides, Zhou et al. determined that only the GSL with a terminal GalNAc saccharide could not

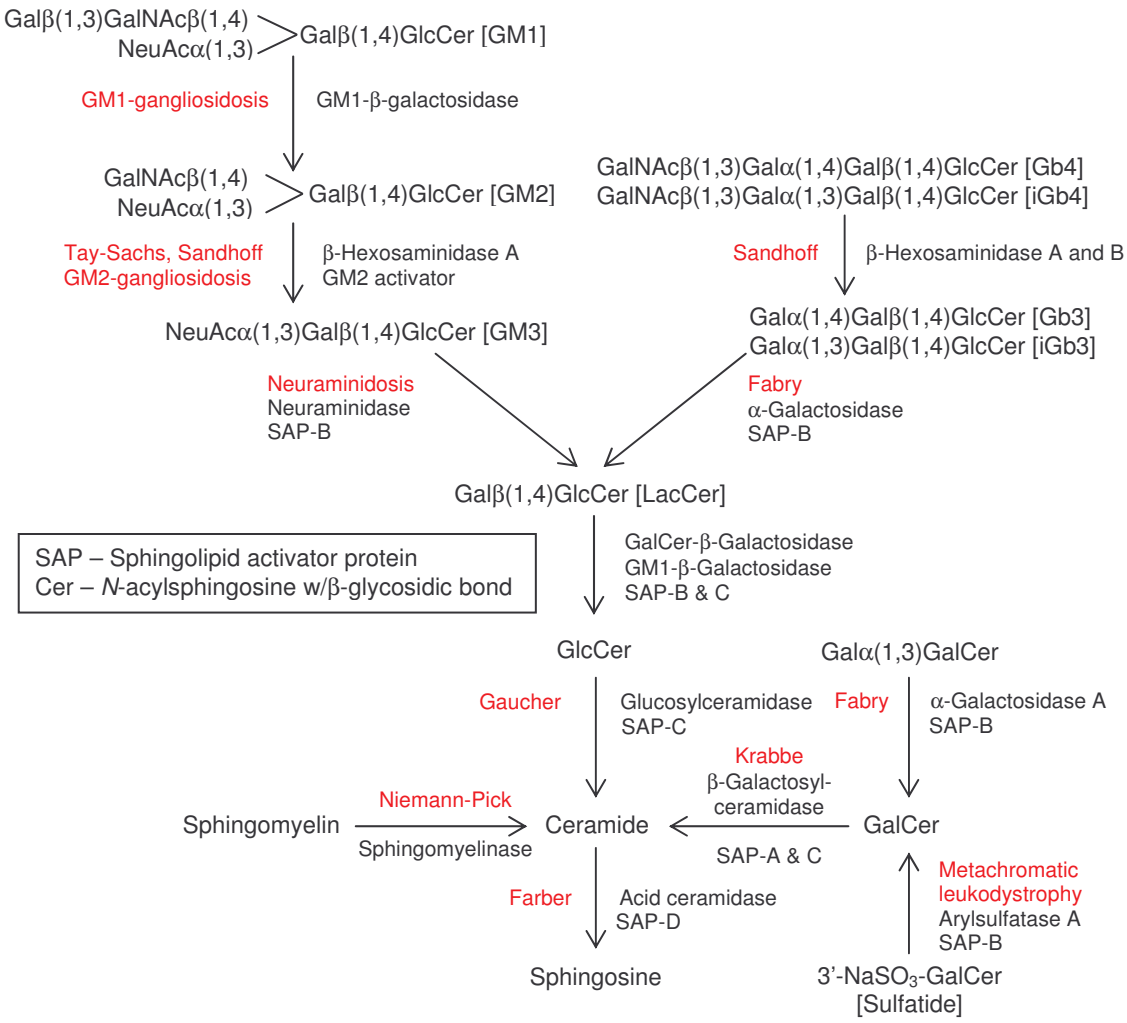

Figure 1.13. Catabolism and Storage Diseases of Glycosphingolipids in Humans.[50]

stimulate IL-2 production via NKT cells in Hexb$^{-/-}$ subjects, an indication that these compounds could not be processed for invariant TCR recognition.[51] Additionally, mice that could not make gangliosides, which also contain GalNAc, did not have impaired NKT cell populations. Studies of the globo- and isogloboside GSLs, the other significant GalNAc-containing endogenous GSL, found that only iGb3 and its tetrasaccharide precursor, iGb4, could cause NKT cell stimulation. When iGb3 was administered to a human Vα24i cell line in the presence of IB4, a lectin responsible for binding the distal Galα(1,3)Gal moiety, neither stimulation nor CD1d-recognition would occur, though it

was possible with αGC as the antigen. More significantly, iGb4 could not elicit an immune response from murine NKT cells when presented by CD1d from Hexb$^{-/-}$ mice, indicating that deletion of the GalNAc tail must occur to form the invariant αTCR.[51]

Since the discovery of αGalCer as a CD1d-restricted antigen of NKT cells in 1997, research has progressed to answer several other questions: Exactly how are antigenic GSLs trafficked and processed in DCs? What is the structure-activity relationship between the binary complement of GSL and CD1d and the ternary complex they form with the Vα14i/Vα24i TCR? Is there a correlation between GSL structure and the ultimate type of immune response (e.g., T_H1 vs. T_H2)? Are there microbial antigens that can stimulate an NKT cell response via CD1d? The research in following chapters attempts to clarify the role of glycosphingolipids as CD1d-restricted cellular antigens of natural killer T cells.

1.4 References

1) Pier, G. B.; Lyczak, J. B.; Wetzler, L. M., Eds. *Immunology, Infection, and Immunity*; ASM Press: Washington, DC, 2004.
2) Medzhitov, R.; Janeway, C. *N. Engl. J. Med*. **2000**, *343*, 338.
3) Janeway, C.; Travers, P.; Walport, M.; Shlomchik, M. *Immunobiology: The Immune System in Health and Disease*, 6th Edition; Garland Science: New York, NY 2005.
4) Delves, P. J.; Roitt, I. M. *N. Engl. J. Med.* **2000**, *343*, 37.
5) Peakman, M.; Vergani, D. *Basic and Clinical Immunology*; Churchill Livingstone: New York, NY 1997.

6) Rabson, A.; Roitt, I. M.; Delves, P. J.; *Really Essential Medical Immunology*, 2nd Edition; Blackwell Publishing: Malden, MA, 2005.

7) Maenaka, K.; Jones, E. Y. *Curr. Opin. Struct. Biol*. **1999**, *9*, 745.

8) Guermonprez, P.; Valladeau, J.; Zitvogel, L.; Thery, C.; Amigorena, S. *Annu. Rev. Immunol*. **2002**, *20*, 621.

9) Delves, P. J.; Roitt, I. M. *N. Engl. J. Med.* **2000**, *343*, 108.

10) Brigl, M.; Brenner, M. R. *Annu. Rev. Immunol*. **2004**, *22*, 817.

11) (a) Zajonc, D. M.; Elsliger, M. A.; Teyton, L.; Wilson, I. A. *Nat. Immunol*. **2003**, *4*, 808. (b) Batuwangala, T.; Shepherd, D.; Gadola, S. D.; Gibson, K. J. C.; Zaccai, N. R.; Fersht, A. R.; Besra, G. S.; Cerundolo, V.; Jones, E. Y. *J. Immunol*. **2004**, *172*, 2382. (c) Gadola, S. D.; Zaccai, N. R.; Harlos, K.; Shepherd, D.; Castro-Palomino, J. C.; Ritter, G.; Schmidt, R. R.; Jones, E. Y.; Cerundolo, V. *Nat. Immunol*. **2002**, *3*, 721. (d) Zeng, Z.-H.; Castano, A. R.; Segelke, B. W.; Stura, E. A.; Peterson, P. A.; Wilson, I. A. *Science* **1997**, *277*, 339.

12) Bauer, A.; Huttinger, R.; Staffler, G.; Hansmann, C.; Schmidt, W.; Majdic, O.; Knapp, W.; Stockinger, H. *Eur. J. Immunol*. **1997**, *27*, 1366.

13) Beckman, E. M.; Porcelli, S. A.; Morita, C. T.; Behar, S. M.; Furlong, S. T.; Brenner, M. B. *Nature* **1994**, *372*. 691.

14) Sieling, P. A.; Chatterjee, D.; Porcelli, S. A.; Prigozy, T. I.; Mazzaccaro, R. J.; Soriano, T.; Bloom, B. R.; Brenner, M. B.; Kronenberg, M.; Brennan, P. J.; Modlin, R. L. *Science* **1995**, *269*, 227.

15) Moody, D. B.; Reinhold, B. B.; Guy, M. R.; Bechman, E. M.; Frederique, D. E.; Furlong, S. T.; Ye, S.; Reinhold, V. N.; Sieling, P. A.; Modlin, S. A.; Besra, G. S.; Porcelli, S. A. *Science* **1997**, *278*, 283.

16) Moody, D. B.; Young, D. C.; Cheng, T.-Y.; Rosat, J.-P.; Roura-mir, C.; O'Connor, P. B.; Zajonc, D. M.; Walz, A.; Miller, M. J.; Levery, S. B.; Wilson, I. A.; Costello, C. E.; Brenner, M. B. *Science* **2004**, *303*, 527.

17) Moody, D. B.; Ulrichs, T.; Muhlecker, W.; Young, D. C.; Gurcha, S. S.; Grant, E.; Rosat, J.-P.; Brenner, M. B.; Costello, C. E.; Besra, G. S.; Porcelli, S. A. *Nature* **2000**, *404*, 884.

18) Shamshiev, A.; Gober H. J.; Donda, A.; Mazorra, Z.; Mori, L.; DeLibero, G. *J. Exp. Med*. **2002**, *195*, 1013.

19) Grant, E. P.; Degano, M.; Rosat, J.-P.; Stenger, S.; Modlin, R. L. *J. Exp. Med*. **1999**, *189*, 195.

20) Kinjo, Y.; Kronenberg, M. *J. Clin. Immunol*. **2005**, *25*, 522.

21) Park, S.-H.; Bendelac, A. *Nature* **2000**, *406*, 788.

22) Godfrey, D. I.; MacDonald, H. R.; Kronenberg, M.; Smyth, M. J.; Van Kaer, L. *Nat. Rev. Immunol*. **2004**, *4*, 231.

23) Benlagha, K.; Weiss, A.; Beavis, A.; Teyton, L.; Bendelac, A. *J. Exp. Med*. **2000**, *191*, 1895.

24) Kronenberg, M.; Gapin, L. *Nat. Rev. Immunol*. **2002**, *2*, 557.

25) Mattner, J.; DeBord, K. L.; Ismail, N.; Goff, R. D.; Cantu, C., III; Zhou, D.; Saint-Mezard, P.; Wang, V.; Gao, Y.; Yin, N.; Hoebe, K.; Schneewind, O.; Walker, D.; Beutler, B.; Teyton, L.; Bendelac, A.; Savage, P. B. *Nature* **2005**, *343*, 525.

26) Chiu, Y.-H.; Jayawardena, J.; Weiss, A.; Lee, D.; Park, S.-H.; Dautry-Varsat, A.; Bendelac, A. *J. Exp. Med*. **1999**, *189*, 103.

27) Chiu, Y.-H.; Park, S.-H.; Benlagha, K.; Forestier, C.; Jawawardena-Wolf, J.; Savage, P. B.; Teyton, L.; Bendelac, A. *Nat. Immunol*. **2002**, *3*, 55.

28) Porcelli, S. A.; Modlin, R. L. *Annu. Rev. Immunol*. **1999**, *17*, 297.

29) Prigozy, T. I.; Naidenko, O.; Qasba, P.; Elewaut, D.; Brossay, L.; Khurana, A.; Natori, T.; Koezuka, Y.; Kulkarni, A.; Kronenberg, M. *Science* **2001**, *291*, 664.

30) Zajonc, D. M.; Cantu, C., III; Mattner, J.; Zhou, D.; Savage, P. B.; Bendelac, A.; Wilson, I. A.; Teyton, L. *Nat. Immunol*. **2005**, *6*, 810.

31) Kishimoto, Y.; Hiraiwa, M.; O'Brien, J. S. *J. Lipid Res*. **1992**, *33*, 1255.

32) Zhou, D.; Cantu, C., III; Sagiv, Y.; Schrantz, N.; Kulkarni, A. B.; Qi, X.; Mahuran, D. J.; Morales, C. R.; Grabowski, G. A.; Benlagha, K.; Savage, P. B.; Bendelac, A.; Teyton, L. *Science* **2004**, *303*, 523.

33) (a) Natori, T.; Koezuka Y.; Higa, T. *Tetrahedron Lett*. **1993**, *34*, 5591. (b) Natori, T.; Morita, M.; Akimoto, K.; Koezuka, Y. *Tetrahedron* **1994**, *50*, 2771.

34) Motoki, K.; Kobayashi, E.; Uchida, T.; Fukushima, H.; Koezuka, Y. *Bioorg. Med. Chem. Lett*. **1995**, *5*, 705.

35) Kundu, S. K. In *Glycoconjugates: Composition, Structure, and Function*; pp. 203-262; Allen, H. J.; Kisailus, E. C., Eds.; Marcel Dekker, Inc.: New York, NY, 1992.

36) Morita, M.; Motoki, K.; Akimoto, K.; Natori, T.; Sakai, T.; Sawa, E.; Yamaji, K.; Koezuka, Y.; Kobayashi, E.; Fukushima, H. *J. Med. Chem*. **1995**, *38*, 2176.

37) Motoki, K.; Morita, M.; Kobayashi, E.; Uchida, T.; Akimoto, K.; Fukushima, H.; Koezuka, Y. *Biol. Pharm. Bull.* **1995**, *18*, 1487.

38) Kawano, T.; Cui, J.; Koezuka, Y.; Toura, I.; Kaneko, Y.; Motoki, K.; Ueno, H.; Nakagawa, R.; Sato, H.; Kondo, E.; Koseki, H.; Taniguchi, M. *Science* **1997**, *278*, 1626.

39) Uchimura, A.; Shimizu, T.; Makajima, M.; Ueno, H.; Motoki, K.; Fukushima, H.; Natori, Y.; Koezuka, Y. *Bioorg. Med. Chem*. **1997**, *5*, 1447.

40) Okamoto, N.; Kanie, O.; Huang, Y.-Y.; Fujii, R.; Watanabe, H. *Chem. Biol*. **2005**, *12*, 677.

41) Kobayashi, E.; Motoki, K.; Uchida, T.; Fukushima, H.; Koezuka, Y. *Oncol. Res*. **1995**, *7*, 529.

42) Nakagawa, R.; Motoki, K.; Ueno, H.; Iijima, R.; Nakamura, H.; Kobayashi, E.; Shimosaka, A.; Koezuka, Y. *Cancer Res.* **1998**, *58*, 1202.

43) Nakagawa, R.; Motoki, K.; Nakamura, H.; Ueno, H.; Iijima, R.; Yamauchi, A.; Tsuyuki, S.; Inamoto, T.; Koezuka, Y. *Oncol. Res.* **1998**, *10*, 561.

44) Nakagawa, R.; Serizawa, I.; Motoki, K.; Sato, M.; Ueno, H.; Iijima, R.; Nakamura, H.; Shimosaka, A.; Koezuka, Y. *Oncol. Res.* **2000**, *12*, 51.

45) Giaccone, G.; Punt, C. J. A.; Ando, Y.; Ruijter, R.; Nishi, N.; Peters, M.; von Blomberg, B. M. E.; Scheper, R. J.; van der Vliet, H. J. J.; van den Eertwegh, A. J. M.; Roelvink, M.; Beijnen, J.; Zwierzina, H.; Pinedo, H. M. *Clin. Canc. Res.* **2002**, *8*, 3702.

46) Hayakawa, Y.; Godfrey, D. I.; Smyth, M. J. *Curr. Med. Chem*. **2004**, *11*, 241.

47) Gapin, L.; Matsuda, J. L.; Surh, C. D.; Kronenberg, M. *Nat. Immunol*. **2001**, *2*, 971.

48) Godfrey, D. I.; Pellicci, D. G.; Smyth, M. J. *Science* **2004**, *306*, 1687.

49) Pellicci, D. G.; Uldrich, A. P.; Kyparissoudis, K.; Crowe, N. Y.; Brooks, A. G.; Hammond, A. J. L.; Sidobre, S.; Kronenberg, M.; Smyth, M. J.; Godfrey, D. I. *Eur. J. Immunol*. **2003**, *33*, 1816.

50) Sandhoff, K.; Kolter, T.; van Echten-Deckert, G. *Ann. NY Acad. Sci*. **1998**, *845*, 139.

51) Zhou, D.; Mattner, J.; Cantu III, C.; Schrantz, N.; Yin, N.; Gao, Y.; Sagiv, Y.; Hudspeth, K.; Wu, Y.-P.; Yamashita, T.; Teneberg, S.; Wang, D.; Proia, R. L.; Levery, S. B.; Savage, P. B.; Teyton, L.; Bendelac, A. *Science* **2004**, *306*, 1786.

CHAPTER 2.

PREPARATION OF *N*-APPENDED 6"-AMINO-α-GALACTOSYLCERAMIDES AND THEIR STIMULATORY EFFECTS ON NKT CELLS

2.1 Introduction

Early research into CD1d-mediated glycosphingolipid stimulation of natural killer T cells was hindered by two deficiencies: a lack of information on the exact trafficking pathway of GSLs in the cell and limited structure-activity relationship studies between antigen, CD1d, and TCR. Due to complexities of this mechanism (i.e., putative cellular processing of antigen, loading onto CD1d, and presentation to NKT cell receptors) little was known about the structural requirements for antigens to cause an immune response by NKT cells.

Although it appeared that both foreign and native antigenic glycosphingolipids must be intracellularly loaded onto CD1d for presentation to natural killer T cell receptors, the precise pathway as to how this is done had yet to be determined. Work by Porcelli and coworkers suggested that the antigenic compound αGalCer must be internalized by an antigen presenting cell for stimulation to occur.[1] When a culture of CD1d-transfected HeLa carcinoma cells were membrane-fixed with EDCI then pulsed for 12 h with αGalCer (**2-1**) and exposed to an NKT cell hybridoma, no stimulatory response was given. Conversely, exposure to antigen followed by EDCI fixation yielded an uptake of ^{3}H-thymidine, suggesting proliferation of lymphocytes. Kawano et al. found it likely that GSL antigens are localized to late endosomes before presentation to NKT cell receptors. Administration of either one of two known late endosomal transport inhibitors,

chloroquine and concanamycin A, to dendritic cells before αGalCer exposure likewise abrogated an NKT cell-mediated immune response.[2] This was corroborated by research from the Bendelac group, which found that tail-deleted CD1d could not be trafficked through to late endosomes or lysosomes, where unbound antigens are apparently reposited, in order to stimulate Vα14i cells.[3] The importance of the lysosome in this pathway was further verified by Kronenberg and coworkers when otherwise active digalactosylceramides could not cause stimulatory activity in the presence of lysosomal inhibitors[4] and more recently by the Bendelac and Teyton groups who identified the requirement for lipid transfer proteins to load CD1d with antigen in this compartment.[5]

Although good evidence has revealed some features of GSL processing, it is possible that there are still unidentified steps along the pathway that antigens must take to be bound and ultimately be recognized. Additionally, a lack of direct observation of cellular trafficking has made it difficult to understand the features of GSL structures that require their processing and allow them to be antigenic to NKT cell receptors. A feasible means to elucidate the cellular mechanism of antigen shuttling to CD1d and to quantify the association of the antigen-CD1d-TCR ternary complex would be through the use of labeled GSLs. This would potentially allow examination into how a GSL is moved through an antigen presenting cell and how it is incorporated with the TCR. It may also provide a means to identify where foreign antigens localize in a host before being engulfed by antigen presenting cells.

Analogs of αGalCer with biotin (**2-2a–2-2d**) or the NBD fluorophore (**2-3**) were created and tested for NKT cell proliferation by the Kirin pharmaceutical research group (Figure 2.1).[6] Their approach to adding these appendages was through binding to the

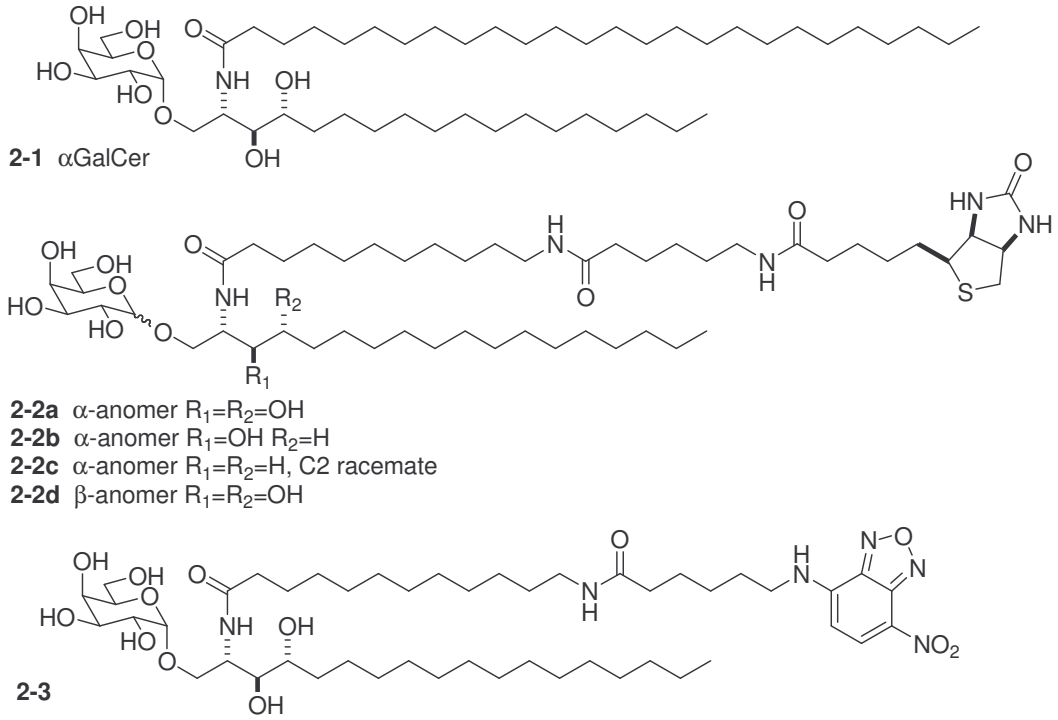

Figure 2.1. αGalCer with Biotinylated and NBD-appended Analogs.[6]

terminal end of the *N*-acyl chain component of the GSL ceramide. They found a significant decrease in the uptake of ^{3}H-thymidine in the biotin-appended compounds when compared to αGalCer. Only a hundred-fold increase in dosage (100 ng/mL) of GSLs **2-2a–2-2c** would provide the same magnitude of response as αGalCer at 1 ng/mL in murine spleen cells.[6a] At lower concentrations, **2-2b–2-2d** stimulated only slightly better than that of vehicle alone. This could be due to the deletion of sphingoid hydroxyl groups (**2-2b**,**c**) or the presence of a β-glycosidic bond (**2-2d**), alterations known to diminish GSL antigenic potency.[7] When **2-3** was used in the same murine spleen cell proliferation assay it was able to induce a greater uptake of tritiated thymidine than **2-1** at lower concentrations (e.g., 100 pg/mL, 1 ng/mL).[6b]

The results generated from these studies may not accurately represent the degree of Vα14i interaction, however. Because there are a wide variety of splenocytes, such as T helper and cytotoxic T cells, measurement of nucleoside assimilation alone would include

proliferation of cells other than those restricted by CD1d. It may also include NKT cell subpopulations that vary in function from the classical invariant type and that are not CD1d dependent.[8] A more specific assay, measurement of cytokine release from a CD1d-restricted NKT cell hybridoma, showed that the ability of **2-2a** to cause IL-2 release was significantly lower than **2-1** at all measured concentrations in a dose-dependent experiment,[9] a result much different than when radiolabeled-thymidine uptake was used as the gauge of activity.

From the original crystal structure of empty mCD1d, it appeared that the two alkyl chains of the GSL ceramide would occupy the A' and F' channels of the binding groove.[10] For adequate binding to occur, the chains would need to fit within these deep hydrophobic pockets leaving the saccharide group in the correct position for TCR recognition. The presence of bulky or hydrophilic groups on the alkyl chains would likely hinder them from being able to enter properly and cause a decrease in the population of antigen-bound CD1d molecules or perhaps binding might occur in such a way that the ligand would not be in a position recognizable by a NKT cell, thus translating into a lower immune response.

From a computer model of αGalCer in mCD1d, it could be seen that the saccharide portion of the antigen may lie just outside the binding cleft so as to not be associated with the protein.[11] If the *N*-acyl chain of the ceramide is docked into the F' channel and the sphingoid into the A', the 2" and 3" hydroxyl groups are close enough to hydrogen bond with the Asp80 and Glu83 residues, respectively. This leaves the 4" and 6" hydroxyls free – a potential place to attach a label that could be used for intracellular identification. From a study of analogs of **2-1** with α-galactose appended at O2", O3", and O6", it was

found that only Galα(1,6)αGalCer did not require cellular processing for NKT cell activity, an indication that alteration at the O6" position would most likely be tolerated.[5]

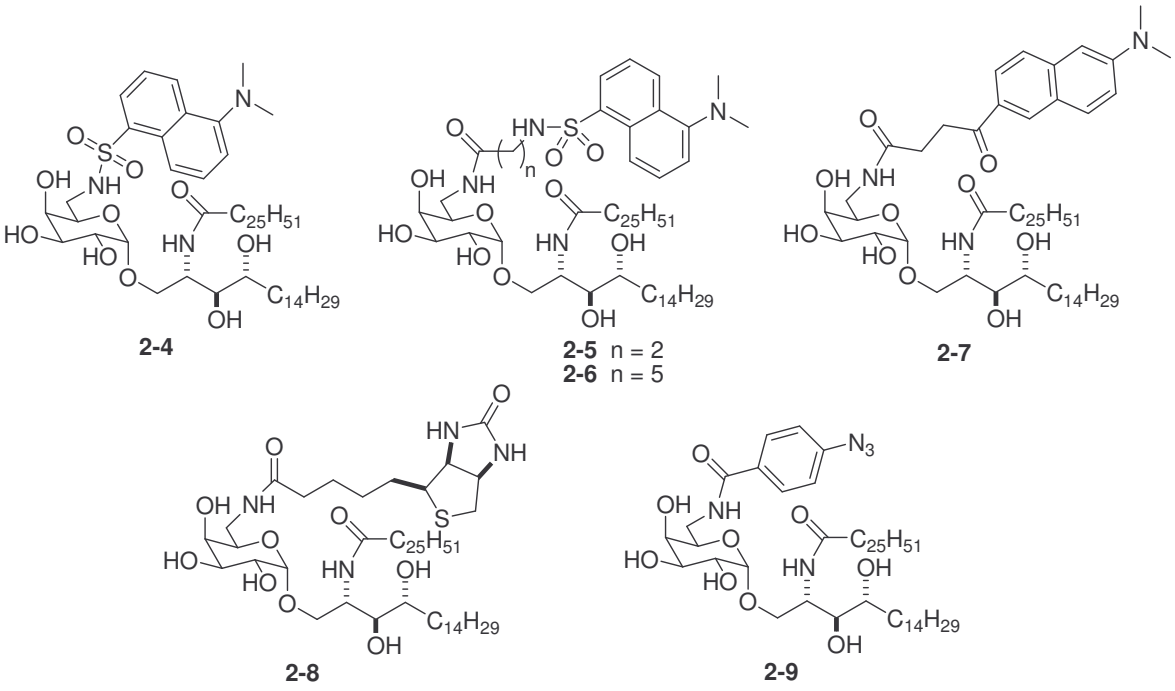

Figure 2.2. Structures of *N*-Appended 6"-amino-α-galactosylceramides.[6]

This led to the design of six compounds, **2-4–2-9**, that have small molecular labels at the 6" position of αGalCer: dansyl and prodan fluorophores, biotin, and the 4-azidobenzoate photoaffinity marker (Figure 2.2).[12] Due to the lack of a crystal structure of a ligand bound to both TCR and CD1d, it is not known how much bulk surrounding the polar head group can be tolerated before an antigen can no longer be recognized. In anticipation of this, three dansylated molecules (**2-4–2-6**) were made with attachments of varying lengths to galactose. Most of these compounds were tested for NKT cell-stimulatory activity and compound **2-7** was further utilized in an intracellular trafficking study of glycosphingolipids in dendritic cells.[13]

2.2 Results and Discussion

These modified GSLs were designed with an amino functional group at the 6" position due to three factors:

1) Successful addition of a dansyl group and other fluorophores to a 6-aminogalactoside had been reported in the literature.[14]

2) Fluorophore attachment via a succinimidyl ester would take place exclusively at an amine, which would allow the use of a deprotected late-stage intermediate for all six compounds.

3) The original patent on KRN-7000 filed by Kirin covered only conventional perhydroxylated GSLs. If these compounds were to be patentable they would require enough modification not to be considered proprietary.[15]

Nitrogen was installed in the form of an azide onto the mesylate of commercially available 1,2:3,4-di-*O*-isopropylidene-α-D-galactose (**2-10**). Concomitant deprotection of the acetonides using acetyl chloride in methanol led to solvolytic formation of 6-azidomethylgalactoside, which was protected at the remaining free hydroxyls with benzyl bromide (**2-12**). After an exchange of protecting groups at the anomeric position, the more labile acetate was substituted with fluoride using HF in pyridine.[16] Using this technique provided a more stable donor (**2-13**; Scheme 2.1).

The ceramide was prepared first by protection of the hydroxyl groups of commercially available phytosphingosine (**2-14**) using TBSOTf with 2,6-lutidine, then by HOBT/DIC coupling of hexacosanoic acid to the sphingoid base (**2-15**).[17] Although glycosidic coupling without the need for substrate protection and deprotection was desirable, it had been reported that attempts at joining the free ceramide, without

protection, to a fluoride donor did not yield product.[17] Removal of the primary silyl ether in the presence of the two secondary groups was done with dilute aqueous trifluoroacetic acid yielding the ceramide acceptor (**2-16**).[18]

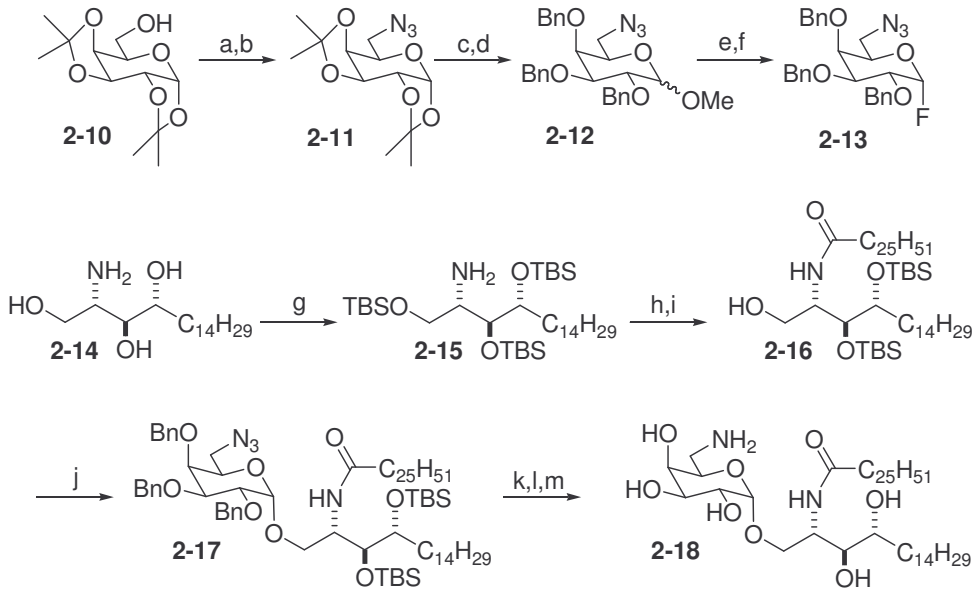

Reagents and conditions: a) MsCl, Et_3N, CH_2Cl_2, 0°C, 1 h; b) NaN_3, DMSO, 80°C, 8 h (51%, 2 steps); c) AcCl, MeOH, 0°C, 12 h (86%); d) BnBr, NaH, 18-c-6, THF, 0°C, 12 h (95%); e) AcOH, H_2SO_4, 0°C, 8 h (84%); f) HF-pyridine, pyridine, -20°C (78%); g) TBSOTf, 2,6-lutidine, CH_2Cl_2, 1 h; h) hexacosanoic acid, DIC, HOBT, CH_2Cl_2, 12 h; i) 10% TFA (aq.), THF, -10°C, 2 h (71%, 3 steps); j) **2-13**, $AgClO_4$, $SnCl_2$, 4A MS, CH_2Cl_2, THF, -10°C, 2 h (44%); k) TBAF, THF, 90 m (81%); l) PPh_3, THF, H_2O, 12 h (99%); m) Na, NH_3, THF, -78°C, 40 m (53%).

Scheme 2.1. Synthesis of 6"-amino-α-galactosylceramide **2-18**.[12]

The glycosphingolipid (**2-17**) was formed using conditions described by Mukaiyama (i.e., $AgClO_4$, $SnCl_2$, 4A molecular sieves, anhydrous CH_2Cl_2) with a somewhat disappointing yield (44%).[19] In the original description of this procedure, yields of glycosylations involving other bulky acceptors, such as cholesterol and protected glucose, were much higher (79-91%). The presence of the azide functional group may have caused the galactosyl fluoride to be a poorer donor since coupling with the 6-hydroxy analog had a greater yield (53%).[17] Deprotection of **2-17** was done sequentially using

TBAF to remove the silyl ethers, aqueous triphenylphosphine to reduce the azide, and reducing metal conditions to eliminate the benzyl ethers, yielding **2-18**.

At this stage, the divergence of the reaction scheme allowed for the six compounds to be made in one coupling step each between amine **2-18** and the *N*-hydroxysuccinimidyl esters of the appendages. However, it was found that it was somewhat difficult manipulating the deprotected intermediate due to its insolubility in many common solvents (e.g., THF, CH_2Cl_2), therefore pyridine or Et_3N/DMF needed to be used. This ultimately did not cause any inconvenience since the crude compounds were purified directly on silica gel with modest yields (43-60%) without requiring aqueous workup (Scheme 2.2).

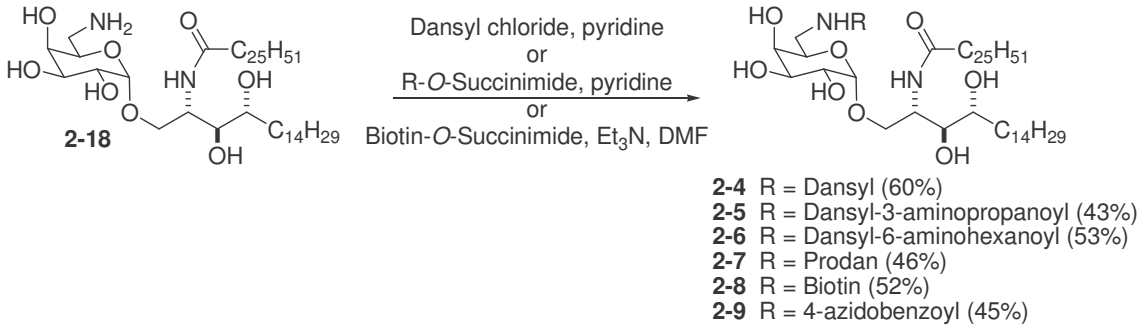

Scheme 2.2. Synthesis of *N*-Appended 6"-amino-α-galactosylceramides **2-4**--**2-9**.[12]

Activated dansyl tethers (**2-19**, **2-20**; Figure 2.3) were made by reacting dansyl chloride with carboxylic acids containing terminal amine groups.[20] The appended acids were then readied for attachment to **2-18** via formation of their *N*-hydroxysuccinimidyl esters. It was originally planned to use *N*-dansyl-4-aminobutanoyl and *N*-dansyl-5-aminopentanoyl linkers in this study but difficulty was met when preparation of the

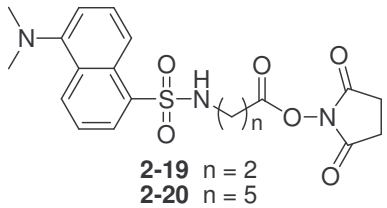

Figure 2.3. *N*-Hydroxysuccinimidyl Esters of Dansyl Tethers.

succinimidyl esters were attempted. Spectral data of the compounds generated from DCC-mediated coupling showed that instead of ester formation intramolecular cyclization had occurred, forming the respective lactams (**2-21** and **2-22**; Figure 2.4). In hindsight this would seem reasonable due to the thermodynamically-favored five- and six-membered rings available using the butanoic and pentanoic chains.

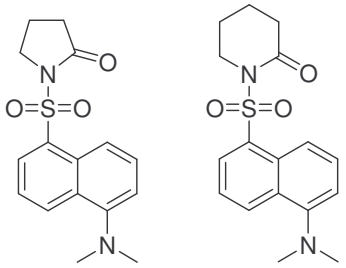

2-21 **2-22**

Figure 2.4. Lactams from DCC-Mediated Intramolecular Cyclization.

The ^{1}H NMR spectrum of cyclized **2-21** showed a lack of proton signals around 2.7-2.8 ppm that would be attributable to the ethylene group of *N*-hydroxysuccinimide. The sulfonamide proton is also not present as is seen in the precursors of **2-21** and **2-22**, the two dansylated straight-chain amino acids (t or br s, from 6.1 to 5.1 ppm). From the ^{13}C NMR data, only one carbonyl carbon is seen (173.25 ppm), which would represent a γ-lactam. The succinimidyl carbonyl peak at 169.22 ppm is absent as well as the signal around 25 ppm for the succinimidyl methylene carbons. A comparison of NMR spectral data between **2-21** and β-alanine straight-chain analog **2-19** is displayed in Table 2.1 (major differences in bold print). For the *N*-dansyl-δ-lactam (**2-22**), similar data from NMR analysis is also seen.

To see if this phenomenon was particular to the NHS/DCC protocol, the acid chloride of *N*-dansyl-4-aminobutanoic acid was made in situ using thionyl chloride then coupled with NHS. Again, the only product attained was γ-lactam **2-21**.

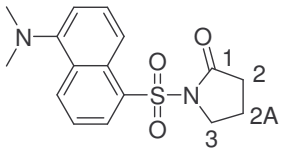

2-21 (γ-lactam)

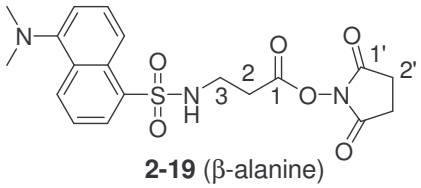

2-19 (β-alanine)

	^{1}H signals (ppm)			^{13}C signals (ppm)	
Proton	**2-21**	**2-19**	Carbon	**2-21**	**2-19**
Ar	8.60 (d, 1 H)	8.57 (d, 1 H)	**C1'**	**- - -**	**169.22**
Ar	8.49 (dd, 1 H)	8.27 (d, 1 H)	**C1**	**173.25**	**167.15**
Ar	8.23 (d, 1 H)	8.26 (dd, 1 H)	Ar	152.39	152.19
Ar	7.58 (dd, 1 H)	7.57 (dd, 1 H)	Ar	133.38	134.75
Ar	7.55 (dd, 1 H)	7.54 (dd, 1 H)	Ar	132.69	Not seen
Ar	7.18 (d, 1 H)	7.19 (d, 1 H)	Ar	131.97	130.88
-N*H*-	**- - -**	**5.65 (t, 1 H)**	Ar	130.25	130.13
H3	**4.06 (t, 2 H)**	**3.30 (dt, 2 H)**	Ar	129.99	129.71
-N(C*H*$_3$)$_2$	2.88 (s, 6 H)	2.89 (s, 6 H)	Ar	128.90	128.68
H2'	**- - -**	**2.84 (s, 4 H)**	Ar	123.44	123.36
H2	**2.40 (t, 2 H)**	**2.78 (t, 2 H)**	Ar	118.25	118.91
H2A	2.08 (m, 2 H)	N/A	Ar	115.39	115.47
			C3	**47.69**	**38.84**
			-N(*C*H$_3$)$_2$	45.58	45.60
			C2	32.53	32.54
			C2'	**- - -**	**25.73**
			C2A	18.56	N/A

Table 2.1. Comparison of NMR Signals Between Cyclic **2-21** and Linear **2-19**.

Linkers of others lengths (3C, **2-19** and 6C, **2-20**) were used to avoid this problem. Since cyclization of the corresponding amino acids would give four- and seven-membered rings, thermodynamically less-favored compounds, these were used instead along with coupling the fluorophore directly to the saccharide.

Attempts were made to measure binding between CD1d and compounds **2-4**, **2-6**, and **2-7** using fluorescence spectroscopy. Both the dansyl and prodan fluorophores have large quantum yields and will undergo a shift in wavelength frequency when introduced into a different environment. For example, in polar protic solutions dansyl will emit at a λ_{max} of around 500 nm (water, 531 nm). When it enters an environment more nonpolar the wavelength will decrease (cyclohexane, 401 nm).[21] It was the intention to combine solutions of appended GSLs and CD1d at nonaggregating concentrations to measure any

binding by the decrease in prodan or dansyl emission wavelengths or change in fluorescent intensity. Using 1.5:1 CD1d:GSL solutions (typically 150 nM:100 nM), compared to controls of 1, 10, and/or 100 nM solutions of GSL only, there was no significant reproducible change in fluorescent intensity or λ_{max} in any of the three studied compounds (**2-4**, **2-6**, **2-7**). In one instance there was an observed decrease to 390 nm from 490 nm and 506 nm with **2-4** and **2-6**, respectively, and an impressive increase in intensity from 10^5 to 10^6, but this result was not repeated in subsequent trials with the same or different batches of **2-4** or **2-6** or with compound **2-7**.

Since the time these measurements were taken, other findings have aided in understanding their meaning. A technique developed by Bendelac and coworkers describes the loading of biotinylated-mCD1d tetramers associated by fluorophore-labeled streptavidin with αGalCer over a period of 18 h.[8] In our measurements, the combined CD1d-GSL solutions were only incubated for ten minutes. Two crystal structures of human and murine CD1d with appended ligands that were recently solved indicate the presence of a 16 carbon long alkyl chain in the A' pocket of the protein.[22] Without removal of the alkyl chain it would be unlikely to fully insert the C26 *N*-acyl chain of αGalCer into CD1d, making association difficult or impossible. These crystal structures also distinctly show the 6" position of the GSL oriented out of the binding groove. This would place the fluorophores in the aqueous environment of the solution, thus leaving their λ_{max} at the longer wavelength.

Regardless of the negative spectroscopy results, these compounds were found to have decent stimulatory effects on natural killer T cells. Compounds **2-4**, **2-6**, **2-7**, and **2-8** were studied for their ability to cause IL-2 production in a Vα24i NKT cell hybridoma.

Using Bendelac's technique, soluble biotinylated CD1d tetramers were loaded onto precoated streptavidin plates and pulsed with various concentrations of appended GSLs. After removing any excess and unbound compound, the hybridoma was introduced and the released IL-2 cytokines were quantified using an enzyme-linked immunosorbent assay (ELISA).[8]

Comparision of fluorophore-appended **2-4**, **2-6**, and **2-7** to **2-1** showed equivalent stimulatory effects at 1 μg/mL, though **2-4** and **2-7** lagged behind at nanogram concentrations (Figure 2.5A). Biotinylated **2-8** was found to produce a larger quantity of IL-2 in the NKT cell hybridoma than **2-1**, though the difference is not considered to be significant (Figure 2.5B). These results were consistent through three separate experiments and the same trend was seen using rat basophilic leukemia cells transfected with CD1d.[12]

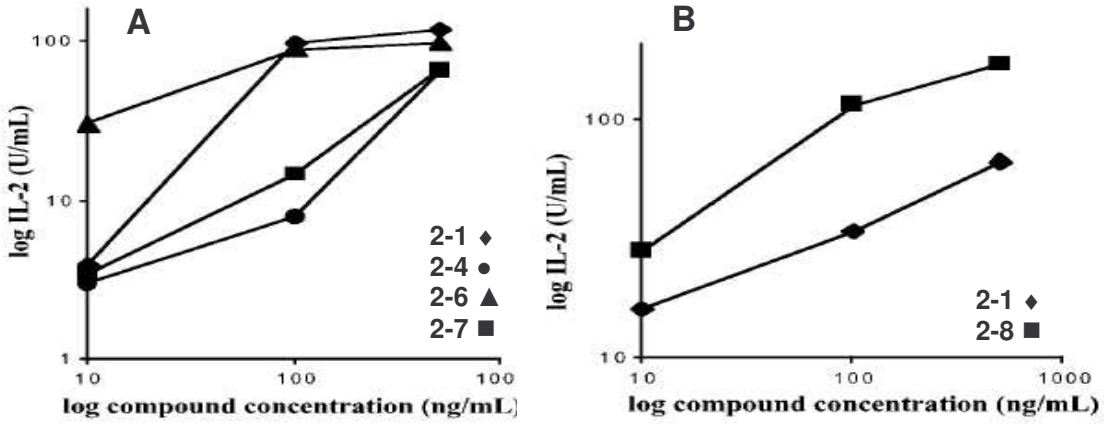

Figure 2.5. IL-2 Production in NKT Cells by Fluorophore (A) and Biotinylated (B) GSLs.[12]

The significance of these findings is that either attachment of a bulky group directly to the C6" position of αGalCer or through a linker is well tolerated in the antigen-CD1d-TCR complex. This was seen regardless of appendage or distance from the sugar,

although slightly better results were obtained using **2-6** and **2-8** whose bulky portions were separated by a seven- and five-carbon linker, respectively. It is possible that the four-carbon spacer between galactose and the naphthyl group of prodan may have been short enough to cause a less-favorable interaction with the NKT cell receptor.

To better understand the cellular process of glycosphingolipid trafficking and processing, **2-7** was used to diagnose the deficiency in individuals with defects in Niemann-Pick Type C1 (NPC1) protein.[13] Niemann-Pick disease is a degenerative disorder that causes unhealthy quantities of lipids to be stored in the spleen, liver, bone marrow, lungs and brain due to mutated enzymes necessary for glycosphingolipid catabolism. Typically it has been associated with problems with sphingomyelinase being unable to metabolize sphingomyelin to ceramide in the lysosome but accumulation of cholesterol can also occur when NPC1 may not be functioning properly.[23]

Sagiv et al. determined that in mice with NPC1 deficiencies there is a lack of Vα14i NKT cells and that these mice could not traffic GSL antigens through to lysosomal compartments from the late endosome.[13] Prodanylated **2-7** was incubated overnight with $NPC1^{+/+}$ or $NPC1^{-/-}$ bone marrow-derived dendritic cells (BMDC) and the $NPC1^{+}$ JP17 and $NPC1^{-}$ A101 cell lines from Chinese hamster ovary (CHO) cells. After incubation they were examined directly by confocal microscopy then fixed using a red dye to visualize the lysosomes. Overlap, giving a yellow color, indicated where **2-7** (green) was able to enter the lysosome (red) for loading onto CD1d. In $NPC1^{-/-}$ murine BMDCs, **2-7** was not found in the lysosome but it did accumulate there in wild type cells (Figure 2.6).

Likewise in NPC1$^-$ A101 CHO cells, **2-7** was trapped in the late endosome and not transported to lysosomes for CD1d loading, unlike the NPC1$^+$ JP17 parent CHO cells that were able to process this ligand. Incremental addition of *N*-butyldeoxygalactono-jirimycin (NBDGJ), an inhibitor of cellular GSL production, caused a modest uptake (yellow color in Figure 2.7) of **2-7** (green) into the lysosome (red) as well as NBD-tagged lactosylceramide. This would indicate that lipid accumulation in the cell blocks GSL antigens from entering the lysosome for CD1d-loading and eventual presentation, an event that could cause

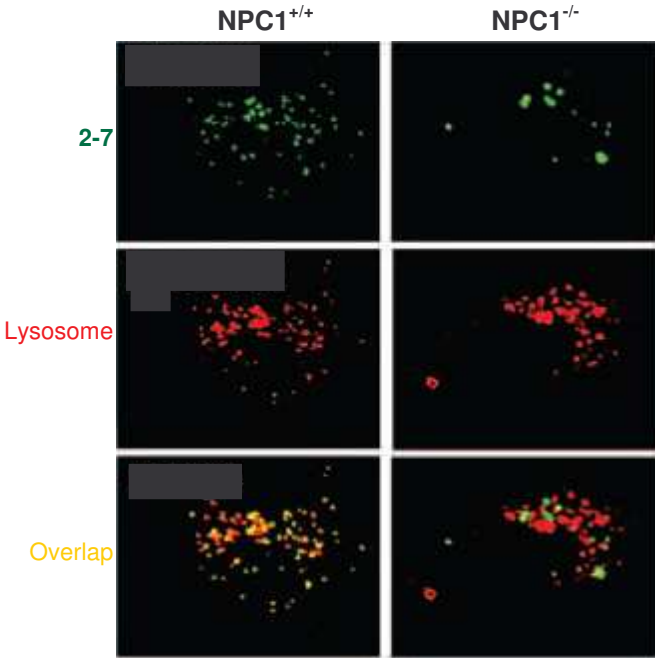

Figure 2.6. BMDC Trafficking of Prodanylated **2-7**.[13]

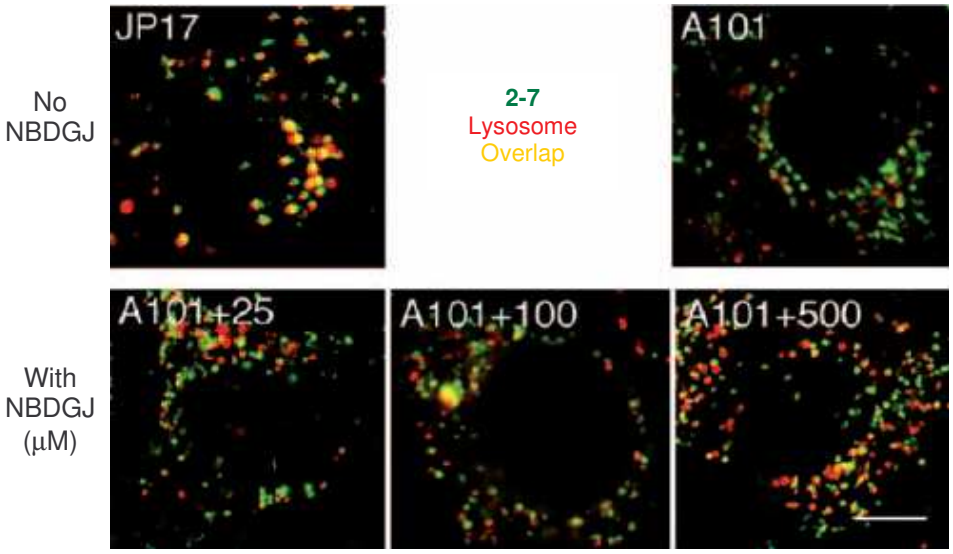

Figure 2.7. Restoration of **2-7** Trafficking in NPC1$^-$ A101 cells by NBDGJ.[13]

maturation of NKT cells to be abrogated in the thymus due to a lack of self-antigens in the lysosomes of dendritic cells.

2.3 Conclusions

To better understand the requirements for NKT cell receptor recognition of glycosphingolipid antigens presented by the CD1d protein and to help elucidate the mechanism of cellular processing of antigen, six analogs of αGalCer have been made. These compounds were appended at the C6" position of 6"-amino-α-galactosylceramide with fluorophores, biotin, and a photoaffinity label. Their synthesis was accomplished using a divergent pathway from the late intermediate **2-18**, which was made in 13 steps from commercially-available starting materials. Addition of these groups did not cause significant loss of NKT cell-stimulating properties and in one case (**2-8**) an increase in cytokine production was seen. This indicates that the GSL-CD1d-TCR ternary complex is accepting of significant modification at the saccharide C6 position. A confocal microscopy study of prodan-appended **2-7** found conclusively that NKT cell antigens must be transported to the lysosome from the late endosome in antigen presenting cells for CD1d loading and antigenic activity.

Use of **2-9** may allow crosslinking of the antigen-CD1d pair to a TCR in future studies. This might aid in probing the surface of CD1d and the receptor to find which amino acid residues closely associate with the ligand's polar head group. Additionally, incorporation of a radiolabel, such as ^{3}H, into the sugar of an analog of αGalCer may help in monitoring substrate trafficking.

2.4 Experimental Section

Materials and General Methods. Mass spectrometric data were obtained on a JEOL SX 102A spectrometer for electron ionization (EI; 70 eV) or fast atom bombardment (FAB; thioglycerol/Na^+ matrix). ^1H and ^{13}C NMR spectra were obtained on a Varian Unity 500 MHz instrument using 99.8% $CDCl_3$ with 0.05% v/v TMS, 99.8% CD_3OD with 0.05% v/v TMS, and/or 99.5% pyridine-d_5 in ampoules. Methanol, methylene chloride, and tetrahydrofuran were dried using columns of activated alumina. Flash chromatography was performed using 230-400 mesh silica gel. Thin layer chromatography was performed on aluminum-backed, 254 nm UV-active plates with a silica gel particle size of 250 μm. Reagents were obtained from Aldrich or Fluka, unless otherwise specified, and were used as received.

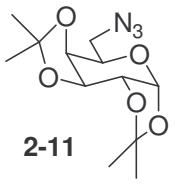

2-11

2-11. Diacetonide **2-10** (25 g, 96 mmol) was dissolved in anhydrous CH_2Cl_2 (100 mL) and Et_3N (20 mL) and cooled to 0°C. Methanesulfonyl chloride (8 mL, 103 mmol) was added slowly and the reaction was allowed to stir for 1 h. Aqueous workup was performed with 10% aqueous HCl (20 mL), saturated aqueous $NaHCO_3$ (20 mL), brine (20 mL), and the organic layer was dried with Na_2SO_4 to yield a white solid (32.5 g, quant. yield. The mesylate (32.5 g, 96.0 mmol) was dissolved in DMSO (100 mL), sodium azide (37.47 g, 576.3 mmol) was added, and the reaction mixture stirred at 80°C for 12 h. Deionized water (50 mL) was added and the aqueous layer was extracted with EtOAc (4 x 50 mL). After drying with Na_2SO_4, flash chromatography (SiO_2, EtOAc:Hex

1:2) yielded the azide as a colorless oil (13.96 g, 51%). ^{1}H NMR ($CDCl_3$, 500 MHz) δ 5.51 (d, *J* = 3.4 Hz, 1 H), 4.60 (dd, *J* = 7.7, 2.3 Hz, 1 H), 4.30 (m, 1 H), 4.16 (d, *J* = 3.6 Hz, 1 H), 3.88 (dd, *J* = 10.7, 3.6 Hz, 1 H), 3.47 (m, 1 H), 3.33 (dd, *J* = 10.7, 9.3 Hz, 1 H), 1.52 (s, 3 H), 1.43 (s, 2 H), 1.33 (s, 3 H), 1.31 (s, 3 H); ^{13}C NMR ($CDCl_3$, 125 MHz) δ 110.34, 108.55, 97.11, 71.87, 71.01, 70.67, 68.83, 51.29, 26.69, 25.46, 24.98, 24.31; HRMS (FAB) *m/z* $C_{12}H_{20}N_3O_5$ ($[M+H]^+$) 286.1421 (3.5%), calc. 286.1397.

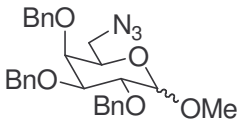

2-12

2-12. Compound **2-11** (1.86 g, 6.52 mmol) was dissolved in MeOH (20 mL), cooled to 0°C, and AcCl (4.35 mL) was added. The mixture was allowed warm to room temperature and stirred for 12 h. The solvent was removed in vacuo and the residue was purified by column chromatography (SiO_2, MeOH:CH_2Cl_2 1:9) yielding the mixture of anomers as a white solid (1.23 g, 86%). ^{1}H NMR ($CDCl_3$:CD_3OD 9:1, 500 MHz) δ 4.79 (d, *J* = 2.5 Hz, 1 H), 4.46 (br s, 1 H), 3.92 (dd, *J* = 8.5, 4.0 Hz, 1 H), 3.84-3.75 (m, 3 H), 3.63 (dd, *J* = 12.5, 8.5 Hz, 1 H), 3.46 (s, 3 H), 3.31 (dd, *J* = 13.0, 4.5 Hz, 1 H); ^{13}C NMR ($CDCl_3$:CD_3OD 9:1, 125 MHz) δ 99.80, 69.84, 69.66, 69.54, 68.55, 55.08, 51.21; HRMS (FAB) *m/z* for $C_7H_{14}N_3O_5$ ($[M+H]^+$) 220.0951 (3.1%), calc. 220.0928. To 6-azido-6-deoxymethylgalactopyranoside (482 mg, 2.2 mmol) in THF (30 mL) was added benzyl bromide (1.57 mL, 13.2 mmol), K_2CO_3 (2.40 g, 17.6 mmol) and 18-crown-6 (120 mg). The suspension was stirred for 15 min, and NaH (0.396 g, 60% in mineral oil, 16.5 mmol) was added. After 12 h, brine (30 mL) was added and the product was extracted with 10% EtOAc in hexane (3 x 20 mL). The combined extracts were dried over Na_2SO_4

and concentrated in vacuo. The desired product (1.02 g, 95%) was obtained as a clear oil after column chromatography (SiO_2, EtOAc:Hex 1:2). ^{1}H NMR ($CDCl_3$, 500 MHz) δ 7.40-7.25 (m, 15 H), 5.02-4.62 (m, 7 H), 4.14-3.76 (m, 4 H), 3.57-3.48 (m, 1 H), 3.39 (s, 3 H), 2.94 (dd, *J* = 12.4, 4.4 Hz, 1 H); ^{13}C NMR ($CDCl_3$, 125 MHz) δ 138.65, 138.58, 138.34, 128.68, 128.61, 128.32, 128.12, 128.01, 127.87, 127.78, 99.01, 79.16, 76.48, 75.45, 74.81, 73.89, 69.98, 55.71, 51.64; HRMS (FAB) *m/z* $C_{28}H_{32}N_3O_5$ ($[M+H]^+$) 490.2347 (3.6%), calc. 490.2336.

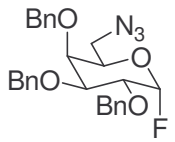

2-13

2-13. Acetic anhydride (0.45 mL) was added to a solution of **2-12** (398 mg, 0.81 mmol) in acetic acid (0.33 mL). The mixture was cooled to 0°C, and conc. H_2SO_4 (6.8 µl) was added. The mixture was stirred at 0°C for 8 h, and water (5 mL) was added. The product was extracted with CH_2Cl_2 (3 x 5 mL), dried over Na_2SO_4 and concentrated in vacuo. After column chromatography (SiO_2, EtOAc:Hex 1:2), 6-azido-2,3,4-tetra-*O*-benzyl-6-deoxy-α-galactosyl-1-acetate (354 mg, 84%) was obtained as a clear oil. 1H NMR ($CDCl_3$, 500 MHz) δ 7.39-7.28 (m, 15 H), 6.38 (d, *J* = 3.5 Hz, 1 H), 5.02-4.58 (m, 6 H), 4.17 (dd, *J* = 11.0, 4.0 Hz, 1 H), 3.91-3.88 (m, 3 H), 3.47 (dd, *J* = 12.5, 7.0 Hz, 1 H), 3.15 (dd, *J* = 12.5, 7.0 Hz, 1 H), 2.12 (s, 3 H); ^{13}C NMR ($CDCl_3$, 125 MHz) δ 169.55, 138.59, 138.13, 138.00, 128.68, 128.62, 128.57, 128.56, 128.53, 128.51, 128.18, 128.13, 128.10, 128.03, 127.98, 127.85, 127.79, 127.60, 90.65, 78.67, 75.45, 75.31, 74.95, 74.69, 74.60, 74.42, 73.57, 73.53, 71.89, 50.85, 21.28; HRMS (FAB) *m/z* $C_{29}H_{31}N_3NaO_6$ ($[M+Na]^+$) 540.2112 (100%), calc. 540.2105. Anhydrous pyridine (0.6 mL) and 70%

hydrogen fluoride-pyridine (1.5 mL) were placed in a polyethylene vial. The mixture was cooled to –20°C and a solution of 6-azido-2,3,4-tetra-*O*-benzyl-6-deoxy-α-galactosyl 1-acetate (401 mg, 0.77 mmol) in toluene (0.3 mL) was added. The mixture was allowed to warm to 0°C and stir for 6 h. It was then poured into a mixture of ether (10 mL) and saturated aqueous KF (30 mL). The product was extracted with a Et_2O:Hex 3:1 solution (2 x 50 mL), and the combined extracts were washed with saturated aqueous KF (30 mL) and brine (30 mL). The organic fraction was dried over Na_2SO_4 and the solvent was removed in vacuo. The residue was purified by flash chromatography (SiO_2, EtOAc:Hex 1:2) to give fluoride **2-13** as a clear oil (230 mg, 78%). ^{1}H NMR ($CDCl_3$, 500 MHz) δ 7.40-7.25 (m, 15 H), 5.63 (dd, *J* = 54.0, 2.5 Hz, 1 H), 5.00 (d, *J* = 11.5 Hz, 1 H), 4.88-4.72 (m, 4 H), 4.61 (d, *J* = 11.0 Hz, 1 H), 4.01-3.88 (m, 4 H), 3.51 (dd, *J* = 12.5, 7.5 Hz, 1 H), 3.13 (dd, *J* = 12.0, 6.0 Hz, 1 H); ^{13}C NMR ($CDCl_3$, 125 MHz) δ 138.38, 138.09, 138.07, 128.74, 128.71, 128.66, 128.56, 128.23, 128.20, 128.16, 128.04, 127.80, 107.12, 105.32, 78.45, 75.85, 75.67, 74.99, 74.48, 73.99, 73.67, 72.14, 72.11, 50.96; HRMS (FAB) *m/e* $C_{27}H_{28}FN_3NaO_4$ ($[M+Na]^+$) 500.1956 (100%), calc. 500.1956.

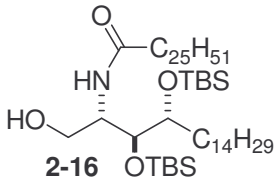

2-16

2-16. Phytosphingosine (**2-14**; 255 mg, 0.803 mmol), commercially available from Avanti Polar Lipids, was stirred vigorously in anhydrous CH_2Cl_2 (4 mL) and 2,6-lutidine (0.64 mL, 5.6 mmol), followed by dropwise addition of TBSOTf (0.64 mL, 2.8 mmol). After 1 h, the solvent was removed in vacuo and was added to a mixture of DIC (131 mg, 1.04 mmol) and HOBT (142 mg, 1.05 mmol) in CH_2Cl_2 (10 mL) that had been

stirring for 20 m. The amide formation was allowed to proceed at room temperature for 12 h, followed by flash chromatography (SiO_2, EtOAc:Hex 5:95), yielding the protected ceramide as a colorless oil (582 mg, 80%), which was used without further characterization. **2-15** (457 mg, 440 mmol) was deprotected at the primary alcohol by dissolving in THF (5 mL), cooling to -10°C, and adding an aqueous solution of TFA (10% v/v) dropwise. After 2 h, a solution of 5% NaOH (2 mL) was added to quench the reaction. Extraction of the product was done with EtOAc (3 x 5 mL) and the organic layer dried with Na_2SO_4. Concentration and purification by flash chromatography (SiO_2, EtOAc:Hex 1:2) provided **2-16** as a colorless oil (361 mg, 89%). ^{1}H NMR ($CDCl_3$, 500 MHz) δ 6.26 (d, *J* = 9.2 Hz, 1 H), 4.23 (dt, *J* = 11.5, 3.0 Hz, 1 H), 4.07 (m, 1 H), 3.92 (m, 1 H), 3.77 (m, 1 H), 3.60 (m, 1 H), 3.17 (dd, *J* = 9.0, 3.5 Hz, 1 H), 2.19 (t, *J* = 7.8 Hz, 2 H), 1.68-1.48 (m, 4 H), 1.26 (br s, 68 H), 0.94 (m, 18 H), 0.88 (t, *J* = 6.8 Hz, 6 H), 0.11 (m, 12 H); ^{13}C NMR ($CDCl_3$, 125 MHz) δ 172.87, 77.67, 76.61, 63.85, 51.42, 37.17, 34.65, 32.15, 30.02, 29.92, 29.88, 29.85, 29.75, 29.71, 29.59, 26.22, 26.17, 26.05, 25.86, 25.83, 22.91, 18.37, 14.34, -3.37, -3.54, -3.85, -4.31; HRMS (FAB) *m/e* $C_{56}H_{117}NNaO_4Si_2$ ($[M+Na]^+$) 946.8422 (100%), calc. 946.8413.

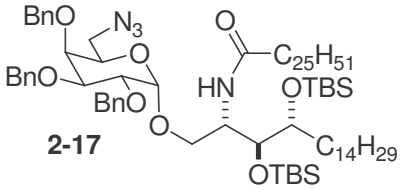

2-17

2-17. To a solution of **2-16** (266 mg, 0.28 mmol) in anhydrous THF (10 mL), $SnCl_2$ (163.7 mg, 0.86 mmol), $AgClO_4$ (179 mg, 0.86 mmol), and freshly crushed 4A molecular sieves (1.34 g) were combined. A solution of **2-13** (214 mg, 0.45 mmol) in anhydrous THF (2 mL) was then added at -10°C. The reaction mixture was allowed to warm to

room temperature over 2 h. The mixture was diluted with Et_2O and filtered through Celite. After concentration, the residue was purified by column chromatgraphy (SiO_2, EtOAc:Hex 1:2) to give the protected glycosphingolipid as a clear oil (175 mg, 44%). ^1H NMR ($CDCl_3$, 500 MHz) δ 7.40-7.31 (m, 15 H), 5.92 (d, *J* = 8.0 Hz, 1 H), 5.02 (d, *J* = 11.0 Hz, 1 H), 4.85-4.59 (m, 6 H), 4.21 (m, 1 H), 4.06-3.99 (m, 2 H), 3.91 (dd, *J* = 13.0, 3.0 Hz, 1 H), 3.86-3.83 (m, 3 H), 3.79 (m, 1 H), 3.50 (dd, *J* = 12.0, 7.5 Hz, 1 H), 3.17 (dd, *J* = 12.0, 7.5 Hz, 1 H), 2.03 (t, *J* = 7.5 Hz, 2 H), 1.58-1.24 (m, 73 H), 0.92 (s, 9 H), 0.91 (s, 9 H), 0.89 (m, 6 H), 0.09 (s, 3 H), 0.08 (s, 3 H), 0.06 (s, 3 H), 0.05 (s, 3 H); ^{13}C NMR ($CDCl_3$, 125 MHz) δ 173.24, 138.69, 138.61, 138.35, 128.64, 128.58, 128.57, 128.06, 128.03, 127.94, 127.85, 127.64, 100.18, 79.16, 76.59, 76.20, 75.99, 75.04, 74.87, 73.71, 73.49, 70.11, 69.56, 51.78, 51.38, 37.05, 33.59, 32.14, 32.13, 30.10, 29.93, 29.91, 29.89, 29.87, 29.81, 29.77, 29.68, 29.66, 29.58, 26.31, 26.24, 25.86, 22.90, 18.52, 18.37, 14.34, -3.47, -3.76, -4.44, -4.71; HRMS (FAB) *m/z* $C_{83}H_{145}N_4O_8Si_2$ ($[M+H]^+$) 1382.0592 (81.3%), calc. 1382.0595.

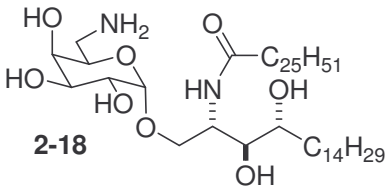

2-18

2-18. To a solution of **2-17** (175 mg, 0.12 mmol) in THF (4 mL), TBAF in THF (1.0 *M*, 0.5 mL, 0.5 mmol) was added dropwise at room temperature. After stirring for 90 m, the mixture was diluted with water and extracted with Et_2O. The extract was washed with water and brine, dried with Na_2SO_4, and concentrated under reduced pressure. The residue was purified by column chromatography (SiO_2, EtOAc:Hex 1:2) to give the corresponding diol as a clear glass (118 mg, 81%). ^1H NMR ($CDCl_3$, 500 MHz) δ 7.39-

7.25 (m, 15 H), 6.25 (d, *J* = 8.0 Hz, 1 H), 4.99 (d, *J* = 11.0 Hz, 1 H), 4.88-4.57 (m, 6 H), 4.27 (m, 1 H), 4.05 (dd, *J* = 9.5, 3.0 Hz, 1 H), 3.93 (dd, *J* = 10.0, 3.0 Hz, 1 H), 3.87-3.80 (m, 2 H), 3.72 (m, 1 H), 3.51-3.45 (m, 3 H), 3.03 (dd, *J* = 13.0, 6.0 Hz, 1 H), 2.25 (d, *J* = 5.5 Hz, 1 H), 2.15 (t, *J* = 7.0 Hz, 2 H), 2.13-1.25 (m, 76 H), 0.88 (t, *J* = 7.5 Hz, 6 H); ^{13}C NMR ($CDCl_3$, 125 MHz) δ 173.07, 138.30, 138.12, 137.84, 128.75, 128.74, 128.64, 128.58, 128.32, 128.29, 128.20, 128.02, 127.72, 99.08, 79.38, 76.41, 75.93, 74.84, 74.60, 74.49, 73.54, 73.27, 70.42, 69.99, 51.22, 49.28, 37.03, 33.58, 32.13, 29.94, 29.91, 29.88, 29.75, 29.63, 29.57, 29.52, 26.12, 25.98, 22.90, 14.33; HRMS (FAB) *m/z* $C_{71}H_{117}N_4O_8$ ($[M+H]^+$) 1153.8873 (89.4%), calc. 1153.8866. To a solution of the diol (118 mg, 0.1 mmol) in THF:H_2O (1.5 mL:0.3 mL) was added triphenylphosphine (40.3 mg). The reaction mixture was stirred at room temperature for 12 h then purified directly by column chromatography (SiO_2, $CHCl_3$:MeOH:NH_4OH 1:0.4:0.02) to yield the amine as a clear glass (114 mg, 99% yield). ^{1}H NMR ($CDCl_3$, 500 MHz) δ 7.59-7.18 (m, 15 H), 6.49 (d, *J* = 8.5 Hz, 1 H), 4.87 (d, *J* = 11.5 Hz, 1 H), 4.78 – 4.52 (m, 6 H), 4.18 (m, 1H), 3.97 (dd, *J* = 10.0, 3.5 Hz, 1 H), 3.81 (dd, *J* = 10.0, 4.5 Hz, 1 H), 3.77 (dd, *J* = 10.0, 2.5 Hz, 1 H), 3.72 (m, 2 H), 3.67 (dd, *J* = 10.0, 4.0 Hz, 1 H), 3.52 (dd, *J* = 8.0, 5.0 Hz, 1 H), 3.41 (m, 2 H), 2.82 (dd, *J* = 13.0, 8.0 Hz, 1 H), 2.42 (dd, *J* = 13.0, 5.0 Hz, 1 H), 2.37 (m, 1 H), 2.04 (t, *J* = 8.0 Hz, 2 H), 1.49-0.82 (m, 74 H), 0.79 (t, *J* = 7.0 Hz, 6 H); ^{13}C NMR ($CDCl_3$, 125 MHz) δ 173.54, 138.60, 138.33, 138.12, 132.96, 132.31, 132.23, 132.19, 132.17, 132.14, 128.76, 128.74, 128.66, 128.59, 128.24, 128.11, 128.09, 127.86, 127.69, 98.86, 79.81, 76.50, 76.35, 74.79, 74.62, 74.08, 73.37, 73.03, 72.58, 68.51, 53.93, 50.42, 42.43, 36.97, 33.88, 32.11, 29.96, 29.90, 29.84, 29.74, 29.61, 29.55, 29.52, 26.16, 25.97, 25.86, 22.88, 20.92, 14.32; HRMS (FAB) *m/z* $C_{71}H_{119}N_2NaO_8$ ($[M+Na]^+$) 1149.8790

(100%), calc. 1149.8780. Sodium metal (20 mg) was added to liquid ammonia (8 mL) under N_2 at -78 °C and the mixture was stirred for 2 m. The amine (18 mg, 0.016 mmol) in anhydrous THF (1 mL) was then added to the blue solution and stirred for 40 m. The reaction was quenched by addition of MeOH (4 mL), ammonia was removed under a stream of N_2, and the residue was purified by column chromatography (SiO_2, $CHCl_3$:MeOH:NH_4OH 1:0.4:0.02) after concentration in vacuo to give the 6"-amino-α-galactosylceramide as a white solid (7.3 mg, 53%). ^{1}H NMR ($CDCl_3$:CD_3OD 95:5) δ 4.91 (d, *J* = 4.0 Hz, 1 H), 4.21 (m, 1 H), 3.88 (m, 2 H), 3.80 (dd, *J* = 10.0, 3.5 Hz, 1 H), 3.75 (m, 1 H), 3.70 (dd, *J* = 10.0, 3.5 Hz, 1 H), 3.62-3.51 (m, 10 H), 3.06 (dd, *J* = 13.0, 7.5 Hz, 1 H), 2.90 (dd, *J* = 13.0, 4.0 Hz, 1 H), 2.19 (t, *J* = 8.0 Hz, 2 H), 1.68-1.25 (m, 73 H), 0.88 (t, *J* = 7.0 Hz, 6 H); ^{13}C NMR ($CDCl_3$:CD_3OD 95:5) δ 174.36, 99.75, 75.17, 72.06, 70.84, 70.37, 70.22, 68.92, 67.31, 50.36, 42.40, 36.62, 33.02, 31.97, 29.83, 29.77, 29.74, 29.71, 29.70, 29.61, 29.46, 29.42, 25.90, 25.87, 22.73, 14.11; HRMS (FAB) *m/z* $C_{50}H_{100}N_2NaO_8$ ($[M+Na]^+$) 879.7384 (100%), calc. 879.7372.

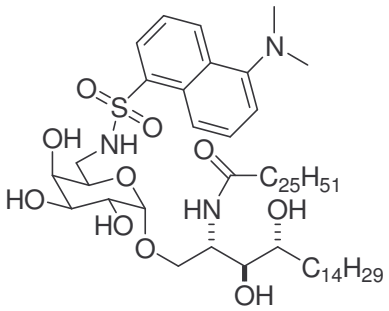

2-4

2-4. Dansyl chloride (1.5 mg, 0.0055 mmol) was added to a solution of **2-18** (4.5 mg, 0.005 mmol) in pyridine (1 mL), and the mixture was stirred for 5 h. The pyridine was removed in vacuo, and the product was purified by column chromatography (SiO_2, 10% MeOH:CH_2Cl_2 1:9) giving a light yellow glass (3.4 mg, 60%). ^{1}H NMR ($CDCl_3$:CD_3OD

95:5, 500 MHz) δ 8.55 (d, *J* = 9.0 Hz, 1 H), 8.26 (d, *J* = 8.5 Hz, 1 H), 8.19 (dd, *J* = 7.0, 1.5 Hz, 1 H), 7.58-7.50 (m, 2 H), 7.20 (d, *J* = 7.5 Hz, 1 H), 6.93 (d, *J* = 8.5 Hz, 1 H), 4.83 (d, *J* = 2.5 Hz, 1 H), 4.22 (m, 1 H), 3.91 (m, 3 H), 3.72 (m, 2 H), 3.64-3.55 (m, 4 H), 3.07 (m, 2 H), 2.88 (s, 6 H), 2.22 (br, 7 H), 1.62-1.25 (m, 72 H), 0.87 (t, *J* = 7.0 Hz, 6 H); ^{13}C NMR ($CDCl_3$:CD_3OD 95:5, 125 MHz) δ 174.45, 152.09, 134.62, 130.69, 130.10, 129.71, 129.36, 123.31, 118.91, 115.43, 99.68, 75.36, 72.41, 70.18, 69.55, 69.13, 69.03, 67.96, 50.42, 45.56, 43.28, 36.78, 33.14, 32.07, 29.93, 29.88, 29.85, 29.82, 29.80, 29.72, 29.57, 29.52, 25.96, 25.94, 22.84, 14.25; HRMS (FAB) *m/z* $C_{62}H_{111}N_3NaO_{10}S$ ($[M+Na]^+$) 1112.7867 (100%), calc. 1112.7882.

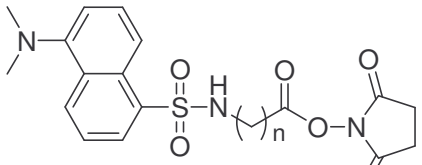

2-19 n = 2
2-20 n = 5

2-19. Dansyl chloride (212 mg, 0.784 mmol) was dissolved in acetone (2 mL) along with separate solutions of β-alanine (100 mg, 1.12 mmol) and $NaHCO_3$ (99 mg, 1.18 mmol) in deionized water (1 mL each). The deep orange color of the dansyl solution turned to a bright yellow upon vigorous mixing. After 4 h, the solution was acidified to a pH of 2 with 5% HCl (3 drops) and extracted with EtOAc (3 x 3 mL). After a wash with brine (1 mL), drying with Na_2SO_4, and concentration of the solvent, the amino acid was crystallized with CH_2Cl_2 to yield fluffy yellow crystals (129 mg, 51%). ^{1}H NMR ($CDCl_3$, 300 MHz) δ 9.25 (br s, 1 H), 8.53 (d, *J* = 8.5 Hz, 1 H), 8.26 (d, *J* = 8.5 Hz, 1 H), 8.24 (dd, *J* = 7.3, 1.2, 1 H), 7.51 (m, 2 H), 7.17 (d, *J* = 7.1 Hz, 1 H), 5.95 (t, *J* = 6.1 Hz, 1 H), 3.16 (dt, *J* = 6.1, 5.9 Hz, 2 H), 2.87 (s, 6 H), 2.50 (t, *J* = 5.9 Hz, 2 H); ^{13}C NMR ($CDCl_3$, 75 MHz) δ 176.60, 151.86, 130.68, 129.98, 129.67, 129.57, 128.61, 123.40,

119.02, 115.53, 45.55, 38.66, 34.22; HRMS (EI) *m/z* for $C_{15}H_{18}N_2O_3S$ ($[M]^+$) 322.0971 (92.0%), calc. 322.0987. The dansyl-linked acid (31 mg, 0.097 mmol) was dissolved in anhydrous CH_2Cl_2 (1 mL) followed by NHS (15 mg, 0.130 mmol) and DCC (26 mg, 0.126 mmol). The solution was stirred at room temperature for 4 h then put in a freezer for 12 h to precipitate DCU and any excess DCC. The yellow mixture was vacuum filtered and purified by column chromatography (SiO_2, EtOAc:Hex, 4:1) to yield a yellow solid (35 mg, 41%). ^{1}H NMR ($CDCl_3$, 300 MHz) δ 8.57 (d, *J* = 8.5 Hz, 1 H), 8.27 (d, *J* = 8.5 Hz, 1 H), 8.26 (dd, *J* = 7.3, 1.2, 1 H), 7.57 (dd, *J* = 8.6, 7.6 Hz, 1 H), 7.54 (dd, *J* = 9.0, 7.3 Hz, 1 H), 7.19 (d, *J* = 7.6 Hz, 1 H), 5.65 (t, *J* = 6.6 Hz, 1 H), 3.30 (dt, *J* = 6.6, 6.3 Hz, 2 H), 2.89 (s, 6 H), 2.84 (s, 4 H), 2.78 (t, *J* = 6.3 Hz, 2 H); ^{13}C NMR ($CDCl_3$, 75 MHz) δ 169.22, 167.15, 152.19, 134.75, 130.88, 130.13, 129.71, 128.68, 123.36, 118.91, 115.47, 45.60, 38.84, 32.54, 25.73; HRMS (EI) *m/z* for $C_{19}H_{21}N_3O_6S$ ($[M]^+$) 419.1166 (100%), calc. 419.1151.

2-20. Same procedure as synthesis of **2-19**, substituting with 6-aminohexanoic acid (30% overall yield). ^{1}H NMR ($CDCl_3$, 300 MHz) δ 8.56 (d, *J* = 8.5 Hz, 1 H), 8.32 (d, *J* = 8.5 Hz, 1 H), 8.26 (dd, *J* = 7.3, 1.2, 1 H), 7.57 (dd, *J* = 8.6, 7.5 Hz, 1 H), 7.54 (dd, *J* = 9.0, 7.3 Hz, 1 H), 7.20 (d, *J* = 7.5 Hz, 1 H), 5.08 (t, *J* = 6.2 Hz, 1 H), 2.99 (m, 2 H), 2.89 (s, 6 H), 2.84 (s, 4 H), 2.19 (t, *J* = 7.3 Hz, 2 H), 1.43 (m, 4 H), 1.21 (m, 2 H); ^{13}C NMR ($CDCl_3$, 75 MHz) δ 169.17, 167.26, 152.11, 134.70, 131.34, 130.75, 130.01, 128.87, 123.86, 119.49, 115.40, 45.60, 38.84, 32.54, 28.65, 26.22, 25.73, 24.70; HRMS (EI) *m/z* for $C_{22}H_{27}N_3O_6S$ ($[M]^+$) 461.1630 (100%), calc. 461.1621.

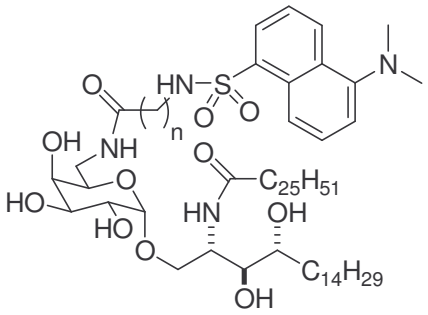

2-5 n = 2
2-6 n = 5

2-5. Ester **2-19** (5.6 mg, 0.01 mmol) was added to a solution of **2-18** (3.8 mg, 0.0044 mmol) in pyridine (1 mL), and the mixture was stirred for 12 h. The pyridine was removed in vacuo, and the product was purified by column chromatography (SiO_2, MeOH:CH_2Cl_2 1:9) giving a light yellow glass (2.2 mg, 43%). ^{1}H NMR ($CDCl_3$:CD_3OD 95:5, 500 MHz) δ 8.55 (d, *J* = 9.0 Hz, 1 H), 8.27 (d, *J* = 8.5 Hz, 1 H), 8.19 (dd, *J* = 7.5, 1.2 Hz, 1 H), 7.59-7.51 (m, 2 H), 7.20 (d, *J* = 7.5 Hz, 1 H), 4.91 (d, *J* = 3.0 Hz, 1 H), 4.27 (m, 1 H), 3.97 (dd, *J* = 10.5, 4.5 Hz, 1 H), 3.90-3.79 (m, 3 H), 3.75 (dd, *J* = 11.0, 4.5 Hz, 1 H), 3.66-3.60 (m, 2 H), 3.57-3.54 (m, 2 H), 3.20 (dd, *J* = 13.5, 5.5 Hz, 1 H), 3.13 (m, 1 H), 3.06 (m, 1 H), 2.89 (s, 6 H), 2.43 (m, 1 H), 2.36 (m, 1 H), 2.16 (td, *J* = 7.5, 3.5 Hz, 2 H), 1.70 (m, 1 H), 1.62-1.50 (m, 3 H), 1.25 (br s, 68 H), 0.88 (t, *J* = 7.5 Hz, 6 H); ^{13}C NMR ($CDCl_3$:CD_3OD 9:1) δ 174.74, 172.70, 152.06, 134.41, 130.69, 130.09, 129.71, 129.48, 128.53, 123.27, 118.93, 115.49, 99.54, 75.31, 72.41, 70.21, 69.31, 69.05, 68.75, 67.39, 50.50, 45.55, 40.05, 39.24, 36.59, 33.15, 32.07, 29.93, 29.88, 29.85, 29.69, 29.52, 29.51, 29.46, 25.98, 22.84, 14.25; HRMS (FAB) *m/z* $C_{65}H_{116}N_4NaO_{11}S$ ($[M+Na]^+$) 1183.8259 (100%), calc. 1183.8254.

2-6. Same procedure as synthesis of **2-5**, substituting with ester **2-20** (53%). ^{1}H NMR ($CDCl_3$:CD_3OD 95:5, 500 MHz) δ 8.53 (d, *J* = 9.0 Hz, 1 H), 8.28 (d, *J* = 8.5 Hz, 1 H),

8.20 (dd, *J* = 7.5, 1.2 Hz, 1 H), 7.59-7.50 (m, 2 H), 7.20 (d, *J* = 7.5 Hz, 1 H), 7.04 (d, *J* = 8.5 Hz, 1 H), 4.91 (d, *J* = 3.0 Hz, 1 H), 4.17 (m, 1 H), 3.90 (dd, *J* = 10.5, 4.5 Hz, 1 H), 3.84 (m, 4 H), 3.75 (dd, *J* = 11.0, 4.5 Hz, 1 H), 3.68-3.64 (m, 2 H), 3.57-3.54 (m, 2 H), 3.20 (dd, *J* = 13.5, 5.5 Hz, 1 H), 2.89 (s, 6 H), 2.80 (m, 1 H), 2.46-2.03 (m, 11 H), 1.62-1.25 (m, 78 H), 0.87 (t, *J* = 7.5 Hz, 6 H); ^{13}C NMR ($CDCl_3$:CD_3OD 9:1) δ 175.38, 174.50, 152.04, 134.69, 130.52, 130.01, 129.72, 129.61, 128.46, 123.31, 118.98, 115.40, 99.71, 74.97, 72.45, 69.94, 69.01, 68.95, 68.03, 50.39, 45.54, 42.76, 42.61, 39.45, 36.57, 35.87, 32.79, 32.06, 29.85, 29.68, 29.50, 29.41, 28.97, 26.85, 26.00, 25.92, 25.49, 25.03, 24.77, 24.37, 22.82, 14.23; HRMS (FAB) *m/z* $C_{68}H_{122}N_4NaO_{11}S$ ($[M+Na]^+$) 1225.8741 (100%), calc. 1225.8723.

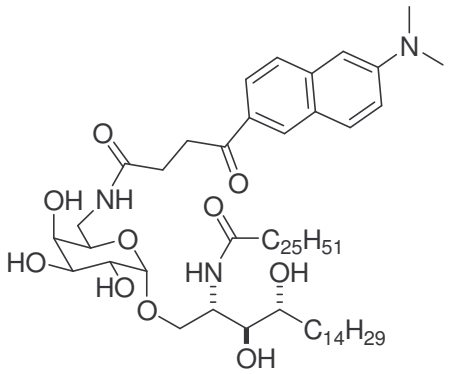

2-7

2-7. *N*-Hydroxysuccinimidyl prodan (6.6 mg, 0.018 mmol) was added to a solution of **2-18** (5.0 mg, 0.0058 mmol) in pyridine (1 mL) and the mixture was stirred for 12 h. The pyridine was removed in vacuo, and the product was purified by column chromatography (SiO_2, MeOH:CH_2Cl_2 9:1) giving a clear glass (3.0 mg, 46%). ^{1}H NMR ($CDCl_3$:CD_3OD 95:5, 500 MHz) δ 8.36 (m, 1 H), 7.89 (dd, *J* = 8.0, 1.5 Hz, 1 H), 7.81 (d, *J* = 8.5 Hz, 1 H), 7.64 (d, *J* = 8.5 Hz, 1 H), 7.18 (dd, *J* = 8.5, 2.5 Hz, 1 H), 7.01 (d, *J* = 8.0 Hz, 1 H), 6.86 (d, *J* = 2.5 Hz, 1 H), 4.89 (d, *J* = 4.0 Hz, 1 H), 4.19 (m, 1 H), 3.92 (dd, *J* =

10.0, 4.5 Hz, 1 H), 3.82-3.38 (m, 9 H), 3.22 (dd, *J* = 13.5, 6.0 Hz, 1 H), 3.19 (s, 6 H), 2.65 (t, *J* = 7.0 Hz, 2 H), 2.34 (br s, 5 H), 2.18 (m, 2H), 2.05-2.08 (m, 2 H), 1.65-1.23 (m, 72 H), 0.87 (t, *J* = 7.0 Hz, 6 H); ^{13}C NMR ($CDCl_3$:CD_3OD 9:1) δ 199.01, 174.46, 150.56, 138.06, 130.98, 130.42, 129.86, 126.43, 125.10, 124.35, 121.72, 116.49, 110.59, 105.36, 99.72, 84.07, 75.29, 72.47, 70.11, 69.23, 68.99, 68.69, 67.80, 60.06, 50.56, 40.54, 36.76, 33.62, 33.11, 32.07, 30.23, 29.86, 29.85, 29.81, 29.80, 29.71, 29.57, 29.51, 25.99, 22.83, 14.25; HRMS (FAB) *m/z* $C_{66}H_{115}N_3NaO_{10}S$ ($[M+Na]^+$) 1132.8484 (100%), calc. 1132.8475.

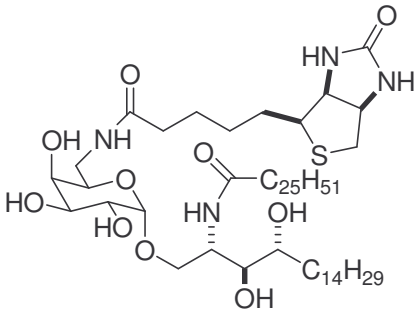

2-8

2-8. *N*-Hydroxysuccinimidyl biotin (5.9 mg, 0.017 mmol) and Et_3N (30 µl) were added to a solution of **2-18** (5.0 mg, 0.0058 mmol) in DMF (1.5 mL). The mixture was stirred for 12 h, and applied directly to a silica gel column. Elution with MeOH:CH_2Cl_2 1:9 gave the product as a clear glass (3.2 mg, 52%). ^{1}H NMR (pyridine-d_5, 500 MHz) δ 8.86 (m, 1 H), 8.61 (d, *J* = 9.0 Hz, 1 H), 7.54-7.40 (m, 4 H), 5.54 (d, *J* = 4.0 Hz, 1 H), 5.28 (br s, 1 H), 4.66-4.61 (m, 2 H), 4.56-4.50 (m, 3 H), 4.41-4.31 (m, 6 H), 4.23 (m, 1 H), 3.92 (m, 1 H), 3.27 (m, 1 H), 3.16 (m, 1 H), 3.00-2.85 (m, 10 H), 2.55-2.44 (m, 6 H), 2.32 (m, 1 H), 1.96-1.50 (m, 20 H), 1.32-1.26 (m, 44 H), 0.87 (t, *J* = 7.0 Hz, 6 H); ^{13}C NMR (pyridine-d_5, 125 MHz) δ 170.36, 169.46, 164.28, 101.41, 76.88, 72.57, 71.30, 71.21, 70.74, 70.10, 68.62, 62.41, 62.36, 60.57, 56.30, 56.13, 51.24, 41.22, 41.15, 36.86,

36.27, 34.52, 32.17, 30.89, 30.46, 30.23, 30.11, 29.98, 29.89, 29.85, 29.67, 29.12, 28.87, 28.53, 26.56, 26.50, 26.27, 26.16, 26.10, 24.85, 22.98, 14.33; HRMS (FAB) *m/z* $C_{60}H_{114}N_4NaO_{10}S$ ($[M+Na]^+$) 1105.8143 (100%), calc. 1105.8148.

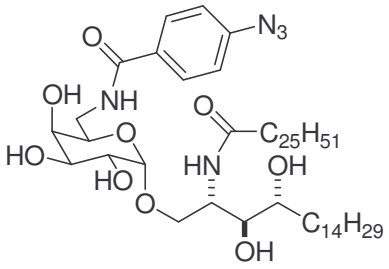

2-9

2-9. Amine **2-18** (11 mg, 0013 mmol) was dissolved in pyridine (5 mL) followed by addition of *N*-hydroxysuccimidyl 4-azidobenzoate (7 mg, 0.026 mmol) with the exclusion of light. The mixture was stirred for 12 h, the solvent was removed in vacuo, and the residue purified by column chromatography (SiO_2, MeOH:$CHCl_3$ 5:95) to yield the solid product (5 mg, 45%). ^{1}H NMR ($CDCl_3$:CD_3OD 9:1, 500 MHz) δ 7.84 (d, *J* = 8.5 Hz, 2 H), 7.09 (d, *J* = 8.5 Hz, 2 H), 4.91 (d, *J* = 3.8 Hz, 1 H), 4.98 (d, *J* = 3.5 Hz, 1 H), 3.91-3.27 (m, 11 H), 2.15-2.13 (m, 2 H), 1.79-1.63 (m, 4 H), 1.26 (br s, 68 H), 0.88 (m, 6 H); ^{13}C NMR ($CDCl_3$:CD_3OD 95:5, 125 MHz) δ 177.73, 173.22, 129.15, 119.12, 100.02, 74.92, 72.16, 70.25, 70.08, 69.88, 69.78, 69.24, 68.99, 67.24, 55.54, 51.53, 50.67, 40.16, 36.63, 32.88, 32.04, 29.82, 29.49, 26.01, 25.43, 22.80, 14.13; HRMS (FAB) *m/z* $C_{57}H_{103}N_5NaO_9$ ($[M+Na]^+$) 1020.7690 (46.5%), calc. 1020.7648.

2.5 References

1) Spada, F. M.; Koezuka, Y.; Porcelli, S. A. *J. Exp. Med*. **1998**, *8*, 1529.

2) Kawano, T.; Cui, J.; Koezuka, Y.; Toura, I.; Kaneko, Y.; Motoki, K.; Ueno, H.; Nakagawa, R.; Sato, H,; Kondo, E,; Koseki, H.; Taniguchi, M. *Science* **1997**, *278*, 1626.

3) Chiu, Y.-H.; Jayawardena, J.; Weiss, A.; Lee, D.; Park, S.-H.; Dautry-Varsat, A.; Bendelac, A. *J. Exp. Med*. **1999**, *189*, 103.

4) Prigozy, T. I.; Naidenko, O.; Qasba, P.; Elewaut, D.; Brossay, L.; Khurana, A.; Natori, T.; Koezuka, Y.; Kulkarni, A.; Kronenberg, M. *Science* **2001**, *291*, 664.

5) Zhou, D.; Cantu, C., III; Sagiv, Y.; Schrantz, N.; Kulkarni, A. B.; Qi, X.; Mahuran, D. J.; Morales, C. R.; Grabowski, G. A.; Benlagha, K.; Savage, P. B.; Bendelac, A.; Teyton, L. *Science* **2004**, *303*, 523.

6) (a) Sakai, T.; Naidenko, O. V.; Iijima, H.; Kronenberg, M.; Koezuka, Y. *J. Med. Chem*. **1999**, *42*, 1836. (b) Sakai, T.; Ehara, H.; Koezuka, Y. *Org. Lett*. **1999**, *1*, 359.

7) Kobayashi, E.; Motoki, K.; Yamaguchi, Y.; Uchida, T.; Fukushima, H.; Koezuka, Y. *Bioorg. Med. Chem*. **1996**, *4*, 615.

8) Benlagha, K.; Weiss, A.; Beavis, A.; Teyton, L.; Bendelac, A. *J. Exp. Med*. **2000**, *191*, 1895.

9) Naidenko, O. V.; Maher, J. K.; Ernst, Y.; Sakai, T.; Modlin, R. L.; Kronenberg, M. *J. Exp. Med*. **1999**, *190*, 1069.

10) Zeng, Z.-H.; Castano, A. R.; Segelke, B. W.; Stura, E. A.; Peterson, P. A.; Wilson, I. A. *Science* **1997**, *277*, 339.

11) Kamada, K.; Iijima, H.; Kimura, K.; Harada, M.; Sminizu, E.; Motohashi, S.; Kawano, T.; Shinkai, H.; Nakayama, T.; Sakai, T.; Brossay, L.; Kronenberg, M.; Taniguchi, M. *Internat. Immunol*. **2001**, *13*, 853.

12) Zhou, X.-T.; Forestier, C.; Goff, R. D.; Li, C.; Teyton, L.; Bendelac, A.; Savage, P. B. *Org. Lett*. **2002**, *4*, 1267. Figure 2.5 is reproduced in part with permission, Copyright 2002 American Chemical Society.

13) Sagiv, Y.; Hudspeth, K.; Mattner, J.; Schrantz, N.; Stern, R. K.; Zhou, D.; Savage, P. B.; Teyton, L.; Bendelac, A. *J. Immunol*. **2006**, *177*, in press. Figures 2.6 and 2.7: Copyright 2006 The American Association of Immunologists, Inc.

14) Ueda, M.; Wada, Y.; Yamamura, S. *Tetrahedron Lett*. **2001**, *42*, 3869.

15) Koezuka, Y.; Kabaya, K.; Motoki, K. Int'l Patent WO 9402168, 1994.

16) Hayashi, M.; Hashimoto, S.; Noyori, R. *Chem. Lett*. **1984**, *13*, 1747.

17) Takikawa, H.; Muto, S.; Mori, K. *Tetrahedron* **1998**, *54*, 3141.

18) Kawai, A.; Hara, O.; Hamada, Y.; Shiari, T. *Tetrahedron Lett*. **1988**, *29*, 6331.

19)Mukaiyama, T.; Murai, Y.; Shoda, S. *Chem. Lett*. **1981**, *10*, 431.

20) Scozzafava, A.; Supuran, C. *Eur. J. Med. Chem*. **2000**, *35*, 299.

21) Weber, G.; Farris, F. J. *Biochemistry* **1979**, *18*, 3075.

22) (a) Zajonc, D. M.; Cantu III, C.; Mattner, J.; Zhou, D.; Savage, P. B.; Bendelac, A.; Wilson, I. A.; Teyton, L. *Nat. Immunol*. **2005**, *6*, 810. (b) Wu, D.; Zajonc, D. M.; Fujio, M.; Sullivan, B. A.; Kinjo, Y.; Kronenberg, M.; Wilson, I. A.; Wong, C.-H. *Proc. Nat. Acad. Sci. USA* **2006**, *103*, 3972.

23) Davies, J. P.; Chen, F. W.; Ioannou, Y. A. *Science* **2000**, *290*, 2295.

CHAPTER 3.

STRUCTURE-ACTIVITY RELATIONSHIP STUDIES OF TRUNCATED GLYCOSPHINGOLIPIDS ON NKT CELL CYTOKINE RELEASE PROFILES

3.1 Introduction

An integral feature of the immune system is its ability to identify endogenous antigens from those of an exogenous source. The receptors on T cells and B cells are able to recognize an abundance of structures due to their genetic and somatic variability and can mount a response according to the type of antigen they recognize. This innate ability of the immune system to differentiate between foreign and self antigens is necessary to keep it from attacking the host organism. Even so, immunity is sophisticated enough to distinguish normal host cells from those that have become diseased. In the case where an endogenous cell has undergone an unnatural transformation (e.g., uncontrolled growth, disruption of the cellular apoptosis function) or has been come corrupted through infection, this system can allow for destruction of those bodies. In adaptive immunity, one such mechanism is absorption of distressed cells by $CD8^+$ T cells through identification of MHC type 1-bound peptides. The other type of effector T lymphocyte, T helper cells, can aid cytotoxic T lymphocytes (CTLs) by secreting cytokines for upregulation of cytotoxic activity and recruitment of other phagocytes.[1]

The ability of activating and assisting CTLs against defective host cells is part of the larger responsibility of T helper cells to mount the adaptive response a host will take against any given type of foreign or abnormal body, though they cannot inactivate or kill

pathogens or defective host cells. Like a conductor of an orchestra indicating the instruments to be played at the proper volume and tempo, T helper cells direct which other types of cells should be activated according to the type of problem the immune system is facing. The basis for immunodeficiency due to the AIDS virus is infection of these $CD4^+$ cells and an erosion of their population so they can no longer recognize a wide variety of antigens to stave off infection. Thus, T_H cells are necessary for a healthy immune system.[2]

These cells are subdivided into two groups based on the types of cytokines they release and the resulting pathway the immune system takes. T helper type 1 (T_H1) cells secrete IFN-γ, IL-2, and tumor necrosis factors (TNF) whereas type 2 (T_H2) produce IL-4, IL-5, IL-6, IL-10, and various other cytokines.[1,3] A T_H1-type response typically involves IL-2 secretion to activate macrophages against intra- and extracellular pathogens and CTLs against corrupted host cells. Messages are also sent to B cells to produce IgG3 antibodies in humans, which make foreign bodies more susceptible to phagocytosis. The cytokines released by the T_H2 subpopulation have an immunomodulatory effect by influencing the humoral adaptive system. B cells are activated to proliferate and motivated to produce a variety of immunoglobulins and/or switch the class of antibodies that are produced. Naïve B cells are activated to proliferate and secrete IgM, which can help initiate the immune response. IL-3, 4, 5, and 10 are used to recruit granuloytes, a subtype of white blood cells. IL-4 appears to have the greatest impact on the T_H2 response and is a major marker for identifying T_H2 cells (Figure 3.1).[4]

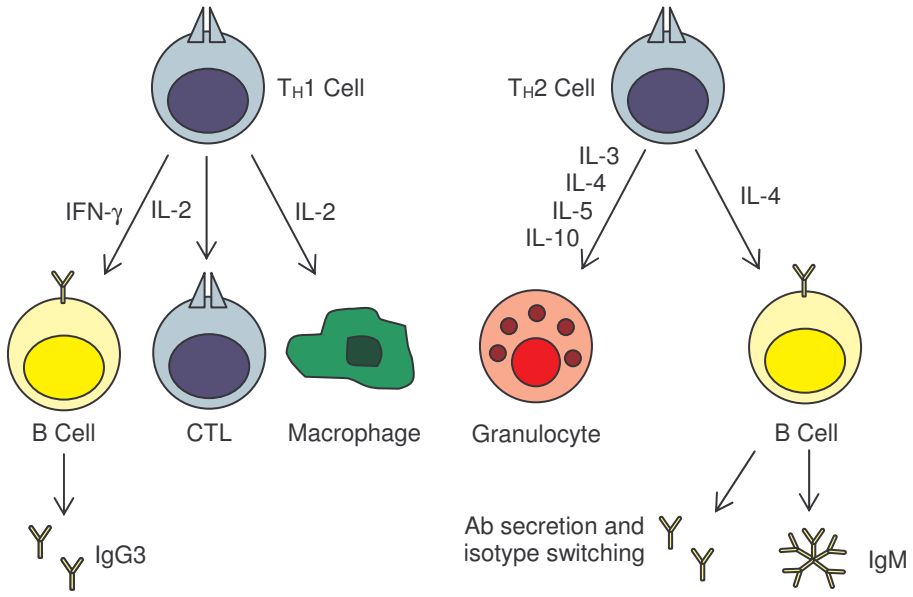

Figure 3.1. T Helper Cell Activation of the Immune System.[1]

Even though they are believed to originate from the same immature T lymphocyte, a T_H0 cell, the effects on the immune system from these different types can be polarizing. It appears T_H1 and T_H2 cells suppress and cross-regulate each other besides causing opposing immune effects. During activation in the proinflammatory T_H1 response, dendritic cells and other APCs can express IL-12. This cytokine supports proliferation of T_H1 cells through directing them to produce IFN-γ and can steer the development of immature T cells toward the T_H1 subtype. Concomitant with this signal is the suppression of selection of T_H2 cells. Conversely, IL-10 promotes T_H2 activity by causing B cells to increase expression of MHC II while serving as an antagonist against IL-2 and IFN-γ cytokines and IL-12 production by antigen presenting cells, downregulating T_H1 cell proliferation (Figure 3.2).[5] Although they offset each other, a failsafe mechanism to prevent permanent polarization toward either T_H cell is in place where respective prevailing cytokines downregulate the type of DC required for

maturation of that specific T helper type (e.g., IL-2 inhibits the development of the specific DC needed for T_H1 development).

Although both T_H1 and T_H2 responses are critical for putting the humoral and cellular sections of the immune system into motion, imbalance of either can cause health problems for the host. Overexpression of T_H2 cells and their associated cytokines (e.g., IL-4) has been associated with type I hypersensitivity causing asthma and allergies through excess promotion of IgE antibodies.[6] When the T_H1 proiflammatory response occurs, which is needed to cause proliferation of mature lymphocytes, macrophages, and NK cells, extreme downregulation of IL-4 can result giving rise to autoimmune problems. Autoimmune diseases have often been linked to hypoactivity of T_H2 cells in producing basal quantities of IL-4, thus abolishing the regulation of the T_H1 response.[7]

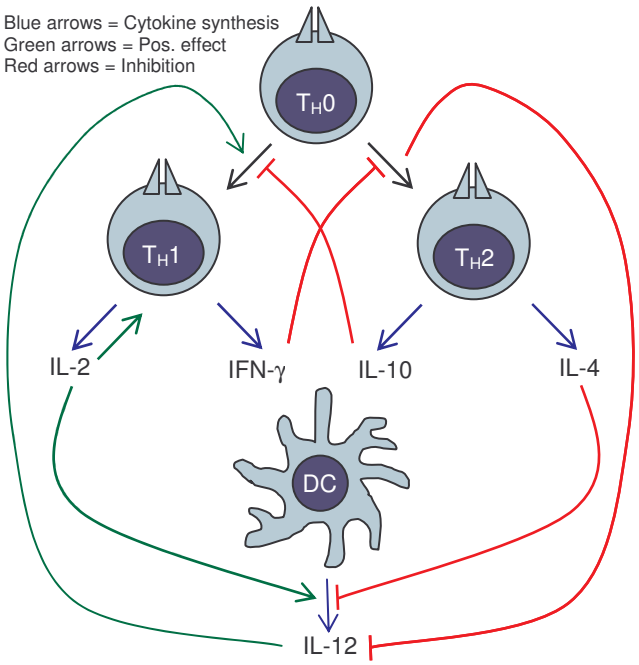

Figure 3.2. Cross-Regulation of T Helper Cell Activity.[1]

Autoimmune disease is the general systematic disorder characterized by cells of the immune system being unable to identify self antigens from foreign ones. This is often prevented in the thymus for T cells during the negative selection process where those cells that have too high an affinity for the MHC complex are instructed to undergo apoptosis. Although the origin of autoimmune disease is not clear, it is understood that T

cells often are responsible for destruction of host cells both directly and through T_H1 cytokine mediation. Therefore, autoimmune diseases are often caused by the lack of IL-4 cytokine production.[1] For example, in diabetes mellitus both T and B cells invade the islets responsible for insulin production but $CD4^+$ T cells also contribute through excessive release of the proinflammatory IFN-γ cytokine. In multiple sclerosis, T cells are directly responsible for destruction of the myelin sheath covering neuronal axons. In the animal model of multiple sclerosis, experimental autoimmune encephalomyelitis (EAE), it is found that the disease is mediated by T_H1 cells. Subjects with EAE display a lack of IL-4 with an abundance of TNF-α and IFN-γ.[8] When T_H1 cytokines are inhibited in mice with EAE and IL-4 is administered, the disease is ameliorated.

Natural killer T cells have a significant role in the balance of T_H1 and T_H2 immune responses. As with T helper cells, in a given NKT cell-mediated response IFN-γ can be emitted to activate T cells, macrophages, and natural killer cells and IL-4 for B cell recruitment. While both types of T_H cells are needed to release the full array of cytokines, it appears that single populations of NKT cells, like Vα14i, are capable of releasing significant amounts of both T_H1 and T_H2 signals.[9] Furthermore, in various studies on T_H-mediated disease states it has often been found that a lack of NKT cells exists.

Numerous studies have been performed on the classical Vα14i/Vα24i NKT cells and their role in antitumor immunity and proinflammatory T_H1 response. In $V\alpha14i^{-/-}$ mice there was a lack of suppression of lung and liver tumor growth even though IL-12 production was normal. However, in $V\alpha14i^{+/+}$ transgenic mice lacking the ability to make other lymphocytes these types of carcinomas were rejected, demonstrating that T,

B, and NK cells are not required for antitumor activity.[10] Additionally, when Vα14i cells are adopted into Vα14i$^{-/-}$ mice infected with B16 melanoma, an inhibition of hepatic metastasis is seen where it once was lacking.[11] Once IL-12-stimulation of NKT cells occurs, IFN-γ is produced prompting NK and CD8^{+} T cells to secrete perforin, a cytolytic protein that produces pores in the plasma membranes of target tumor cells. The IFN-γ also produced by NKT cells can directly inhibit tumor angiogenesis (Figure 3.3).[9] In several other cancer studies, it has been reported that human Vα24i NKT cells are often deficient along with a lack of IFN-γ production in patients with solid tumors or other cancerous growths.[12] This would suggest a correlation between advanced cancer and a lack of NKT cells.

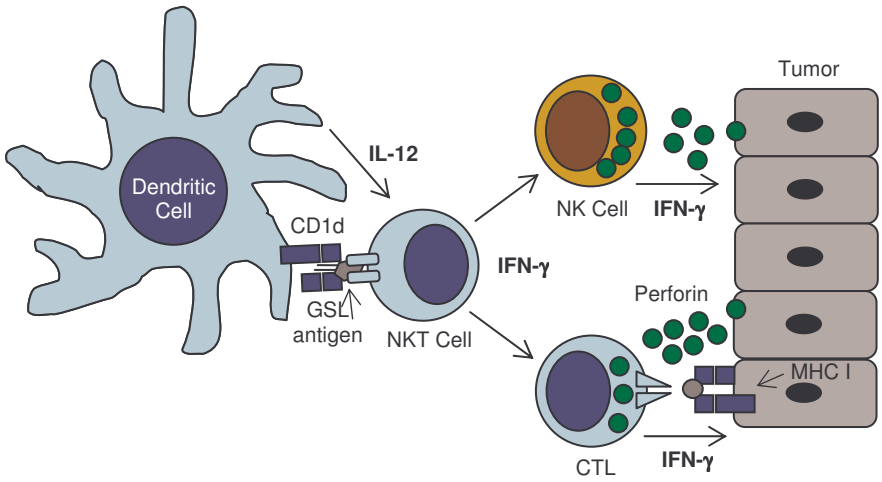

Figure 3.3. NKT Cell-mediated T_H1 Antitumor Response.[9]

In autoimmune diseases, NKT cells are often found lacking as well. Investigation into the role of NKT cells in type I diabetes suggests that their populations are severely decreased, as in subjects with advanced tumors. In non-obese diabetic (NOD) mice, which are easily susceptible to attain this disorder, NKT cells are lower in number than in healthy animals, IL-4 levels are decreased, and pancreatic islet β cell-autoreactive T cells accumulate. When Vα14i NKT cells are directly transplanted or introduced genetically to NOD mice, the disease is ameliorated through an increase of IL-4 and IL-10 and a

decrease in IFN-γ.[13] In humans, the same trend is seen. With twins or triplets, the populations of Vα24 cells and their ability to produce IL-4 were much lower in diabetics than in their healthy siblings.[14]

Because NKT cells are stimulated to proliferate and recruit other lymphocytes by glycosphingolipids, αGalCer is often used to gauge immune reactions in both T_H1- and T_H2-type responses. In initial biological studies of the agelasphin GSLs, αGalCer (**3-1**) was found to be effective at promoting cancer rejection, inhibiting metastasis of carcinomas,[15] and was used in a Phase I clinical trial against solid tumors (see Chapter 1, section 1.3.1.2).[12b] This antitumor behavior is accomplished through its ability to cause a sustained IFN-γ response when loaded onto DCs.[16] In animal models of autoimmunity disorders, αGalCer was found to delay the onset of type I diabetes in NOD mice by decreasing the T_H1-type response through an increase in the IL-4 cytokine,[17] and in a similar fashion was able to prevent EAE in susceptible mice due to creation of a T_H2 bias.[18]

A question raised from these findings is how can the same ligand produce a T_H1 and a T_H2 bias? It would make sense for a given compound to produce cytokines of one type or the other to bias the immune system toward one of the two responses, not to simultaneously produce the opposing reactions when used to ameliorate a disorder; especially so since one T_H response downregulates the other. Several ideas exist, such as the presence of NKT cells with a functionally distinct T_H-like property (subset model) or secondary factors (environmental model) that may dictate the T_H response (Figure 3.4).[14] Although αGalCer is a remarkable immunostimulatory glycolipid, further studies into exactly how it directs NKT cells toward one type of T_H response or the other is needed.

In an important investigation by Yamamura and coworkers, more information was gleaned about the overall stimulatory effects of αGalCer on biasing the T_H outcome.[19] This work differed from previous studies where αGalCer was used in repeated injections[20] or with an adjuvant[21] to sensitize the subject to its effects. The degree of T_H2 bias may have attributed to the resulting sensitization and not solely to the actual mechanism of the function of αGalCer. Additionally, some of these studies did not utilize knockout mice with cytokine-producing genes removed from their chromosomes to compare the overall effects of αGalCer when either IL-4 or IFN-γ could not be produced.[17,20,21] In this particular body of work, Yamamura claimed that with a single injection of αGalCer (100 μg/kg), wild-type B6 mice initially produced more IL-4 than IFN-γ and IL-12 combined (2 h after administration).[19] Over time there was a greater sustaining presence of IFN-γ than the other two signals (12-36 h). This translated into no delay of onset of EAE in B6 mice that had also been injected with myelin oligodendrocyte glycoprotein (MOG), an EAE-inducing antigen, nor did it improve the condition of these mice after EAE inducement. Due to the ratio of T_H1/T_H2 cytokines, any kind of T_H2 response would be

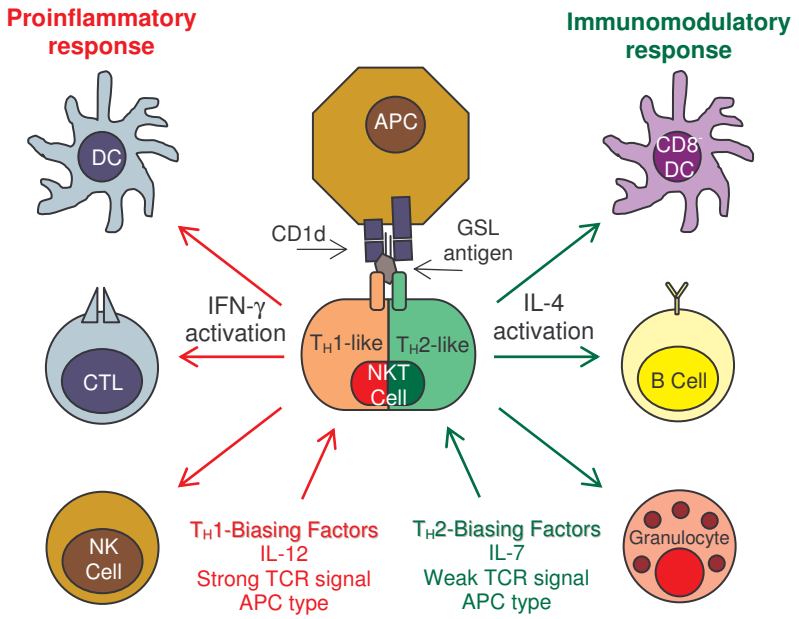

Figure 3.4. Environmental and Subset Models of NKT Cell T_H-Bias.[14]

downplayed, thus decreasing the opportunity for an autoimmunity problem to be ameliorated.

To verify the potential counteracting role of IFN-γ, IL-4 and IFN-γ, knockout mice were studied for cytokine release and EAE activity when αGalCer was injected in a single dose (100 μg/kg). In IL-4 knockout mice, the onset of EAE was not delayed (16 days after inoculation) and the mean disease score was higher than in wild-type B6 mice. In IFN-$\gamma^{-/-}$ mice, however, the disease onset was delayed two days later with EAE having a significantly lower effect. More significantly, it was found that the T_H0 phenotype in B6 mice could be steered towards either T_H1 or T_H2-type cells depending on murine antibody-blocking of costimulatory proteins from αGalCer-loaded antigen presenting cells. When the pro-T_H1 protein B7.2 was bound by anti-B7.2, IFN-γ production was inhibited and the effect of EAE was minimized. Conversely, blocking pro-T_H2 B7.1 protein upon αGalCer administration had the same effect as dosing with the GSL alone, demonstrating that αGalCer has a bias toward T_H1.[19] Thus, it is seen that αGalCer induces both significant quantities of IFN-γ and IL-4 cytokines, but in ratios that favor a T_H1 response overall.

To effectively utilize αGalCer or similar GSLs as therapeutic agents, it would be advantageous to eliminate the adversarial results of a T_H1 effect over the T_H2 counterpart that they cause. Due to the apparent T_H1 bias it produces, it would be desirable to use αGalCer in the treatment of disease in a proinflammatory pathway, being potentially more effective as an antitumor or anti-infectious agent.

To effect a GSL-mediated bias toward either a proinflammatory or immunomodulatory therapy, structure-activity work would need to be performed on

αGalCer derivatives to determine the vital features for skewing toward the desired outcome. Only minimal work had been done by chemists to make GSL analogs for T_H-type studies, though they suggest that alteration of the ceramide portion has an influence on T_H1/T_H2 ratios. The Kirin pharmaceutical group found that greater antitumor behavior was achieved with a tetracosanoyl chain or longer.[15] In another study, truncation of the phytosphingosine base of αGalCer caused an bias toward T_H2 in B6 mice.[22] When this same strain was induced towards EAE with the MOG protein, the cumulative clinical scores were half those of subjects injected instead with αGalCer or a PBS solution control, indicating a positive therapeutic affect. Although not as effective as causing proliferation of Vα14i NKT cells as αGalCer, the shortened glycosyl ceramide did not appear to be a weaker agonist of EAE nor did the T_H2 bias seem to be dose-dependent. At differing concentrations, both glycolipids maintained their same relative IL-4/IFN-γ ratios and therapeutic effects on EAE mice, respectively.[22]

These two publications have been enlightening as to structural features important for immunobiasing by CD1d-restricted GSLs. However, there have been no systematic studies on the effect of ceramide alteration toward a T_H bias. To examine this phenomenon, three analogs of αGalCer with shortened phytosphingosine bases (**3-2a–c**) and three with shortened acyl chains (**3-3a–c**) were synthesized using an efficient synthetic method. Their ability to load CD1d tetramers was gauged and their cytokine release profiles were measured.[23] An additional GSL (**3-4**) was made with mammalian sphingosine and a truncated acyl group for immunological comparison to **3-3b** (Figure 3.5).

3.2 Results and Discussion

Unlike **3-1** or the *N*-appended 6"-amino-α-galactosylceramides discussed in Chapter 2, compounds **3-2** could not be created using phytosphingosine due to their shortened alkyl chain lengths. These unnatural sphingoids are also not commercially available. Most published syntheses of phytosphingosine, including many of those that were performed in past decades, use saccharides as chiral building blocks.[24] Morita et al. describes the use of semiprotected galactose that can undergo oxidative cleavage of the anomeric carbon and azide-mediated inversion of the galactosyl C4 stereocenter to provide the natural phytosphingosyl geometry.[15] More recently diacetonidylmannose[25] and protected lyxose[26] have been used with S_N2 azide inversion to install the required nitrogen with the proper (2*S*) configuration. These syntheses use inexpensive starting materials, yet they suffer from multiple protection/deprotection steps and are dependent on nitrogen fixation and saturation of the alkene that results from Wittig installation of the alkyl tail, which must be added early in the reaction scheme. These pathways also have typically low overall yields (<10%).

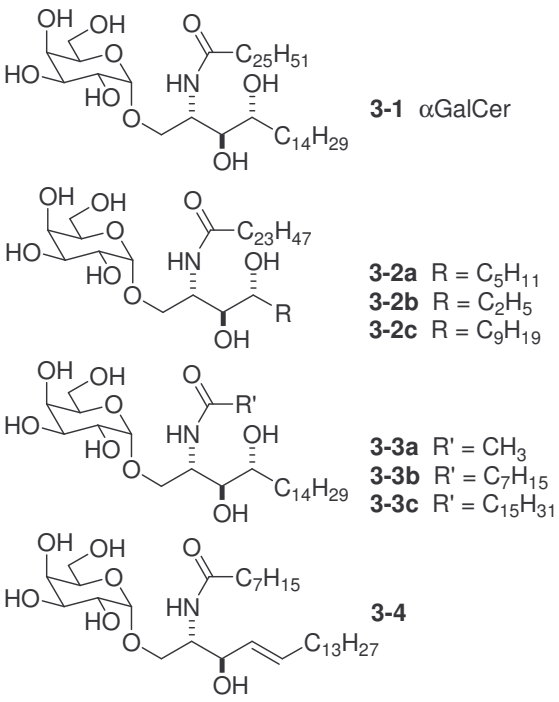

Figure 3.5. αGalCer and Truncated Analogs.

A protocol published by Berova and coworkers described an alternate source of chirality to make phytosphingosine: L-serine. By using this readily-available compound,

they were able to make phytosphingosine in seven steps on a multigram scale with a 34% overall yield.[27] The divergent nature of the protocol also made this pathway attractive as an intermediate-stage compound, Garner's aldehyde (**3-5**),[28] could be used to make the three shortened sphingoids without noticeable racemization of the constrained stereocenter. Phytosphingosine was also made in this manner due to its high commercial cost at the time ($530/g, Avanti Polar Lipids, Inc.).

Using an improved method, Garner's aldehyde was made from L-serine in four steps with an overall 88% yield requiring only one purification by silica gel.[29] The alkyl tail was installed using Wittig chemistry between **3-5** and the proper alkyltriphenylphosphonium bromide salts (Scheme 3.1). Use of an unstabilized ylide at -78°C gave predominantly the *Z*-alkene (95:5 *Z*:*E*), which could be separated using chromatographic methods. The yield in the Wittig step was typically low (44-63%) due to the inability to fully react **3-5** in this step. It was universally encountered that a significant amount of aldehyde went unused (17%), even when the reaction was allowed to continue for prolonged periods (>12 h). Attempts were made to improve this yield by

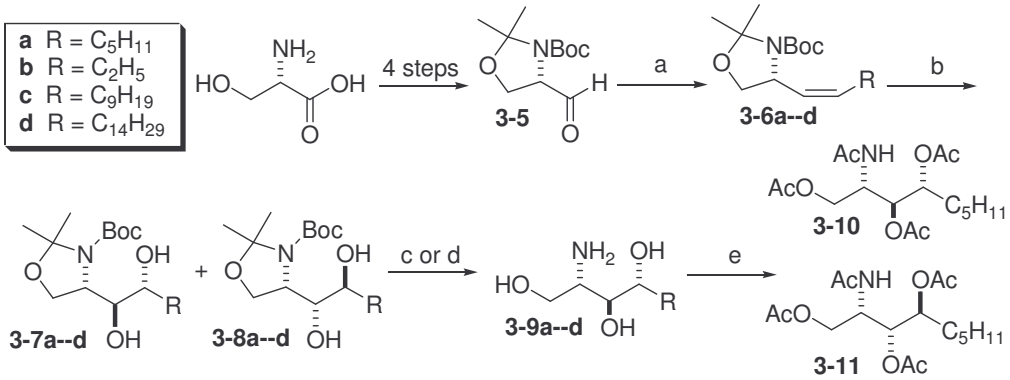

Reagents and conditions: a) *n*BuLi, Ph_3BrPCH_2R, THF, -78°C (44-63%); b) OsO_4 (aq., 2 mol%), NMO, 1:1 *t*BuOH:H_2O, 0°C (61-66% α, 22-32% β); c) HCl (g), THF; d) 20:1 TFA:H_2O; e) Ac_2O, DMAP, pyridine.

Scheme 3.1. Synthesis of Phytosphingosine Bases **3-9**.

minimizing the amount of water that the aldehyde contained (e.g., coevaporation with toluene, storage over activated molecular sieves) but this apparently did not have an effect on the reaction. Aldehyde **3-5** could be recovered, purified, and reused, however.

The hydroxyl groups at C3 and C4 were installed stereoselectively using Upjohn dihydroxylation conditions (i.e., catalytic aqueous OsO_4 solution, excess NMO).[30] Typically, only 2 mol% of OsO_4 needed to be used for full conversion of alkene to diol. Substrate control using the C2 stereocenter was found to be fairly effective at delivering the osmate reagent to the desired alkenyl face (appx. 2:1 **3-7**:**3-8**). Interestingly, the original procedure described the use of AD-mix-β as the hydroxyl source, which provided a 1:1 ratio of diastereomers.[27] When this was tried, the diol products were not produced. It is possible that trace amounts of triphenylphosphine oxide, a byproduct generated from the Wittig reaction, were carried over with the alkene and fouled the 0.2% quantity of $K_2OsO_2(OH)_4$ reagent used to generate active OsO_4.

The two diastereomers could be completely separated using silica gel column chromatography (TLC, 1:3 EtOAc:Hex, $R_{f\ 3\text{-}7}$ = 0.24, $R_{f\ 3\text{-}8}$ = 0.35), though with prolonged elution times. When eluent was allowed to gravity drip through the column, two visible bands from colored contaminants were fully resolved. Elution of the desired compound could occur with full purity after the second band was fully removed when proceeding at this pace.

The shortened sphingoids (**3-7a–c**) and **3-7d** were deprotected by dissolving them in anhydrous THF and bubbling in hydrogen chloride gas for a few minutes followed by removal of the solvent to yield the amines as colorless syrups. This was usually done in situ before coupling with an acyl group, but for prolonged storage times the preferred

method was using a 20:1 TFA:H_2O solution followed by coevaporation with toluene. Shorter chained **3-7a** and **3-7b** were formed as semisolids while the C13 and C18 compounds were white powders, which could also be purified by $NaHCO_3$ neutralization, filtration, and lyophilization.

To identify the diol with the desired stereochemistry, diastereomers **3-7a** and **3-8a** were deprotected and peracetylated using acetic anhydride and DMAP. ^{1}H NMR comparison of the signals from protons H1 through H4 of **3-10** and **3-11** with a peracetylated sample of natural phytosphingosine confirmed that the major compound from dihydroxylation had the desired stereochemistry.

Phytosphingosines **3-9a–c** were coupled with tetracosanoic acid using NHS/DCC conditions, though the resulting yields were lower than desirable (37-39%). This was due to the amphiphilic nature of the unprotected ceramides, which could not be isolated without triacetylation (**3-12a–c**). This was also the case for coupling phytosphingosine (**3-9d**) to octanoic (**3-12f**), hexadecanoic (**3-12g**), and hexacosanoic acids (**3-12d**; 41-43%). Peracetylation of phytosphingosine (**3-12e**) did proceed at a much higher yield (88%), though this is likely due to the difference in reaction conditions (Scheme 3.2).

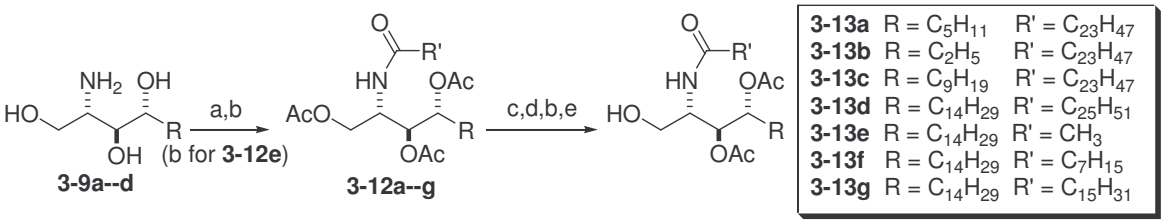

3-13a	R = C_5H_{11}	R' = $C_{23}H_{47}$
3-13b	R = C_2H_5	R' = $C_{23}H_{47}$
3-13c	R = C_9H_{19}	R' = $C_{23}H_{47}$
3-13d	R = $C_{14}H_{29}$	R' = $C_{25}H_{51}$
3-13e	R = $C_{14}H_{29}$	R' = CH_3
3-13f	R = $C_{14}H_{29}$	R' = C_7H_{15}
3-13g	R = $C_{14}H_{29}$	R' = $C_{15}H_{31}$

Reagents and conditions: a) R'CO_2H, DCC, NHS, Et_3N, THF; b) Ac_2O, DMAP, Et_3N, THF (45-88% from **3-7**); c) NaOMe, MeOH; d) TBSCl, imidazole, THF, 60°C; e) HF (aq.), THF (50-59% from **3-12**).

Scheme 3.2. Synthesis of Ceramide Acceptors **3-13**.

After purification, the triacetoxyceramides were prepared for coupling to a saccharide donor by complete deacetylation with sodium methoxide in methanol. Instead of using the previously described di-*O*-TBS analog (**2-16**; see section 2.2) to make ceramides **3-13**, a less-bulky version was sought. It was thought that due to the size of the tert-butydimethylsilyl group, coupling with the glycosyl donor may have been negatively affected reducing the anticipated yield. Instead, a smaller protecting group at C3 and C4 was installed. This was accomplished by selectively silylating the primary alcohol with TBSCl in imidazole then diacetylation of the secondary alcohols with Ac_2O and DMAP. Removal of the silyl ether was rapidly achieved in aqueous HF/THF solution.

During the workup and purification steps it was found that migration of the acetyl group at O3 to O1 in **3-13** occurred readily when either the acid was not fully neutralized by aqueous $NaHCO_3$ or there was incomplete drying of the organic solution (Scheme 3.3). In either of these two cases the migrated product **3-14** was invariably attained as the major compound, requiring another sequence of protection/deprotection steps.

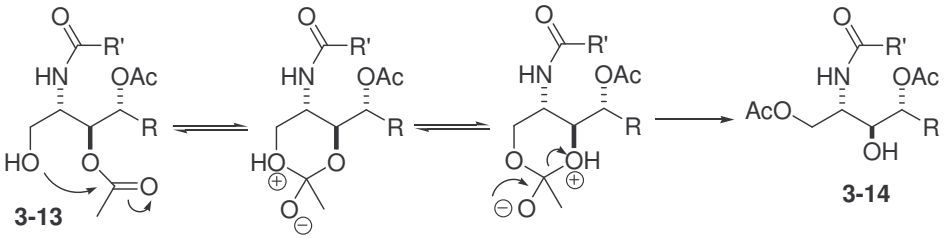

Scheme 3.3. 1,3-Acetyl Migration in Di-*O*-Acetylceramides.

Galactosyl bromide **3-15** was used as the donor to bind with these seven ceramides (**3-13a–g**).[23] Use of this donor over perbenzylated sugars was desirable due to a step-wise deprotection plan that was anticipated to aid in purification of the final compound. Coupling using an altered Koenigs-Knorr method with silver (I) triflate[31] gave

predominantly the desired α-anomers (**3-16a-g**; 3-4:1 α:β) with decent yields (62-75%) when the reaction was performed on a 100 mg scale or larger. Separation of the anomeric mixture was difficult but possible using column chromatography (TLC, EtOAc:Hex 1:2, $R_{f\,\alpha} = 0.38$, $R_{f\,\beta} = 0.23$). After debenzylation with palladium on carbon under H_2, α-anomers **3-17a–g** were more easily separable from their β-counterparts, however (Scheme 3.4).

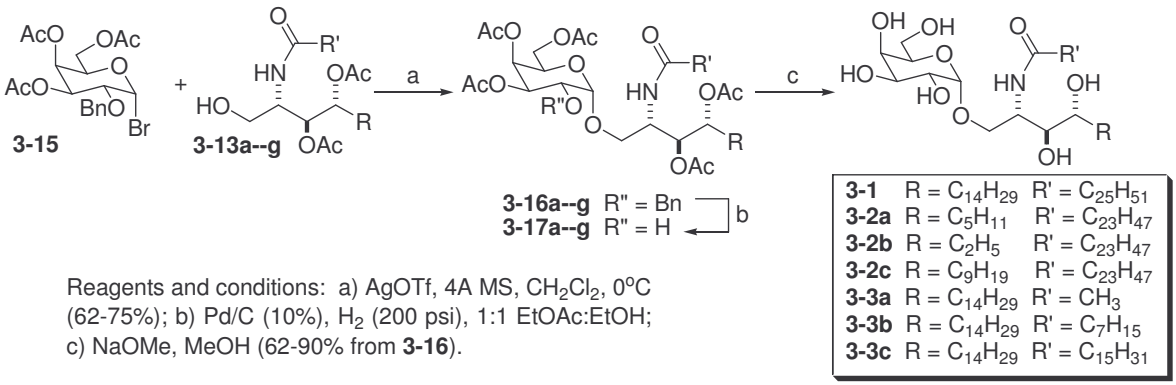

Reagents and conditions: a) AgOTf, 4A MS, CH_2Cl_2, 0°C (62-75%); b) Pd/C (10%), H_2 (200 psi), 1:1 EtOAc:EtOH; c) NaOMe, MeOH (62-90% from **3-16**).

Scheme 3.4. Galactosylation and Deprotection of GSL Antigens **3-1--3-3**.

Final deprotection of the GSLs was performed with NaOMe in MeOH. With longer chain compounds **3-17a,c,d,g**, removal of the acetates promoted insolubility and the compounds were precipitated from methanol, which was aided by small amounts of water. This convenient event often allowed for isolation by centrifugation, removal of supernatant, and rinsing with clean methanol. Those glycosphingolipids with a shorter alkyl chain (**3-17b,e,f**) often did not precipitate, necessitating silica gel purification. Comparison of NMR spectra of compound isolated by both processes did not show a difference in purity.

Sphingosine-containing compound **3-4** was made in a similar fashion to the phytosphingosine GSLs. Sphingosine (**3-18**), made in two steps from Garner's

aldehyde,[32] was acylated selectively at the amine using octanoic anhydride. Due to its greater lipophilic character, ceramide **3-19** did not require acetylation for purification. After a similar protection/deprotection scheme used for ceramides **3-13**, acceptor **3-20** was coupled to galactosyl donor **3-15** with an increased selectivity towards the α-anomer (6:1 α:β) than **3-16**. Due to the *E*-alkene, deprotection was performed without hydrogenation in one step with reducing metal conditions (e.g, sodium metal in liquid ammonia), which required column chromatography for purification (Scheme 3.5).

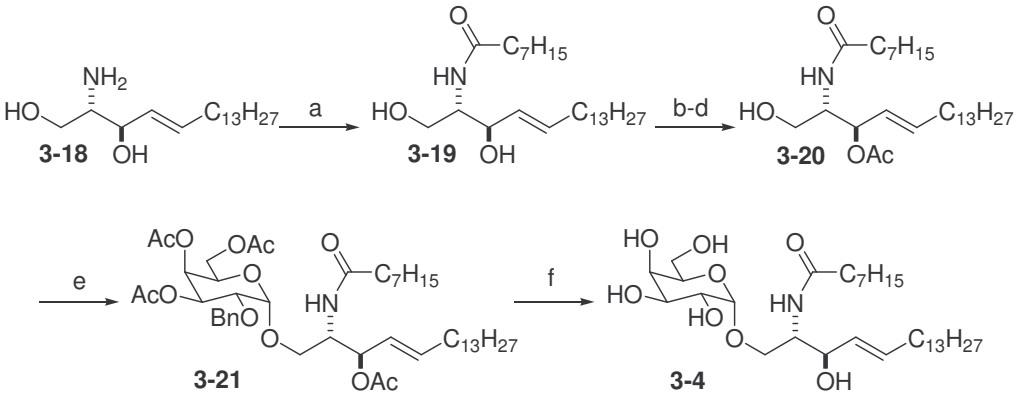

Reagents and conditions: a) $(C_7H_{15}CO)_2O$, Et_3N, THF, reflux (97%); b) TBSCl, imidazole, THF, 60°C; c) Ac_2O, DMAP, Et_3N, THF; d) HF (aq.), THF (58% from **3-19**); e) **3-15**, AgOTf, 4A MS, CH_2Cl_2, 0°C (70%); f) Na°, NH_3, THF, -78°C (53%).

Scheme 3.5. Preparation of Unsaturated GSL **3-4**.

Before cytokine release profiles on **3-2** and **3-3** were performed to gauge their potential T_H1/T_H2 bias, measurement of binding between these GSL ligands and CD1d were taken. To effectively interpret the results from a cytokine profile, it is desirable to understand to what degree the antigens are binding to their APC receptors. This was performed in vitro according to a procedure developed by Bendelac and coworkers where ligands were dissolved in an aqueous PBS solution with detergent (Tween 20), DMSO, and biotinylated mCD1d.[33] After incubation at 37°C for 4 h and dialysis purification,

fluorophore-appended streptavidin was added to bind the loaded CD1d into tetramers (Figure 3.6). The GSL-CD1d tetramers were analyzed for association with two different NKT cell hybridomas, one expressing TCRs (solid line) and a control without TCRs (dashed line). Those CD1d proteins complexed with GSL were able to fluorescently stain plate-immobilized NKT cells and be identified (labeled M1 in Figure 3.6) using the tetramer's fluorophore as a differentiating marker by flow cytometry. Only acetamidyl GSL **3-3a** did not display any loading onto mCD1d, though αGalCer was bound with a smaller frequency than the other CD1d-associated GSL.[23]

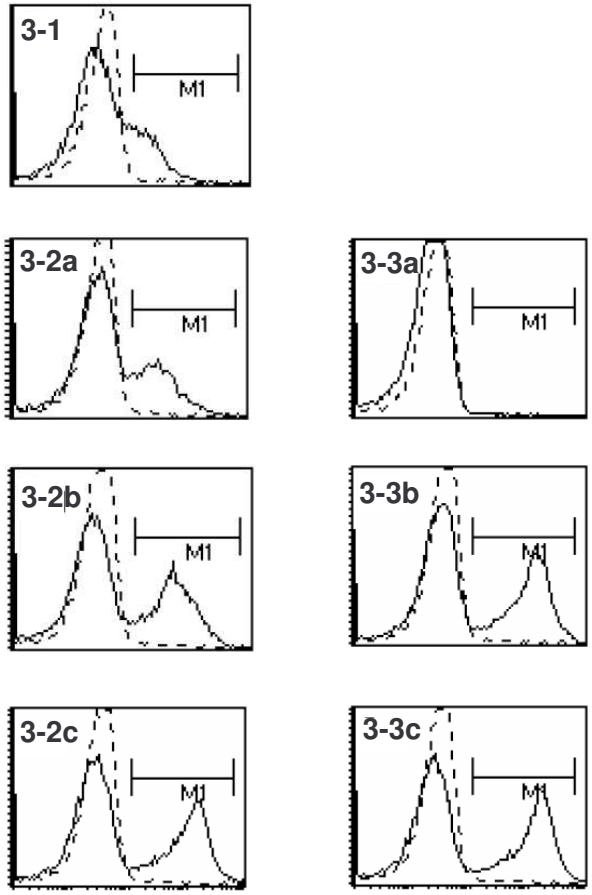

Figure 3.6. Flow Cytometric Analysis of CD1d-Restricted GSLs **3-1–3-3** Bound to NKT Cells.[23]

These truncated GSLs were then measured for their ability to cause IL-4 and IFN-γ release by NKT cells. Spleen cells from B6 and BALB/C mice strains were used due to their relatively high concentrations of NKT cells and APCs. GSLs **3-1–3-3** were added in vitro at a concentration of 100 ng/mL and allowed to associate for 60 h in a 96 well plate. Cytokine measurement using ELISA and calculation of the ratio of secreted IL-4 to IFN-γ indicate a trend that shortening of either alkyl chain of the ceramide results in a greater ratio of T_H2/T_H1 cytokines (Figure 3.7A). The lone exception is **3-3a**, which

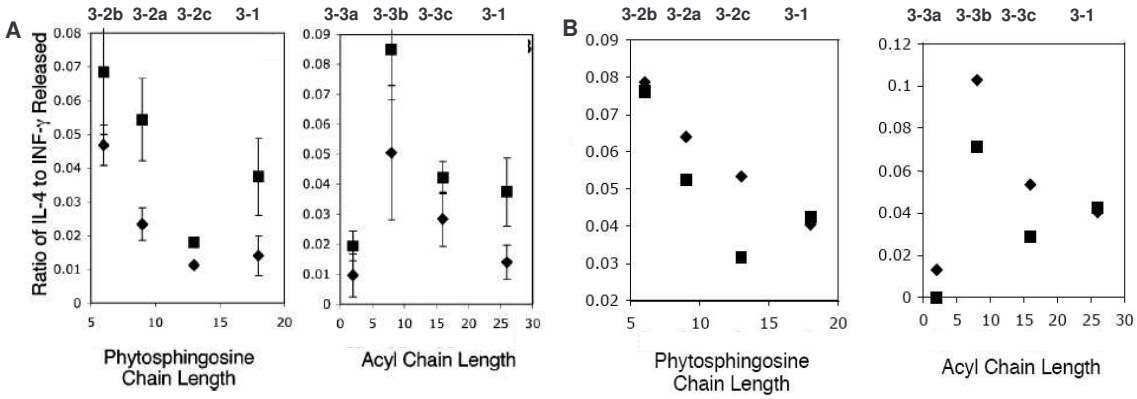

Figure 3.7. Cytokine Release Profiles of **3-1–3-3** Using Murine Spleen Cells.
A. B6 (♦) and BALB/C (■).[23]
B. B6 at 10 ng/mL(■) and 100 ng/mL (♦).[23]

was not loaded onto tetramers like the other compounds. It was not as effective at promoting an immune response in mice. Concentration-dependence was evaluated using spleens from B6 mice at 10 and 100 ng/mL of GSL. Again, the same trend was seen with a greater relative amount of IL-4 released in NKT cells except for **3-3a** (Figure 3.7B).

To verify if this was a species-dependent event, human NKT cell clones from peripheral blood lymphocytes (PBLs) were also exposed at the same concentration of GSL. The same tendency was found, although it appears that **3-3a** was able to be loaded onto human CD1d due to its resulting stimulatory activity (Figure 3.8).[23]

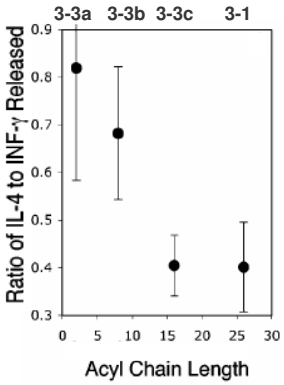

Figure 3.8. Cytokine Release Profiles of **3-1** & **3-3** on Human PBL NKT Cells.[23]

GSL **3-3b** and its sphingosine-containing counterpart **3-4** were used in the same assay with B6 mouse spleen cells to compare their cytokine release profiles. The only difference in the two GSLs is the sphingoid base, which has a deleted C4 hydroxyl group and C4-C5 *E*-alkene in **3-3b**. Both compounds stimulated IL-4 and IFN-γ secretion to

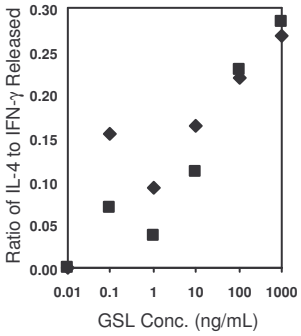

Figure 3.9. Comparison of T_H Biasing Between GSL Analogs **3-3b** (♦) and **3-4** (■) Using Murine B6 Spleen Cells.

similar ratios at different concentrations, respectively, yet **3-4** caused a release of IFN-γ slightly greater than that of **3-3b** at lower concentrations (0.1-10 ng/mL) that translated to a decreased IL-4 ratio (Figure 3.9). Therefore, it is possible that at least in acyl-shortened GSLs the type of sphingoid base may have an impact on overall stimulation or the resulting T_H response.

Compounds **3-1**, **3-2a**, and **3-3b** were further evaluated for their ability in making and maintaining a stable binding partnership with CD1d.[34] As was seen in the binding assay with the six truncated GSLs,[23] an aliquot of tetrameric CD1d-**3-3b** stained a murine DN32.D3 and equivalent human NKT cell hybridoma with greater fluorescent intensity than αGalCer and maintained a stable ternary association for 240 m (Figure 3.10). **3-3b** is also much more soluble in aqueous solutions than **3-2a** and αGalCer, and did not require detergent or sonication. Enhanced solubility translated into a greater degree of CD1d loading as measured by isoelectric focusing and a quicker 'on rate' in which **3-3b** was able to cause a maximal amount of NKT cell activation (8 h) much sooner than αGalCer (24 h; Figure 3.11A).[34] The 'off rate,' or measure of GSL-CD1d complex stability, was equivalent to that of αGalCer by virtue of NKT cell stimulatory activity up to the measured maximum

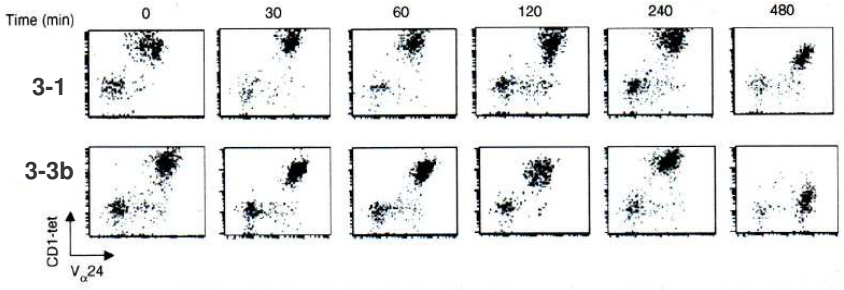

Figure 3.10. CD1d Binding Stability of **3-3b** vs. **3-1**.[34]

of 24 h (Figure 3.11B). A thermal denaturation experiment demonstrated that both CD1d-αGalCer and CD1d-**3-2a** complexes, as measured by circular dichroism, were able to maintain integrity at elevated temperatures, though **3-3b** was found to shift the curve 5°C higher, suggesting that it is able to form a more stable complex with CD1d (Figure 3.11C).

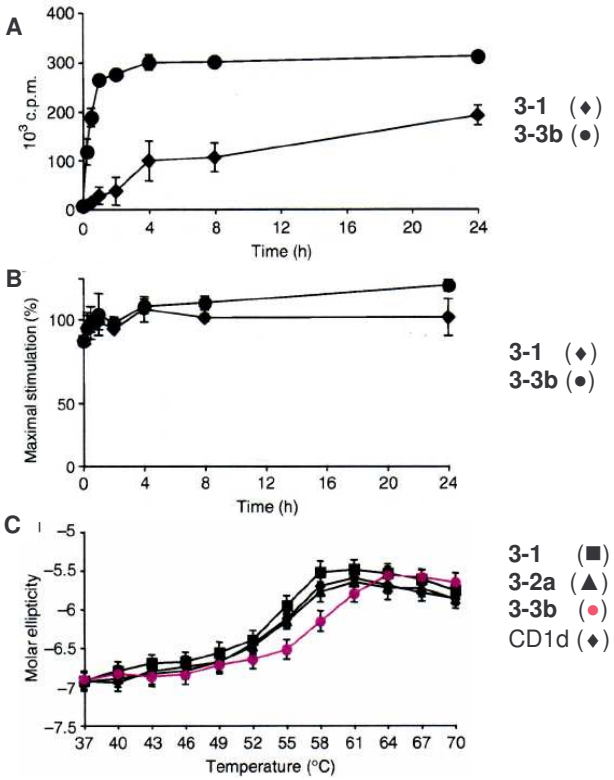

Figure 3.11. **A**. Rate of GSL Association with CD1d.[34]
B. Stability and NKT Cell-Stimulatory Effects of CD1d-GSL Complexes.[34]
C. Thermal Stability of CD1d-GSL Complexes.[34]

Recently, three different research groups were able to successfully produce X-ray crystal structures of CD1d complexed with **3-3b** (PBS-25),[34] αGalCer,[35] or an α-galacuronoside with a C18 sphinganine base and myristic acid ceramide (**3-22**; Figure 3.12).[36] These studies have aided in understanding how the general GSL-CD1d interaction affects antigenic activity with NKT cells.

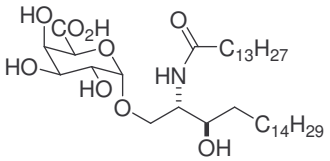

Figure 3.12. Galacturonoside **3.22**.[36]

From the association of **3-3b** with CD1d, it can be seen that GSLs interact in a fashion differently than previously believed,[37] where the acyl chain is inserted into the A'

pocket and the sphingoid into the F', instead of the opposite way (Figure 3.13). Near the polar end of the molecule the chains are oriented perpendicular to the β-sheet that forms the floor of the binding groove with the ends turning outward to either end of the side of the protein (Figure 3.14). Van der Waal stabilization is seen between lipophilic residues lining the groove (e.g., Tyr73, Phe77, Trp133) and the alkyl chains for a total of 67 contacts. The phytosphingosine base fully occupies the F' channel, which appears to be able to accept a maximum chain length of 18 carbons.[35]

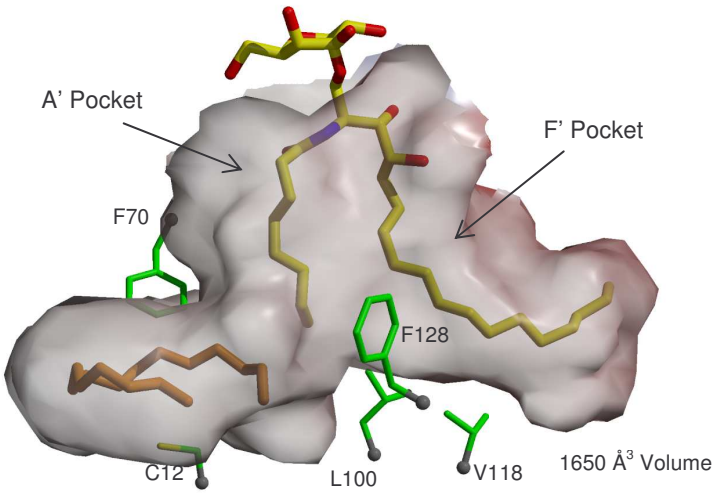

Figure 3.13. Orientation of **3-3b** in the Binding Space of mCD1d.[34]

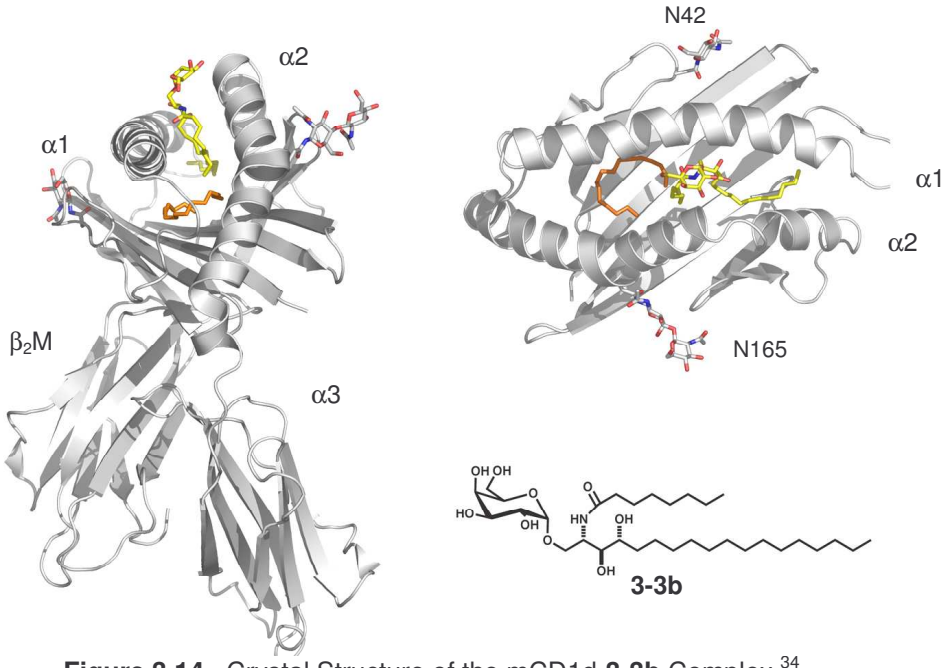

Figure 3.14. Crystal Structure of the mCD1d-**3-3b** Complex.[34]

The acyl group shares the A' channel with a lipid compound of 16 carbons, a spacer that possibly stabilizes the pocket in the absence of a longer acyl chain, like that found in αGalCer (Figure 3.15). The presence of such a compound was alluded to in the original

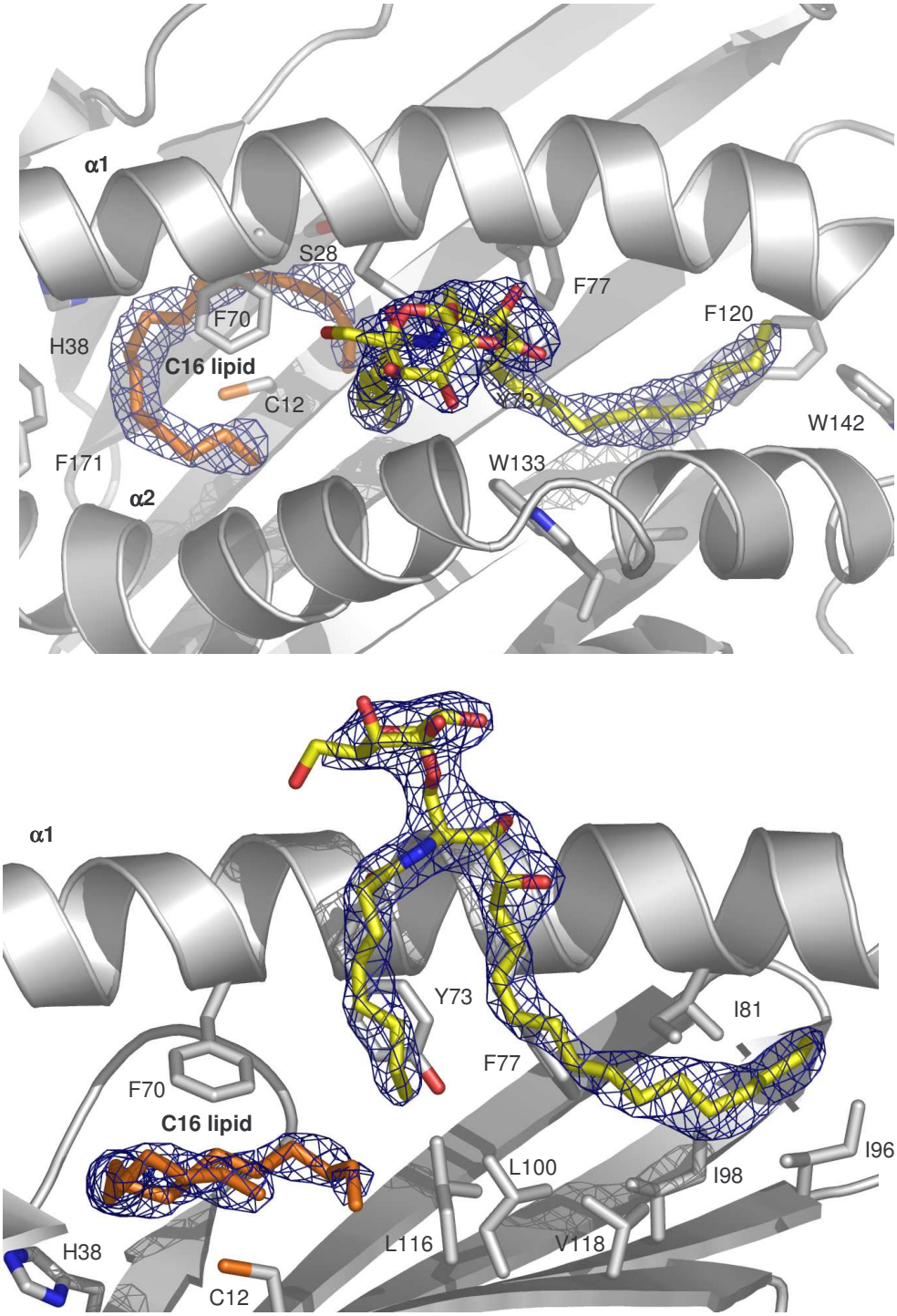

Figure 3.15. Top (upper) and Side (lower) Views of **3-3b** and Spacer Ligand in CD1d.[34]

crystal structure of mCD1d.[38] A different mCD1d crystal structure with tetradecanamide GSL **3-22** had a spacer compound with the same length. Methanolysis of the complex and GC/MS isolation determined that this spacer is likely palmitic acid, a ubiquitous component of eukaryotic cellular membranes.[36] Interestingly, the distance between **3-3b** and the C16 lipid is the right length for an ethylene group to be inserted, connecting the two halves and giving a 26-carbon chain, the length of the acyl group in αGalCer.

The polar head moiety of **3-3b**, comprised of the saccharide and the hydroxylated and amide groups of the ceramide, forms seven hydrogen bonds with CD1d. Galactose is stabilized through hydrogen bonding between the O2" and O3" groups with Asp153 and the anomeric oxygen with Thr156, allowing the O4" and O6"hydroxyls to be oriented towards the outside of the binding pocket (Figure 3.16). The ceramide is involved with interactions between the amide nitrogen and Thr156, O3 with Arg79 and Asp80, and O4

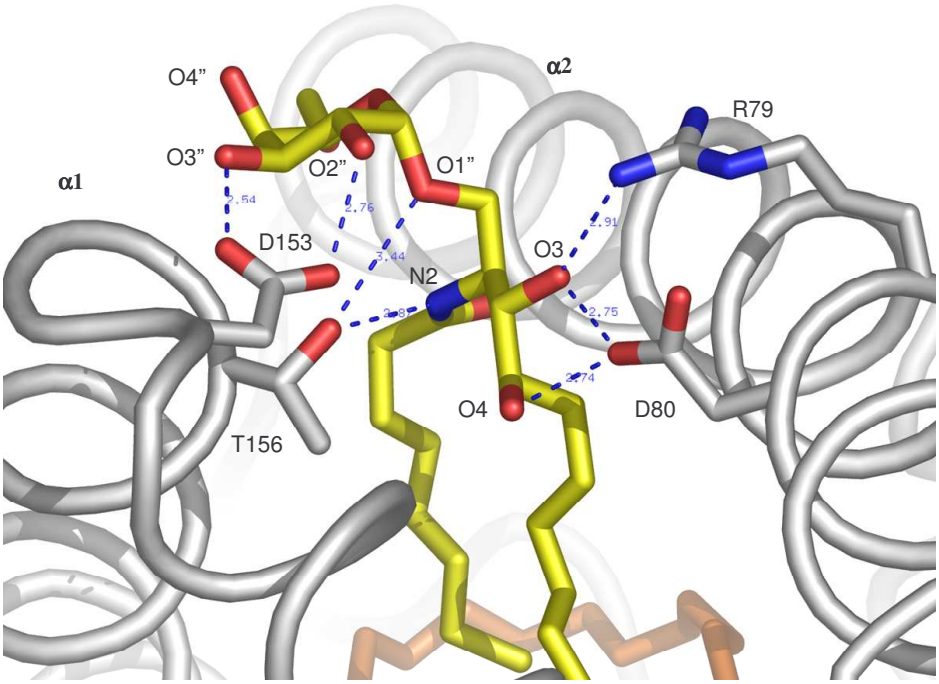

Figure 3.16. Hydrogen Bonding Interactions between the Polar Head Group of **3-3b** and CD1d.[34]

also with Asp80.[34] Modeling with the mannosyl derivative of **3-3b** shows hydrogen bonding is unavailable at O2"with the axial oxygen being oriented outside the pocket. Also, when modeled ceramide hydroxyls are deleted, destabilization of the association occurs.

This appears to be the case with **3-22** (green, in Figure 3.17), which lacks the O4 hydroxide radical.[36] The antigen is oriented slightly differently than **3-3b** (orange), presumably due to decreased hydrogen bonding to Asp80 (yellow with **3-3b**, gray with **3-22**) by the ceramide. Arg79 is unable to reach the O3 oxygen for further stabilization, thus the saccharide is pulled more into the binding groove than **3-3b**, which sits outside the protein.

Nonantigenic βGalCer also shows a diminished capacity for hydrogen bonding with CD1d, losing two interactions with Asp153. When modeled instead with mammalian

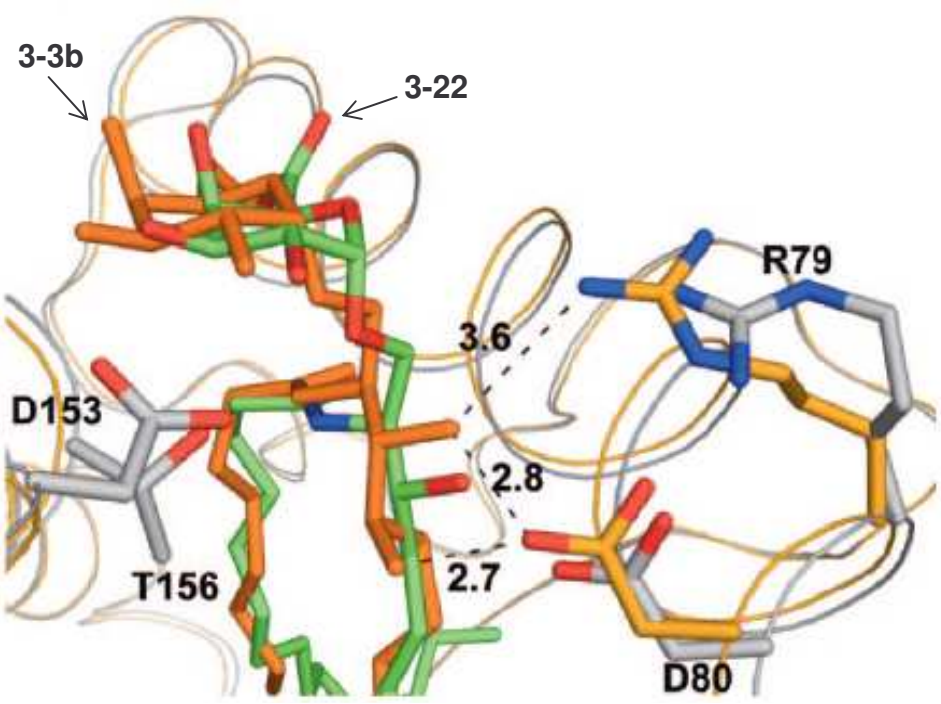

Figure 3.17. Modeling comparison of **3-3b** with CD1d-bound **3-22** CD1d.[36]

sulfatide, the 3”-sulfosphingosinyl analog of βGalCer, a potential hydrogen bond is added back in between the sulfate group and Arg79,[34] explaining how this endogenous compound could possibly be antigenic to NKT cells when bound by CD1d.

The simplest conclusion that can be drawn from these data (i.e., cytokine release profiles and ligand-protein structures) is that truncation of the ceramide causes a difference in binding between ligand and CD1d and that the altered orientation of the ligand is identified differently by the TCR, causing a relative change in the ratios of released cytokines. It is more likely that the differentiation in T_H bias is due to other factors.

According to Oki et al., shortening of phytosphingosine in a GSL antigen (**3-2a**) causes a two-fold effect.[39] First, binding of CD1d-**3-2a** to murine NKT cells caused an initial upregulation of IL-4 transcription gene (1.5 h) that was eventually eclipsed by activation of the IFN-γ gene (6 h). Second, **3-2a** forms a complex that is less stable with CD1d than αGalCer and dissociates quicker. Due to the shorter half-life of **3-2a**, the amount of IFN-γ that could have potentially been released by NKT cells is diminished, thus augmenting a T_H2 response. This claim is based solely on the measurement of calcium influx of proliferating NKT cells, however, and appears to be contrary to the thermal denaturation assay that found comparable stabilities of CD1d-**3-2a** and CD1d-αGalCer.[34]

It is possible that the differing T_H responses are due to presentation to multiple subpopulations of NKT cells. CD1d-tetramers loaded with αGalCer were able to isolate two distinct subsets of Vα24 NKT cells from human PBLs, one that contains the T cell receptor assistant CD4 protein and another that lacks both CD4 and CD8 ($CD4^-CD8^-$

double negative [DN]). Both of these types have greatly different cytokine release profiles. While they are mutually able to produce TNF-α and IFN-γ T_H1 cytokines, only the $CD4^+$ phenotype could generate IL-4 and IL-13 to yield a T_H2 response.[40] This may explain why a ligand, such as αGalCer, is able to produce a dual response in antitumor and antiautoimmune disorder models. It has not been established, however, whether either of these two types have a greater affinity for antigen-loaded CD1d or if one population is expressed in greater numbers than another, which could help explain T_H biasing further. However, this phenomenon is not present in murine Vα14 $CD4^+$ and DN cells, which can both express IL-4 and IFN-γ.

A third possibility may be presentation of antigen through another type of APC, B cells. It has been established that besides dendritic cells, macrophages, and hepatocytes, B cells also express CD1d and can bind glycolipid antigen. In fact, a subset of B cells, the splenic marginal zone B cell, expresses CD1d with a greater frequency than the potent DC.[41] Research by Joyce and coworkers indicate that presentation of αGalCer to Vα14i NKT cells by CD1d-associated B cells results in poor overall stimulation with a release of only T_H2 cytokines and suppression of DC-mediated immunity, while DC-restriction of antigen causes a robust release of both T_H types.[42] In a DC-deficient mice strain, $hDTR^{tg}$, production of cytokines was severely diminished when αGalCer was administered; IL-4 levels were decreased by 50% than levels in B6 mice and IFN-γ secretion was not detected. Conversely, in B cell-deficient μMT mice, the levels of IL-4 and IL-2 were elevated 3 to 5 times greater of those in wild-type B6 individuals with normal levels of IFN-γ. They also found evidence that macrophages and hepatocytes were incapable of presenting αGalCer to Vα14i cells in vivo, leaving DCs and B cells as

the two known modes of GSL delivery to NKT cells. One of the most interesting findings is that NOD mice had difficulty presenting αGalCer via DCs, yet B cells that were able to do so elicited levels of IL-4 enough to prevent type I diabetes.[42]

While these data have provided more insight about the structure-activity relationship between GSLs and immune response, the mechanism of T_H bias by NKT cells remains unclear. It has been shown unequivocally in in vitro models that truncation of either portion of the ceramide in GSL antigens causes a T_H2 bias and in αGalCer-like compounds (i.e., those GSLs with longer acyl chains) a proinflammatory skewing of cytokines appears to be favored.[23] In light of these findings, it is possible that truncated GSLs like **3-2a** and **3-3b** may be preferentially presented by B cells to the NKT cell receptor, while the more "traditional" glycosylceramides are associated with dendritic cells. It is possible that administration of chain-shortened GSLs preloaded onto B cells may serve as a therapeutic agent in autoimmune disorders by causing an elevation of the T_H2 response. On the other hand, a T_H1 reaction may be heightened through B cell suppression, causing greater proinflammatory action against infection and tumorous growths.

3.3 Conclusions

Understanding the nature of T helper cell-type responses by natural killer T cells has been difficult due to the lack of structure-activity relationship studies on glycosphingolipid antigens. Cytokine release profiles by αGalCer have shown conflicting responses can occur in proinflammatory and immunomodulatory therapies and concern exists over its use as a therapeutic agent due to regimens that have been established arbitrarily.[43]

To better understand these elusive SAR features in GSL antigens, a series of α-galactosylceramides have been synthesized with ceramides systematically shortened in either the phytosphingosine base (**3-2**) or acyl chain (**3-3**).[23] The use of the chiral building block Garner's aldehyde (**3-5**) allowed for a divergence to the four sphingoids at an intermediate stage rather than early in the reaction sequence, which would have been necessary using a saccharide-based starting material. This aldehyde also eliminated the need for a lengthy protection-deprotection strategy that is required when making sphingoids via a carbohydrate. Compounds **3-2** and **3-3** were made in twelve steps from the intermediate **3-5** requiring typically only six chromatographic separations with an average overall yield of 5-10%. The reaction scheme has been easily scaled up to produce these glycolipids in relatively large quantities (500 mg), though production of only a few milligrams is acceptable due to their potencies as NKT cell agonists at nanogram amounts.

It has been demonstrated through this in vitro study that using these truncated GSLs can cause a bias of secreted IL-4 over IFN-γ in CD1d-restricted NKT cells that is strain-independent, species-independent, and concentration-independent. Alteration of the long chain base from phytosphingosine to sphingosine in **3-4** caused a slight decrease in IFN-γ production at lower nanogram quantities, thus potentially skewing the T_H response profile but not likely enough to be clinically significant. Synthesis of other sphingosine analogs of **3-2** and **3-3** may establish if there is a noteworthy SAR on cytokine release profiles due to this structural change.

Compound **3-3b** also provides stable complexes with CD1d and the ternary CD1d-antigen-TCR association. Its use has aided in attaining a ligand-bound crystal structure

of CD1d, demonstrating how GSLs bind to this protein and verifying the stabilization provided by hydrogen bonding of the polar head group to hydrophilic amino acid residues.

Though the exact mechanism of GSL-mediated biasing of NKT cell response has not been identified, future work with truncated glycosylceramides is needed to understand how they cause differentiating immune responses. They are the only known compounds of this class able to consistently produce an immodulatory response that may be beneficial in treating autoimmune disorders, such as type I diabetes, multiple sclerosis, or lupus.

3.4 Experimental Section

Materials and General Methods. Mass spectrometric data were obtained on either a JEOL SX 102A spectrometer for electron ionization (EI; 70 eV) or fast atom bombardment (FAB; thioglycerol/Na^+ matrix) or an Agilent Technologies LC/MSD TOF spectrometer for electrospray ionization (ESI; 3500 eV, positive ion mode). ^1H and ^{13}C NMR spectra were obtained on a Varian Unity 300 or 500 MHz instrument using 99.8% $CDCl_3$ with 0.05% v/v TMS, 99.8% CD_3OD with 0.05% v/v TMS, or 99.5% pyridine-d_5 and 99.96% DMSO-d_6 in ampoules. Methanol, methylene chloride, and tetrahydrofuran were dried using columns of activated alumina. Flash chromatography was performed using 230-400 mesh silica gel. Thin layer chromatography was performed on aluminum-backed, 254 nm UV-active plates with a silica gel particle size of 250 μm. Reagents were obtained from Aldrich or Fluka, unless otherwise specified, and were used as received.

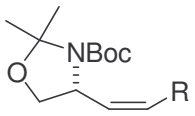

3-6a R = C_5H_{11}
3-6b R = C_2H_5
3-6c R = C_9H_{19}
3-6d R = $C_{14}H_{29}$

3-6a. A solution of *n*-BuLi in hexanes (1.6 *M*, 18.1 mL, 29.0 mmol) was added dropwise to a suspension of hexyltriphenylphosphonium bromide (14.06 g, 32.90 mmol; prepared from 1-bromohexane and triphenylphosphine refluxed in toluene for five days, 92%) in anhydrous THF (65 mL) at –78°C under N_2. The resulting orange suspension was allowed to warm to room temperature then stirred for 1 h. The reddish solution was cooled to -78°C, and a solution of Garner's aldehyde (5.80 g, 25.3 mmol) in anhydrous THF (25 mL) was added over 30 m. The suspension was allowed to warm to room temperature and was stirred for another 2 h. Quenching was performed with saturated aqueous NH_4Cl (50 mL) followed by extraction with Et_2O (3 x 50 mL). The organic layer was washed with brine, dried over Na_2SO_4, and concentrated in vacuo. The crude product was adsorbed onto silica gel, after dissolving in CH_2Cl_2, then purified by column chromatography (SiO_2, EtOAc:Hex 5:95 to 1:9 to 1:1), which yielded both *Z*- and *E*-alkenes as colorless oils (*Z*: 4.98 g, 60%, R_f = 0.41 EtOAc:Hex 5:95; *E*: 0.21 g, 3%, R_f = 0.38 EtOAc:Hex 5:95; *Z*:*E* 96:4 as determined by weight), as well as recovered aldehyde starting material (980 mg). *Z*-alkene: ^{1}H NMR ($CDCl_3$, 300 MHz) δ 5.43 (m, 2 H), 4.58 (br s, 1 H), 4.05 (dd, *J* = 8.5, 6.1 Hz, 1 H), 3.63 (dd, *J* = 8.6, 3.3 Hz, 1 H), 2.12 (br s, 2 H), 1.59 (s, 3 H), 1.52 (s, 3 H), 1.45 (s, 9 H), 1.29 (br s, 6 H), 0.89 (t, *J* = 6.6 Hz, 3 H); ^{13}C NMR ($CDCl_3$, 75 MHz) δ 151.96, 131.98 (br), 130.67 (br), 130.42 (br), 129.51 (br), 93.92 (br), 79.53 (br), 69.03, 54.56, 31.52, 29.43, 28.48, 27.42, 22.54, 14.03; HRMS (EI) *m/z* for $C_{17}H_{32}NO_3$ ($[M+H]^+$) 298.2396 (34.5%), calc. 298.2377.

3-6b. Same procedure as the synthesis of **3-6a**, substituting with propyltriphenylphosphonium bromide (*Z*: 63%; *E*: 3%; *Z*:*E* 96:4 as determined by weight). ^{1}H NMR ($CDCl_3$, 300 MHz) δ 5.33 (m, 2 H), 4.55 (br s, 1 H), 3.98 (dd, *J* = 8.5, 6.1 Hz, 1 H), 3.56 (dd, *J* = 8.5, 3.2 Hz, 1 H), 2.06 (br s, 2 H), 1.51 (s, 3 H), 1.44 (s, 3 H), 1.38 (s, 9 H), 0.91 (t, *J* = 7.4 Hz, 3 H); ^{13}C NMR ($CDCl_3$, 75 MHz) δ 151.92, 133.47 (br), 132.20 (br), 129.74 (br), 128.86 (br), 93.85 (br), 79.49 (br), 68.99, 54.44, 28.44, 26.42, 24.03, 20.66, 14.36; HRMS (EI) *m/z* for $C_{14}H_{26}NO_3$ ($[M+H]^+$) 256.1900 (93.5%), calc. 256.1913.

3-6c. Same procedure as synthesis of **3-6a**, substituting with decyltriphenylphosphonium bromide (*Z*: 44%; *E*: 2%; *Z*:*E* 96:4 as determined by weight). ^{1}H NMR ($CDCl_3$, 300 MHz) δ 5.43 (m, 2 H), 4.60 (br s, 1 H), 4.05 (dd, *J* = 8.6, 6.2 Hz, 1 H), 3.64 (dd, *J* = 8.5, 3.4 Hz, 1 H), 2.12 (br s, 2 H), 1.59 (s, 3 H), 1.52 (s, 3 H), 1.45 (s, 9 H), 1.26 (br s, 14 H), 0.88 (t, *J* = 6.7 Hz, 3 H); ^{13}C NMR ($CDCl_3$, 75 MHz) δ 152.18, 133.78 (br), 130.92 (br), 130.50 (br), 129.55 (br), 94.12 (br), 79.81 (br), 69.24, 54.74, 32.08, 29.93, 29.75, 29.70, 29.50, 28.67, 27.64, 22.86, 14.29; HRMS (FAB) *m/z* for $C_{21}H_{40}NO_3$ ($[M+H]^+$) 354.3021 (26.1%), calc. 354.3008.

3-6d. Same procedure as synthesis of **3-6a**, substituting with pentadecyltriphenylphosphonium bromide (*Z*: 86%; *E*: 4%; *Z*:*E* 96:4 as determined by weight). ^{1}H NMR ($CDCl_3$, 300 MHz) δ 5.42 (m, 2 H), 4.58 (br s, 1 H), 4.04 (dd, *J* = 8.6, 6.2 Hz, 1 H), 3.64 (dd, *J* = 8.5, 3.4 Hz, 1 H), 2.12 (br s, 2 H), 1.59 (s, 3 H), 1.52 (s, 3 H), 1.45 (s, 9 H), 1.27 (br s, 24 H), 0.88 (t, *J* = 6.8 Hz, 3 H); ^{13}C NMR ($CDCl_3$, 75 MHz) δ 152.09, 133.60 (br), 131.45 (br), 130.87 (br), 129.74 (br), 94.01 (br), 79.76 (br), 69.22, 54.68, 32.02, 29.93, 29.87, 29.74, 29.70, 29.61, 29.50, 28.73, 27.50, 22.75, 14.24; HRMS (FAB) *m/z* for $C_{26}H_{50}NO_3$ ($[M+H]^+$) 424.3779 (95.6%), calc. 424.3785.

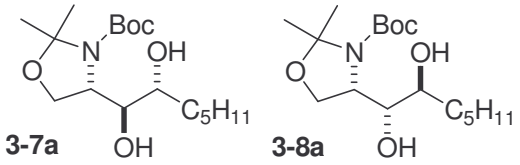

3-7a **3-8a**

3-7a and **3-8a**. Aqueous OsO_4 (4% v/v, 1.8 mL, 0.28 mmol) was added to a solution of NMO (1.63 mg, 13.9 mmol) in *t*-BuOH and water (10 mL, 1:1). The colorless solution was cooled to 0°C and an emulsion of **3-6a** (3.42 g, 11.5 mmol) in the same solvent (11.5 mL) was added dropwise. The resulting brown solution was allowed to warm to room temperature overnight then was quenched with solid Na_2SO_3. The solution was extracted with CH_2Cl_2 (2 x 25 mL), washed with 5% NaOH and brine, then dried with Na_2SO_4, and concentrated. Purification was performed by column chromatography (SiO_2, EtOAc:Hex 1:3), which yielded two diastereomers as colorless oils (**3-7a**: 3.91 g, 68%, R_f = 0.24; **3-8a**: 1.75 g, 30%, R_f = 0.35; 38% de). **3-7a**: ^{1}H NMR ($CDCl_3$, 300 MHz) δ 4.15 (m, 2 H), 4.00 (m, 1 H), 3.61 (m, 2 H), 3.30 (br s, 2 H), 1.70-1.55 (br s, 5 H), 1.51 (s, 3 H), 1.48 (s, 9 H), 1.30 (br s, 6 H), 0.89 (t, *J* = 6.7 Hz, 3 H); ^{13}C NMR ($CDCl_3$, 75 MHz) δ 153.71, 93.88, 81.25, 74.61, 73.97, 64.97, 59.10, 33.32, 31.86, 28.39, 25.91, 22.64, 14.04; HRMS (EI) *m/e* for $C_{17}H_{34}NO_5$ ($[M+H]^+$) 332.2433 (100%), calcd 332.2437. **3-8a**: ^{1}H NMR ($CDCl_3$, 300 MHz) δ 4.37 (br s, 2 H), 4.08 (dd, *J* = 9.3, 6.1 Hz, 1 H), 3.99 (dd, *J* = 9.3, <1 Hz, 1 H), 3.43 (m, 1 H), 3.29 (br s, 1 H), 2.88 (br s, 1 H), 1.80-1.65 (m, 2 H), 1.62 (s, 3 H), 1.53 (s, 3 H), 1.51 (s, 9 H), 1.31 (br s, 6 H), 0.89 (t, *J* = 6.7 Hz, 3 H); ^{13}C NMR ($CDCl_3$, 75 MHz) δ 155.11, 94.68, 81.79, 78.71, 71.72, 66.95, 57.60, 32.74, 32.14, 28.42, 26.63, 25.52, 22.83, 14.24; HRMS (EI) *m/z* for $C_{17}H_{34}NO_5$ ($[M+H]^+$) 332.2437 (100%), calc. 332.2437.

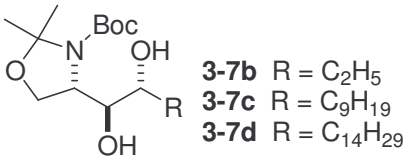

3-7b R = C_2H_5
3-7c R = C_9H_{19}
3-7d R = $C_{14}H_{29}$

3-7b. Same procedure as synthesis of **3-7a** (**3-7b**: 66%; **3-8b**: 34%; 32% de). ^{1}H NMR ($CDCl_3$, 300 MHz) δ 4.17 (m, 2 H), 3.99 (m, 1 H), 3.63 (br s, 2 H), 3.52 (br s, 2 H), 1.60 (s, 3 H), 1.51 (s, 3 H), 1.49 (s, 9 H), 1.26 (s, 2H), 0.90 (t, *J* = 6.6 Hz, 3 H); ^{13}C NMR ($CDCl_3$, 75 MHz) δ 153.50, 94.16, 81.50, 75.32, 74.85, 65.37, 59.61, 29.85, 28.53, 27.01, 26.29, 14.63; HRMS (EI) *m/z* for $C_{14}H_{28}NO_5$ ($[M+H]^+$) 290.1951 (100%), calc. 290.1967.

3-7c. Same procedure as synthesis of **3-7a** (**3-7c**: 93%; **3-8c**: not isolated). ^{1}H NMR ($CDCl_3$, 300 MHz) δ 4.16 (m, 2 H), 4.00 (m, 1 H), 3.60 (br s, 2 H), 3.31 (br s, 2 H), 1.75-1.55 (br s, 2 H), 1.62 (s, 3 H), 1.52 (s, 3H), 1.50 (s, 9 H), 1.26 (br s, 14 H), 0.88 (t, *J* = 6.7 Hz, 3 H); ^{13}C NMR ($CDCl_3$, 75 MHz) δ 153.69, 94.00, 81.92, 75.39, 73.92, 67.04, 57.56, 33.46, 32.10, 29.97, 29.89, 29.83, 29.79, 29.53, 28.60, 28.49, 26.70, 25.93, 22.89, 14.32; HRMS (FAB) *m/z* for $C_{21}H_{41}NNaO_5$ ($[M+Na]^+$) 410.2880 (100%), calc. 410.2882.

3-7d. Same procedure as synthesis of **3-7a** (**3-7d**: 61%; **3-8d**: 22%; 39% de). ^{1}H NMR ($CDCl_3$, 300 MHz) δ 4.16 (m, 2 H), 4.00 (m, 1 H), 3.61 (br s, 2 H), 3.31 (br s, 2 H), 1.78-1.54 (br s, 2 H), 1.62 (s, 3 H), 1.52 (s, 3H), 1.50 (s, 9 H), 1.25 (br s, 24 H), 0.88 (t, *J* = 6.6 Hz, 3 H); ^{13}C NMR ($CDCl_3$, 75 MHz) δ 153.60, 93.98, 81.77, 75.42, 74.01, 66.74, 58.56, 33.39, 32.17, 29.96, 29.90, 29.82, 29.77, 29.85, 29.53, 28.60, 28.50, 26.76, 26.00, 22.88, 14.34; HRMS (FAB) *m/z* for $C_{26}H_{51}NNaO_5$ ($[M+Na]^+$) 480.3649 (100%), calc. 480.3659.

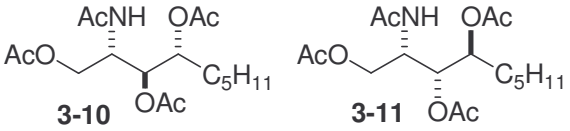

3-10 and **3-11**. Each diastereomer (**3-7a**, **3-8a**; 100 mg, 0.302 mmol) was separately dissolved in TFA (1.5 mL) and three drops of MeOH. Immediately after acidification, TLC (MeOH:CH_2Cl_2 5:95) showed complete deprotection (from **3-8a**: R_f = 0.46; from **3-7a**: R_f = 0.31). The solvent was removed in vacuo and then pyridine (2 mL) and acetic anhydride (1 mL) were added. DMAP (150 mg, 1.23 mmol) was included and the reaction continued at room temperature for 1 h. The reaction was quenched with ice, the product extracted with EtOAc (2 x 5 ml), washed with saturated aqueous $NaHCO_3$, 5% HCl, and brine, dried with Na_2SO_4, and concentrated. Both peracetylated diastereomers were characterized by NMR after flash chromatography (SiO_2, MeOH:CH_2Cl_2 5:95) and compared to that of a commercial sample of phytosphingosine ((2S,3S,4R)-2-amino-1,3,4-octadecanetriol; **3-9d**) that was peracetylated in the same manner. The methine proton splitting patterns of the major triol product were consistent with those of peracetylphytosphingosine, while those of the minor triol varied greatly. Major product (**3-10**) from dihydroxylation: ^{1}H NMR ($CDCl_3$, 300 MHz) δ 6.04 (d, *J* = 9.3 Hz, 1 H), 5.11 (dd, *J* = 8.3, 2.9 Hz, 1 H), 4.94 (dt, *J* = 9.5, 3.4 Hz, 1 H), 4.48 (m, 1 H), 4.29 (dd, *J* = 11.5, 4.9 Hz, 1 H), 4.01 (dd, *J* = 11.5, 3.1 Hz, 1 H), 2.09 (s, 3 H), 2.05 (s, 6 H), 2.03 (s, 3 H), 1.75-1.50 (br s, 2 H), 1.29 (br s, 6 H), 0.89 (t, *J* = 6.7 Hz, 3 H); ^{13}C NMR ($CDCl_3$, 75 MHz) δ 171.34, 171.06, 170.29, 170.00, 73.14, 72.23, 63.04, 47.85, 31.59, 28.30, 25.31, 23.46, 22.66, 21.22, 20.96, 20.93, 14.15; HRMS (FAB) *m/z* for $C_{17}H_{30}NO_7$ ($[M+H]^+$) 360.2025 (100%), calc. 360.2022. Minor product (**3-11**) from dihydroxylation: ^{1}H NMR ($CDCl_3$, 300 MHz) δ 5.64 (d, *J* = 9.8 Hz, 1 H), 5.20 (dd, *J* = 6.7, 3.3 Hz, 1 H), 5.00 (dd, *J*

= 12.2, 6.8 Hz, 1 H), 4.61 (m, 1 H), 4.00 (d, J = 6.1 Hz, 2 H), 2.12 (s, 3 H), 2.06 (s, 3 H), 2.05 (s, 3H), 1.97 (s, 3 H), 1.60-1.45 (br s, 2 H), 1.28 (br s, 6 H), 0.89 (t, *J* = 6.7 Hz, 3 H); ^{13}C NMR ($CDCl_3$, 75 MHz) δ 170.86, 170.46, 170.02, 169.88, 72.20, 71.13, 63.23, 47.27, 31.75, 30.43, 24.89, 23.42, 22.64, 21.17, 20.98, 20.92, 14.14; HRMS (FAB) *m/z* for $C_{17}H_{30}NO_7$ ($[M+H]^+$) 360.2017 (100%), calc. 360.2022. Peracetylphytosphingosine: ^{1}H NMR ($CDCl_3$, 300 MHz) δ 6.07 (d, *J* = 9.4 Hz, 1 H), 5.12 (dd, *J* = 8.3, 3.0 Hz, 1 H), 4.96 (dt, *J* = 9.5, 3.2 Hz, 1 H), 4.51 (m, 1 H), 4.30 (dd, *J* = 11.5, 4.9 Hz, 1 H), 4.02 (dd, *J* = 11.6, 3.1 Hz, 1 H), 2.09 (s, 3 H), 2.06 (s, 6 H), 2.04 (s, 3 H), 1.75-1.55 (br s, 2 H), 1.26 (br s, 6 H), 0.89 (t, *J* = 6.7 Hz, 3 H); ^{13}C NMR ($CDCl_3$, 125 MHz) δ 171.06, 170.80, 170.03, 169.68, 72.88, 71.91, 62.79, 47.53, 31.86, 29.63, 29.62, 29.61, 29.59, 29.56, 29.52, 29.44, 29.30, 29.24, 28.09, 25.45, 23.22, 22.63, 20.98, 20.72, 20.69, 14.06; HRMS (FAB) *m/z* for $C_{26}H_{47}NNaO_7$ ($[M+Na]^+$) 508.3199 (100%), calc. 508.3250.

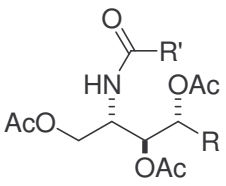

3-12a R = C_5H_{11} R' = $C_{23}H_{47}$
3-12b R = C_2H_5 R' = $C_{23}H_{47}$
3-12c R = C_9H_{19} R' = $C_{23}H_{47}$
3-12d R = $C_{14}H_{29}$ R' = $C_{25}H_{51}$
3-12e R = $C_{14}H_{29}$ R' = CH_3
3-12f R = $C_{14}H_{29}$ R' = C_7H_{15}
3-12g R = $C_{14}H_{29}$ R' = $C_{15}H_{31}$

3-12a. Tetracosanoic acid (298 mg, 0.808 mmol) was dissolved in anhydrous THF (8 mL) at 50°C followed by NHS (101 mg, 0.878 mmol) and DCC (180 mg, 0.872 mmol). The mixture was heated to reflux for 3 h before being cooled to room temperature. Triethylamine (1 mL) and **3-9a** (288 mg, 0.870 mmol; prepared from protected parent compound **3-7a** by dissolving in THF and adding hydrogen chloride gas) in anhydrous THF (3 ml) were added to the reaction mixture and refluxed for 3 h. After cooling and stirring at rt overnight, the solvent was removed in vacuo. Purification was performed by peracetylation of the ceramide with acetic anhydride (2 mL), triethylamine (2 mL),

DMAP (700 mg, 5.73 mmol), in anhydrous THF (10 mL) and heating to reflux for 1 h. The reaction was quenched with ice, extracted with EtOAc (2 x 20 mL), washed with saturated aqueous $NaHCO_3$, 5% HCl, and brine, dried with $MgSO_4$, and concentrated. Pure triacetate was isolated by flash chromatography (SiO_2, EtOAc:Hex 1:3) as a white oily semisolid (273 mg, 47%, R_f = 0.39 EtOAc:Hex 1:3). ^{1}H NMR ($CDCl_3$, 300 MHz) δ 5.94 (d, *J* = 9.3 Hz, 1 H), 5.11 (dd, *J* = 8.5, 2.9 Hz, 1 Hz), 4.93 (dt, *J* = 9.8, 3.3 Hz, 1 H), 4.49 (m, 1 H), 4.30 (dd, *J* = 11.6, 5.0 Hz, 1 H), 3.99 (dd, *J* = 11.6, 3.0 Hz, 1 H), 2.21 (t, *J* = 7.5 Hz, 2 H), 2.08 (s, 3 H), 2.05 (s, 3H), 2.04 (s, 3H), 1.70-1.55 (m, 4 H), 1.25 (br s, 46 H), 0.88 (t, *J* = 6.7 Hz, 6 H); ^{13}C NMR ($CDCl_3$, 75 MHz) δ 173.21, 171.37, 171.05, 170.26, 73.18, 72.02, 63.08, 47.57, 36.88, 32.10, 31.57, 29.88, 29.68, 29.53, 29.40, 28.10, 25.82, 25.35, 22.86, 22.67, 21.18, 20.93, 20.89, 14.28, 14.14; HRMS (FAB) *m/z* for $C_{39}H_{74}NO_7$ ($[M+H]^+$) 668.5463 (100%), calc. 668.5460.

3-12b. Same procedure as synthesis of **3-12a**, substituting with **3-7b** (45%). ^{1}H NMR ($CDCl_3$, 300 MHz) δ 5.89 (d, *J* = 9.5 Hz, 1 H), 5.11 (dd, *J* = 8.3, 3.2 Hz, 1 H), 4.86 (dt, *J* = 10.0, 3.3 Hz, 1 H), 4.49 (m, 1 H), 4.30 (dd, *J* = 11.7, 4.9 Hz, 1 H), 3.99 (dd, *J* = 11.7, 3.2 Hz, 1 H), 2.21 (t, *J* = 7.6 Hz, 2 H), 2.08 (s, 3 H), 2.06 (s, 3H), 2.05 (s, 3H), 1.69-1.57 (m, 4 H), 1.25 (br s, 40 H), 0.91 (t, *J* = 7.3 Hz, 3 H), 0.88 (t, *J* = 67.1 Hz, 3 H); ^{13}C NMR ($CDCl_3$, 75 MHz) δ 173.12, 171.35, 171.10, 170.27, 74.49, 72.09, 63.07, 47.65, 36.96, 32.14, 29.92, 29.84, 29.72, 29.58, 29.55, 29.43, 25.80, 22.91, 21.65, 21.22, 20.98, 14.34; HRMS (FAB) *m/z* for $C_{36}H_{67}NNaO_7$ ($[M+Na]^+$) 648.4797 (100%), calc. 648.4815.

3-12c. Same procedure as synthesis of **3-12a**, substituting with **3-7c** (47%). ^{1}H NMR ($CDCl_3$, 300 MHz) δ 6.05 (d, *J* = 9.5 Hz, 1 H), 5.11 (dd, *J* = 8.4, 3.1 Hz, 1 H), 4.93 (dt, *J* = 9.7, 3.2 Hz, 1 H), 4.49 (m, 1 H), 4.29 (dd, *J* = 11.6, 5.0 Hz, 1 H), 3.99 (dd, *J* = 11.7, 2.9

Hz, 1 H), 2.20 (t, *J* = 7.6 Hz, 2 H), 2.07 (s, 3 H), 2.04 (s, 6 H), 1.75-1.54 (m, 4 H), 1.25 (br s, 54 H), 0.88 (t, *J* = 6.6 Hz, 6 H); ^{13}C NMR ($CDCl_3$, 75 MHz) δ 173.03, 171.33, 171.02, 170.28, 73.18, 72.19, 63.10, 47.61, 37.00, 32.15, 29.75, 29.58, 29.51, 28.34, 25.85, 25.77, 22.92, 21.27, 21.00, 14.34; HRMS (FAB) *m/z* for $C_{43}H_{82}NO_7$ ($[M+H]^+$) 724.6211 (100%), calc. 724.6086

3-12d. Same procedure as synthesis of **3-12a**, substituting with **3-7d** and hexacosanoic (cerotic) acid (50%). ^{1}H NMR ($CDCl_3$, 500 MHz) δ 5.87 (d, *J* = 9.8 Hz, 1 H), 5.11 (dd, *J* = 8.3, 2.9 Hz, 1 H), 4.93 (dt, *J* = 10.3, 2.9 Hz, 1 H), 4.49 (m, 1 H), 4.30 (dd, *J* = 11.2, 4.9 Hz, 1 H), 3.98 (dd, *J* = 11.2, 2.9 Hz, 1 H), 2.21 (t, *J* = 7.6 Hz, 2 H), 2.08 (s, 3 H), 2.05 (s, 6 H), 1.72-1.56 (m, 4 H), 1.25 (br s, 68 H), 0.88 (t, *J* = 7.1 Hz, 6 H); ^{13}C NMR ($CDCl_3$, 125 MHz) δ 173.02, 171.32, 171.09, 170.27, 73.16, 72.13, 63.09, 47.58, 36.98, 32.15, 29.93, 29.75, 29.59, 29.52, 29.46, 28.29, 25.85, 25.77, 22.92, 21.26, 21.00, 20.99, 14.35; HRMS (FAB) *m/z* for $C_{50}H_{95}NNaO_7$ ($[M+Na]^+$) 844.7009 (100%), calc. 844.7001.

3-12e. **3-7d** (250 mg, 546 mmol) was deprotected in the same manner as **3-7a**, yielding a crude oil, which was peracetylated in THF (10 mL), with excess acetic anhydride (2 mL) and Et_3N (2 mL) along with DMAP (100 mg, 0.82 mmol). After 30 m, the reaction mixture was concentrated and the crude product purified by flash chromatography (SiO_2, EtOAc:Hex 1:3) yielding a white solid (200 mg, 88%, R_f = 0.38 1:1 EtOAc:Hex). ^{1}H NMR ($CDCl_3$, 500 MHz) δ 5.96 (d, *J* = 9.4 Hz, 1 H), 5.10 (dd, *J* = 8.2, 3.1 Hz, 1 H), 4.93 (dt, *J* = 9.4, 3.3 Hz, 1 H), 4.47 (m, 1 H), 4.29 (dd, *J* = 11.8, 4.9 Hz, 1 H), 3.99 (dd, *J* = 11.8, 3.1 Hz, 1 H), 2.08 (s, 3 H), 2.05 (s, 6 H), 2.03 (s, 3 H), 1.72-1.58 (m, 2 H), 1.25 (br s, 24 H), 0.88 (t, *J* = 6.7 Hz, 3 H); ^{13}C NMR ($CDCl_3$, 125 MHz)

δ 171.50, 171.05, 170.30, 169.98, 73.10, 72.20, 63.10, 47.88, 31.68, 29.05, 28.85, 25.49, 21.12, 20.99, 20.91, 14.22; HRMS (FAB) *m/z* for $C_{26}H_{47}NNaO_7$ ($[M+Na]^+$) 508.3232 (100%), calc. 508.3250.

3-12f. Same procedure as synthesis of **3-12a**, substituting with **3-7d** and octanoic acid (51%). ^{1}H NMR ($CDCl_3$, 300 MHz) δ 6.09 (d, *J* = 9.4 Hz, 1 H), 5.10 (dd, *J* = 8.3, 3.1 Hz, 1 H), 4.94 (dt, *J* = 9.4, 3.2 Hz, 1 H), 4.48 (m, 1 H), 4.29 (dd, *J* = 11.8, 4.8 Hz, 1 H), 4.01 (dd, *J* = 11.8, 3.1 Hz, 1 H), 2.28 (t, *J* = 7.7 Hz, 2 H), 2.07 (s, 3 H), 2.05 (s, 3 H), 2.02 (s, 3 H), 1.74-1.52 (m, 4 H), 1.26 (br s, 32 H), 0.88 (t, *J* = 6.8 Hz, 6 H); ^{13}C NMR ($CDCl_3$, 75 MHz) δ 173.19, 171.24, 171.00, 170.21, 73.16, 72.13, 63.13, 47.60, 36.83, 32.09, 31.87, 29.86, 29.76, 29.46, 28.25, 25.71, 22.85, 21.15, 20.90, 20.86, 14.26, 14.21; HRMS (FAB) *m/z* for $C_{32}H_{59}NNaO_7$ ($[M+Na]^+$) 592.4181 (100%), calc. 592.4189.

3-12g. Same procedure as synthesis of **3-12a**, substituting with **3-7d** and hexadecanoic (palmitic) acid (52%). ^{1}H NMR ($CDCl_3$, 300 MHz) δ 6.03 (d, *J* = 9.4 Hz, 1 H), 5.10 (dd, *J* = 8.4, 3.2 Hz, 1 H), 4.93 (dt, *J* = 9.3, 3.1 Hz, 1 H), 4.48 (m, 1 H), 4.28 (dd, *J* = 11.7, 4.9 Hz, 1 H), 4.01 (dd, *J* = 11.7, 3.2 Hz, 1 H), 2.21 (t, *J* = 7.7 Hz, 2 H), 2.08 (s, 3 H), 2.06 (s, 3 H), 2.02 (s, 3 H), 1.71-1.54 (m, 4 H), 1.26 (br s, 48 H), 0.89 (t, *J* = 6.7 Hz, 6 H); ^{13}C NMR ($CDCl_3$, 75 MHz) δ 173.10, 171.25, 170.94, 170.29, 73.17, 72.19, 63.10, 47.30, 37.00, 32.24, 31.76, 29.96, 29.88, 29.73, 29.44, 29.02, 28.75, 28.22, 25.71, 23.02, 21.14, 20.89, 20.89, 14.22; HRMS (FAB) *m/z* for $C_{40}H_{75}NNaO_7$ ($[M+Na]^+$) 704.5431 (100%), calc. 704.5441.

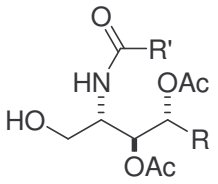

3-13a R = C_5H_{11} R' = $C_{23}H_{47}$
3-13b R = C_2H_5 R' = $C_{23}H_{47}$
3-13c R = C_9H_{19} R' = $C_{23}H_{47}$
3-13d R = $C_{14}H_{29}$ R' = $C_{25}H_{51}$
3-13e R = $C_{14}H_{29}$ R' = CH_3
3-13f R = $C_{14}H_{29}$ R' = C_7H_{15}
3-13g R = $C_{14}H_{29}$ R' = $C_{15}H_{31}$

3-13a. Ceramide **3-12a** (523 mg, 0.783 mmol) was deacetylated by dissolving in MeOH (10 mL) then adding a solution of sodium methoxide (0.30 *M*, 5 mL, 1.5 mmol). The suspension was agitated for 45 m and centrifuged (3500 rpm, 5 m) to isolate the solid triol product. The supernatant was removed, the solid rinsed with fresh MeOH (5 mL) to remove any remaining base, and centrifuged again. After removal of the solvent and drying under vacuum, a white flaky solid (346 mg, 82%) was isolated and used without further purification. The primary alcohol was selectively protected by stirring in anhydrous THF (25 mL) at 60°C and adding TBSCl (289 mg, 1.92 mmol) and imidazole (130 mg, 1.92 mmol). The temperature was increased to 80°C and allowed to proceed for 15 m before quenching with water (15 mL). Extraction of the mixture was done with EtOAc (3 x 15 mL), washed with brine, dried with Na_2SO_4, and concentrated. The resulting colorless oil was dissolved in THF (5 mL) and diacetylated with acetic anhydride (1 mL), triethylamine (1 mL), and DMAP (76 mg, 0.63 mmol) at room temperature for 1.5 h. The reaction was quenched with ice and extracted with EtOAc (2 x 10 mL). The organic layer was washed with saturated aqueous $NaHCO_3$, 5% HCl, and brine, dried with $NaSO_4$, and concentrated. The crude oil was taken back up into THF (3 mL) and aqueous HF (1 mL, 49%). TLC (EtOAc:Hex 2:1) showed an immediate disappearance of starting material and formation of the desilylated ceramide (R_f = 0.54). The reaction was poured carefully into saturated aqueous $NaHCO_3$ (10 mL), extracted with EtOAc (10 mL), rewashed with $NaHCO_3$ (10 mL), back extracted with EtOAc (2 x

10 mL), washed with brine (5 mL), and dried thoroughly with Na_2SO_4 before concentrating. Purification by flash chromatography (SiO_2, EtOAc:Hex 2:1) yielded the product as a white powder (245 mg, 50% from triacetate). ^{1}H NMR ($CDCl_3$, 500 MHz) δ 6.19 (d, *J* = 9.3 Hz, 1 H), 5.02 (dd, *J* = 9.3, 2.4 Hz, 1 H), 4.96 (dt, *J* = 10.3, 2.4 Hz, 1 H), 4.15 (tt, *J* = 9.3, 2.9 Hz, 1 H), 3.57 (br s, 2 H), 2.52 (t, *J* = 6.6 Hz, 1 H), 2.22 (t, *J* = 7.5 Hz, 2 H), 2.16 (s, 3 H), 2.04 (s, 3 H), 1.72-1.62 (m, 4 H), 1.25 (br s, 46 H), 0.89 (t, *J* = 6.8 Hz, 6 H); ^{13}C NMR ($CDCl_3$, 125 MHz) δ 173.18, 171.80, 170.80, 73.06, 61.56, 49.51, 36.81, 31.92, 31.46, 29.70, 29.49, 29.34, 29.27, 27.83, 25.69, 25.34, 22.69, 22.55, 21.04, 20.91, 14.13, 14.01; HRMS (FAB) *m/z* for $C_{37}H_{71}NNaO_6$ ($[M+Na]^+$) 648.5183 (100%), calc. 648.5174.

3-13b. Same procedure as synthesis of **3-13a** (51%). ^{1}H NMR ($CDCl_3$, 500 MHz) δ 6.18 (d, *J* = 9.3 Hz, 1 H), 5.02 (dd, *J* = 9.3, 2.9 Hz, 1 H), 4.89 (dt, *J* = 10.3, 2.9 Hz, 1 H), 4.15 (tt, *J* = 9.3, 2.9 Hz, 1 H), 3.57 (m, 2 H), 2.48 (t, *J* = 6.6 Hz, 1 H), 2.23 (t, *J* = 7.8 Hz, 2 H), 2.15 (s, 3 H), 2.05 (s, 3 H), 1.72-1.60 (m, 4 H), 1.26 (br s, 40 H), 0.91 (t, *J* = 7.3 Hz, 3 H), 0.89 (t, *J* = 6.8 Hz, 3 H); ^{13}C NMR ($CDCl_3$, 125 MHz) δ 173.25, 171.75, 170.91, 74.43, 73.08, 61.60, 49.62, 36.77, 31.93, 29.70, 29.49, 29.33, 29.25, 25.63, 22.69, 21.27, 20.98, 20.87, 14.11; HRMS (FAB) *m/z* for $C_{34}H_{65}NNaO_6$ ($[M+Na]^+$) 606.4712 (100%), calc. 606.4710.

3-13c. Same procedure as synthesis of **3-13a** (57%). ^{1}H NMR ($CDCl_3$, 300 MHz) δ 6.44 (d, *J* = 9.3 Hz, 1 H), 5.06 (dd, *J* = 9.3, 2.4 Hz, 1 H), 4.95 (dt, *J* = 9.9, 2.8 Hz, 1 H), 4.17 (tt, *J* = 9.4, 2.6 Hz, 1 H), 3.57 (m, 2 H), 2.80 (t, *J* = 6.5 Hz, 1 H), 2.22 (t, *J* = 7.6 Hz, 2 H), 2.14 (s, 3 H), 2.04 (s, 3 H), 1.78-1.56 (m, 4 H), 1.25 (br s, 54 H), 0.88 (t, *J* = 6.6 Hz, 6 H); ^{13}C NMR ($CDCl_3$, 75 MHz) δ 173.39, 171.67, 171.31, 73.42, 72.90, 61.69,

49.76, 36.96, 32.12, 32.10, 29.91, 29.86, 29.77, 29.73, 29.58, 29.56, 29.51, 28.00, 25.91, 22.88, 21.24, 21.08, 14.31; HRMS (FAB) *m/z* for $C_{41}H_{79}NNaO_6$ ($[M+Na]^+$) 704.5798 (100%), calc. 704.5805.

3-13d. Same procedure as synthesis of **3-13a** (57%). ^1H NMR ($CDCl_3$, 500 MHz) δ 6.36 (d, *J* = 9.2 Hz, 1 H), 5.05 (dd, *J* = 9.3, 2.4 Hz, 1 H), 4.96 (dt, *J* = 10.3, 2.4 Hz, 1 H), 4.18 (tt, *J* = 9.3, 2.9 Hz, 1 H), 4.30 (dd, *J* = 11.2, 4.9 Hz, 1 H), 3.58 (m, 2 H), 2.72 (br s, 1 Hz), 2.22 (t, *J* = 7.6 Hz, 2 H), 2.15 (s, 3 H), 2.04 (s, 3 H), 1.70-1.58 (m, 4 H), 1.25 (br s, 68 H), 0.88 (t, *J* = 6.8 Hz, 6 H); ^{13}C NMR ($CDCl_3$, 125 MHz) δ 173.43, 171.81, 171.26, 73.37, 72.01, 61.72, 49.73, 36.97, 32.13, 29.91, 29.80, 29.73, 29.58, 29.51, 28.03, 25.91, 22.90, 21.25, 21.10, 14.33; HRMS (FAB) *m/z* for $C_{50}H_{93}NNaO_6$ ($[M+Na]^+$) 802.68930 (100%), calc. 802.68951.

3-13e. Same procedure as synthesis of **3-13a** (50%). ^1H NMR ($CDCl_3$, 500 MHz) δ 6.57 (d, *J* = 9.0 Hz, 1 H), 5.09 (dd, *J* = 9.4, 2.6 Hz, 1 H), 4.97 (dt, *J* = 9.6, 3.0 Hz, 1 H), 4.18 (tt, *J* = 9.6, 2.8 Hz, 1 H), 3.61 (m, 2 H), 2.85 (br s, 1 H), 2.16 (s, 3 H), 2.07 (s, 3 H), 2.05 (s, 3H), 1.80-1.58 (m, 4 H), 1.27 (br s, 22 H), 0.90 (t, *J* = 6.7 Hz, 3 H); ^{13}C NMR ($CDCl_3$, 125 MHz) δ 173.05, 171.52, 171.15, 73.70, 72.99, 61.82, 49.88, 36.98, 32.13, 29.91, 29.82, 29.52, 28.54, 25.37, 21.22, 21.00, 20.91, 14.31; HRMS (FAB) *m/z* for $C_{24}H_{45}NNaO_6$ ($[M+Na]^+$) 466.3144 (100%), calc. 466.3145.

3-13f. Same procedure as synthesis of **3-13a** (51%). ^1H NMR ($CDCl_3$, 300 MHz) δ 6.40 (d, *J* = 9.5 Hz, 1 H), 5.06 (dd, *J* = 9.5, 2.4 Hz, 1 H), 4.95 (dt, *J* = 9.8, 2.9 Hz, 1 H), 4.17 (tt, *J* = 9.3, 2.4 Hz, 1 H), 3.58 (m, 2 H), 2.75 (br s, 1 H), 2.22 (t, *J* = 7.5 Hz, 2 H), 2.14 (s, 3 H), 2.04 (s, 3H), 1.80-1.58 (m, 4 H), 1.25 (br s, 32 H), 0.88 (t, *J* = 6.8 Hz, 6 H); ^{13}C NMR ($CDCl_3$, 75 MHz) δ 173.41, 171.69, 171.29, 73.42, 72.99, 61.75, 49.80, 36.97,

32.13, 31.90, 29.90, 29.86, 29.82, 29.79, 29.56, 29.45, 29.21, 28.08, 25.90, 22.88, 22.81, 21.23, 21.08, 14.31, 14.26; HRMS (FAB) *m/z* for $C_{30}H_{57}NNaO_6$ ($[M+Na]^+$) 550.4072 (34.3%), calc. 550.4084.

3-13g. Same procedure as synthesis of **3-13a** (59%). ^{1}H NMR ($CDCl_3$, 300 MHz) δ 6.47 (d, *J* = 9.5 Hz, 1 H), 5.04 (dd, *J* = 9.5, 2.5 Hz, 1 H), 4.95 (dt, *J* = 9.7, 3.0 Hz, 1 H), 4.19 (tt, *J* = 9.5, 2.4 Hz, 1 H), 3.59 (m, 2 H), 2.77 (br s, 1 H), 2.20 (t, *J* = 7.5 Hz, 2 H), 2.13 (s, 3 H), 2.04 (s, 3H), 1.79-1.58 (m, 4 H), 1.25 (br s, 48 H), 0.89 (t, *J* = 6.7 Hz, 6 H); ^{13}C NMR ($CDCl_3$, 75 MHz) δ 173.52, 171.73, 171.39, 73.51, 73.01, 61.79, 49.81, 36.88, 32.13, 31.95, 29.91, 29.89, 29.85, 29.82, 29.76, 29.66, 29.57, 29.42, 29.23, 28.62, 25.93, 23.01, 22.94, 21.23, 21.10, 14.32, 14.25; HRMS (FAB) *m/z* for $C_{38}H_{73}NNaO_6$ ($[M+Na]^+$) 662.5331 (100%), calc. 662.5336.

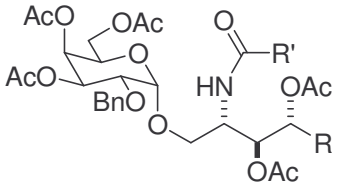

3-16a R = C_5H_{11} R' = $C_{23}H_{47}$
3-16b R = C_2H_5 R' = $C_{23}H_{47}$
3-16c R = C_9H_{19} R' = $C_{23}H_{47}$
3-16d R = $C_{14}H_{29}$ R' = $C_{25}H_{51}$
3-16e R = $C_{14}H_{29}$ R' = CH_3
3-16f R = $C_{14}H_{29}$ R' = C_7H_{15}
3-16g R = $C_{14}H_{29}$ R' = $C_{15}H_{31}$

3-16a. Bromide donor **3-15** (540 mg, 1.18 mmol) and ceramide **3-13a** (503 mg, 0.804 mmol) were dissolved in anhydrous CH_2Cl_2 (26 mL) and cooled to 0^{o}C. Freshly crushed 4 Å molecular sieves (2.0 g) were added and the mixture was allowed to stir for 10 m before addition of AgOTf (620 mg, 2.41 mmol) in the dark. The reaction vessel was wrapped in aluminum foil and allowed to warm to room temperature overnight. After 12 h, the slurry was filtered through Celite after dilution with EtOAc (20 mL). The resulting colorless solution was concentrated and purified by column chromatography (SiO_2, EtOAc:Hex 1:2), which yielded both α- and β-anomers as a white, waxy solid and colorless oil, respectively (α: 611 mg, 75%, R_f = 0.38 EtOAc:Hex 1:2; β: 161 mg, 20%,

R_f = 0.23 EtOAc:Hex 1:2; α:β 3.75:1 as determined by weight). ^{1}H NMR ($CDCl_3$, 500 MHz) δ 7.33 (m, 4 H), 7.28 (m, 1 H), 6.30 (d, *J* = 9.3 Hz, 1 H), 5.41 (dd, *J* = 3.4, <1 Hz, 1 H), 5.25 (t, *J* = 2.7 Hz, 1 H), 5.23 (d, *J* = 2.9 Hz, 1 H), 4.96 (dt, *J* = 10.2, 2.9 Hz, 1 H), 4.88 (d, *J* = 3.4 Hz, 1 H), 4.70 (d, *J* = 12.2 Hz, 1 H), 4.60 (d, *J* = 12.2 Hz, 1 H), 4.38 (tt, *J* = 9.3, 3.4 Hz, 1 H), 4.18 (t, *J* = 6.8 Hz, 1 H), 4.09 (m, 1 H), 4.03 (dd, *J* = 11.2, 6.8 Hz, 1 H), 3.82 (dd, *J* = 10.7, 3.4 Hz, 1 H), 3.65 (qd, *J* = 11.2, 3.4 Hz, 2 H), 2.17 (td, *J* = 7.7, 3.4 Hz, 2 H), 2.09 (s, 3 H), 2.08 (s, 3 H), 2.04 (s, 3 H), 1.99 (s, 3 H), 1.96 (s, 3 H), 1.72-1.66 (m, 4 H), 1.26 (br s, 46), 0.87 (m, 6 H); ^{13}C NMR ($CDCl_3$, 125 MHz) δ 172.92, 170.63, 170.36, 170.09, 169.99, 169.84, 137.97, 128.37, 127.86, 98.59, 73.47, 72.96, 72.91, 71.95, 69.34, 68.31, 67.77, 66.83, 61.77, 48.09, 36.64, 31.93, 31.42, 29.71, 29.52, 29.37, 29.29, 27.87, 25.65, 25.20, 22.69, 22.53, 20.91, 20.85, 20.70, 20.66, 20.57, 14.12, 13.99; HRMS (ESI) *m/z* for $C_{56}H_{93}NNaO_{14}$ ($[M+Na]^+$) 1026.64966 (100%), calc. 1026.64883.

3-16b. Same procedure as synthesis of **3-16a**, substituting with **3-13b** (62%). ^{1}H NMR ($CDCl_3$, 300 MHz) δ 7.38 (m, 5 H), 6.39 (d, *J* = 8.7 Hz, 1 H), 5.43 (m, 1 H), 5.28 (m, 2 H), 5.25 (d, *J* = 3.3 Hz, 1 H), 4.91 (d, *J* = 3.3 Hz, 1 H), 4.74 (d, *J* = 12.0 Hz, 1 H), 4.62 (d, *J* = 12.0 Hz, 1 H), 4.38 (m, 1 H), 4.17-4.05 (m, 3 H), 3.84 (dd, *J* = 10.1, 3.3 Hz, 1 H), 3.66 (dd, *J* = 9.6, 3.3 Hz, 1 H), 2.23-2.18 (m, 4 H), 2.11 (s, 3 H), 2.10 (s, 3 H), 2.07 (s, 3 H), 1.99 (s, 3 H), 1.27 (br s, 40 H), 0.92-0.87 (m, 6 H); ^{13}C NMR ($CDCl_3$, 75 MHz) δ 173.31, 171.06, 170.69, 170.45, 170.29, 170.19, 138.12, 128.65, 128.17, 128.14, 98.79, 74.69, 73.74, 73.20, 72.03, 69.54, 68.58, 67.75, 67.12, 62.03, 48.34, 36.91, 32.17, 29.96, 29.91, 29.62, 25.87, 22.95, 21.48, 21.18, 21.143, 21.00, 20.96, 20.88, 14.37, 10.29; HRMS (FAB) *m/z* for $C_{53}H_{87}NNaO_{14}$ ($[M+Na]^+$) 984.6014 (100%), calc. 984.6019.

3-16c. Same procedure as synthesis of **3-16a**, substituting with **3-13c** (80%). ^{1}H NMR ($CDCl_3$, 300 MHz) δ 7.38-7.29 (m, 5 H), 6.62 (d, *J* = 9.6 Hz, 1H), 5.43 (d, *J* = 2.7 Hz, 1 H), 5.32-5.26 (m, 2 H), 4.97-4.94 (m, 1 H), 4.91 (d, *J* = 3.3 Hz, 1 H), 4.61 (d, *J* = 12 Hz, 1 H), 4.38 (m, 1 H), 4.19-4.01 (m, 3 H), 3.84 (dd, *J* = 9.0, 3.6 Hz, 1 H), 3.69 (dd, *J* = 11.1, 3.6 Hz, 1 H), 3.60 (dd, *J* = 11.4, 3.0 Hz, 1 H), 2.23-2.18 (m, 4 H), 2.12 (s, 3 H), 2.11 (s, 3 H), 2.07 (s, 3 H), 2.01 (s, 3 H), 1.99 (s, 3 H), 1.67-1.58 (m, 4 H), 1.28 (br s, 56 H), 0.90 (t, *J* = 6.3 Hz, 6 H); ^{13}C NMR ($CDCl_3$, 75 MHz) δ 173.26, 171.12, 170.71, 170.29, 138.07, 128.65, 128.16, 98.65, 73.75, 73.42, 73.15, 71.86, 69.50, 68.60, 67.61, 62.05, 48.26, 36.93, 32.18, 29.96, 29.82, 29.56, 27.98, 25.94, 22.94, 21.22, 21.18, 21.00, 20.88, 14.37; HRMS (FAB) *m/z* for $C_{60}H_{101}NNaO_{14}$ ($[M+Na]^+$) 1082.7107 (100%), calc. 1082.7114.

3-16d. Same procedure as synthesis of **3-16a**, substituting with **3-13d** (64%). ^{1}H NMR ($CDCl_3$, 500 MHz) δ 7.33 (m, 4 H), 7.29 (m, 1 H), 6.27 (d, *J* = 9.2 Hz, 1 H), 5.41 (d, *J* = 2.4, 1 H), 5.24 (m, 2 H), 4.94 (dt, *J* = 10.3, 2.9 Hz, 1 H), 4.87 (d, *J* = 3.9 Hz, 1 H), 4.71 (d, *J* = 11.7 Hz, 1 H), 4.60 (d, *J* = 11.7 Hz, 1 H), 4.36 (tt, *J* = 9.3, 3.4 Hz, 1 H), 4.16 (t, *J* = 6.8 Hz, 1 H), 4.09 (m, 1 H), 4.03 (dd, *J* = 11.2, 6.8 Hz, 1 H), 3.82 (dd, *J* = 10.7, 3.4 Hz, 1 H), 3.65 (qd, *J* = 11.2, 3.4 Hz, 2 H), 2.17 (td, *J* = 7.7, 4.4 Hz, 2 H), 2.09 (s, 3 H), 2.08 (s, 3 H), 2.04 (s, 3 H), 1.99 (s, 3 H), 1.96 (s, 3 H), 1.70-1.56 (m, 4 H), 1.26 (br s, 68), 0.88 (t, *J* = 7.0 Hz, 6 H); ^{13}C NMR ($CDCl_3$, 125 MHz) δ 173.05, 170.83, 170.52, 170.27, 170.13, 170.00, 138.07, 128.52, 128.00, 98.73, 73.63, 73.18, 73.07, 72.08, 69.48, 68.48, 67.80, 67.02, 61.91, 48.23, 36.82, 32.07, 29.84, 29.71, 29.51, 29.45, 28.10, 25.78, 25.71, 22.82, 21.07, 21.01, 20.85, 20.81, 20.72, 14.25; HRMS (ESI) *m/z* for $C_{67}H_{116}NO_{14}$ ($[M+H]^+$) 1158.83782 (100%), calc. 1158.83903.

3-16e. Same procedure as synthesis of **3-16a**, substituting with **3-13e** (57%). ^{1}H NMR ($CDCl_3$, 300 MHz) δ 7.34 (m, 5 H), 6.48 (d, *J* = 9.6 Hz, 1 H), 5.45 (d, *J* = 2.4 Hz, 1 H), 5.32-5.23 (m, 2 H), 4.99-4.94 (m, 1 H), 4.90 (d, *J* = 3.6 Hz, 1 H), 4.73 (d, *J* = 11.7 Hz, 1 H), 4.62 (d, *J* = 11.7 Hz, 1 H), 4.37 (m, 1 H), 4.19-4.04 (m, 4 H), 3.85 (dd, *J* = 10.5, 3.3 Hz, 1 H), 3.67 (dd, *J* =11.1, 3.3 Hz, 1 H), 2.11 (s, 3 H), 2.07 (s, 3 H), 2.02 (s, 3 H), 2.02 (s, 3 H), 2.01 (s, 3 H), 1.99 (s, 3 H), 1.68 (m, 2 H), 1.27 (br s, 24 H), 0.9 (t, *J* = 7.2 Hz, 6 H); ^{13}C NMR ($CDCl_3$, 75 MHz) δ 171.06, 170.74, 170.48, 170.29, 170.24, 170.13, 138.10, 128.67, 128.19, 128.14, 127.79, 98.81, 72.12, 69.55, 68.62, 67.79, 67.42, 67.14, 62.12, 48.56, 32.17, 29.94, 29.90, 29.78, 29.61, 29.54, 28.23, 25.75, 23.51, 22.94, 21.23, 21.16, 21.00, 20.96, 20.88, 14.37; HRMS (FAB) *m/z* for $C_{43}H_{67}NNaO_{14}$ ($[M+Na]^+$) 844.4468 (100%), calc. 844.4454.

3-16f. Same procedure as synthesis of **3-16a**, substituting with **3-13f** (68%). ^{1}H NMR ($CDCl_3$, 500 MHz) δ 7.33 (m, 4 H), 7.29 (m, 1 H), 6.32 (d, *J* = 9.3 Hz, 1 H), 5.41 (d, *J* = 3.4, 1 H), 5.25 (dd, *J* = 10.2, 2.9 Hz, 2 H), 4.96 (dt, *J* = 10.2, 2.4 Hz, 1 H), 4.88 (d, *J* = 3.4 Hz, 1 H), 4.71 (d, *J* = 12.2 Hz, 1 H), 4.59 (d, *J* = 12.2 Hz, 1 H), 4.36 (m, 1 H), 4.16 (t, *J* = 6.3 Hz, 1 H), 4.12-4.01 (m, 2 H), 3.82 (dd, *J* = 10.7, 3.4 Hz, 1 H), 3.64 (qd, *J* = 11.2, 3.4 Hz, 2 H), 2.19-2.16 (m, 2 H), 2.09 (s, 3 H), 2.08 (s, 3 H), 2.04 (s, 3 H), 1.99 (s, 3 H), 1.97 (s, 3 H), 1.68-1.56 (m, 4 H), 1.26 (br s, 30 H), 0.88 (m, 6 H); ^{13}C NMR ($CDCl_3$, 125 MHz) δ 173.90, 170.89, 170.57, 170.32, 170.18, 170.06, 138.03, 128.53, 128.12, 128.03, 98.70, 73.60, 73.18, 73.07, 71.99, 69.44, 68.47, 67.76, 67.00, 61.93, 48.21, 36.81, 32.06, 31.85, 29.83, 29.79, 29.76, 29.72, 29.50, 29.45, 29.37, 29.16, 28.06, 25.78, 25.71, 22.83, 22.77, 21.10, 21.05, 20.88, 20.84, 20.76, 14.27, 14.22; HRMS (ESI) *m/z* for $C_{49}H_{79}NNaO_{14}$ ($[M+Na]^+$) 928.53939 (100%), calc. 928.53928.

3-16g. Same procedure as synthesis of **3-16a**, substituting with **3-13g** (56%). ^{1}H NMR ($CDCl_3$, 300 MHz) δ 7.40-7.20 (m, 5 H), 6.42 (dd, *J* = 9.3 Hz, 1 H), 5.43 (d, *J* = 3.3 Hz, 1 H), 5.29-5.24 (m, 2 H), 4.97-4.94 (m, 1 H), 4.90 (d, *J* = 3.6 Hz, 1 H), 4.74 (d, *J* = 12.0 Hz, 1 H), 4.61 (d, *J* = 12.0 Hz, 1 H), 4.41-4.35 (m, 1 H), 4.17-4.04 (m, 3 H), 3.84 (dd, *J* = 10.5, 3.6 Hz, 1 H), 3.71-3.60 (m, 2 H), 2.19-2.18 (m, 4 H), 2.12 (s, 3 H), 2.11 (s, 3 H), 2.06 (s, 3 H), 2.01 (s, 3 H), 1.99 (s, 3 H), 1.68-1.58 (m, 4 H), 1.27 (br s, 46 H), 0.90 (m, 6 H); ^{13}C NMR ($CDCl_3$, 75 MHz) δ 173.12, 171.81, 170.67, 170.64, 170.52, 170.38, 170.23, 136.55, 129.63, 129.72, 129.16, 99.62, 73.25, 73.13, 72.98, 71.76, 69.32, 68.46, 67.99, 67.41, 62.01, 48.36, 36.44, 32.12, 31.84, 29.82, 29.79, 29.56, 29.57, 29.32, 28.54, 25.86, 25.57, 22.79, 22.35, 21.24, 21.16, 20.98, 20.87, 14.70; HRMS (FAB) *m/z* for $C_{57}H_{95}NNaO_{14}$ ([M+Na]$^+$) 1040.6666 (100%), calc. 1040.6645.

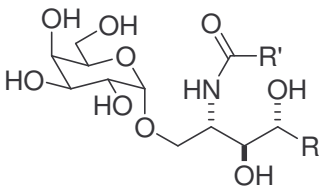

3-1 R = $C_{14}H_{29}$ R' = $C_{25}H_{51}$
3-2a R = C_5H_{11} R' = $C_{23}H_{47}$
3-2b R = C_2H_5 R' = $C_{23}H_{47}$
3-2c R = C_9H_{19} R' = $C_{23}H_{47}$
3-3a R = $C_{14}H_{29}$ R' = CH_3
3-3b R = $C_{14}H_{29}$ R' = C_7H_{15}
3-3c R = $C_{14}H_{29}$ R' = $C_{15}H_{31}$

3-2a. The waxy, protected glycosphingolipid (611 mg, 0.609 mmol) was dissolved in a solution of EtOH (95%) and EtOAc (20 mL; 1:1) and placed inside a hydrogenation vessel. Palladium on carbon (10%, 300 mg) was added slowly and the container filled with H_2 (200 psi). After 12 h, the vessel was evacuated, the suspension was filtered through a Celite plug using EtOAc as a diluent, the solution concentrated in vacuo, and purified performed by flash chromatography (SiO_2, EtOAc:Hex 1:1) to yield a white, sticky solid (458 mg, 82%, R_f = 0.25, EtOAc:Hex 1:2). ^{1}H NMR ($CDCl_3$, 500 MHz) δ 6.47 (d, *J* = 9.2 Hz, 1 H), 5.42 (d, *J* = 2.9 Hz, 1 H), 5.24 (dd, *J* = 9.0, 3.6 Hz, 1 H), 5.06 (dd, *J* = 10.2, 3.2 Hz, 1 H), 5.00 (dt, *J* = 9.8, 3.4, 1 H), 4.86 (d, *J* = 3.9, 1 H), 4.44 (tt, *J* =

9.0, 3.2 Hz, 1 H), 4.15 (t, *J* = 6.3 Hz, 1 H), 4.10 (m, 1 H), 4.05 (dd, *J* = 11.2, 7.3 Hz, 1 H), 3.91 (td, *J* = 10.7, 2.9, 1 H), 3.77 (dd, *J* = 10.2, 3.9 Hz, 1 H), 3.49 (dd, *J* = 10.2, 3.4 Hz, 1 H), 2.77 (d, *J* = 11.2 Hz, 1 H), 2.24 (t, *J* = 7.5 Hz, 2 H), 2.13 (s, 3 H), 2.12 (s, 3 H), 2.05 (s, 3 H), 2.04 (s, 6 H), 1.70-1.58 (m, 4 H), 1.26 (br s, 46 H), 0.88 (m, 6 H); ^{13}C NMR ($CDCl_3$, 125 MHz) δ 173.02, 171.06, 170.97, 170.76, 170.44, 170.13, 99.50, 72.82, 72.05, 70.72, 68.06, 67.96, 67.00, 66.79, 61.95, 61.95, 47.72, 36.64, 31.96, 31.49, 29.73, 29.57, 29.44, 29.39, 28.14, 25.70, 25.20, 22.72, 22.54, 21.02, 20.92, 20.88, 20.68, 20.62, 14.16, 14.01; HRMS (ESI) *m/z* for $C_{49}H_{87}NNaO_{14}$ ($[M+Na]^+$) 936.60324 (100%), calc. 936.60188. The pentaacetate was dissolved in a minimal amount of MeOH (7 mL) in a conical vial followed by addition of a solution of NaOMe (prepared by cleaning a 300 mg chunk of Na metal in 10 mL of MeOH for 1 m, then dissolving in 2 mL fresh MeOH). After 5 m, a white precipitate formed. The reaction was monitored by ESI-MS for disappearance of starting material, which was complete after 20 m. The reaction was centrifuged (4500 rpm, 5 m), the supernatant was removed, and fresh MeOH (2 mL) was added. After 5 m of agitation, the vial was centrifuged, rinsed, and agitated again twice more. The solid was dried in vacuo then dissolved with sonication in a solution of MeOH and $CHCl_3$ (5 mL; 3:17, respectively). The solution was purified by flash chromatography (SiO_2, MeOH:$CHCl_3$ 3:17) and the resulting fine, white granules were dissolved in DMSO (25 mL) with sonication and lyophilized to yield a fluffy white powder (335 mg, 95%, R_f = 0.33 MeOH:$CHCl_3$ 3:17). ^{1}H NMR ($CDCl_3$:CD_3OD 3:1, 500 MHz) δ 7.34 (d, *J* = 8.3 Hz, 1 H), 4.90 (d, *J* = 3.9 Hz, 1 H), 3.94 (d, *J* = 3.4 Hz, 1 H), 3.89 (m, 1 H), 3.81-3.66 (m, 7 H), 3.57-3.51 (m, 2 H), 2.20 (t, *J* = 7.8 Hz, 2 H), 1.71-1.52 (m, 4 H), 1.26 (m, 46 H), 0.89 (m, 6 H); ^{13}C NMR ($CDCl_3$:CD_3OD 3:1, 125 MHz)

δ 174.53, 99.66, 74.78, 71.89, 70.66, 70.20, 69.69, 68.85, 67.29, 61.82, 50.40, 36.47, 32.52, 31.81, 29.60, 29.47, 29.33, 29.28, 25.80, 25.36, 22.56, 13.89, 13.84; HRMS (ESI) *m/z* for $C_{39}H_{77}NNaO_9$ ($[M+Na]^+$) 726.54899 (100%), calc. 726.54905; mp 145°C. Anal. Calc. for $C_{39}H_{77}NO_9$: C, 66.53; H, 11.02; N, 1.99. Found: C, 66.20; H, 11.00; N, 2.29.

3-2b. Same procedure as synthesis of **3-2a** (84% over two steps). ^{1}H NMR (pyridine-d_5, 500 MHz) δ 8.55 (d, *J* = 9.0 Hz, 1 H), 5.60 (d, *J* = 3.59 Hz, 1 H), 5.29 (m, 1H), 4.70-4.66 (m, 2 H), 4.57 (d, *J* = 2.4 Hz, 1 H), 4.52 (t, *J* = 5.9 Hz, 1 H), 4.46-4.38 (m, 4 H), 4.30 (dd, *J* = 8.3, 3.9 Hz, 1 H), 4.21 (m, 1 H), 2.46 (t, *J* = 7.5 Hz, 2 H), 2.31-2.28 (m, 1 H), 1.88-1.78 (m, 3 H), 1.26 (br s, 40 H), 0.87 (t, *J* = 6.7 Hz, 6 H); ^{13}C NMR (pyridine-d_5, 125 MHz) δ 171.51, 99.76, 74.78, 71.98, 71.33, 69.87, 69.25, 68.56, 66.76, 60.90, 49.64, 35.04, 30.39, 28.29, 28.12, 28.07, 28.01, 27.88, 25.48, 24.66, 21.21, 12.55, 9.00; HRMS (FAB) *m/z* for $C_{36}H_{71}NNaO_9$ ($[M+Na]^+$) 684.5026 (100%), calc. 684.5021.

3-2c. Same procedure as synthesis of **3-2a** (86% over two steps). ^{1}H NMR (pyridine-d_5, 500 MHz) δ 8.51 (d, *J* = 8.5 Hz, 1H), 6.68 (d, *J* = 6 Hz, 1 H), 6.58 (t, *J* = 5.0 Hz, 1 H), 6.49 (d, *J* = 6.0 Hz, 1 H), 6.37 (d, *J* = 4.5 Hz, 1 H), 6.12 (d, *J* = 5.5 Hz, 1 H), 5.60 (d, *J* = 4.0 Hz, 1 H), 5.29-5.28 (m, 1 H), 4.71-4.66 (m, 1 H), 4.57 (m, 1 H), 4.53 (t, *J* = 6.0 Hz, 1 H), 4.46-4.33 (m, 6 H), 2.45 (t, *J* = 7.0 Hz, 2 H), 2.28 (m, 1 H), 1.90-1.80 (m, 3 H), 1.67 (m, 1 H), 1.26 (br s, 54 H), 0.88 (m, 6 H); ^{13}C NMR (pyridine-d_5, 125 MHz) δ 173.26, 101.52, 76.54, 73.76, 73.10, 71.62, 71.03, 70.30, 68.54, 62.68, 51.38, 36.81, 32.15, 30.05, 29.88, 29.82, 29.64, 27.24, 26.42, 22.97, 14.32, 10.76; HRMS (FAB) *m/z* for $C_{43}H_{85}NNaO_9$ ($[M+Na]^+$) 782.6130 (100%), calc. 782.6117.

3-3a. Same procedure as synthesis of **3-2a** (89% over two steps). ^{1}H NMR (pyridine-d_5, 500 MHz) δ 8.50 (d, J = 9.0 Hz, 1 H), 6.71 (s, 1 H), 6.59 (s, 1 H), 6.47 (d, J = 6.0 Hz, 1 H), 6.38 (s, 1 H), 6.16 (s, 1 H), 5.59 (d, J = 3.5 Hz, 1 H), 4.70-4.66 (m, 2 H), 4.56 (s, 1 H), 4.52 (t, J = 6.0 Hz, 1 H), 4.46-4.4.37 (m, 4 H), 4.28 (s, 1 H), 4.21 (s, 1 H), 2.45 (t, J = 7.5 Hz, 2 H), 2.32-2.27 (m, 1 H), 1.90-1.79 (m, 3 H), 1.26 (m, 40 H), 0.87 (t, J = 5.0 Hz, 3 H); ^{13}C NMR (pyridine-d_5, 125 MHz) δ 171.51, 99.76, 74.78, 71.98, 71.33, 69.87, 69.25, 68.56, 66.76, 60.90, 49.64, 35.04, 30.39, 28.29, 28.12, 28.07, 28.01, 27.88, 25.48, 24.66, 21.21, 12.55, 9.00; HRMS (FAB) *m/z* for $C_{36}H_{71}NNaO_9$ ([M+Na]$^+$) 684.5026 (100%), calc. 684.5021.

3-3b. Same procedure as synthesis of **3-2a** (62% over two steps). ^{1}H NMR (pyridine-d_5, 500 MHz) δ 8.48 (d, J = 8.8 Hz, 1H), 7.02 (br s, 1 H), 6.68 (br s, 1 H), 6.56 (t, J = 5.4 Hz, 1 H), 6.48 (d, J = 5.4 Hz, 1 H), 6.35 (d, J = 2.9 Hz, 1 H), 6.12 (d, J = 5.4 Hz, 1 H), 5.57 (d, J = 3.4 Hz, 1 H), 5.26 (dt, J = 8.3, 3.9, 1 H), 4.69-4.64 (m, 2 H), 4.55 (br s, 1 H), 4.51 (t, J = 5.9 Hz, 1 H), 4.44-4.38 (m, 4 H), 4.32 (m, 2 H), 2.42 (td, J = 7.5, 1.4 Hz, 2 H), 2.40-2.24 (m, 1 H), 1.96-1.84 (m, 2 H), 1.77 (m, 2 H), 1.72-1.60 (m, 1 H), 1.24 (br s, 30 H), 0.86 (t, J = 6.8 Hz, 3 H) 0.79 (t, J = 6.9 Hz, 3 H); ^{13}C NMR (pyridine-d_5, 125 MHz) δ 173.61, 101.89, 77.09, 73.42, 72.84, 71.97, 71.36, 70.66, 68.98, 63.02, 51.77, 37.14, 34.73, 32.49, 32.27, 30.73, 30.52, 30.37, 30.30, 29.99, 29.74, 26.87, 26.72, 23.31, 23.23, 14.66, 14.59; HRMS (FAB) *m/z* for $C_{32}H_{63}NNaO_9$ ([M+Na]$^+$) 628.4412 (100%), calc. 628.4395.

3-3c. Same procedure as synthesis of **3-2a** (90% over two steps). ^{1}H NMR (pyridine-d_5, 500 MHz) δ 8.52 (d, J = 9.0 Hz, 1 H), 5.60 (d, J = 3.4 Hz, 1 H), 5.29 (m, 1 H), 4.71-4.66 (m, 2 H), 4.57 (d, J = 3.0 Hz, 1 H), 4.53 (t, J = 6.0 Hz, 1 H), 4.46-4.34 (m,

6 H), 2.45 (t, J = 7.0 Hz, 2 H), 2.30 (m, 1 H), 1.92-1.90 (m, 2 H), 1.82 (t, J = 4.0 Hz, 2 H), 1.64 (m, 1 H), 1.24 (br s, 46 H), 0.87 (t, J = 7.0 Hz, 6 H); ^{13}C NMR (pyridine-d_5, 125 MHz) δ 168.67, 96.99, 72.18, 68.51, 67.92, 67.06, 66.44, 65.75, 64.09, 58.10, 46.85, 32.23, 29.79, 27.57, 25.81, 25.59, 25.44, 25.37, 25.30, 25.25, 25.19, 25.06, 21.95, 21.84, 18.38, 9.73; HRMS (FAB) m/z for $C_{40}H_{79}NNaO_9$ ([M+Na]$^+$) 740.5659 (100%), calc. 740.5647.

3-1. Same procedure as synthesis of **3-2a** (78% over two steps). ^{1}H NMR (pyridine-d_5, 500 MHz) δ 8.50 (d, J = 10.8 Hz, 1 H), 6.12 (br s, 6 H), 5.58 (d, J = 3.9 Hz, 1 H), 5.27 (d, J = 3.9 Hz, 1 H), 4.69-4.64 (m, 2 H), 4.55 (d, J = 2.0 Hz, 1 H), 4.52 (t, J = 5.6 Hz, 1 H), 4.44-4.38 (m, 4 H), 4.33 (m, 2 H), 2.45 (t, J = 7.3 Hz, 2 H), 2.29 (m, 1 H), 1.98-1.85 (m, 2 H), 1.84-1.76 (m, 2 H), 1.68 (m, 1 H), 1.24 (m, 66 H), 0.87 (m, 6 H); ^{13}C NMR (pyridine-d_5, 125 MHz) δ 173.61, 101.93, 77.11, 73.44, 72.89, 71.99, 71.37, 70.69, 69.05, 63.04, 51.81, 37.18, 34.73, 32.52, 30.76, 30.55, 30.41, 30.27, 30.22, 30.15, 30.02, 26.90, 26.79, 23.31, 23.34, 14.68; HRMS (ESI) m/z for $C_{50}H_{99}NNaO_9$ ([M+Na]$^+$) 880.72144 (100%), calc. 880.72120.

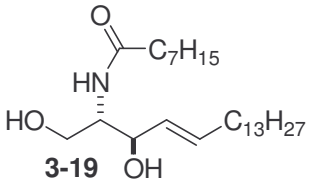

3-19

3-19. Octanoic anhydride (1.0 mL, 3.6 mmol; prepared from stirring octanoic acid, triethylamine, trichloroactonitrile, and triphenylphosphine in CH_2Cl_2 for 4 h) was dissolved in anhydrous THF (15 mL) and warmed to reflux. A solution of sphingosine (**3-18**) (1.02 g, 3.41 mmol) and Et_3N (2 mL, 27.2 mmol) in anhydrous THF (7 mL) was added and stirred for 1 h. The solvent was removed in vacuo and the residue purified by

flash chromatography (SiO_2, MeOH:CH_2Cl_2 5:95) yielding a white solid (1.41 g, 97%, R_f = 0.31 MeOH:CH_2Cl_2 5:95). ^{1}H NMR ($CDCl_3$, 500 MHz) δ 6.87 (d, *J* = 7.8 Hz, 1 H), 5.73 (m, 1 H), 5.48 (dd, *J* = 15.6, 6.8 Hz, 1 H), 4.23 (m, 1 H), 3.87 (m, 2 H), 3.66 (dd, *J* = 12.2, 4.4 Hz, 1 H), 2.29 (t, *J* = 7.3 Hz, 1 H), 2.21 (t, *J* = 7.3 Hz, 2 H), 2.03 (dt, *J* = 7.3, 6.8 Hz, 2 H), 1.60 (m, 3 H), 1.28 (br s, 30 H), 0.88 (t, *J* = 6.8 Hz, 6 H); ^{13}C NMR ($CDCl_3$, 125 MHz) δ 174.76, 133.94, 128.86, 73.62, 61.94, 54.96, 36.74, 32.48, 32.01, 31.83, 31.78, 29.80, 29.76, 29.67, 29.46, 29.38, 29.23, 29.17, 29.07, 25.94, 25.00, 22.76, 22.72, 14.16, 14.12; HRMS (FAB) *m/z* for $C_{26}H_{51}NNaO_3$ ($[M+Na]^+$) 448.3773 (100%), calc. 448.3761.

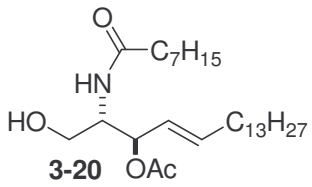

3-20

3-20. Ceramide **3-19** (1.41 g, 3.31 mmol) was selectively protected at the primary alcohol by dissolving in anhydrous THF (15 mL) at 60°C and adding TBSCl (1.50 g, 9.93 mmol) and imidazole (676 mg, 9.93 mmol). The temperature was increased to 80°C and allowed to proceed for 10 m before quenching with water (10 mL). The aqueous layer was extracted with EtOAc (3 x 15 mL), followed by a brine wash, drying with Na_2SO_4, and concentration. The resulting colorless oil was dissolved in THF (10 mL) and acetylated with acetic anhydride (1 mL), triethylamine (1 mL), and DMAP (100 mg, 0.818 mmol) at room temperature for 10 m. The solvent was removed in vacuo and the crude oil was purified by flash chromatography (SiO_2, EtOAc:Hex 1:8) to provide a colorless oil (1.24 g, 62%, R_f = 0.21 EtOAc:Hex 1:8). ^{1}H NMR ($CDCl_3$, 500 MHz) δ 5.73 (m, 1 H), 5.70 (d, *J* = 9.7 Hz, 1 H), 5.41 (dd, *J* = 15.6, 7.3 Hz, 1 H), 5.28 (t, *J* = 7.3

Hz, 1 H), 4.22 (m, 1 H), 3.74 (dd, *J* = 10.3, 2.9 Hz, 1 H), 3.57 (dd, *J* = 10.3, 4.4, 1 H), 2.15 (td, *J* = 7.3, 2.9 Hz, 1 H), 2.03 (s, 3 H), 2.00 (dt, *J* = 7.3, 6.8 Hz, 2 H), 1.65-1.55 (m, 2 H), 1.24 (br s, 30 H), 0.88 (m, 15 H), 0.03 (d, *J* = 2.0 Hz, 6 H); ^{13}C NMR ($CDCl_3$, 125 MHz) δ 172.84, 170.01, 136.99, 125.20, 73.67, 61.69, 52.03, 37.15, 34.21, 32.51, 32.11, 31.87, 29.88, 29.70, 29.55, 29.42, 29.37, 29.24, 29.18, 26.01, 25.94, 24.98, 22.87, 22.81, 21.40, 18.39, 14.30, 14.24, -5.30, -5.40; HRMS (FAB) *m/z* for $C_{34}H_{67}NNaO_4Si$ ($[M+Na]^+$) 604.4739 (100%), calc. 604.4732. The protected ceramide (1.00 g, 1.72 mmol) was taken back up into THF (7 mL) and aqueous HF (2 mL, 49%). TLC (EtOAc:Hex 2:1) showed an immediate disappearance of starting material and formation of the desilylated ceramide (R_f = 0.30). The reaction was poured carefully into saturated aqueous $NaHCO_3$ (10 mL), extracted with EtOAc (10 mL), rewashed with $NaHCO_3$ (10 mL), back extracted with EtOAc (2 x 10 mL), washed with brine (5 mL), and dried thoroughly with Na_2SO_4 before concentrating. Purification by flash chromatography (SiO_2, EtOAc:Hex 2:1) yielded the product as a white powder (750 mg, 93%). ^{1}H NMR ($CDCl_3$, 500 MHz) δ 6.36 (d, *J* = 9.3 Hz, 1 H), 5.70 (m, 1 H), 5.36 (dd, *J* = 15.6, 7.3 Hz, 1 H), 5.24 (t, *J* = 7.3 Hz, 1 H), 4.09 (m, 1 H), 3.71 (br s, 1 H), 3.55 (m, 2 H), 2.09 (td, *J* = 7.3, 2.9 Hz, 1 H), 1.98 (s, 3 H), 1.94 (dt, *J* = 7.3, 6.8 Hz, 2 H), 1.51 (m, 2 H), 1.17 (br s, 30 H), 0.80 (t, *J* = 6.8 Hz, 6 H); ^{13}C NMR ($CDCl_3$, 125 MHz) δ 173.65, 170.63, 137.07, 124.83, 73.84, 61.26, 52.95, 36.78, 32.35, 31.93, 31.75, 29.71, 29.66, 29.53, 29.37, 29.28, 29.12, 29.00, 25.82, 22.69, 22.64, 21.18, 14.09, 14.05; HRMS (FAB) *m/z* for $C_{28}H_{53}NNaO_4$ ($[M+Na]^+$) 490.3878 (100%), calc. 490.3867.

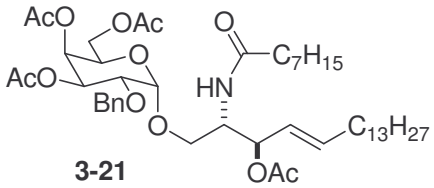

3-21

3-21. Same procedure as synthesis of **3-16a**, substituting with **3-20** (70%). ^{1}H NMR ($CDCl_3$, 500 MHz) δ 7.35 (m, 5 H), 5.86 (d, *J* = 9.3 Hz, 1 H), 5.65 (m, 1 H), 5.42 (d, *J* = 2.9, 1 H), 5.34 (dd, *J* = 15.6, 7.3 Hz, 1 H), 5.27 (m, 1 H), 4.93 (d, *J* = 3.4 Hz, 1 H), 4.73 (d, *J* = 11.7 Hz, 1 H), 4.64 (d, *J* = 11.7 Hz, 1 H), 4.34 (m, 1 H), 4.18-4.01 (m, 4 H), 3.86 (dd, *J* = 10.7, 3.4 Hz, 1 H), 3.71 (dd, *J* = 10.7, 3.9 Hz, 1 H), 3.63 (dd, *J* = 10.7, 2.9 Hz, 1 H), 2.13 (t, *J* = 6.3 Hz, 2 H), 2.11 (s, 3 H), 2.05 (s, 3 H), 2.03 (s, 3 H), 1.99 (s, 3 H), 1.95 (dt, *J* = 7.3, 6.8 Hz, 2 H), 1.58 (m, 2 H), 1.26 (br s, 30), 0.88 (t, *J* = 6.8 Hz, 6 H); ^{13}C NMR ($CDCl_3$, 125 MHz) δ 172.82, 170.839, 170.10, 170.03, 169.96, 137.96, 137.58, 128.53, 128.44, 127.94, 127.84, 127.63, 124.89, 98.29, 73.70, 73.58, 73.12, 69.56, 68.34, 67.18, 66.70, 61.86, 50.69, 36.79, 32.29, 31.95, 31.75, 29.73, 29.68, 29.53, 29.39, 29.27, 29.09, 28.94, 25.71, 22.72, 22.67, 21.26, 20.78, 20.69, 20.65, 14.15, 14.10; HRMS (FAB) *m/z* for $C_{47}H_{75}NNaO_{12}$ ($[M+Na]^+$) 868.5190 (100%), calc. 868.5181.

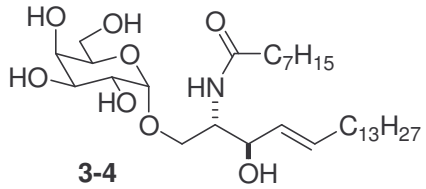

3-4

3-4. Sodium metal (63 mg) was added to liquid ammonia (10 mL) under N_2 at -78 °C and the mixture was stirred until a blue color persisted. Protected GSL **3-21** (95 mg, 0.11 mmol) in anhydrous THF (3 mL) was then added to the blue solution and stirred for 75 m. The reaction was quenched by addition of MeOH (5 mL), ammonia was removed under a stream of N_2 overnight, and the residue was purified by flash chromatography

(SiO_2, MeOH:$CHCl_3$ 15:85). The α-galactosylceramide was lyophilized to remove any residual water yielding a white fluffy solid (35 mg, 53%). ^{1}H NMR (DMSO-d_6, 500 MHz) δ 7.51 (d, *J* = 8.8 Hz, 1 H), 5.53 (m, 1 H), 5.35 (dd, *J* = 15.2, 6.8 Hz, 1 H), 4.86 (d, *J* = 5.9 Hz, 1 H), 4.65 (d, *J* = 3.4 Hz, 1 H), 4.50 (m, 2 H), 4.37 (d, *J* = 4.4 Hz, 1 H), 4.18 (d, *J* = 8.3 Hz, 1 H), 3.93 (dt, *J* = 7.3, 5.9 Hz, 1 H), 3.76 (m, 1 H), 3.68 (m, 1 H), 3.58-3.46 (m, 6 H), 3.41 (m, 1 H), 2.03 (td, *J* = 7.3, 2.9 Hz, 2 H), 1.94 (m, 2 H), 1.45 (m, 2 H), 1.23 (br s, 30 H), 0.85 (m, 6 H); ^{13}C NMR (DMSO-d_6, 125 MHz) δ 171.74, 131.34, 131.18, 99.74, 71.22, 70.50, 69.77, 68.87, 68.74, 66.66, 60.57, 53.17, 35.61, 31.74, 31.30, 31.24, 29.07, 29.02, 28.80, 28.71, 28.63, 25.41, 22.13, 22.10, 13.96; HRMS (FAB) *m/z* for $C_{32}H_{61}NNaO_8$ ([M+Na]$^+$) 610.4291 (100%), calc. 610.4289.

3.5 References

1) Pier, G. B.; Lyczak, J. B.; Wetzler, L. M., Eds. *Immunology, Infection, and Immunity*; ASM Press: Washington, DC, 2004.

2) Delves, P. J.; Roitt, I. M. *N. Engl. J. Med.* **2000**, *343*, 108.

3) Mosman, T. R.; Cherwinski, H.; Bond, M. W.; Giedlin, M. A.; Coffman, R. L. *J. Immunol*. **1986**, *136*, 2348.

4) Janeway, C.; Travers, P.; Walport, M.; Shlomchik, M. *Immunobiology: The Immune System in Health and Disease*, 6th Edition; Garland Science: New York, NY 2005.

5) Mosmann, T. R.; Sad S. *Immunol. Today* **1996**, *17*, 138.

6) O'Hehir, R. E.; Garman, R. D.; Greenstein, J. L.; Lamb, J. R. *Annu. Rev. Immunol*. **1991**, *9*, 67.

7) Nicholson, L. B.; Kuchroo, V. K. *Curr. Opin. Immunol*. **1996**, *8*, 837.

8) Steinman, L. *Neuron* **1999**, *24*, 511.

9) Brigl, M.; Brenner, M. D. *Annu. Rev. Immunol*. **2004**, *22*, 817.

10) Cui, J.; Shin, T.; Kawano, T.; Sato, H.; Kondo, E.; Toura, I.; Kaneko, Y.; Koseki, H.; Kanno, M.; Taniguchi, M. *Science* **1997**, *278*, 1623.

11) Shin, T.; Nakayama, T.; Akutsu, Y.; Motohashi, S.; Shibata, Y.; Harada, M.; Kamada, N.; Shimizu, C.; Shimizu, E.; Saito, T.; Ochiai, T.; Taniguchi M. *Int. J. Cancer* **2001**, *91*, 523.

12) (a) Sahir, S. M. A.; Cheng, O.; Shaulov, A.; Koezuka, Y.; Bubley, G. J.; Wilson, S. B.; Balk, S. P.; Exley, M. A. *J. Immunol*. **2001**, *167*, 4046. (b) Giaccone, G.; Punt, C. J. A.; Ando, Y.; Ruijter, R.; Nishi, N.; Peters, M.; von Blomberg, B. M. E.; Scheper, R. J.; van der Vliet, H. J. J.; van den Eertwegh, A. J. M.; Roelvink, M.; Beijnen, J.; Zwierzina, H.; Pinedo, H. M. *Clin. Canc. Res.* **2002**, *8*, 3702. (c) Kenna, T.; Mason, L. G.; Porcelli, S. A.; Koezuka, Y.; Hegarty, J. E.; O'Farrelly, C.; Doherty, D. G. *J. Immunol*. **2003**, *171*, 1775.

13) Zouali, M., Ed. In *Molecular Autoimmunity*; Springer: New York, NY, 2005.

14) Godfrey, D. I.; Kronenberg, M. *J. Clin. Invest*. **2004**, *114*, 1379.

15) Morita, M.; Motoki, K.; Akimoto, K.; Natori, T.; Sakai, T.; Sawa, E.; Yamaji, K.; Koezuka, Y.; Kobayashi, E.; Fukushima, H. *J. Med. Chem*. **1995**, *38*, 2176.

16) Fujii, S.; Shimizu, K.; Kronenberg, M.; Steinman, R. M. *Nat. Immunol*. **2002**, *3*, 867.

17) Hong, S.; Wilson, M. T.; Serizawa, I.; Wu, L.; Singh, N.; Naidenko, O. V.; Miura, T.; Haba, T.; Scherer, D. C.; Wei, J.; Kronenberg, M.; Koezuka, Y.; van Kaer, L. *Nat. Med*. **2001**, *7*, 1052.

18) Singh, A. K.; Wilson, M. T.; Hong, S.; Olivares-Villagomez, D.; Du, C.; Stanic, A. K.; Joyce, S.; Sriram, S.; Koezuka, Y.; van Kaer, L. *J. Exp. Med*. **2001**, *194*, 1801.

19) Pal, E.; Tabira, T.; Kawano, T.; Taniguchi, M.; Miyake, S.; Yamamura, T. *J. Immunol*. **2001**, *166*, 662.

20) Singh, N.; Hong, S.; Scherer, D. C.; Serizawa, I.; Burdin, N.; Kronenberg, M.; Koezuka, Y.; van Kaer, L. *J. Immunol*. **1999**, *163*, 2373.

21) Burdin, N.; Brossay, L.; Kronenberg, M. *Eur. J. Immunol*. **1999**, *29*, 2014.

22) Miyamoto, K.; Miyake, S.; Yamamura, T. *Nature* **2001**, *413*, 531.

23) Goff, R. D.; Gao, Y.; Mattner, J.; Zhou, D.; Yin, N.; Cantu, C., III; Teyton, L.; Bendelac, A.; Savage, P. B. *J. Am. Chem. Soc*. **2004**, *126*, 13602. Figures 3.6-3.8 are reproduced in part with permission, Copyright 2004 American Chemical Society.

24) (a) Gigg, J.; Gigg, R.; Warren, C. D. *J. Chem. Soc. C* **1966**, 1872. (b) Mulzer, J.; Brand C. *Tetrahedron* **1986**, *42*, 5961. (c) Schmidt, R. R.; Maier, T. *Carbohydr. Res*. **1988**, *174*, 169. (d) Murakami, T.; Minamikawa, H.; Hato, M. *Tetrahedron Lett*. **1994**, *35*, 745.

25) Chiu, H.-Y.; Tzou, D.-L. M.; Patkar, L. N.; Lin, C.-C. *J. Org. Chem*. **2003**, *68*, 5788.

26) Lin, C.-C.; Fan, G.-T.; Fang, J.-M. *Tetrahedron Lett*. **2003**, *44*, 5281.

27) Shirota, O.; Nakanishi, K.; Berova, N. *Tetrahedron* **1999**, *55*, 13643.

28) Garner, P.; Park, J. M. *J. Org. Chem. 1987*, **52**, 2361.

29) Campbell, A. D.; Raynham, T. M.; Taylor, R. M. *Synthesis* **1998**, *8*, 1707.

30) VanRheenen, V.; Kelly, R. C.; Cha, D. Y. *Tetrahedron Lett*. **1976**, *23*, 1973.

31) Hanessian, S.; Banoub, J. *Methods Carbohydr. Chem*. **1980**, *8*, 247.

32) Garner, P.; Park, J. M.; Malecki, E. *J. Org. Chem*. **1988**, *53*, 4395.

33) Benlagha, K.; Weiss, A.; Beavis, A,; Teyton, L.; Bendelac, A. *J. Exp. Med*. **2000**, *191*, 1895.

34) Zajonc, D. M.; Cantu, C., III; Mattner, J.; Zhou, D.; Savage, P. B.; Bendelac, A.; Wilson, I. A.; Teyton, L. *Nat. Immunol*. **2005**, *6*, 810. Figures 3.10 and 3.11 are adapted by permission, Copyright 2005 Macmillan Publishers Ltd.

35) Koch, M.; Stronge, V. S.; Shepherd, D.; Gadola, S. D.; Mathew, B.; Ritter, G.; Fersht, A. R.; Besra, G. S.; Schmidt, R. R.; Jones, E. Y.; Cerundolo, V. *Nat. Immunol*. **2005**, *6*, 819.

36) Wu, D.; Zajonc, D. M.; Fujio, M.; Sullivan, B. S.; Kinjo, Y.; Kronenberg, M.; Wilson, I. A.; Wong, C.-H. *Proc. Nat. Acad. Sci. USA* **2006**, *103*, 3972. Figure 3.17 is reproduced with permission, Copyright 2006 National Academy of Sciences.

37) Kamada, K.; Iijima, H.; Kimura, K.; Harada, M.; Sminizu, E.; Motohashi, S.; Kawano, T.; Shinkai, H.; Nakayama, T.; Sakai, T.; Brossay, L.; Kronenberg, M.; Taniguchi, M. *Internat. Immunol*. **2001**, *13*, 853.

38) Zeng, Z.-H.; Castano, A. R.; Segelke, B. W.; Stura, E. A.; Peterson, P. A.; Wilson, I. A. *Science* **1997**, *277*, 339.

39) Oki, S.; Chiba, A.; Yamamura, T.; Miyake, S. *J. Clin. Invest*. **2004**, *113*, 1631.

40) Lee, P. T.; Benlagha, K.; Teyton, L.; Bendelac, A. *J. Exp. Med*. **2002**, *195*, 637.

41) Roark, J. H.; Park, S.-H.; Jayawardena, J.; Kavita, U.; Shannon, M.; Bendelac, A. *J. Immunol*. **1998**, *160*, 3121.

42) Bezbradica, J. S.; Stanic, A. K.; Matsuki, N.; Bour-Jordan, H.; Bluestone, J. A.; Thomas, J. W.; Unutmaz, D.; Van Kaer, L.; Joyce, S. *J. Immunol*. **2005**, *174*, 4696.

43) Van Kaer, L. *Immunol. Cell. Biol*. **2004**, *82*, 315.

CHAPTER 4.

STRUCTURE-ACTIVITY RELATIONSHIP STUDIES OF *N*-ALKENOYL GLYCOSPHINGOLIPIDS AND NKT CELL ACTIVITY

4.1 Introduction

It has been recognized that the length of the *N*-acyl chain of glycosphingolipid ceramides can influence the stimulatory activity of natural killer T cells, specifically those populations with the mVα14 or hVα24 invariant receptors. Longer amide groups (≥ C24) tend to promote a proinflammatory function[1] and those that are shorter (≤ C8) cause a bias toward an immunomodulatory role.[2] As was mentioned in Chapter 3, the reason for this inclination is not known although several hypotheses have been proffered.[3] One of these is based on the premise that analog compounds of αGalCer bind to CD1d with an altered relationship. In other words, changes in the structure of αGalCer, such as shortening of the ceramide alkyl groups or deletion of sphingoid hydroxides, could cause orientation of the exposed polar head group in a fashion other than that of αGalCer when restricted by CD1d. Such a change may cause the NKT cell receptor to recognize it in an different manner[4] or produce weaker binding to CD1d resulting in accelerated 'off rates.'[5] According to these propositions, the resulting bias in natural killer T cell activity would occur due to an alternative CD1d-GSL association.

To more thoroughly uncover the nature of varying NKT cell responses through the use of GSLs as antigens, further structure-activity relationship work is required. An effective way to provide several structural analogs of the model antigen αGalCer for further study would be simple modification of the GSL ceramide. As was previously

seen, alteration of this segment gave drastically different results in the type of NKT cell activity.[2] Implementing other changes in the lipid portion might also yield further information about the antigenic nature of GSLs on NKT cells due to the association that must occur between ceramide and CD1d for effective TCR presentation. Changing the sphingoid base to one with an unnatural length required syntheses with an increased number of steps, while only modifying the type of amide allowed a simplified procedure to be used.

Besides truncation of the amide, the only other modification of this group had been addition of bulky appendages (e.g., prodan and biotin).[6] This type of derivatization suffered from two problems: addition of synthetic steps to make the altered acyl group and decreased stimulatory activity due to installation of these functionalities at the acyl terminus (see Chapter 2, section 2.1).[7] A simpler way to create multiple GSLs for immunological evaluation would be using an array of commercially-available lipophilic carboxylic acids to introduce variation on the amide tail. This could accomplish two goals at one time: probing the binding pocket of CD1d to find ligands that may have a more intimate association and aiding in ligand solubility for biological assays.

Before the structure of ligand-bound CD1d had been solved,[8] it was thought that adding permanent bends in the ceramide tails of αGalCer might improve binding, which could possibly heighten the overall immune response given by NKT cells. Examination of the original crystal structure of murine CD1d shows that its two binding pockets are not straight but rather angle away from the interior of the protein. The A' pocket curls around clockwise from the point of insertion and the F' pocket has a slight curve aiming down towards the floor and exterior of the binding cavity.[9] Addition of an invarying

curve(s) in GSL alkyl chains may allow compounds to fit more snugly into CD1d, decreasing any tendency to dissociate, and potentially increasing antigenic efficacy. Incorporation of such a feature could be done with unsaturated alkenes in the *Z* configuration or cyclopropyl rings, which could conceivably be made in one step from an alkene using Simmons-Smith reaction conditions.[10]

CD1d shares homology and basic structural features with those of CD1b, which can be used as a model to indicate that kinking of the lipid portion of the GSL ceramide may be beneficial to overall binding. There is evidence from the crystal structure of CD1b that a natural ligand has these types of crimping substructures located at bends in the protein binding groove. When CD1b was cocrystallized with a bound mycobacterial glucose monomycolate (GMM), a homogenous group of glycolipids composed of a variety of dialkyl mycolic acids, the meromycolate chain of the ligand was found to curl throughout the A'-T'-F' superchannel (Figure 4.1). The two *Z*-alkenes

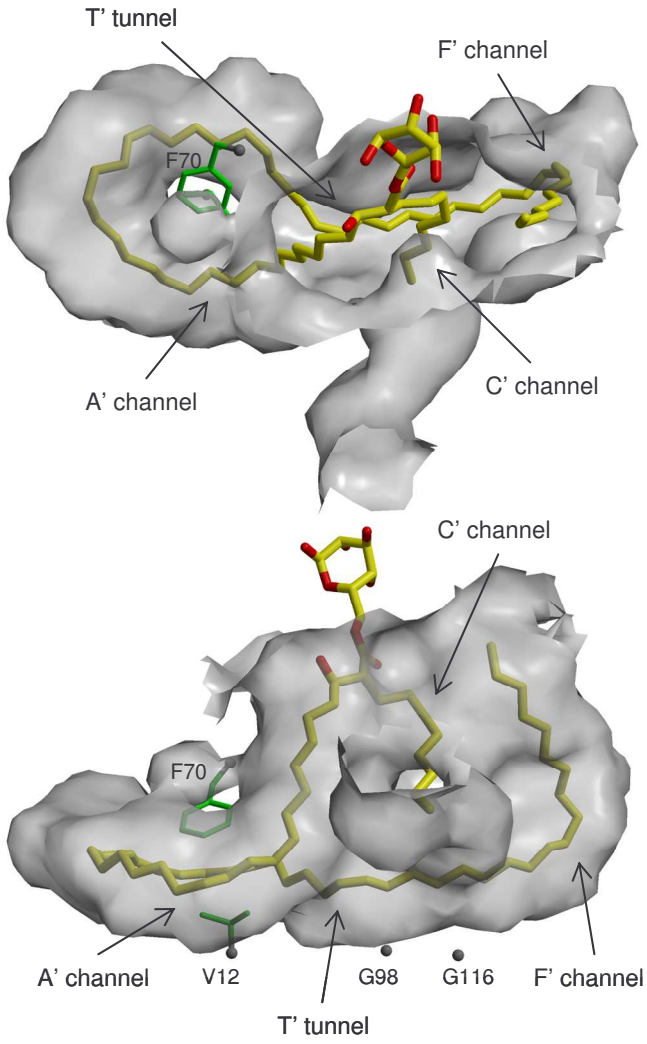

Figure 4.1. Crystal Structure of CD1b Bound with GMM.[11]

identified in this particular C49 GMM structure are located at the curve in the A' channel, where the lipid group is initially inserted, and at the bent junction of the A' channel and T' tunnel, a constrained conduit located deep within the protein.[11] The crystal structure shows that these points of unsaturation allow the polar glucose and β-hydroxy ester groups to be outside the binding pocket and available for presentation to the complimentary T cell receptor. Though not as voluminous as CD1b, the two channels in the homologous CD1d protein may be apt to more easily accept lipids with this type of substructure.

The other factor of concern in dealing with glycolipids is compound solubility. When αGalCer and other GSLs are used in vitro or in vivo they are typically dissolved in aqueous media after initially solubilizing in a DMSO solution with detergent and sonication.[12] Due to their denaturing properties in biological systems, the final concentration of DMSO and detergent must be residual, which is accomplished through serial dilutions of the GSL stock solution. A disadvantage of using αGalCer is that it is notoriously insoluble in most solvents except for pyridine or combinations of $CHCl_3$/MeOH or THF/MeOH, liquids not suitable for biological assays. αGalCer insolubility is largely due to its amphiphilic nature imparted by both the polar head group and lipid tail, providing a balance between hydrophilicity and hydrophobicity. Compounds **3-3b** and **3-4** (see Chapter 3), which contain much shorter acyl chains than αGalCer, have decreased amphiphilicity making them more soluble in DMSO; especially so for **3-4** due to its unsaturated sphingosine base. Increasing GSL solubility in DMSO through alkenyl incorporation may cause a decrease in compound aggregation and allow for aqueous solutions of greater dilution to be made, thus minimizing any potential

negative effects of DMSO in biological assays. Making GSL antigens more soluble may also have a positive effect on both efficiency of loading onto CD1d and stability of the ligand-protein complex [8a]

Unsaturated fatty acids can potentially accomplish the goals of causing improved GSL binding to CD1d and increasing compound solubility simultaneously. They are commercially available, usually at a relatively low cost if they are naturally abundant, and have greater solubilities than their saturated counterparts. Accessible alkenyl carboxylates are also widely varied in the position and number of double bonds in the alkyl chain, allowing systematic structural variations to be created in a highly divergent fashion through simple peptide coupling at the sphingoid amine group.

To probe the ability of unsaturated fatty acids to imbue αGalCer with increased binding affinity to CD1d and greater solubility in DMSO solutions, five glycosphingolipids with varying points of unsaturation on the *N*-acyl group were synthesized and evaluated for these two physical properties. Three GSLs, **4-1a–c,** were modified by incrementally moving the *Z*-alkene two carbons further from the carboxylate. Two others, **4-2a** and **4-2b**, were made with amides from polyunsaturated eicosenoids, a family of C20 fatty acids naturally found in mammalian liver and brain tissue. Optimization of the properties discovered from the structure-activity studies of these and the *N*-appended 6”-amino GSLs led to the synthesis of an effective surrogate of αGalCer, **4-3**, which is also designated as PBS-57 (Figure 4.2).

4.2 Results and Discussion

Compounds **4-1a–c** were synthesized following the same pathway as truncated ceramides **3-2** and **3-3** (see Chapter 3, section 3.2). Although DCC/NHS-mediated

ceramide formation suffered from undesirable yields (45-52%) and needed a peracetylation step to be purified, the reaction scheme worked well and generated functional glycosidic acceptors that could be coupled to an α-bromogalactoside resulting in nominal quantities and anomeric selectivity.[13] Additionally, an inexpensive commercial source for phytosphingosine had been located since the creation of **3-3** ($2.60/g, Centerchem, Inc.), rendering the lower yields from amide formation to be not as significant because the sphingoid no longer needed to be made from Garner's aldehyde.

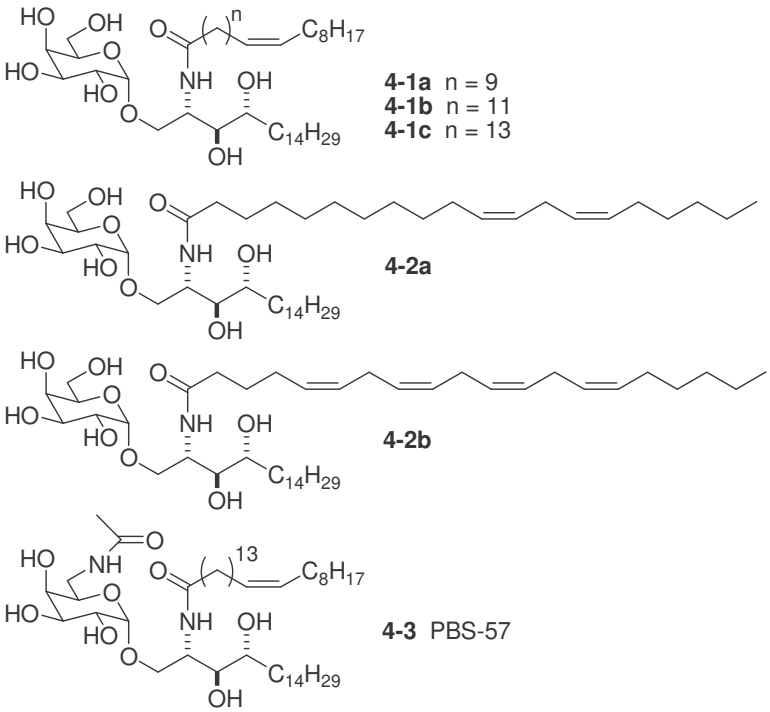

Figure 4.2. Unsaturated GSLs and αGalCer Surrogate **4-3**.

Due to the presence of the alkenyl groups, amide formation via coupling to the *N*-hydroxysuccinimidyl esters of (11*Z*)-eicosenoic, erucic, and nervonic acids were able to be identified through TLC stain (e.g., *p*-anisaldehyde, $KMnO_4$, cerium molybdate) unlike their saturated counterparts, which made it easier to identify when reactions were completed. Purification via acetylation provided the protected ceramides (**4-5a–c**) in slightly higher yields (49-56%) than **3-12**. Silylation of the primary alcohol, followed by diacetylation and fluoride deprotection of the silyl ether provided ceramide acceptors **4-6** in amounts comparable to those obtained in the synthesis of **3-13** (50-55%; Scheme 4.1).

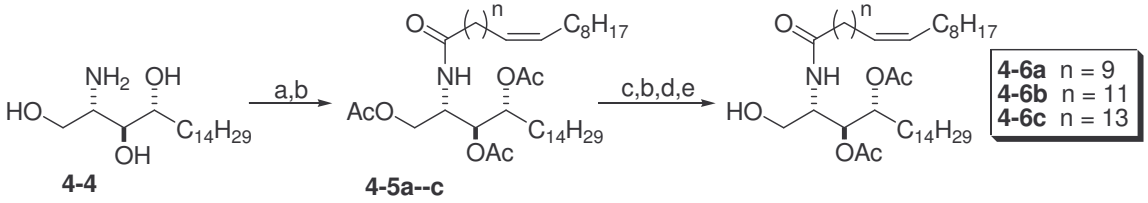

Reagents and conditions: a) $HO_2C(CH_2)_nCH{=}CHC_8H_{17}$, DCC, NHS, Et_3N, THF; b) Ac_2O, DMAP, Et_3N, THF (49-56% from **4-4**); c) NaOMe, MeOH; d) TBSCl, imidazole, THF, 60°C; e) HF (aq.), THF (50-55% from **4-5**).

Scheme 4.1. Synthesis of Ceramide Acceptors **4-6**.

The final compounds (**4-1a–c**) were synthesized in the same manner as **3-4** (Scheme 4.2). Bromide donor **4-7** was activated by AgOTf in the presence of crushed 4A molecular sieves and coupled to **4-6a–c** yielding protected unsaturated GSLs **4-8a–c**, again in quantities (57-68%) and anomeric selectivity (3-4:1 α:β) comparable to those of the truncated ceramides in Chapter 3. Reducing metal conditions (Na^o, NH_3) were used to remove the benzyl ether at the C2" hydroxyl group, along with the acetate protecting groups, to avoid saturation of the double bond by hydrogenation. Because compounds **4-1a–c** could not be isolated by precipitation in methanol, like **3-3a** and other GSLs, they required column chromatography. This caused a small decrease of the resulting yields (45-55%) yet they were equivalent to that of **3-4** (53%), which was purified in the same fashion.

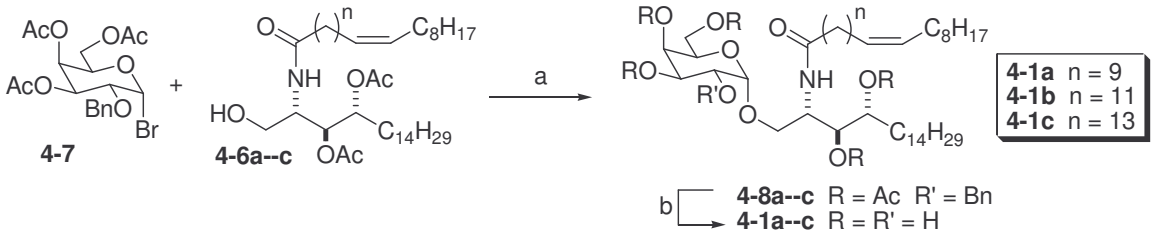

Reagents and conditions: a) AgOTf, 4A MS, CH_2Cl_2, 0°C (57-68%); b) Na^o, NH_3, THF, -78°C (44-55%).

Scheme 4.2. Preparation of Unsaturated GSLs **4-1a--c**.

Compounds **4-1a–c** were assayed for their ability to be loaded onto CD1d and stain NKT cells using a method described by Bendelac and coworkers.[14] NKT cells from a murine DN32.D3 NKT cell hybridoma that were restricted by GSL-CD1d tetramers were sorted by flow cytometry and quantified. It was found that all three compounds were able to load extremely well onto CD1d at 1 μg/mL and 10 μg/mL. In comparison to αGalCer, C6"-acetamidyl-αGalCer, and **3-3b**, **4-1a–c** had a greater amount of NKT cell staining, which indicates these unsaturated compounds are able to load onto CD1d in superior quantities than saturated GSLs (Figure 4.3).

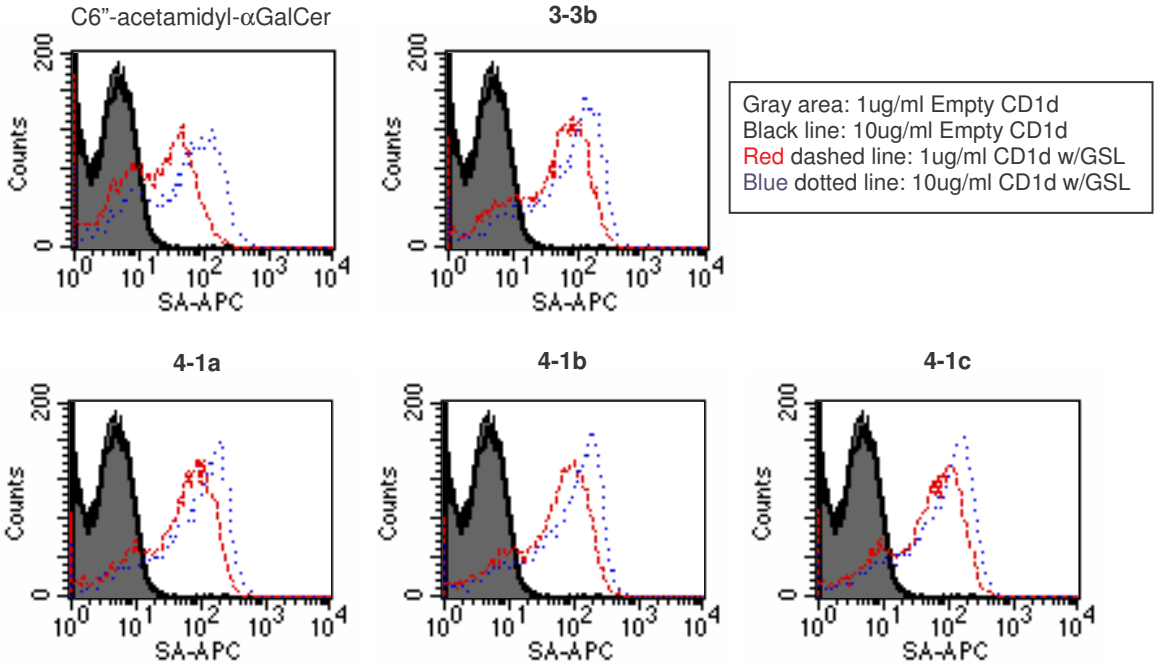

Figure 4.3. NKT Cell Hybridoma Staining by CD1d/GSL Tetramers.

An in vitro assay was used to gauge the NKT cell-stimulatory activity of **4-1a–c**. Bone marrow dendritic cells (BMDCs) from B6 mice were loaded separately with each of the three GSLs at a concentration of 100 ng/mL then exposed to Vα14i NKT cells that had been purified by cell sorting (Figure 4.4). GSL **4-1c** induced a greater quantity of IFN-γ cytokine than the other two compounds in reproducible experiments. This could

be indicative that the double bond in the ceramide of **4-1c** is in an appropriate position to allow for an association with CD1d such that a superior binding partnership is formed. To verify if this supposition is valid, a crystal structure of CD1d loaded with **4-1c** should be obtained.

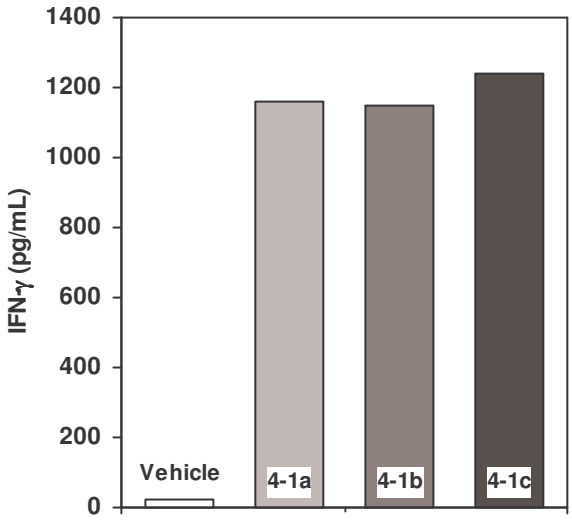

Figure 4.4. Stimulation of Vα14i NKT Cells by **4-1** at 100 ng/mL.

To probe a possible connection between ceramide unsaturation and improved CD1d binding, GSLs with polyunsaturated *N*-acyl chains were synthesized (**4-2a**, **4-2b**). The eicosenoid (C20) family of carboxylic acids was used because the locations of their alkenes are widely varied while maintaining a constant chain length and numerous polyunsaturated versions are available. Their alkyl chains are also long enough to provide extensive hydrophobic interactions with CD1d. Eicosenoids are also naturally abundant and thus could be obtained at lower cost than those of similar lengths.

In using polyunsaturated fatty acids (PUFAs), care was taken to avoid unwanted side reactions. Although polyalkenyl eicosenoids are not conjugated and thus are not particularly light sensitive, they are susceptible to oxidation upon exposure to air. Initially, the same synthetic pathway to create **4-1a–c** was used but there were several difficulties. Every reaction step required not only exclusion of atmospheric oxygen but sparging of all solvents and liquid reagents with argon for at least 30 m. NHS/DCC

coupling to phytosphingosine solely under nitrogen provided lower amounts of triacetylceramide (30-35%) than when oxygen was removed from reagents (50-55%). Due to their decreased amphiphilicity, peracetylation to purify the ceramide followed by deacetylation in preparation for glycosidic bonding was not required; the ceramides were purified directly by column chromatography under argon using polar eluent (MeOH:CH_2Cl_2 5:95). Although this worked well and higher yields were apparently gained, NMR spectroscopy of the "purified" ceramides found a considerable amount of contamination from dicyclohexylurea, which coeluted with the products. Switching to another reagent, such as DIC or EDCI, or attempting to precipitate out the urea side product did not improve the purity.

Problems also occurred during the protection/deprotection portion of the acceptor synthesis. Silylation of the primary alcohol using TBSCl and imidazole required three equivalents of each reagent to prompt the reaction, yet polysilylation often resulted without full conversion of the free alcohol. This possibly is a solubility issue due to the triol ceramide being fairly insoluble in THF or CH_2Cl_2. Desilylation using aqueous hydrofluoric acid often would be accompanied by acetyl migration during workup, even when care was taken to thoroughly dry the solution and fully neutralize the acid. Switching to TBAF was not viable due to its propensity to cause acyl migration as well.

Reduced yields of the prepared acceptors (<20 mg) made coupling to the bromide donor difficult, often resulting in no reaction. This is likely to due to oxidation during storage. To collect enough compound for an effective glycosylation, two or three batches of material were made and grouped together. It was discovered that ceramide storage, even under argon at -20^{o}C, for more than a week resulted in oxidation of the polyenes.

The undesired polyhydroxylated GSLs, as evidenced by multiple ^{1}H NMR signals from 3.5-4.5 ppm, would not undergo glycosylation without adequate protection.[15] When attempting to make the acceptors on a larger scale, greatly diminished reaction yields occurred, necessitating that other batches be made. Due to the numerous problems encountered in this pathway, and the possibility that the protected glycolipid would not be stable enough to withstand reducing metal deprotection in the final step, it was abandoned and another scheme was devised.

Since the problems encountered by using the typical GSL synthetic procedure were due to polyunsaturation, installing the acid toward the end of the scheme would minimize exposure to oxidizing conditions. This was achieved by first attaching protected phytosphingosine to galactose then forming the amide bond, reducing the number of reation steps involving the PUFAs to two. This type of approach would also introduce an effective divergent point in the scheme for making several other GSLs because the varying element would be installed in the penultimate step.

The amine on phytosphingosine (**4-4**) was protected as an azide. This was advantageous due to ease of formation and stability in the planned synthetic pathway. Adapting a procedure from Wong and coworkers, triflic azide was used to transfer a diazo group, via copper catalysis, to the amine in near quantitative yield without the need for column purification.[16] 2-Azidophytosphingosine (**4-9**) was protected in a similar fashion as a ceramide prior to glycosylation but with pivaloyl (trimethylacetyl) esters (**4-11**) instead of acetates. It was thought that during the deprotection of the amine, possible acetyl migration could occur making the stable acetamide. It was hoped that the bulkier 'Piv' groups would make this less likely to happen (Scheme 4.3).

Coupling to bromide donor **4-7** provided **4-12** in excellent yield (85%) and heightened α-selectivity (6.5:1 α:β). It is likely that the reduced size of the acceptor is the cause for this improvement in yield. The presence of an amide, especially a lengthy one, may somewhat hinder the attacking hydroxyl group on the acceptor. The smaller, linear azide would not cause such an obstruction. Also, yields of silyl ether formation, acylation, and desilylation in phytosphingosine were greatly-improved over those from bulky ceramides.

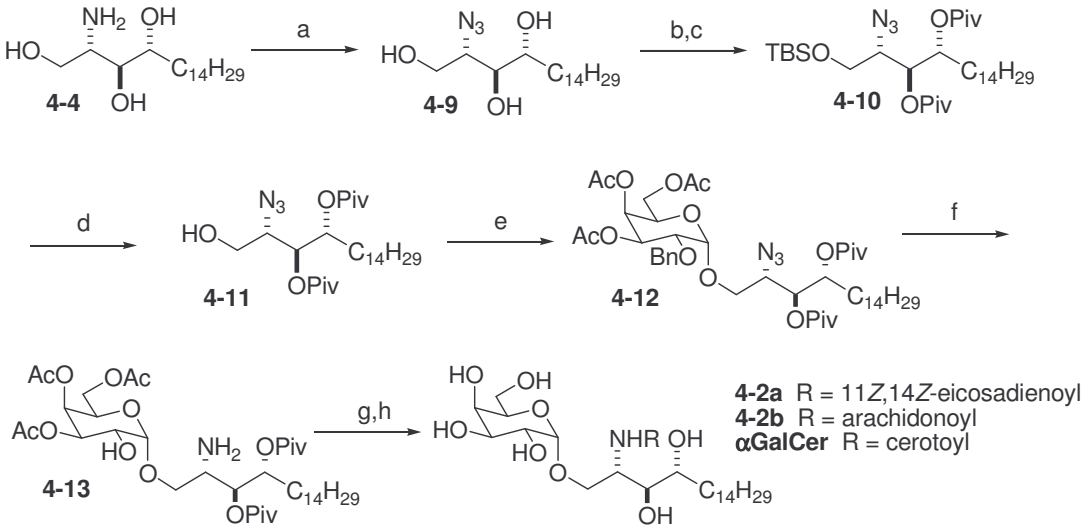

Reagents and conditions: a) NaN_3, Tf_2O, K_2CO_3, $CuSO_4$, CH_2Cl_2, MeOH, H_2O, 0°C (99%); b) TBSCl, imidazole, THF, 60°C; c) PivCl, DMAP, Et_3N, THF (90% 2 steps); d) HF (aq.), THF (97%); e) **4-7**, AgOTf, 4 A MS, CH_2Cl_2 (85%); f) H_2, Pd/C, THF, MeOH (60%); g) 11*Z*,14*Z*-eicosadienoic, arachidonic, or cerotic acid, HBTU, Et_3N, CH_2Cl_2, *p*-dioxane (32-44%); h) NaOMe, MeOH, 40°C (65-78%).

Scheme 4.3. Preparation of Polyunsaturated GSLs **4-2** and αGalCer via Intermediate **4-13**.

Compounds **4-2a** and **4-2b** were completed in three steps after glycosylation. Reduction of the benzyl ether at the O2" position and the azide were done concomitantly by hydrogenation. From the ^{1}H and ^{13}C NMR spectra of amine **4-13**, the two Piv groups remained at O3 and O4 with no detectable amide formation. Due to the increased potential for PUFA oxidation from the heat needed to drive peptide bond formation using DCC and NHS, the HBTU reagent (*O*-(benzotriazol-1-yl)-*N*,*N*,*N*',*N*'-tetramethyluronium

hexafluorophosphate) was used instead. It can be employed at room temperature with shorter reaction times and without the need of an external dehydrating agent (e.g., DCC, DIC).[17] Coupling with this reagent was successful with no oxidized side products observed, yet yields were very low (32-44%).

Deprotection of the GSLs using sodium methoxide in argon-sparged methanol was successful, but slight heating (40°C) was required to remove the pivaloyl esters. Cooling to room temperature induced the precipitation of **4-2a**, while **4-2b** required purification on a silica gel column due to its formation as a colorless oil. To gauge its usefulness, intermediate **4-13** was also used to make αGalCer. HBTU-acylation with saturated hexacosanoic acid also resulted in a low yield (38%), which may be attributed to steric hindrance due to the bulk of the amine. A comparison of the reaction pathway described in Chapter 3 and the one used to make compounds **4-2** shows that the two methods are similar in overall yield (14% and 13% from phytosphingosine, respectively) and in the number of steps (nine and eight, respectively) to make αGalCer. However, this second scheme holds an advantage due to the divergent acylation step late in the protocol.

Evaluation of **4-2a** as an antigen of NKT cells was performed (see Figure 4.9 below). Besides having improved solubility in DMSO (~10 mg/mL) over αGalCer (<5 mg/mL), its stimulatory activity was slightly greater than αGalCer as well, with a modest increase in the ratio of secreted IL-4 to IFN-γ. Due to the propensity of **4-2a** and **4-2b** to oxidize, resulting in shorter viable lifetimes, and because **4-2a** did not show markedly greater activity than other unsaturated compounds, SAR work on PUFA-appended GSLs was not pursued further.

Structure-activity research on monoalkenoyl and *N*-appended C6"-amino-glycosphingolipids provided inspiration to combine useful elements into one compound. The monoalkenoic acids in **4-1a–c** increased solubility and NKT cell staining over αGalCer while the bulky groups on the C6"-amino compounds were tolerated by TCRs and retained the potency of αGalCer to induce the release of cytokine. Also, an assay of immunological activity by compounds **4-1b**, **4-1c**, and C6"-acetamidyl-αGalCer showed that all three were able to induce NKT cell proliferation to a greater extent than αGalCer (Figure 4.5). Therefore, hybrid GSL **4-3** was created using a C6" acetamide group and a

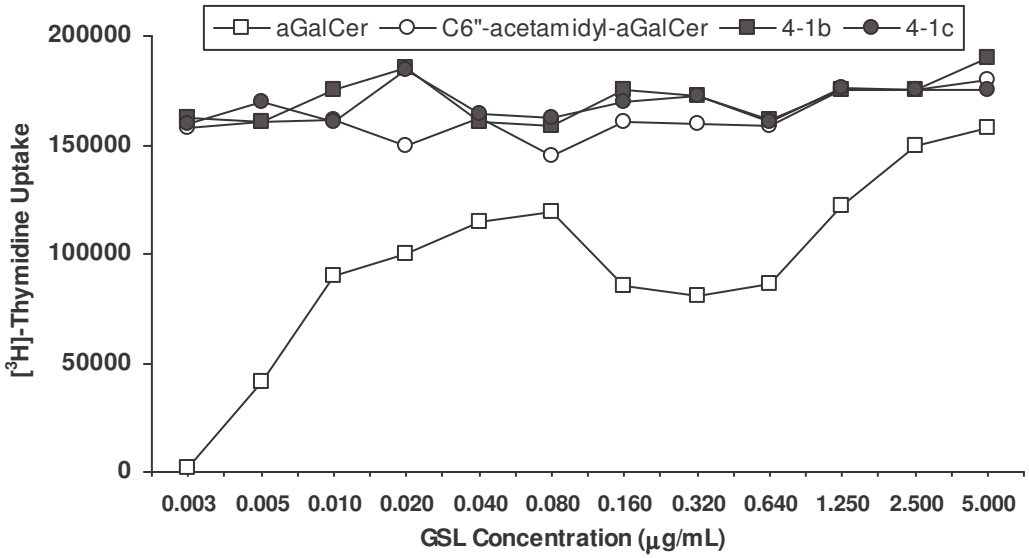

Figure 4.5. GSL-Induced NKT Cell Proliferation at Varying Concentrations.

monoalkenoyl acid. Because **4-1c** had slightly higher activity at causing IFN-γ production than **4-1a** and **4-1b**, nervonic acid was used. It was anticipated that these two elements would do the following:

1) Retain or improve the NKT cell-stimulatory activity of αGalCer.

2) Improve binding with CD1d and provide more stable protein-antigen complexes.

3) Increase compound solubility to aid with immunological testing.

Successful implementation of these properties into a GSL would provide researchers with a useful alternative of αGalCer, which is under patent and has recently become difficult to obtain.

The synthesis of **4-3** was straightforward because its individual components had been made previously (Scheme 4.4). Ceramide **4-6c** was coupled to fluoride donor **4-14** (see Chapter 2, section 2.2) followed by azide reduction and acetylation with acetic anhydride to form protected compound **4-16**. Deprotection was achieved by reducing metal conditions with a yield higher than those from making **4-1a–c** (68%), likely due to decreased polarity from the acetamide group. Though the synthesis of **4-3** requires more steps than αGalCer, it can be prepared in good overall yields and in fairly large quantities (500 mg).

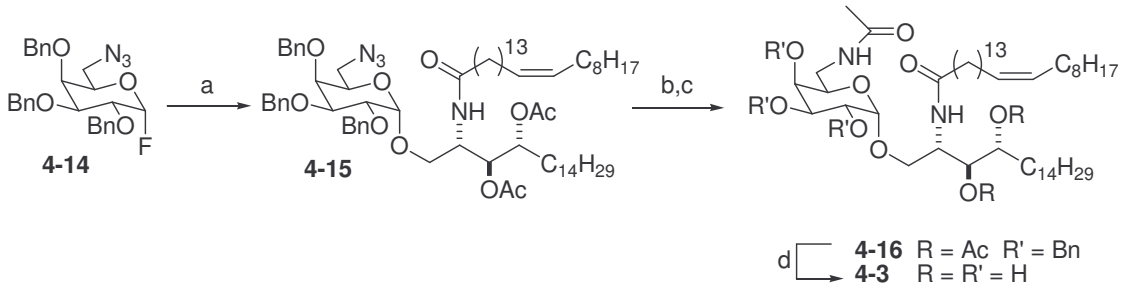

Reagents and Conditions: a) **4-6c**, $AgClO_4$, $SnCl_2$, 4A MS, CH_2Cl_2, 0°C (53%); b) PPh_3, THF, H_2O; c) Ac_2O, DMAP, Et_3N, THF (89% over two steps); d) Na^o, NH_3, THF, -78°C (68%).

Scheme 4.4. Preparation of αGalCer Surrogate **4-3**.

This optimized ligand was evaluated and found to have improved properties as an immunological stimulant compared to αGalCer.[18] Solutions of **4-3** can be prepared in the same manner as αGalCer, but with greater solubility in DMSO (20 mg/mL and <5 mg/mL, respectively), allowing the final concentration of the solvent to be negligible (<1

%) in a standard 10 μg/mL solution. Unsaturated **4-3** was able to load CD1d tetramers and bind to Vα14i NKT cells to a comparable degree as αGalCer (Figure 4.6).[18]

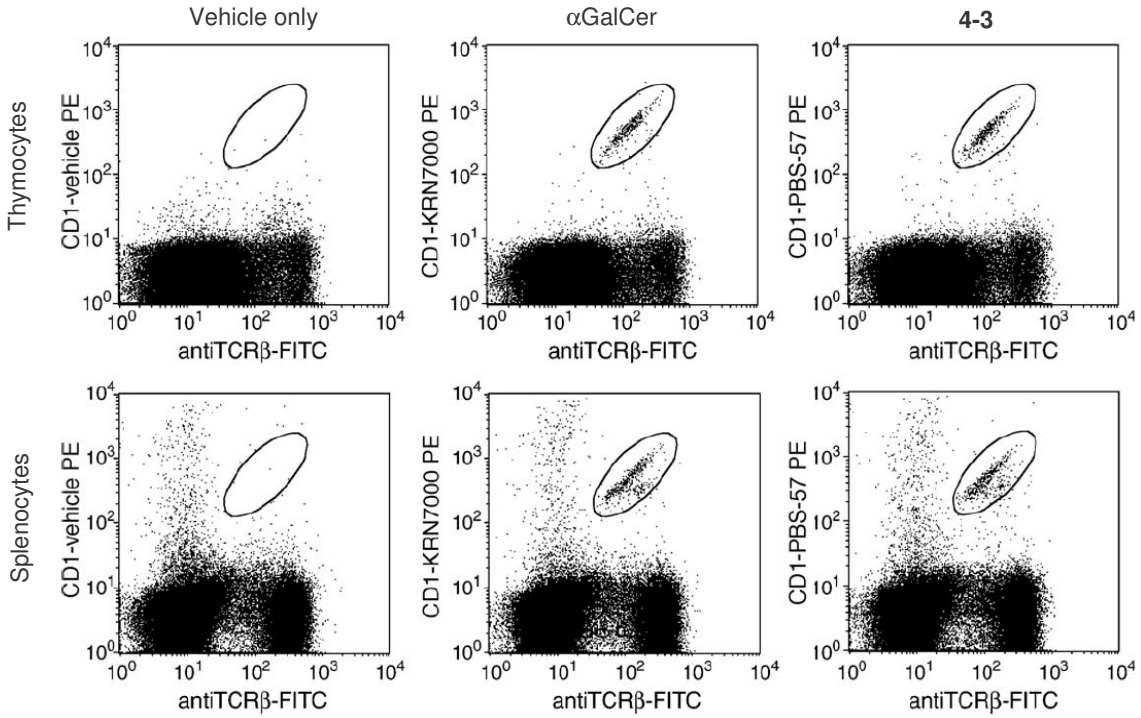

Figure 4.6. Comparative Staining of Vα14i NKT Cells from Different Cell Populations.[18]

NKT cells were also sufficiently engaged by CD1d-restricted **4-3**. Various NKT cell hybridomas, each with a different TCR β-chain, were used to measure the ability of **4-3** to act as a universal agent with the Vα14i NKT cell population. Using flow cytometry, fluorescent CD1d tetramers, formed by association with biotinylated, **4-3**-loaded CD1d molecules and streptavidin-appended cychrome, were found to stain NKT cells from all six different hybridomas. This demonstrates the ability of **4-3** to interact with TCRs independently of the type of Vβ subunit (Figure 4.7).[18]

The ability of **4-3** to interact with NKT cells from other mammals was gauged by the Altman group at the Emory Vaccine Research Center. Using both murine and human CD1d tetramers, blood samples from humans and primates were assayed for

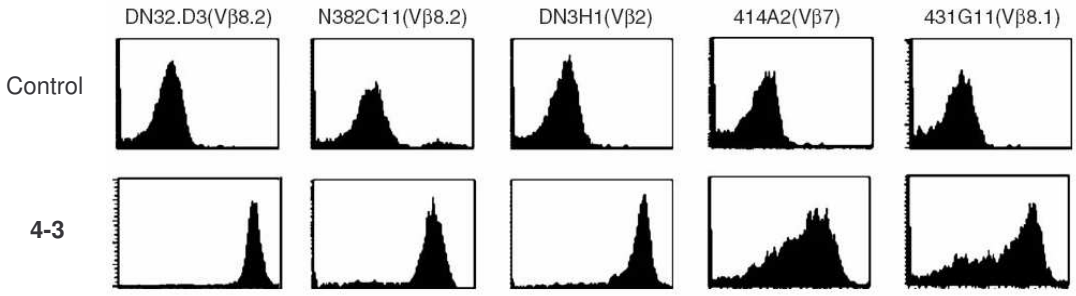

Figure 4.7. Staining of Murine NKT Cell Hybridomas with Variant Vβ Chains by **4-3** and Nonreactive Lipid Control α-Galactosylcholesterol.[18]

NKT cell staining (NKT cells typically comprise >0.08% of all human blood cells). Significant staining was seen in human blood (fourteen of seventeen samples) as well as in chimpanzees (six of ten) and rhesus macaques (four of twelve), though staining was not seen in pigtail macaques or sooty mangabeys (six each).[18] According to Lee et al., this may be due to certain individuals having samples with an NKT cell population to few to be detected.[19] If the sampling pool had been larger for both these two primates, the likelihood of NKT detection would be greater (Figure 4.8).

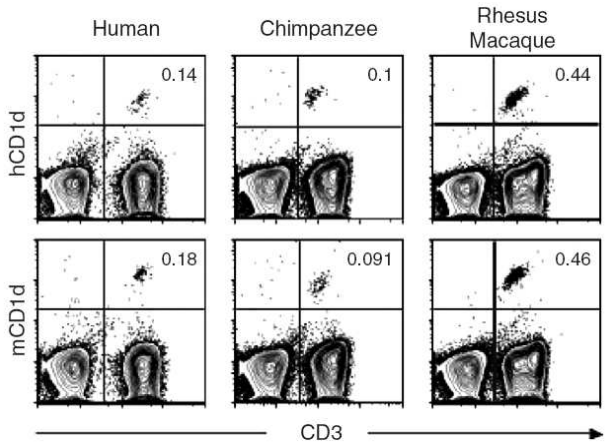

Figure 4.8. Staining of Mammalian NKT Cells by **4-3** Loaded into Human and Murine CD1d Tetramers.[18]

NKT cell cytokine release from **4-3** stimulation was measured in vitro and in vivo on mice. Splenocytes harvested from B6 mice were exposed to varying concentrations of αGalCer and **4-3** along with polyene **4-2a** and sphingosine-containing **3-3b**. From ELISA testing, it was found that **4-3** consistently induced a greater amount of in vitro IL-4 secretion than αGalCer, yet at higher concentrations **3-3b** and **4-2a** were able to stimulate to an even greater extent. **4-3** also produced comparable quantities of IFN-γ as αGalCer, plateauing

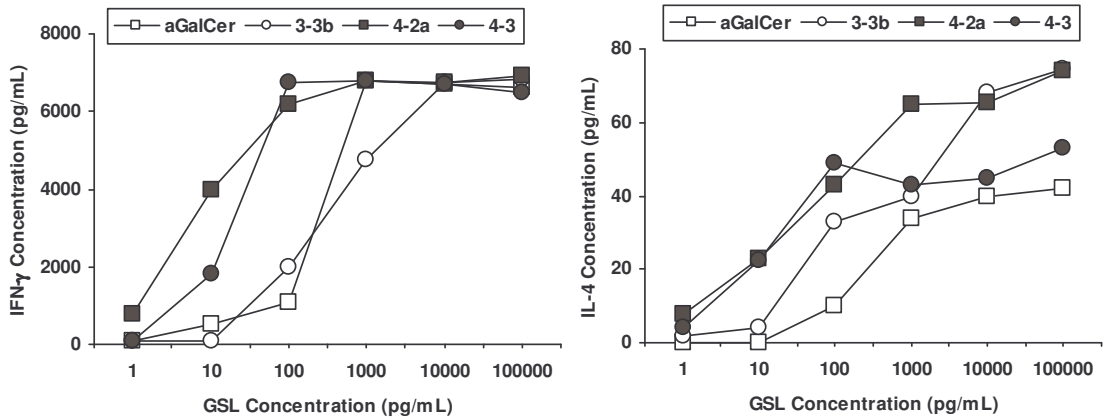

Figure 4.9. In Vitro Cytokine Release from Murine B6 Splenocytes Stimulated with GSLs.

at 100 ng/mL and 1000 pg/mL, respectively. Interestingly, **4-2a** leveled off at the same concentration as **4-3** (Figure 4.9). In vivo measurement of IFN-γ in B6 mice showed that at a higher concentration (100 ng in 100 µL), the activity of **4-3** and αGalCer was similar, yet smaller doses significantly diminished the activity of αGalCer (Figure 4.10). This may be explained by the increased solubility and greater ability of CD1d loading of **4-3** over αGalCer, translating into greater NKT cell stimulatory activity at lower concentrations. Due to the activity of **4-3** surpassing that of αGalCer, it has been requested by and provided to the National Institutes of Health's Tetramer Core Facility for widespread distribution to immunologists.[20]

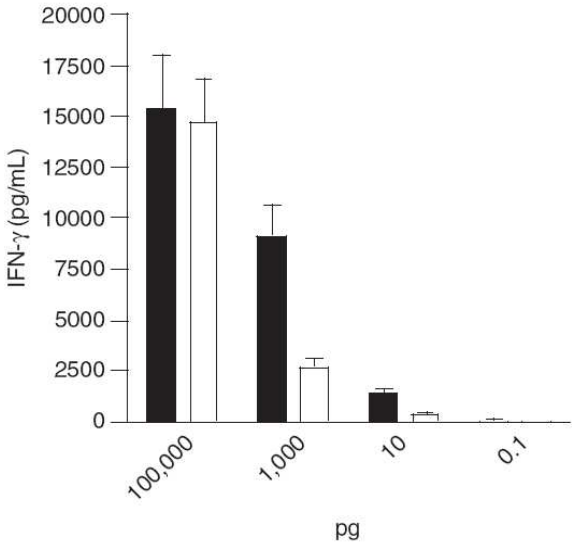

Figure 4.10. In Vivo Secretion of IFN-γ in B6 Mice Injected with 100 µL of GSL.[18]

4.3 Conclusions

Compounds **4-1a–c** were synthesized to expand the library of known NKT cell antigens and aid in understanding the structural requirements for CD1d-restricted recognition by NKT cell receptors. Following a known procedure, GSLs **4-1a–c** were made in eight steps from phytosphingosine and monoalkenoic acids with an overall yield of 7-10%. Aliquots of these compounds were able to load CD1d and stain NKT cells to a greater degree than saturated GSLs, like αGalCer. Their ability to cause NKT cell proliferation was also heightened compared to αGalCer, likely due to a more favorable TCR association.

Although difficult to manipulate becase they are easily oxidized, *N*-polyenoyl compounds **4-2a** and **4-2b** were synthesized in a highly divergent fashion by installation of the acyl chain at the end of the reaction sequence. This pathway is also applicable for adding other types of carboxylic acids for further SAR studies. Compound **4-2a** was found to have in vitro stimulatory activity comparable to αGalCer, though it has a smaller probability of being used as a therapeutic agent due to its shorter shelf life.

Combination of different attributes from active GSL-based antigens led to the formulation of **4-3**, a modified version of αGalCer. Addition of an acetamide moiety at C6" and introduction of acyl unsaturation on the ceramide has provided an improved agonist that universally stains NKT cells, has increased solubility, and has equivalent in vivo activity as αGalCer. Cocrystallization with the CD1d protein may elucidate how these structural features aid in improving binding over αGalCer. Importantly, availability of **4-3** through the NIH will allow other researchers to have unrestricted access to GSL antigens needed for studies on NKT cell activity.[21]

4.4 Experimental Section

Materials and General Methods. Mass spectrometric data were obtained on either a JEOL SX 102A spectrometer for electron ionization (EI; 70 eV) or fast atom bombardment (FAB; thioglycerol/Na^+ matrix) or an Agilent Technologies LC/MSD TOF spectrometer for electrospray ionization (ESI; 3500 eV, positive ion mode). ^1H and ^{13}C NMR spectra were obtained on a Varian Unity 300 or 500 MHz instrument using 99.8% $CDCl_3$ with 0.05% v/v TMS, 99.8% CD_3OD with 0.05% v/v TMS, and 99.9% D_2O or 99.96% DMSO-d_6 and 99.5% pyridine-d_5 in ampoules. Methanol, methylene chloride, pyridine, and tetrahydrofuran were dried using columns of activated alumina. Flash chromatography was performed using 230-400 mesh silica gel. Thin layer chromatography was performed on aluminum-backed, 254 nm UV-active plates with a silica gel particle size of 250 μm. Reagents were obtained from Aldrich, Fluka, or Nu-Chek Prep, unless otherwise specified, and were used as received.

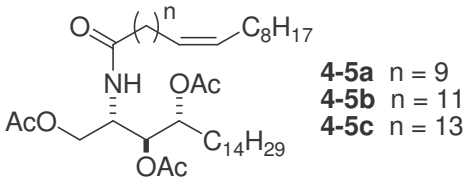

4-5a n = 9
4-5b n = 11
4-5c n = 13

4-5a. (11*Z*)-Eicosenoic acid (309 mg, 0.995 mmol) was dissolved in anhydrous THF (10 mL) and warmed to reflux under N_2 before adding NHS (140 mg, 1.21 mmol) and DCC (235 mg, 1.14 mmol). After refluxing for 3 h, a solution of phytosphingosine (316 mg, 0.995 mmol) in anhydrous THF (5 mL) and pyridine (2 mL) was added to the reaction mixture, which was allowed to reflux for another 2 h before cooling to room temperature overnight and removing the solvent in vacuo. Purification was performed by peracetylation of the ceramide with acetic anhydride (2 mL), triethylamine (2 mL),

DMAP (700 mg, 5.73 mmol), in anhydrous THF (10 mL) and heating to reflux for 1 h. The reaction was quenched with ice, extracted with EtOAc (2 x 20 mL), washed with saturated aqueous $NaHCO_3$, 5% HCl, and brine, dried with $MgSO_4$, and concentrated. Pure triacetate was isolated by flash chromatography (SiO_2, EtOAc:Hex 1:3) as a white solid (410 mg, 56%, R_f = 0.37 EtOAc:Hex 1:3). ^{1}H NMR ($CDCl_3$, 300 MHz) δ 5.95 (d, *J* = 9.3 Hz, 1 H), 5.33 (m, 2 H), 5.13 (dd, *J* = 8.5, 2.9 Hz, 1 Hz), 4.94 (dt, *J* = 9.5, 3.2 Hz, 1 H), 4.50 (m, 1 H), 4.28 (dd, *J* = 11.6, 5.0 Hz, 1 H), 4.01 (dd, *J* = 11.6, 2.9 Hz, 1 H), 2.21 (t, *J* = 7.6 Hz, 2 H), 2.07 (s, 3 H), 2.03 (s, 6 H), 2.00 (m, 4 H), 1.72-1.56 (m, 4 H), 1.26 (br s, 48 H), 0.88 (m, 6 H); ^{13}C NMR ($CDCl_3$, 75 MHz) δ 172.98, 171.24, 171.00, 170.21, 130.08, 129.99, 73.12, 72.11, 64.09, 63.07, 47.55, 36.90, 32.09, , 32.07, 29.93, 29.86, 29.83, 29.77, 29.69, 29.65, 29.53, 29.48, 29.41, 28.25, 27.38, 25.79, 25.71, 25.43, 22.86, 21.18, 21.10, 20.93, 14.28; HRMS (FAB) *m/z* for $C_{44}H_{81}NNaO_7$ ($[M+Na]^+$) 758.5915 (22.8%), calc. 758.5905.

4-5b. Same procedure as synthesis of **4-5a**, substituting with (13*Z*)-docosenoic (erucic) acid (49%). ^{1}H NMR ($CDCl_3$, 300 MHz) δ 6.01 (d, *J* = 9.5 Hz, 1 H), 5.34 (m, 2 H), 5.11 (dd, *J* = 8.3, 2.9 Hz, 1 Hz), 4.93 (dt, *J* = 9.5, 3.4 Hz, 1 H), 4.49 (m, 1 H), 4.29 (dd, *J* = 11.5, 5.1 Hz, 1 H), 3.99 (dd, *J* = 11.5, 2.9 Hz, 1 H), 2.21 (t, *J* = 7.3 Hz, 2 H), 2.07 (s, 3 H), 2.04 (s, 6 H), 2.01 (m, 4 H), 1.70-1.55 (m, 4 H), 1.26 (br s, 52 H), 0.88 (m, *J* = 6.8 Hz, 6 H); ^{13}C NMR ($CDCl_3$, 75 MHz) δ 172.97, 171.21, 170.97, 170.18, 130.02, 130.00, 73.09, 72.07, 63.06, 47.52, 36.86, 32.81, 32.06, 32.04, 30.89, 29.93, 29.91, 29.84, 29.78, 29.73, 29.67, 29.51, 29.48, 29.46, 29.39, 28.20, 27.34, 26.45, 25.78, 25.69, 25.66, 24.88, 22.83, 21.15, 20.90, 20.87, 14.26; HRMS (FAB) *m/z* for $C_{46}H_{85}NNaO_7$ ($[M+Na]^+$) 786.6226 (82.8%), calc. 786.6218.

4-5c. Same procedure as synthesis of **4-5a**, substituting with (15*Z*)-tetracosenoic (nervonic) acid (51%). ^{1}H NMR ($CDCl_3$, 300 MHz) δ 5.89 (d, *J* = 9.5 Hz, 1 H), 5.35 (m, 2 H), 5.11 (dd, *J* = 8.5, 2.9 Hz, 1 Hz), 4.93 (dt, *J* = 9.3, 3.2 Hz, 1 H), 4.49 (m, 1 H), 4.29 (dd, *J* = 11.7, 4.9 Hz, 1 H), 3.99 (dd, *J* = 11.7, 2.9 Hz, 1 H), 2.21 (t, *J* = 7.8 Hz, 2 H), 2.08 (s, 3 H), 2.05 (s, 6 H), 2.01 (m, 4 H), 1.70-1.54 (m, 4 H), 1.25 (br s, 56 H), 0.88 (m, *J* = 6.6 Hz, 6 H); ^{13}C NMR ($CDCl_3$, 125 MHz) δ 173.20, 171.38, 171.08, 170.28, 130.07, 73.20, 72.07, 63.08, 60.60, 47.58, 36.91, 32.10, 29.96, 29.88, 29.79, 29.72, 29.55, 29.51, 29.43, 28.23, 27.39, 25.83, 25.83, 25.74, 22.88, 21.23, 20.96 20.92, 14.37, 14.30; HRMS (FAB) *m/z* for $C_{48}H_{90}NO_7$ ($[M+H]^+$) 792.6724 (100%), calc. 792.6712.

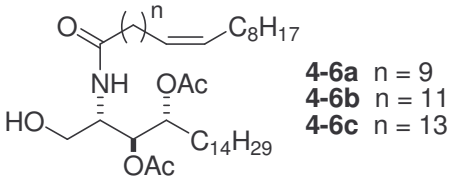

4-6a n = 9
4-6b n = 11
4-6c n = 13

4-6a. Ceramide **4-5a** (410 mg, 0.557 mmol) was deacetylated by dissolving in MeOH (15 mL) then adding a solution of sodium methoxide (0.30 *M*, 5 mL, 1.5 mmol). The suspension was agitated for 45 m and centrifuged (3500 rpm, 5 m) to isolate the solid triol product. The supernatant was removed and the solid rinsed with fresh MeOH (5 mL) to remove any remaining base and centrifuged again. After removal of the solvent and drying under vacuum, a white flaky solid (271 mg, 80%) was isolated and used without further purification. The primary alcohol was selectively protected by dissolving in pyridine (10 mL) then adding dimethylthexylsilyl chloride (174 mg, 0.977 mmol). The reaction was monitored closely by TLC (R_f = 0.56, EtOAc:Hex 1:2) to avoid polysilylation. After proceeding for 1 h, excess Ac_2O (2 mL) and DMAP (100 mg, 0.818 mmol) were added to the reaction mixture. After 30 m, the solvent was removed in

vacuo, the crude oil was adsorbed onto silica gel after dissolving in CH_2Cl_2, and the protected ceramide purified by flash chromatography (SiO_2, EtOAc:Hex 1:8). The colorless oil (249 mg, 67%, R_f = 0.5 EtOAc:Hex 1:8), which was used without further characterization, was taken up into THF (5 mL) and aqueous HF (1 mL, 49%). TLC (EtOAc:Hex 2:1) showed an immediate disappearance of starting material and formation of the desilylated ceramide (R_f = 0.56). The reaction was poured carefully into saturated aqueous $NaHCO_3$ (10 mL), extracted with EtOAc (10 mL), rewashed with $NaHCO_3$ (10 mL), back extracted with EtOAc (2 x 10 mL), washed with brine (5 mL), and dried thoroughly with Na_2SO_4 before concentrating. Purification by flash chromatography (SiO_2, EtOAc:Hex 2:1) yielded the product as a colorless oil (193 mg, 50% from triacetate). ^{1}H NMR ($CDCl_3$, 300 MHz) δ 6.53 (d, *J* = 9.3 Hz, 1 H), 5.34 (m, 2 H), 5.08 (dd, *J* = 9.8, 2.4 Hz, 1 H), 4.95 (dt, *J* = 9.8, 2.6 Hz, 1 H), 4.17 (tt, *J* = 9.3, 2.6 Hz, 1 H), 3.58 (br s, 2 H), 2.91 (br s, 1 H), 2.22 (t, *J* = 7.5 Hz, 2 H), 2.14 (s, 3 H), 2.04 (s, 3 H), 2.01 (m, 4 H), 1.74-1.57 (m, 4 H), 1.25 (br s, 48 H), 0.88 (t, *J* = 6.3 Hz, 6 H); ^{13}C NMR ($CDCl_3$, 75 MHz) δ 173.40, 171.55, 171.38, 130.08, 130.03, 73.46, 72.72, 61.64, 49.74, 36.92, 32.12, 32.10, 29.98, 29.96, 29.89, 29.85, 29.81, 29.78, 29.74, 29.71, 29.69, 29.56, 29.51, 27.94, 27.42, 27.40, 25.90, 22.88, 21.23, 21.06, 14.30; HRMS (FAB) *m/z* for $C_{42}H_{79}NNaO_6$ ($[M+Na]^+$) 716.5809 (100%), calc. 716.5800.

4-6b. Same procedure as synthesis of **4-6a** (51% from triacetate). ^{1}H NMR ($CDCl_3$, 300 MHz) δ 6.43 (d, *J* = 9.3 Hz, 1 H), 5.34 (m, 2 H), 5.07 (dd, *J* = 9.5, 2.4 Hz, 1 H), 4.95 (dt, *J* = 9.5, 2.7 Hz, 1 H), 4.17 (tt, *J* = 9.3, 2.7 Hz, 1 H), 3.57 (m, 2 H), 2.79 (t, *J* = 6.7 Hz, 1 H), 2.22 (t, *J* = 7.5 Hz, 2 H), 2.14 (s, 3 H), 2.04 (s, 3 H), 2.01 (m, 4 H), 1.72-1.56 (m, 4 H), 1.26 (br s, 52 H), 0.88 (t, *J* = 6.8 Hz, 6 H); ^{13}C NMR ($CDCl_3$, 75 MHz) δ 173.39,

171.67, 171.31, 130.08, 73.42, 72.89, 61.69, 49.76, 36.96, 32.13, 32.11, 30.00, 29.97, 29.91, 29.86, 29.83, 29.79, 29.73, 29.56, 29.52, 28.00, 27.43, 27.40, 25.91, 22.88, 21.24, 21.08, 14.32; HRMS (FAB) *m/z* for $C_{44}H_{83}NNaO_6$ ($[M+Na]^+$) 744.6116 (100%), calc. 744.6113.

4-6c. Same procedure as synthesis of **4-6a** (55% from triacetate). ^{1}H NMR ($CDCl_3$, 300 MHz) δ 6.46 (d, *J* = 9.3 Hz, 1 H), 5.34 (m, 2 H), 5.05 (dd, *J* = 9.8, 2.4 Hz, 1 H), 4.95 (dt, *J* = 9.8, 2.9 Hz, 1 H), 4.17 (tt, *J* = 9.3, 2.9 Hz, 1 H), 3.57 (br s, 2 H), 2.73 (br s, 1 H), 2.22 (t, *J* = 7.6 Hz, 2 H), 2.14 (s, 3 H), 2.04 (s, 3 H), 2.02 (m, 4 H), 1.80-1.59 (m, 4 H), 1.25 (br s, 56 H), 0.88 (t, *J* = 6.7 Hz, 6 H); ^{13}C NMR ($CDCl_3$, 75 MHz) δ 173.42, 171.78, 171.25, 130.09, 73.38, 73.04, 61.74, 49.77, 36.98, 32.13, 32.11, 29.98, 29.91, 29.87, 29.83, 29.73, 29.58, 29.55, 29.53, 28.06, 27.41, 25.91, 22.89, 21.25, 21.09, 14.32; HRMS (FAB) *m/z* for $C_{46}H_{87}NNaO_6$ ($[M+Na]^+$) 772.6429 (100%), calc. 772.6426.

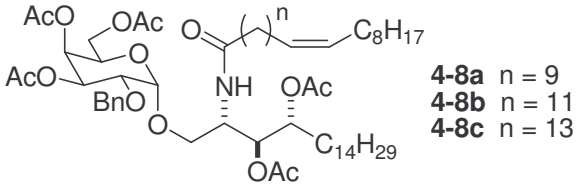

4-8a. Bromide donor **4-7** (326 mg, 0.711 mmol) and ceramide **4-6a** (329 mg, 0.474 mmol) were dissolved in anhydrous CH_2Cl_2 (14 mL) and cooled to 0°C. Freshly crushed 4 Å molecular sieves (800 mg) were added and the mixture was allowed to stir for 10 m before addition of AgOTf (365 mg, 1.42 mmol) in the dark. The reaction vessel was wrapped in aluminum foil and allowed to warm to room temperature overnight. After 12 h, the slurry was filtered through Celite after dilution with EtOAc (20 mL). The resulting colorless solution was concentrated and purified by column chromatography (SiO_2, EtOAc:Hex 1:2), which yielded both α- and β-anomers as a white, waxy solid and

colorless oil, respectively (α: 305 mg, 60%, R_f = 0.46 EtOAc:Hex 1:2; β: 91 mg, 18%, R_f = 0.36 EtOAc:Hex 1:2; α:β 3.3:1 as determined by weight). ^{1}H NMR ($CDCl_3$, 500 MHz) δ 7.33 (m, 5 H), 6.70 (d, *J* = 9.3 Hz, 1 H), 5.40 (d, *J* = 3.0 Hz, 1 H), 5.34 (m, 2 H), 5.34-5.25 (m, 2 H), 4.93 (dt, *J* = 10.3, 2.9 Hz, 1 H), 4.88 (d, *J* = 3.4 Hz, 1 H), 4.73 (d, *J* = 12.0 Hz, 1 H), 4.58 (d, *J* = 12.0 Hz, 1 H), 4.35 (tt, *J* = 9.3, 3.4 Hz, 1 H), 4.14 (t, *J* = 6.5 Hz, 1 H), 4.08 (m, 1 H), 4.02 (dd, *J* = 11.2, 6.8 Hz, 1 H), 3.82 (dd, *J* = 10.2, 3.4 Hz, 1 H), 3.61 (qd, *J* = 11.2, 3.4 Hz, 2 H), 2.19 (td, *J* = 7.6, 2.9 Hz, 2 H), 2.09 (s, 3 H), 2.08 (s, 3 H), 2.04 (s, 3 H), 2.02 (m, 4 H), 1.99 (s, 3 H), 1.96 (s, 3 H), 1.68-1.57 (m, 4 H), 1.26 (br s, 48 H), 0.88 (t, *J* = 6.8 Hz, 6 H); ^{13}C NMR ($CDCl_3$, 125 MHz) δ 173.25, 171.13, 170.69, 170.49, 170.27, 170.23, 138.00, 130.11, 128.63, 128.16, 98.55, 73.73, 73.44, 73.12, 71.71, 69.45, 68.58, 67.49, 67.10, 62.04, 48.22, 36.89, 32.14, 30.05, 30.01, 29.95, 29.91, 29.83, 29.77, 29.65, 29.60, 29.56, 27.86, 27.49, 27.45, 25.93, 25.83, 22.93, 21.21, 21.17, 20.98, 20.95, 20.86, 14.37; HRMS (FAB) *m/z* for $C_{61}H_{101}NNaO_{14}$ ($[M+Na]^+$) 1094.7109 (100%), calc. 1094.7114.

4-8b. Same procedure as synthesis of **4-8a**, substituting with **4-6b** (α: 57%; β: 15%; 3.8:1 α:β). ^{1}H NMR ($CDCl_3$, 300 MHz) δ 7.33 (m, 5 H), 6.71 (d, *J* = 9.2 Hz, 1 H), 5.40 (d, *J* = 3.0 Hz, 1 H), 5.35 (m, 2 H), 5.31-5.24 (m, 2 H), 4.93 (m, 1 H), 4.89 (d, *J* = 3.7 Hz, 1 H), 4.73 (d, *J* = 12.0 Hz, 1 H), 4.58 (d, *J* = 12.0 Hz, 1 H), 4.35 (tt, *J* = 9.3, 3.4 Hz, 1 H), 4.13 (m, 1 H), 4.03 (m, 2 H), 3.82 (dd, *J* = 10.5, 3.7 Hz, 1 H), 3.61 (qd, *J* = 11.2, 3.4 Hz, 2 H), 2.19 (t, *J* = 7.3 Hz, 2 H), 2.10 (s, 3 H), 2.08 (s, 3 H), 2.04 (s, 3 H), 2.02 (m, 4 H), 1.98 (s, 3 H), 1.96 (s, 3 H), 1.68-1.55 (m, 4 H), 1.25 (br s, 52 H), 0.88 (t, *J* = 6.7 Hz, 6 H); ^{13}C NMR ($CDCl_3$, 75 MHz) δ 173.23, 171.11, 170.66, 170.46, 170.25, 170.20, 137.99, 130.12, 130.09, 128.61, 128.13, 98.53, 73.71, 73.42, 73.09, 71.70, 69.43, 68.56,

67.46, 67.08, 62.01, 48.20, 36.87, 32.12, 30.03, 29.99, 29.92, 29.83, 29.73, 29.63, 29.59, 29.53, 27.84, 27.45, 27.42, 25.91, 22.90, 21.18, 21.13, 20.95, 20.91, 20.83, 14.33; HRMS (FAB) *m/z* for $C_{63}H_{105}NNaO_{14}$ ($[M+Na]^+$) 1122.7422 (100%), calc. 1122.7427.

4-8c. Same procedure as synthesis of **4-8a**, substituting with **4-6c** (α: 68%; β: 17%; 4:1 α:β). ^{1}H NMR ($CDCl_3$, 500 MHz) δ 7.33 (m, 4 H), 7.30 (m, 1H), 6.71 (d, *J* = 9.3 Hz, 1 H), 5.41 (d, *J* = 3.4 Hz, 1 H), 5.33 (m, 2 H), 5.25-5.21 (m, 2 H), 4.95 (dt, *J* = 10.3, 2.9 Hz, 1 H), 4.88 (d, *J* = 3.4 Hz, 1 H), 4.71 (d, *J* = 12.2 Hz, 1 H), 4.60 (d, *J* = 12.2 Hz, 1 H), 4.36 (tt, *J* = 9.3, 3.4 Hz, 1 H), 4.17 (t, *J* = 6.5 Hz, 1 H), 4.10 (m, 1 H), 4.03 (dd, *J* = 11.2, 6.8 Hz, 1 H), 3.82 (dd, *J* = 10.2, 3.4 Hz, 1 H), 3.66 (qd, *J* = 11.2, 3.4 Hz, 2 H), 2.19 (m, 2 H), 2.09 (s, 3 H), 2.08 (s, 3 H), 2.04 (s, 3 H), 2.02 (m, 4 H), 1.99 (s, 3 H), 1.96 (s, 3 H), 1.68-1.57 (m, 4 H), 1.26 (br s, 56 H), 0.88 (t, *J* = 6.8 Hz, 6 H); ^{13}C NMR ($CDCl_3$, 125 MHz) δ 173.02, 170.77, 170.49, 170.23, 170.11, 169.96, 138.07, 129.99, 129.97, 128.49, 127.96, 98.73, 73.61, 73.12, 73.05, 72.14, 69.46, 68.45, 67.85, 66.98, 61.88, 48.22, 37.79, 32.50, 32.01, 30.64, 29.88, 29.81, 29.72, 29.68, 29.51, 29.42, 28.14, 27.32, 27.75, 25.68, 21.05, 20.98, 20.82, 20.79, 20.70, 14.30, 14.22; HRMS (ESI) *m/z* for $C_{65}H_{109}NNaO_{14}$ ($[M+Na]^+$) 1150.77364 (100%), calc. 1150.77403.

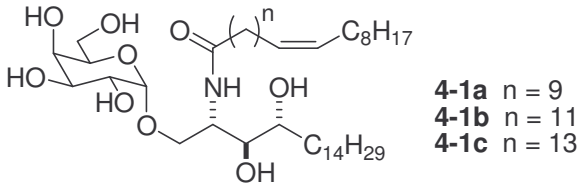

4-1a n = 9
4-1b n = 11
4-1c n = 13

4-1a. Sodium metal (90 mg, 3.9 mmol) was added to liquid ammonia (25 mL) at -76°C under N_2 and allowed to dissolve over 10 m. A solution of **4-8a** (129 mg, 0.118 mmol) in anhydrous THF (7 mL) was added to the blue mixture dropwise and allowed to react for 1 h. The reaction was then quenched with MeOH (6 mL) and dried under a

stream of N_2 overnight. The resulting whitish solid was taken up into a minimal amount of MeOH and $CHCl_3$ and adsorbed onto silica gel before purifying by gradient flash chromatography (SiO_2, MeOH:$CHCl_3$ 5:95 to 10:90 to 15:85). The purified product was dissolved in DMSO (4 mL) and lyophilized to yield a white fluffy solid (41 mg, 45%, R_f = 0.42 MeOH:$CHCl_3$ 15:85). ^{1}H NMR (pyridine-d_5, 500 MHz) δ 8.43 (d, J = 9.3 Hz, 1 H), 6.93 (br s, 1 H), 6.59 (br s, 1 H), 6.50 (br s, 1 H), 6.42 (br s, 1 H), 6.28 (br s, 1 H), 6.08 (br s, 1 H), 5.57 (d, J = 3.4 Hz, 1 H), 5.49 (m, 2 H), 5.26 (m, 1 H), 4.66 (m, 2 H), 4.55 (br s, 1 H), 4.51 (t, J = 6.0 Hz, 1 H), 4.44-4.38 (m, 4 H), 4.32 (br s, 2 H), 2.43 (t, J = 7.5 Hz, 2 H), 2.32-2.24 (m, 1 H), 2.10 (m, 4 H), 1.95-1.84 (m, 2 H) 1.84-1.76 (m, 2 H), 1.67 (br s, 1 H), 1.25 (br s, 46 H), 0.87 (m, 6 H); ^{13}C NMR (pyridine-d_5, 125 MHz) δ 173.57, 130.58, 101.21, 76.42, 72.71, 72.18, 71.29, 70.67, 69.98, 68.35, 62.34, 51.12, 36.46, 34.04, 31.79, 31.75, 30.03, 29.80, 29.77, 29.66, 29.59, 29.52, 29.45, 29.27, 29.26, 29.21, 27.23, 27.19, 26.16, 26.04, 22.58, 13.93; HRMS (FAB) *m/z* for $C_{44}H_{85}NNaO_9$ ($[M+Na]^+$) 794.6121 (93.8%), calc. 794.6117.

4-1b. Same procedure as synthesis of **4-1a** (52%). ^{1}H NMR (pyridine-d_5, 500 MHz) δ 8.47 (d, J = 9.3 Hz, 1 H), 5.60 (d, J = 3.4 Hz, 1 H), 5.51 (m, 2 H), 5.25 (m, 1 H), 4.66 (m, 2 H), 4.55 (br s, 1 H), 4.51 (m, 1 H), 4.44-4.39 (m, 4 H), 4.32 (br s, 2 H), 2.45 (t, J = 7.3 Hz, 2 H), 2.32-2.24 (m, 1 H), 2.12 (m, 4 H), 1.96-1.85 (m, 2 H), 1.85-1.76 (m, 2 H), 1.67 (br s, 1 H), 1.26 (br s, 50 H), 0.87 (m, 6 H); ^{13}C NMR (pyridine-d_5, 75 MHz) δ 173.62, 130.72, 102.02, 77.21, 73.50, 72.97, 72.08, 71.47, 70.77, 69.16, 63.014, 51.84, 37.27, 34.83, 32.60, 30.83, 30.58, 30.47, 30.23, 30.09, 30.02, 28.03, 26.97, 26.85, 26.42, 23.40, 14.74; HRMS (FAB) *m/z* for $C_{46}H_{89}NNaO_9$ ($[M+Na]^+$) 822.6432 (100%), calc. 822.6430.

4-1c. Same procedure as synthesis of **4-1a** (55%). ^{1}H NMR (pyridine-d_5, 500 MHz) δ 8.47 (d, J = 9.3 Hz, 1 H), 6.97 (br s, 1 H), 6.63 (br s, 1 H), 6.52 (br s, 1 H), 6.45 (br s, 1 H), 6.31 (br s, 1 H), 6.08 (br s, 1 H), 5.57 (d, J = 3.4 Hz, 1 H), 5.51 (m, 2 H), 5.26 (m, 1 H), 4.66 (m, 2 H), 4.55 (br s, 1 H), 4.51 (t, J = 5.9 Hz, 1 H), 4.44-4.38 (m, 4 H), 4.32 (br s, 2 H), 2.45 (t, J = 7.5 Hz, 2 H), 2.32-2.24 (m, 1 H), 2.13 (m, 4 H), 1.96-1.86 (m, 2 H) 1.86-1.78 (m, 2 H), 1.67 (br s, 1 H), 1.26 (br s, 54 H), 0.87 (m, 6 H); ^{13}C NMR (pyridine-d_5, 125 MHz) δ 173.63, 130.65, 101.93, 77.12, 73.43, 72.89, 72.00, 71.39, 70.70, 69.07, 63.06, 51.83, 37.19, 34.75, 32.52, 32.49, 30.79, 30.54, 30.40, 30.33, 30.30, 30.22, 30.17, 30.02, 29.96, 27.93, 27.95, 26.90, 26.79, 23.34, 14.67; HRMS (ESI) *m/z* for $C_{48}H_{93}NNaO_9$ ([M+Na]$^+$) 850.67576 (100%), calc. 850.67425.

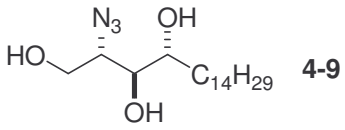

4-9

4-9. Sodium azide (11.52 g, 177.2 mmol) was dissolved in deionized water (30 mL) followed by addition of CH_2Cl_2 (45 mL) with vigorous stirring. The mixture was cooled to 0^{o}C then Tf_2O (6 mL, 35 mmol) was added dropwise. After stirring for 2 h, the aqueous layer was separated, extracted with CH_2Cl_2 (2 x 25 mL), and washed with saturated aqueous $NaHCO_3$ (15 mL). Phytosphingosine (5.63 g, 17.7 mmol; from Degussa) was suspended in deionized water (60 mL) followed by addition of K_2CO_3 (3.66 g, 26.5 mmol), $CuSO_4$ (30 mg, 0.19 mmol), and MeOH (100 mL). The azide solution was added and the reaction mixture was homogenized by adding aliquots of MeOH (7 x 5 mL). After stirring at room temperature for 12 h, TLC (MeOH:$CHCl_3$ 1:9) showed full conversion of the amine (R_f = 0.03) to azide (R_f = 0.51). The solvent was removed in vacuo, homogenized in MeOH:CH_2Cl_2 15:85, and filtered through a silica gel

plug to yield a white powder (6.035 g, 99%) after solvent evaporation. ^{1}H NMR ($CDCl_3$, 500 MHz) δ 4.01 (dd, *J* = 11.7, 5.9 Hz, 1 H), 3.92 (dd, *J* = 11.7, 4.4, 1 H), 3.85 (m, 1 H), 3.80 (t, *J* = 4.9 Hz, 1 H), 3.66 (q, *J* = 4.9 Hz, 1 H), 1.68-1.48 (m, 2 H), 1.26 (br s, 24 H), 0.88 (t, *J* = 6.8 Hz, 3 H); ^{13}C NMR ($CDCl_3$, 125 MHz) δ 74.49, 72.36, 63.36, 61.45, 32.08, 32.04, 29.80, 29.76, 29.47, 25.94, 22.80, 14.20; HRMS (EI) *m/z* for $C_{18}H_{37}N_3NaO_3$ ($[M+Na]^+$) 366.2736 (100%), calc. 366.2727.

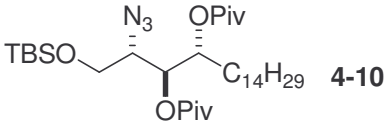

4-10

4-10. 2-Azidophytosphingosine (**4-9**; 1.0 g, 2.9 mmol) was dissolved in anhydrous THF (50 mL) and warmed to 60°C. TBSCl (1.3 g, 8.6 mmol) and imidazole (590 mg, 8.6 mmol) were added and the reaction quenched slowly with water (20 mL) after 20 m. The aqueous layer was extracted with EtOAc (3 x 30 mL), the organic fractions combined and washed with 5% HCl (10 mL) and brine (20 mL), and the solution dried with Na_2SO_4. Concentration of the solvent yielded the crude silane as a colorless oil (1.55 g, R_f = 0.73 EtOAc:Hex 1:2). Dipivoylation was performed by dissolving the oil in THF (20 mL) and adding excess Et_3N (1 mL), DMAP (100 mg, 0.818 mmol), then pivaloyl chloride (900 µL, 7.3 mmol) dropwise. The white mixture was allowed to stir for 16 h at room temperature before the solvent was removed in vacuo and the residue purified by flash chromatography (SiO_2, EtOAc:Hex 1:8) yielding a colorless oil (1.64 g, 90%, R_f = 0.53 EtOAc:Hex 1:8). ^{1}H NMR ($CDCl_3$, 500 MHz) δ 5.11 (m, 1 H), 5.08 (dd, *J* = 7.3, 3.4 Hz,1 H), 3.86 (dd, *J* = 10.3, 2.9 Hz, 1 H), 3.70 (dd, *J* = 10.3, 7.3 Hz, 1 H), 3.54 (ddd, *J* = 10.3, 7.3, 2.9 Hz, 1 H), 1.70-1.60 (m, 2 H), 1.26 (br s, 24 H), 1.21 (s, 9 H), 1.19 (s, 9 H), 0.88 (m, 12 H), 0.75 (s, 6 H); ^{13}C NMR ($CDCl_3$, 125 MHz) δ 177.70, 176.92, 72.54,

71.49, 63.87, 62.49, 39.14, 39.06, 32.15, 29.89, 29.72, 29.63, 29.59, 29.49, 29.29, 27.38, 27.31, 26.73, 25.97, 25.50, 22.92, 18.41, 14.35, -5.33, -5.40; HRMS (FAB) *m/z* for $C_{34}H_{67}N_3NaO_5Si$ ($[M+Na]^+$) 648.4742 (100%), calc. 648.4740.

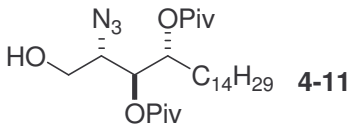

4-11

4-11. Azide **4-10** (1.64 g, 2.62 mmol) was dissolved in THF (12 mL) and aqueous HF (3 mL, 49%). After 10 m, TLC (EtOAc:Hex 1:1) showed all starting material gone and formation of the desilylated ceramide (R_f = 0.67). The reaction was poured carefully into saturated aqueous $NaHCO_3$ (10 mL), extracted with EtOAc (10 mL), rewashed with $NaHCO_3$ (10 mL), back extracted with EtOAc (3 x 30 mL), washed with brine (10 mL), and dried thoroughly with Na_2SO_4 before concentrating. Flash chromatography (SiO_2, EtOAc:Hex 1:1) yielded the product as a colorless oil (1.30 g, 97%). ^{1}H NMR ($CDCl_3$, 500 MHz) δ 5.16-5.12 (m, 2 H), 3.86 (m, 1 H), 3.65 (m, 1 H), 3.55 (m, 1 H), 2.38 (br s, 1 H), 1.76-1.61 (m, 2 H), 1.25 (br s, 24 H), 1.22 (s, 9 H), 1.19 (s, 9 H), 0.88 (t, *J* = 6.8 Hz, 3 H); ^{13}C NMR ($CDCl_3$, 125 MHz) δ 178.04, 177.86, 72.52, 71.97, 62.82, 62.21, 39.25, 39.09, 32.13, 29.86, 29.82, 29.69, 29.61, 29.56, 29.45, 27.20, 27.31, 25.56, 22.90, 14.33; HRMS (FAB) *m/z* for $C_{28}H_{53}N_3NaO_5$ ($[M+Na]^+$) 534.3877 (100%), calc. 534.3885.

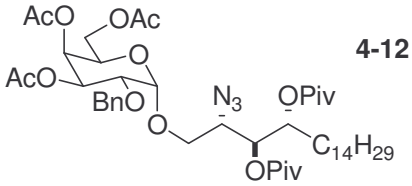

4-12

4-12. Bromide donor **4-7** (340 mg, 0.619 mmol) and azide **4-11** (215 mg, 0.420 mmol) were dissolved in anhydrous CH_2Cl_2 (12 mL) under N_2 and cooled to 0°C. Freshly crushed 4 Å molecular sieves (500 mg) were added and the mixture was allowed

to stir for 10 m before addition of AgOTf (330 mg, 1.28 mmol) in the dark. The reaction vessel was wrapped in aluminum foil and allowed to warm to room temperature. After 12 h, the slurry was filtered through Celite after dilution with EtOAc (15 mL). The resulting colorless solution was concentrated and purified by flash chromatography (SiO_2, EtOAc:Hex 1:2), which yielded a colorless oil (401 mg). ^{1}H NMR analysis of the mixture ($CDCl_3$, 500 MHz) revealed a 6:1 mixture of α:β anomers (H1' α: 5.45 ppm, J = 3.4 Hz; β: 5.34 ppm, J = 7.8 Hz). Complete separation of the anomers was realized by gravity column chromatography (SiO_2, MeOH:CH_2Cl_2 1.5:98.5) providing both as colorless oils (α: 318 mg, 85%, R_f = 0.29; β: 49 mg, 13%, R_f = 0.68; 6.5:1 α:β). α-anomer: ^{1}H NMR ($CDCl_3$, 500 MHz) δ 7.34 (m, 4 H), 7.29 (m, 1 H), 5.45 (d, *J* = 3.4, 1 H), 5.29 (dd, *J* = 10.7, 3.4 Hz, 1 H), 5.10 (m, 2 H), 4.91 (d, *J* = 3.4 Hz, 1 H), 4.66 (s, 2 H), 4.18 (t, *J* = 7.8 Hz, 1 H), 4.05 (m, 2 H), 3.92 (dd, *J* = 10.7, 2.4 Hz, 1 H), 3.85 (dd, *J* = 10.7, 3.4 Hz, 1 H), 3.80 (m, 1 H), 3.48 (dd, *J* = 10.7, 9.3 Hz, 1 H), 2.10 (s, 3 H), 2.03 (s, 3 H), 1.97 (s, 3 H), 1.68-1.62 (m, 2 H), 1.25 (br s, 24), 1.22 (s, 9 H), 1.19 (s, 9H), 0.88 (t, *J* = 6.7 Hz, 3 H); ^{13}C NMR ($CDCl_3$, 125 MHz) δ 177.78, 177.04, 170.60, 170.31, 170.21, 138.26, 128.60, 128.02, 127.91, 98.70, 73.44, 73.15, 72.16, 72.10, 69.60, 68.59, 68.47, 66.83, 61.80, 61.62, 39.18, 39.07, 32.14, 29.89, 29.71, 29.63, 29.60, 29.57, 29.48, 27.35, 27.28, 25.37, 22.90, 20.99, 20.87, 14.34; HRMS (FAB) *m/z* for $C_{47}H_{75}N_3NaO_{13}$ ($[M+Na]^+$) 912.5198 (100%), calc. 912.5187.

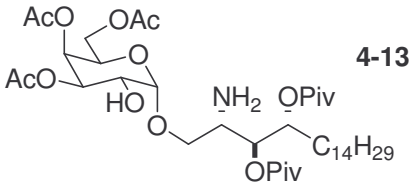

4-13

4-13. Protected glycosphingolipid **4-12** (318 mg, 0.357 mmol) was dissolved in THF (10 mL), MeOH (3 mL), and concentrated aqueous HCl (100 μL) and placed in a hydrogenation vessel. Palladium on carbon (10%, 62 mg) was added slowly and the container filled with H_2 (200 psi). After 6 h, the vessel was evacuated and the reaction progress checked by TLC (R_f = 0.41, MeOH:CH_2Cl_2 5:95). The suspension was filtered through a Celite plug using MeOH:CH_2Cl_2 1:9 as a diluent, concentrated in vacuo, and purified by column chromatography (SiO_2, MeOH:CH_2Cl_2 5:95) to yield a white amorphous solid (166 mg; 60%). ^{1}H NMR ($CDCl_3$, 500 MHz) δ 5.41 (d, *J* = 3.0 Hz, 1 H), 5.21 (dt, *J* = 9.8, 3.4 Hz, 1 H), 5.14 (dd, *J* = 10.7, 3.4 Hz, 1 H), 5.10 (m, 1 H), 4.89 (d, *J* = 3.9, 1 H), 4.21 (t, *J* = 6.8, 1 H), 4.09 (m, 2 H), 3.95 (dd, *J* = 10.2, 3.4 Hz, 1 H), 3.91 (dd, *J* = 10.2, 2.4 Hz, 1 H), 3.29 (dd, *J* = 9.4, 7.6 Hz, 1 H), 3.16 (td, *J* = 6.8, 2.4 Hz, 1 H), 2.13 (s, 3 H), 2.13 (s, 3 H), 2.05 (s, 3 H), 2.04 (s, 3 H), 1.70-1.56 (m, 2 H), 1.25 (br s, 24 H), 1.22 (s, 9 H), 1.18 (s, 9 H), 0.88 (t, *J* = 6.3 Hz, 3 H); ^{13}C NMR ($CDCl_3$, 125 MHz) δ 178.06, 177.92, 171.01, 170.64, 170.44, 99.98, 74.16, 72.36, 70.74, 70.02, 68.25, 67.07, 66.89, 61.74, 51.70, 50.63, 39.21, 39.04, 32.06, 29.81, 29.65, 29.59, 29.50, 29.05, 27.27, 25.42, 22.83, 21.02, 20.84, 20.79, 14.27; HRMS (FAB) *m/z* for $C_{40}H_{71}NNaO_{13}$ ($[M+Na]^+$) 796.4818 (100%), calc. 796.4818.

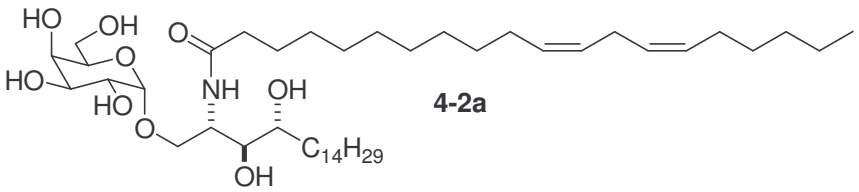

4-2a

4-2a. (11*Z*,14*Z*)-Eicosadienoic acid (70 mg, 0.227 mmol) was dissolved in anhydrous CH_2Cl_2 (4 mL) that had been sparged with argon for 30 m. HBTU (79 mg, 0.208 mmol), Et_3N (100 μL), and *p*-dioxane (500 μL) were added and the reaction stirred for 20 m under argon. An argon-sparged solution of deprotected amine **4-13** (129 mg, 0.167 mmol) in CH_2Cl_2 (3 mL) and Et_3N (100 μL) was then added and the reaction allowed to proceed for 16 h. The solvent was removed in vacuo and the crude product purified by column chromatography (SiO_2, EtOAc:Hex 1:2) under argon. The product was isolated as a colorless oil (57 mg, 32%, R_f = 0.42 EtOAc:Hex 1:2). ^{1}H NMR ($CDCl_3$, 500 MHz) δ 6.45 (d, *J* = 9.3 Hz, 1 H), 5.42 (d, *J* = 3.0 Hz, 1 H), 5.35 (m, 5 H), 5.10 (dd, *J* = 10.7, 3.4 Hz, 1 H), 4.94 (td, *J* = 7.3, 3.4 Hz, 1 H), 4.78 (d, *J* = 3.9 Hz, 1 H), 4.43 (tt, *J* = 9.7, 3.2 Hz, 1 H), 4.13 (t, *J* = 6.9 Hz, 1 H), 4.10-4.01 (m, 2 H), 3.92 (td, *J* = 10.7, 3.4 Hz, 1 H), 3.77 (dd, *J* = 10.3, 2.4 Hz, 1 H), 3.38 (dd, *J* = 10.3, 2.9 Hz, 1 H), 2.77 (t, *J* = 6.8, 2 H), 2.67 (d, *J* = 11.2 Hz, 1 H), 2.28 (t, *J* = 7.8 Hz, 2 H), 2.12 (s, 3 H), 2.06 (s, 3 H), 2.04 (m, 4 H), 2.02 (s, 3 H), 1.76-1.60 (m, 4 H), 1.25 (br s, 42 H), 1.22 (s, 9 H), 1.15 (s, 9 H), 0.88 (m, 6 H); ^{13}C NMR ($CDCl_3$, 125 MHz) δ 178.42, 178.36, 173.30, 171.06, 170.62, 170.36, 130.39, 128.15, 99.48, 72.92, 70.88, 70.82, 68.19, 67.98, 67.18, 66.89, 62.03, 47.91, 39.32, 39.04, 32.09, 31.69, 29.87, 29.75, 29.71, 29.66, 29.53, 29.34, 27.59, 27.42, 27.35, 27.27, 27.21, 25.88, 25.78, 25.66, 22.86, 22.75, 21.07, 20.82, 20.79, 14.30, 14.25; HRMS (FAB) *m/z* for $C_{60}H_{105}NNaO_{14}$ ($[M+Na]^+$) 1086.7441 (29.1%), calc. 1086.7427. The protected glycosphingolipid (57 mg, 0.54 mmol) was dissolved in

anhydrous MeOH (1 mL) follwed by the addition of a methanolic solution of NaOMe (1.15 *M*, 1.50 mL, 1.74 mmol). The solution was warmed to 40°C and gently sparged with argon. After 10 m, TLC showed the disappearance of the triacetate (R_f = 0.55, MeOH:CH_2Cl_2 1:9). The reaction proceeded for 5.5 h until total depivoylation was seen (R_f = 0.36). The reaction was cooled to room temperature with precipitation of a white solid. Deionized water (150 µL) was added to aid precipitation and the reaction vessel was centrifuged (4000 rpm, 6 m). The supernatant was removed, another aliquot of MeOH:H_2O (10:1, 1.1 mL) added, and the flask centrifuged again twice more. The solid was dissolved in DMSO (3 mL) and lyophilized for 12 h yielding **4-2a** as white fluffy powder (31 mg, 76%). ^{1}H NMR (DMSO-d_6, 500 MHz) δ 7.70 (d, *J* = 8.3 Hz, 1 H), 5.32 (m, 4 H), 4.80 (br s, 1 H), 4.72 (br s, 1 H), 4.67 (d, *J* = 3.4 Hz, 1 H), 4.56 (br s, 2 H), 4.37 (br s, 1 H), 4.14 (br s, 1 H), 3.98 (br s, 1 H), 3.68 (br s, 1 H), 3.64 (dd, *J* = 10.0, 4.6 Hz, 1 H), 3.58 (t, *J* = 6.3 Hz, 1 H), 3.52 (br s, 2 H), 3.50-3.35 (m, 5 H), 2.73 (t, *J* = 6.8 Hz, 2 H), 2.05 (m, 2 H), 2.01 (q, *J* = 6.8 Hz, 4 H), 1.58-1.38 (m, 4 H), 1.23 (br s, 42 H), 0.86 (m, 6 H); ^{13}C NMR (DMSO-d_6, 125 MHz) δ 171.68, 129.72, 127.75, 99.47, 73.80, 72.10, 71.27, 70.52, 70.06, 69.78, 68.77, 68.59, 66.56, 60.50, 49.73, 35.49, 31.55, 31.34, 30.95, 29.28, 29.14, 29.07, 29.02, 28.77, 26.69, 26.64, 25.45, 25.23, 22.15, 22.02, 13.99; HRMS (FAB) *m/z* for $C_{44}H_{83}NNaO_9$ ([M+Na]$^+$) 792.5969 (100%), calc. 792.5960.

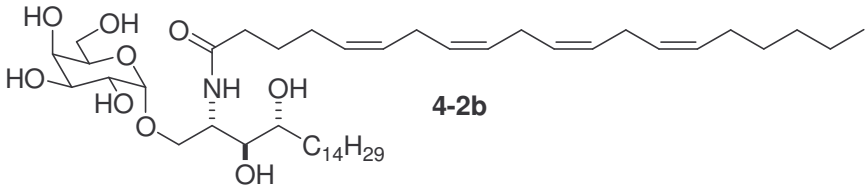

4-2b

4-2b. Same procedure as acylation of **4-2a**, substituting with arachidonic acid (44%). Protected compound: ^{1}H NMR ($CDCl_3$, 500 MHz) δ 6.52 (d, *J* = 9.3 Hz, 1 H), 5.40 (d, *J*

= 3.0 Hz, 1 H), 5.39-5.27 (m, 8 H), 5.28 (dd, *J* = 10.2, 2.4 Hz, 1 H), 5.09 (dd, *J* = 10.7, 3.4 Hz, 1 H), 4.92 (td, *J* = 7.3, 2.4 Hz, 1 H), 4.77 (d, *J* = 3.9 Hz, 1 H), 4.42 (tt, *J* = 9.8, 3.4 Hz, 1 H), 4.13 (t, *J* = 6.3 Hz, 1 H), 4.10-4.00 (m, 2 H), 3.90 (td, *J* = 10.3, 2.9 Hz, 1 H), 3.75 (dd, *J* = 10.3, 2.4 Hz, 1 H), 3.37 (dd, *J* = 10.3, 2.9 Hz, 1 H), 2.81 (m, 6 H), 2.67 (d, *J* = 11.2 Hz, 1 H), 2.28 (t, *J* = 7.8 Hz, 2 H), 2.11 (s, 3 H), 2.06 (s, 3 H), 2.04 (m, 4 H), 2.02 (s, 3 H), 1.78-1.66 (m, 4 H), 1.26 (br s, 30 H), 1.22 (s, 9 H), 1.14 (s, 9 H), 0.87 (m, 6 H); ^{13}C NMR ($CDCl_3$, 125 MHz) δ 178.56, 178.32, 173.00, 171.02, 170.57, 170.30, 130.63, 129.14, 128.99, 128.74, 128.41, 128.35, 128.06, 127.73, 99.47, 72.92, 70.93, 70.86, 68.19, 67.99, 67.20, 66.90, 62.01, 47.98, 39.32, 39.06, 36.23, 32.09, 31.68, 29.86, 29.70, 29.65, 29.54, 29.49, 29.37, 27.67, 27.38, 27.27, 27.22, 26.93, 25.79, 25.65, 22.86, 22.75, 21.08, 20.83, 20.79, 14.30, 14.25; HRMS (FAB) *m/z* for $C_{60}H_{101}NNaO_{14}$ ($[M+Na]^+$) 1082.7120 (93.1%), calc. 1082.7114. Deprotection was done following the same procedure as **4-2a** (Protected **4-2b** precursor: 51 mg, 0.048 mmol), except isolation needed to be done in a different manner due to the product being formed as an oil. After deprotection, the solvent was removed and the crude compound was purified by flash chromatography under argon (SiO_2, MeOH:$CHCl_3$ 15:85) to yield a colorless oil (24 mg, 65% R_f = 0.46 MeOH:$CHCl_3$ 15:85). ^{1}H NMR (DMSO-d_6, 500 MHz) δ 7.61 (d, *J* = 8.8 Hz, 1 H), 5.32 (m, 8 H), 4.67 (d, *J* = 2.9 Hz, 1 H), 4.64 (d, *J* = 5.4 Hz, 1 H), 4.54 (m, 2 H), 4.43 (d, *J* = 7.3 Hz, 1 H), 4.37 (d, *J* = 4.4 Hz, 1 H), 4.32 (d, *J* = 6.3 Hz, 1 H), 4.02 (m, 1 H), 3.72-3.64 (m, 2 H), 3.59 (t, *J* = 6.3 Hz, 1 H), 3.54-3.38 (m, 7 H), 2.79 (m, 6 H), 2.09 (t, *J* = 7.3 Hz, 2 H), 2.02 (m, 4 H), 1.58-1.45 (m, 4 H), 1.23 (br s, 30 H), 0.86 (m, 6 H); ^{13}C NMR (DMSO-d_6, 125 MHz) δ 171.48, 129.94, 129.48, 128.13, 128.03, 127.95, 127.81, 127.68, 127.53, 99.43, 74.07, 71.25, 70.56, 69.80, 68.83, 68.52, 66.46, 60.54,

49.65, 34.98, 31.32, 30.91, 29.12, 28.74, 26.63, 26.33, 25.43, 25.21, 22.12, 13.98; HRMS (FAB) *m/z* for $C_{44}H_{79}NNaO_9$ ($[M+Na]^+$) 788.5665 (100%), calc. 788.5647.

αGalCer. Same procedure as acylation of **4-2a**, substituting with hexacosanoic acid and omitting the use of argon (38%). ^{1}H NMR ($CDCl_3$, 500 MHz) δ 6.78 (d, *J* = 9.8 Hz, 1 H), 5.41 (d, *J* = 2.9 Hz, 1 H), 5.36 (dd, *J* = 10.7, 2.4 Hz, 1 H), 5.15 (dd, *J* = 10.7, 2.9 Hz, 1 H), 4.93 (m, 1 H), 4.78 (d, *J* = 3.9 Hz, 1 H), 4.42 (tt, *J* = 9.8, 2.4 Hz, 1 H), 4.13 (t, *J* = 6.3 Hz, 1 H), 4.08 (m, 1 H), 4.03 (dd, *J* = 11.2, 7.3 Hz, 1 H), 3.92 (td, *J* = 10.3, 2.4 Hz, 1 H), 3.76 (dd, *J* = 10.3, 2.4 Hz, 1 H), 3.36 (dd, *J* = 10.3, 2.4 Hz, 1 H), 2.72 (d, *J* = 11.2 Hz, 1 H), 2.28 (t, *J* = 7.8 Hz, 2 H), 2.12 (s, 3 H), 2.06 (s, 3 H), 2.03 (s, 3 H), 1.74-1.60 (m, 4 H), 1.25 (br s, 68 H), 1.22 (s, 9 H), 1.15 (s, 9 H), 0.88 (t, *J* = 6.8 Hz, 6 H); ^{13}C NMR ($CDCl_3$, 125 MHz) δ 178.75, 178.32, 173.34, 171.20, 170.61, 170.36, 99.27, 73.12, 70.91, 70.57, 68.31, 67.67, 67.29, 66.96, 62.07, 47.91, 39.33, 39.11, 36.79, 32.13, 29.90, 29.78, 29.74, 29.57, 29.35, 27.46, 27.31, 27.24, 25.93, 25.70, 22.89, 21.12, 20.85, 14.32; HRMS (FAB) *m/z* for $C_{66}H_{121}NNaO_{14}$ ($[M+Na]^+$) 1174.8684 (100%), calc. 1174.8679. Deprotection was done following the same procedure as **4-2a** (Protected αGalCer precursor: 48 mg, 0.042 mmol), omitting the use of argon (78%). ^{1}H NMR (pyridine-d_5, 500 MHz) δ 8.60 (d, *J* = 9.3 Hz, 1 H), 6.68 (d, *J* = 5.9 Hz, 1 H), 6.39 (d, *J* = 2.9 Hz, 1 H), 6.36 (t, *J* = 5.9 Hz, 1 H), 5.98 (d, *J* = 9.8 Hz, 1 H), 5.59 (d, *J* = 10.7 Hz, 1 H), 5.29 (d, *J* = 3.9 Hz, 1 H), 5.25 (d, *J* = 8.8 Hz, 1 H), 5.10-4.98 (m, 1 H), 4.58 (m, 2 H), 4.48-4.40 (m, 2 H), 4.25 (m, 4 H), 4.02 (m, 2 H), 2.50 (t, *J* = 7.3 Hz, 2 H), 2.24 (m, 1 H), 2.00-1.98 (m, 1 H), 1.96-1.81 (m, 3 H), 1.60 (m, 1 H), 1.27 (m, 66 H), 0.88 (m, 6 H); ^{13}C NMR (pyridine-d_5, 125 MHz) δ 173.94, 102.54, 76.89, 73.88, 73.67, 72.60, 71.84, 71.28, 71.00, 63.13,

50.59, 37.04, 32.55, 30.43, 30.32, 30.14, 30.05, 29.96, 26.72, 26.50, 23.35, 14.70; HRMS (FAB) *m/z* for $C_{50}H_{99}NNaO_9$ ($[M+Na]^+$) 880.7220 (100%), calc. 880.7212.

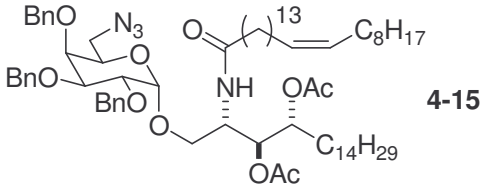

4-15

4-15. Fluoride donor **4-14** (3.39 g, 7.10 mmol) and ceramide **4-6c** (2.35 g, 3.13 mmol) were dissolved in anhydrous CH_2Cl_2 (470 mL) and cooled to 0°C. Freshly crushed 4 Å molecular sieves (10 g) were added and the mixture was allowed to stir for 10 m before addition of $AgClO_4$ (1.94 g, 9.36 mmol) and $SnCl_2$ (1.78 g, 9.39 mmol) in the dark. The reaction vessel was wrapped in aluminum foil and stirred under N_2 for 2 h. The reaction mixture was filtered through Celite, the resulting colorless solution was concentrated, and purification performed by column chromatography (SiO_2, EtOAc:Hex 1:4), which yielded a colorless oil (2.0 g, 53%, R_f = 0.42 EtOAc:Hex 1:4). ^{1}H NMR ($CDCl_3$, 500 MHz) δ 7.42-7.29 (m, 15 H), 6.67 (d, *J* = 9.3 Hz, 1 H), 5.36 (m, 2 H), 5.23 (m, 1 H), 4.98 (dd, *J* = 11.0, 3.0 Hz, 1 H), 4.93 (dt, *J* = 10.5, 3.0 Hz, 1 H), 4.86-4.55 (m, 6 H), 4.35 (tt, *J* = 9.3, 3.4 Hz, 1 H), 4.03 (dd, *J* = 10.5, 3.4 Hz, 1 H), 3.92-3.86 (m, 2 H), 3.82-3.78 (m, 2 H), 3.61-3.54 (m, 2 H), 3.05 (dd, *J* = 12.5, 4.5 Hz, 1 H), 2.15 (t, *J* = 7.6 Hz, 2 H), 2.06 (s, 3 H), 2.04 (m, 4 H), 2.02 (s, 3 H), 1.72-1.56 (m, 4 H), 1.26 (br s, 56 H), 0.88 (t, *J* = 6.8 Hz, 6 H); ^{13}C NMR ($CDCl_3$, 125 MHz) δ 173.20, 171.22, 170.38, 138.76, 138.40, 138.23, 130.14, 128.78, 128.67, 128.36, 128.23, 128.11, 127.85, 127.67, 99.95, 78.73, 76.65, 75.01, 74.90, 73.71, 73.42, 71.64, 70.59, 69.80, 51.50, 48.40, 36.96, 32.16, 29.96, 29.69, 29.57, 27.75, 27.46, 25.96, 25.88, 22.94, 21.26, 21.17, 14.38; HRMS (FAB) *m/z* for $C_{73}H_{114}N_4NaO_{10}$ ($[M+Na]^+$) 1229.8434 (21.6%), calc. 1229.8427.

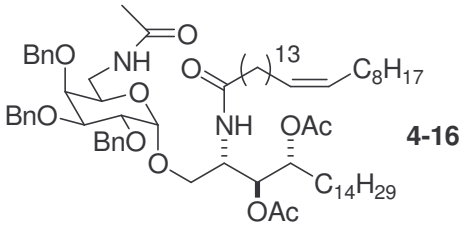

4-16

4-16. Azidoglycosphingolipid **4-15** (2.0 g, 1.7 mmol) was dissolved in THF (107 mL) followed by dropwise addition of deionized water (21 mL). Triphenylphosphine (1.5 g, 5.7 mmol) was added and the reaction allowed to stir for 16 h at room temperature. The solvent was removed in vacuo and the white solid taken up into THF (100 mL) before the addition of Ac_2O (320 µL, 3.4 mmol), Et_3N (470 µL, 3.4 mmol), and DMAP (200 mg, 1.63 mmol). After 2 h, TLC showed complete formation of the acetamide (R_f = 0.23, EtOAc:Hex 1:1). After solvent removal, the crude product was taken up into CH_2Cl_2 (75 mL). The solution was washed with $NaHCO_3$ (25 mL) and brine (25 mL), dried with Na_2SO_4, and purified by flash chromatography (SiO_2, EtOAc:Hex 1:1) yielding the product as a colorless oil (1.85 g, 89%). ^{1}H NMR ($CDCl_3$, 500 MHz) δ 7.42-7.28 (m, 15 H), 6.73 (d, *J* = 9.3 Hz, 1 H), 6.12 (t, *J* = 6.5 Hz, 1 H), 5.36 (m, 2 H), 5.24 (dd, *J* = 9.5, 3.0 Hz, 1 H), 4.97 (d, *J* = 11.5, Hz, 1 H), 4.88 (dt, *J* = 10.5, 3.0 Hz, 1 H), 4.83-4.65 (m, 6 H), 4.31 (tt, *J* = 9.3, 3.0 Hz, 1 H), 4.04 (dd, *J* = 10.5, 3.4 Hz, 1 H), 3.93 (dd, *J* = 11.5, 3.4 Hz, 1 H), 3.86 (dd, *J* = 9.5, 2.5 Hz, 1 H), 3.82 (s, 1 H), 3.79 (t, *J* = 6.5 Hz, 1 H), 3.53-3.47 (m, 2 H), 3.30 (dt, *J* = 13.5, 6.0 Hz, 1 H), 2.13 (t, *J* = 8.0 Hz, 2 H), 2.06 (s, 3 H), 2.03 (s, 3 H), 2.01 (m, 4 H), 1.88 (s, 3 H), 1.74-1.66 (m, 1 H), 1.65-1.54 (m, 3 H), 1.26 (br s, 56 H), 0.89 (t, *J* = 6.8 Hz, 6 H); ^{13}C NMR ($CDCl_3$, 125 MHz) δ 173.49, 171.75, 170.51, 170.41, 138.89, 138.64, 138.57, 130.14, 129.21, 128.65, 128.31, 128.11, 127.79, 100.91, 79.14, 76.64, 74.91, 74.91, 73.85, 73.65, 71.32, 71.10, 70.27, 48.68, 40.24, 36.84, 32.14, 29.94, 29.90, 29.86, 29.82, 29.76, 29.68, 29.60, 29.55,

27.89, 27.45, 25.95, 25.79, 23.37, 22.92, 21.41, 21.19, 14.35; HRMS (FAB) *m/z* for $C_{75}H_{118}N_2NaO_{11}$ ($[M+Na]^+$) 1245.8634 (92.8%), calc. 1245.8628.

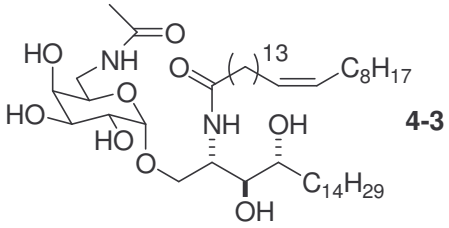

4-3

4-3. Sodium metal (48 mg, 2.1 mmol) was added to liquid ammonia (25 mL) under N_2 at -78°C and allowed to dissolve over 10 m. A solution of **4-16** (127 mg, 0.104 mmol) in anhydrous THF (2 mL) was added to the blue mixture dropwise and allowed to react for 2 h. The reaction was then quenched with MeOH (5 mL) and dried under a stream of N_2 overnight. The crude solid was taken up into a minimal amount of MeOH and $CHCl_3$ and adsorbed onto silica gel before purifying by flash chromatography (SiO_2, MeOH:$CHCl_3$ 1:9). The purified product was dissolved in DMSO (5 mL) and lyophilized to yield a white fluffy solid (62 mg, 68%, R_f = 0.24 MeOH:$CHCl_3$ 1:9). ^{1}H NMR ($CDCl_3$:CD_3OD:D_2O 9:1:0.1, 500 MHz) δ 5.35 (m, 2 H), 4.87 (d, *J* = 3.4 Hz, 1 H), 4.14 (q, *J* = 4.4 Hz, 1 H), 3.84 (dd, *J* = 10.2, 4.4 Hz, 1 H), 3.79 (d, *J* = 2.9 Hz, 1 H), 3.77 (d, *J* = 3.4 Hz, 1 H), 3.73 (m, 2 H), 3.65 (m, 2 H), 3.55 (m, 2 H), 3.22 (dd, *J* = 13.7, 6.8 Hz, 1 H), 2.20 (t, *J* = 7.3 Hz, 2 H), 2.01 (m, 4 H), 1.99 (s, 3 H), 1.66-1.50 (m, 4 H), 1.26 (br s, 56 H), 0.88 (t, *J* = 6.8 Hz, 6 H); ^{13}C NMR ($CDCl_3$:CD_3OD:D_2O 9:1:0.1, 125 MHz) δ 174.61, 172.60, 129.96, 99.57, 74.72, 72.16, 69.92, 69.12, 68.88, 67.14, 50.53, 39.70, 36.58, 32.70, 31.97, 29.83, 29.77, 29.65, 29.56, 29.50, 29.45, 29.42, 29.39, 29.36, 27.25, 25.95, 25.91, 22.72, 22.76, 14.10; HRMS (ESI) *m/z* for $C_{50}H_{96}N_2NaO_9$ ($[M+Na]^+$) 891.70102 (100%), calc. 891.70080.

4.5 References

1) Morita, M.; Motoki, K.; Akimoto, K.; Natori, T.; Sakai, T.; Sawa, E.; Yamaji, K.; Koezuka, Y.; Kobayashi, E.; Fukushima, H. *J. Med. Chem*. **1995**, *38*, 2176.

2) Goff, R. D.; Gao, Y.; Mattner, J.; Zhou, D.; Yin, N.; Cantu, C., III; Teyton, L.; Bendelac, A.; Savage, P. B. *J. Am. Chem. Soc*. **2004**, *126*, 13602.

3) (a) Bezbradica, J. S.; Stanic, A. K.; Matsuki, N.; Bour-Jordan, H.; Bluestone, J. A.; Thomas, J. W.; Unutmaz, D.; van Kaer, L.; Joyce, S. *J. Immunol*. **2005**, *174*, 4696. (b) van Kaer, L. *Nat. Rev. Immunol*. **2005**, *5*, 31.

4) Wu, D.; Zajonc, D. M.; Fujio, M.; Sullivan, B. S.; Kinjo, Y.; Kronenberg, M.; Wilson, I. A.; Wong, C.-H. *Proc. Nat. Acad. Sci. USA* **2006**, *103*, 3972.

5) Oki, S.; Chiba, A.; Yamamura, T.; Miyake, S. *J. Clin. Invest*. **2004**, *113*, 1631.

6) (a) Sakai, T.; Naidenko, O. V.; Iijima, H.; Kronenberg, M.; Koezuka, Y. *J. Med. Chem*. **1999**, *42*, 1836. (b) Sakai, T.; Ehara, H.; Koezuka, Y. *Org. Lett*. **1999**, *1*, 359.

7) Naidenko, O. V.; Maher, J. K.; Ernst, Y.; Sakai, T.; Modlin, R. L.; Kronenberg, M. *J. Exp. Med*. **1999**, *190*, 1069.

8) (a) Zajonc, D. M.; Cantu, C., III; Mattner, J.; Zhou, D.; Savage, P. B.; Bendelac, A.; Wilson, I. A.; Teyton, L. *Nat. Immunol*. **2005**, *6*, 810. (b) Koch, M.; Stronge, V. S.; Shepherd, D.; Gadola, S. D.; Mathew, B.; Ritter, G.; Fersht, A. R.; Besra, G. S.; Schmidt, R. R.; Jones, E. Y.; Cerundolo, V. *Nat. Immunol*. **2005**, *6*, 819.

9) Zeng, Z.-H.; Castano, A. R.; Segelke, B. W.; Stura, E. A.; Peterson, P. A.; Wilson, I. A. *Science* **1997**, *277*, 339.

10) Simmons, H. E.; Smith, R. D. *J. Am. Chem. Soc*. **1958**, *80*, 5323.

11) Batuwangala, T.; Shepherd, D.; Gadola, S. D.; Gibson, K. J. C.; Zaccai, N. R.; Fersht, A. R.; Besra, G. S.; Cerundolo, V.; Jones, E. Y. *J. Immunol*. **2004**, *172*, 2382.

12) Benlagha, K.; Weiss, A.; Beavis, A.; Teyton, L.; Bendelac, A. *J. Exp. Med*. **2000**, *191*, 1895.

13) Hanessian, S.; Banoub, J. *Methods Carbohydr. Chem*. **1980**, *8*, 247.

14) Benlagha, K.; Weiss, A.; Beavis, A,; Teyton, L.; Bendelac, A. *J. Exp. Med*. **2000**, *191*, 1895.

15) Takikawa, H.; Muto, S.; Mori, K. *Tetrahedron* **1998**, *54*, 3141.

16) Alper, P. B.; Hung, S.-C.; Wong, C.-H. *Tetrahedron Lett*. **1996**, *37*, 6029.

17) Knorr, R.; Trzeciak, A.; Bannwarth, W.; Gillessen, D. *Tetrahedron Lett*. **1998**, *30*, 1927.

18) Liu, Y.; Goff, R. D.; Zhou, D.; Mattner, J.; Sullivan, B. A.; Khurana, A.; Cantu, C., III; Ravkov, E. V.; Ibegbu, C. C.; Altman, J. D.; Teyton, L. T.; Bendelac, A.; Savage, P. B. *J. Immunol. Methods* **2006**, *312*, 34. Figures 4.6-4.8 and 4.10 are reproduced with permission, Copyright 2006 Elsevier.

19) Lee, P. T.; Putnam, A.; Benlagha, K.; Teyton, L.; Gottlieb, P. A.; Bendelac, A. *J. Clin. Invest*. **2002**, *110*, 793.

20) NIH Tetramer Core Facility website - http://www.yerkes.emory.edu/TETRAMER/CD1d_Tetramers.html.

21) Campos-Martin, Y.; Colmenares, M.; Gozalbo-Lopez, B.; Lopez-Nunez, M.; Savage, P. B.; Martinez-Naves, E. *J. Immunol*. **2006**, *176*, 6172.

CHAPTER 5.

PREPARTION OF A β-*C*-GLYCOSPHINGOLIPID FOR SUPPRESSION OF NKT CELL ACTIVITY

5.1 Introduction

Natural killer T cells are important for the clearance of disease in mammalian immune systems. In individuals with advanced cancerous growths and autoimmunity disorders, NKT cell populations have often been found to be deficient.[1] It has also been implied that NKT cells in mice play a role in allergic reactions and resulting inflammatory responses via secretion of cytokines. Allergen contact sensitivity[2] and airway inflammation and hyperreactivity due to asthma[3] have been found to be mediated by IL-4 production by mVα14i cells. These findings are significant because murine systems are often used as models for humans in immunological research.

In an ongoing effort to understand the underlying basis of natural killer T cell activity as influenced by CD1d-restricted glycosphingolipid antigens, several analogs of the model αGalCer compound have been made. The discovery that biasing immunological activity (i.e., T_H1 or T_H2 response) can be imposed by αGalCer variants[4] has led to better comprehension of structure-activity relationships between GSL antigens and NKT cell responses (see Chapter 3, section 3.2),[5] though the pathway through which this variability happens is still not known.

An alternative to tuning the immune system towards a specific T_H response through NKT cell stimulation is to inhibit their activity in peripheral tissues, such as the circulatory system or spleen. In individuals with ailments due to hyperresponsive

performance or where their regulatory functions have become overactive,[6] suppression of NKT cells may be a viable therapeutic option. This could potentially be accomplished by making the CD1d protein unavailable for antigen restriction and presentation to NKT cell receptors. Competitive inhibition could be possible through administration of a nonantigenic agent either with greater binding affinity for CD1d than an activating ligand or in quantities that would 'outpopulate' those of NKT cell antigens. Because little is known about the scope of natural endogenous and exogenous ligands and their binding affinities, CD1d saturation using an inactive TCR binding partner would serve more effectively in elucidating how undesirable NKT cell effects may be inhibited.

CD1d and other CD1 family members are promiscuous binders; many lipophilic compounds associate with them due to the hydrophobic environment of their ligand binding regions.[7] Although hydrocarbons may readily bind to CD1d, it appears that only glycosphingolipids are able to induce activity in NKT cells through TCR recognition. Furthermore, stimulatory effects are often limited to those GSLs with a composition similar to that of αGalCer (i.e., α-galactosides, ceramides with *N*-acyl chains); GSLs with β-anomeric connectivity between saccharide and ceramide have been found not to have significant antigenic activity when restricted to CD1d.[8] Inactive β-galactosylceramide analogs of αGalCer have the potential to be effective inhibitors because βGalCer has been shown to associate with mouse and human CD1d to a slightly greater degree than αGalCer (**5-1**) and dissociates at the same rate.[9]

To aid the stability of β-GSL-based inhibitors, inclusion of a *C*-glycosidic bond may help prolong their lifetimes in vivo. Replacing the anomeric oxygen of carbohydrates with a methylene group often imparts stability without significantly increasing steric

interactions. *C*-Glycosides also have increased longevity in vivo because of resistance to degradation by glycosidases, reaction with glycosyltrasferases, and hydrolysis due to the lack of the anomeric hemiacetal functional group.[10] These isosteres can frequently function as enzyme inhibitors due to their greater stability in vivo.[11] GSLs with *C*-glycosidic bonds should also be more impervious to ceramidases, intracellular enzymes involved specifically in the metabolism of glycosphingolipids. According to Sandhoff, ceramidases are ubiquitous in lysosomal compartments and serve as catabolic agents to break down monoglycosylceramides, a process necessary not only for GSL component use in signaling pathways and but also to avoid lipid storage disorders (e.g., Krabbe and Farber diseases). Various pH-sensitive ceramidases, along with sphingolipid activator proteins, exist to selectively cleave ceramdes under acidic, alkaline, or neutral conditions.[12] Therefore, substitution of oxygen with a carbon bond to the ceramide at the anomeric position should allow an αGalCer analog to bind to CD1d with similar affinity yet impart a greater amount of resistance to enzymatic and chemical degredation. When coadministered at the same (or greater) concentration as αGalCer, a β-*C*-glycoside is expected to cause a diminished stimulatory response due to its potential of sequestering a portion of CD1d from being bound by the NKT cell agonist. Combined with the stability afforded by the cyclic ether functional group, such an altered compound should posses a longer viable lifetime in vivo than conventional GSLs, like αGalCer, thus increasing the potential to bring about diminished activity of NKT cells.

Conversely, administration of *C*-glycoside analogs of NKT cell antigens potentially have increased potency due to the durability imparted by the carbon-carbon bond. The *C*-glycoside of αGalCer (α-C-GalCer, **5-2**; Figure 5.1) was found to induce greater T_H1-

type activity in Vα14i NKT cells than the parent compound.[13] In B6 mice that had been inoculated with **5-2** there was a greater prophylactic effect in inhibiting liver stage growth and proliferation of *Plasmodium yoelii*, a sporozoite responsible for malarial infection, 1000 times that of αGalCer at nanogram quantities. Additionally, B6 mice that had been infected with B16 melanoma cells responded better to α-C-GalCer than αGalCer at preventing metastatic tumors in the lungs by a factor of 100. The length of stimulatory activity between these two analogs is also significantly different. It was reported that in B6 mice αGalCer-mediated secretion of IFN-γ lasted 24 h after injection, while those subjects dosed with α-C-GalCer required 48 h for a return to a basal cytokine level. Although the reason for this T_H1 bias is still not known, these data demonstrate that making this small change in glycosidic linkage can appreciably change the effect on the immune system.

From research into suppression of NKT cell activity by the Strober research group at Stanford University,[14] a *C*-glycoside-based GSL (**5-3**; Figure 5.1) was developed to act as an inhibitor. When *N*-acyl variants of β-*O*-galactosylceramides were injected intra-peritoneally into mice, Strober and coworkers found that NKT cell activity was suppressed. Expression of NKT cell TCRs was diminished and serum levels of IFN-γ and IL-4 were greatly decreased. The structure with the greatest in vivo inhibitory activity, as

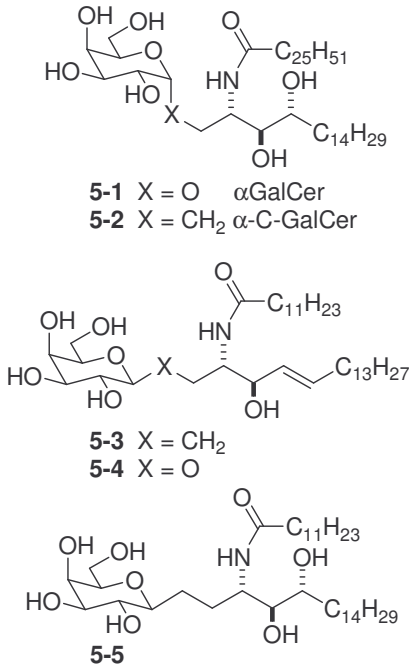

Figure 5.1. αGalCer (**5-1**) and Variant GSLs with β- and/or *C*-Glycosidic Linkages.

found by this study, was compound **5-4**, a β-*O*-galactoside with a sphingosine base and lauroyl (C12) *N*-acyl group. Based on these findings, compound **5-3** was synthesized with the same amide chain length but with a carbon glycosidic bond instead. A second compound, **5-5**, with a phytosphingosine base was also designed and its synthesis was attempted with the intent to compare inhibitory activity against **5-4**.

5.2 Results and Discussion

There are several approaches at making *C*-glycosides, which can be more flexible to create than *O*-analogs due to the ability of saccharide donors to act as electrophiles, nucleophiles, or glycosyl radicals with their compliment acceptors.[15] One method involves the use of activated, electron-rich ("armed") glycosidic donors and nucleophilic silyl acceptors.[16] This results in the preferential formation of α-anomer, which is not the desired product in this case.[10] Another method for making this type of linkage is the Ramburg-Backlund reaction involving stitching together the two halves of a sulfone to make a carbon-carbon bond. It was used by Franck and coworkers in the original synthesis of **5-2**, between an acetylthio sugar and homophytosphingosine.[17]

A general method of *C*-glycosidation is the reaction of a protected glyconolactone with an organometallic nucleophile, such as a Grignard reagent.[18] This is typically done with a reactive tag on the nucleophile for subsequent component addition to fully elaborate the desired structure of the molecule, often to make carbon-linked glycopeptides.[19] Recently, Grubbs' method of cross-metathesis has been found to be a favorable method of attaching tethers onto *C*-glycosidic alkenyl groups.[20] Such a method was used to accomplish a more efficient synthesis of **5-2** by Chen et al.[20c]

Further searching of published research led to the finding of two papers discussing the preparation of β-*C*-galactosylceramides, one using cross-metathesis[21] and the other using Wittig chemistry to make the crucial carbon-carbon bond.[22] Both described lengthy syntheses of more than ten linear steps from starting materials that in themselves required multiple steps from commercially available reagents, though one did not reach the fully deprotected product.[22] These pathways were somewhat attractive due to their use of synthetic techniques that had been previously performed with good results in the Savage research group. Also, the installation of the amide functional group was performed in the penultimate step to provide potential divergence. However, the drawback of these schemes is that many subsequent reactions were required after *C*-glycosylation to finish the ceramide moiety.[21,22] It was envisioned that a glycosyl ylide (**5-12**) could be coupled with a fully elaborated ceramide (**5-14**) in a more efficient synthetic route, rather than needing several linear steps to construct the ceramide from the scaffold of **5-12**.

Both halves of the *C*-glycoside were prepared according to known procedures. Triphenylphosphonium iodide **5-12** was prepared for Wittig coupling by following a procedure by Xie et al. to add vinyl Grignard reagent to 2,3,4,6-tetra-*O*-benzylgalactonolactone (**5-8**) and subsequent reduction of the hemiacetal with triethylsilane.[23] Ozonolysis, in situ reduction to the alcohol, iodination, and triphenylphosphine addition followed, providing **5-12** at an overall yield of 26% from the lactone.[24] Ceramide **5-14** was initially prepared in the same fashion as nonformylated ceramides,[5] except that benzyl ethers were used to protect the secondary alcohols rather than acetyl esters to shorten the number of deprotection steps. Oxidation of the free

primary alcohol with catalytic TPAP and excess NMO as a cooxidant provided aldehyde **5-14** (Scheme 5.1).

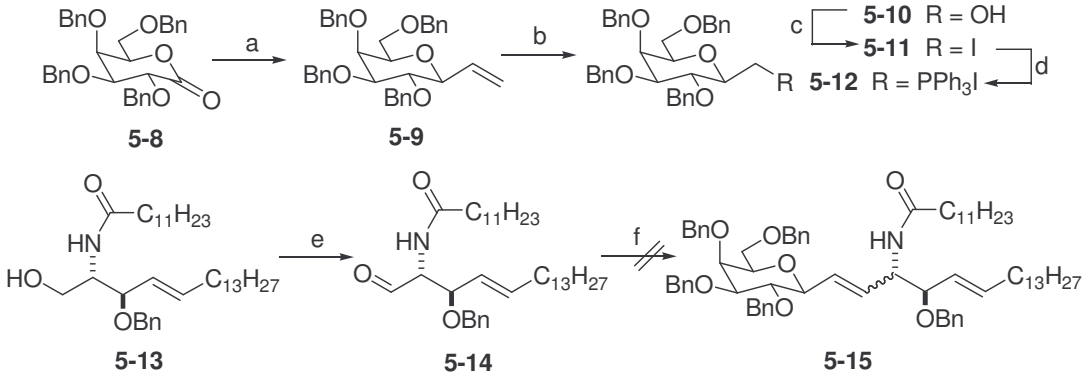

Reagents and conditions: a) i - vinylMgBr, THF, -78°C, ii - TES, BF_3-Et_2O, AcCN, -40°C (50%); b) i - O_3, CH_2Cl_2, -78°C, ii - $NaBH_4$, MeOH, 0°C (73%); c) I_2, PPh_3, imidazole, toluene, reflux (77%); d) PPh_3, 120°C (92%); e) TPAP (8 mol%), NMO, 3A MS, CH_2Cl_2 (34%); f) **5-12**, *n*BuLi, HMPA, THF, -78°C to 0°C (desired product not isolated).

Scheme 5.1. Attempted Wittig Coupling Between *C*-Galactoside **5-12** and Aldehyde **5-14**.

The Wittig reaction of **5-12** and **5-14** was performed using *n*BuLi as a base in THF either with or without HMPA at both low (-78°C) and higher temperatures (-40°C, 0°C) during aldehyde addition. Though the reactions proceeded to completion to provide a coupled product, it was not the desired glycosphingolipid (**5-15**). It appeared that the amide portion of the ceramide was eliminated from the product independent of the reaction temperature. There was no spectral evidence, by ^1H or ^{13}C NMR, of the amide group (i.e., amido nitrogen proton, α-carbonyl methylene group, amide carbonyl carbon) and only four benzyl groups were retained with a signal from a free alcohol (doublet at 3.1 ppm, J = 5.6 Hz, 1 H), although upfield signals indicate one long alkyl chain remained. Also, only three alkenyl protons are evident, not four, with signals more representative of a vinyl group (ddd at 5.88 ppm, 1 H; 2 d at 5.3 ppm, 2 H), than sphingosine (five-tiered multiplet at 5.7 ppm, 1 H; dd at 5.4 ppm, 1 H).

Similar procedures were attempted using altered components to attempt the synthesis of **5-5**, the phytosphingosine analog of **5-3**. Ceramide **5-16** was used to make a formyl analog of **5-14** (**5-17**) that was reacted with **5-12** under the same conditions. From the ^{1}H and ^{13}C NMR spectra of the product, it appears that the same compound from the combination of **5-8** and **5-14** was made instead of desired alkene **5-18** (Scheme 5.2).

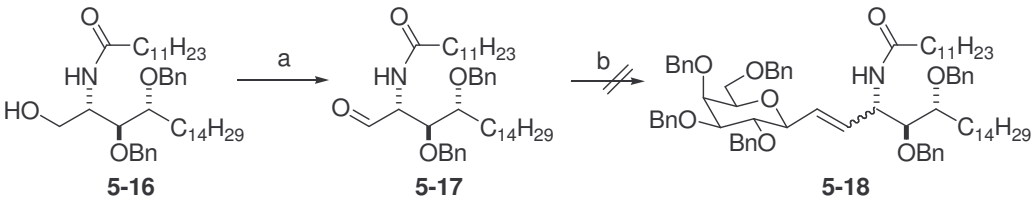

Reagents and conditions: a) TPAP (8 mol%), NMO, 3A MS, CH_2Cl_2 (64%);
b) **5-12**, *n*BuLi, HMPA, THF, -78°C to 0°C (desired product not isolated).

Scheme 5.2. Attempted Wittig Coupling Between *C*-Galactoside **5-12** and Aldehyde **5-17**.

It was thought that the bulk of the ceramide may have a negative impact on the reaction, but a review of the literature demonstrated that successful Wittig reactions have been performed using α-amino aldehydes with the amine singly protected by the large butoxycarbonyl (Boc) or carboxybenzoyl (Cbz) groups.[25] Interestingly, when the amide was exchanged with an azide (**5-20**) and Wittig coupling was attempted with compound **5-12**, the product was different than that of other aldehydes (Scheme 5.3). ^{1}H NMR signals indicating the presence of four benzyl groups were observed, along with two sets of alkenyl peaks (i.e., ddd at 5.87 ppm, 1 H; 2 d at 5.3 ppm, 2 H), and patterns for seven

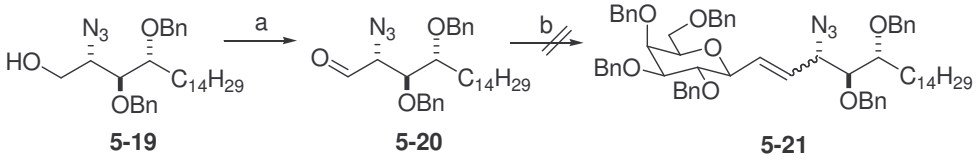

Reagents and conditions: a) TPAP (8 mol%), NMO, 3A MS, CH_2Cl_2 (63%);
b) **5-12**, *n*BuLi, HMPA, THF, -78°C to 0°C (desired product not isolated).

Scheme 5.3. Attempted Wittig Coupling Between *C*-Galactoside **5-12** and Aldehyde **5-20**.

other polar protons between 4.2 and 3.0 ppm with the same splitting pattern as seen in reactions with aldehydes **5-14** and **5-17**. However, there were no signals at 1.6, 1.26, or 0.88 ppm to indicate the presence of alkyl chains. Since **5-20** lacks an amide group, it is more likely that the alkyl portion of the sphingoid is being eliminated during these three reactions and migration of the amide carbonyl moiety is occurring. Because **5-12** does not form a stabilized ylide when deprotonated with *n*BuLi, it is possible that excess base is available for direct reaction with aldehydes **5-14**, **5-17**, and **5-20** along a different, undesired pathway.

To avoid the problem of using an ylide that may not be stable enough, a last attempt to couple a formyl ceramide was performed but by using a phosphonate as a *C*-glycoside. Horner-Wadsworth-Emmons (HWE) reactions are typically more robust than those using phosphonium ylides,[26] so altered conditions were used because a more stabilized nucleophile could cause aldehyde coupling to occur quicker than the observed elimination if they were competing reactions. A recent paper by Blasdel and Myers described the use of HWE phosphonate coupling to epimerizable carbonyl compounds, such as α-amido aldehydes in short peptide chains.[27] This was found to be encouraging because many of the reported reactions involved bulky or long aldehyde substrates. Both aldehydes **5-14** and **5-17** were again used to make the crucial carbon-carbon linkages, but

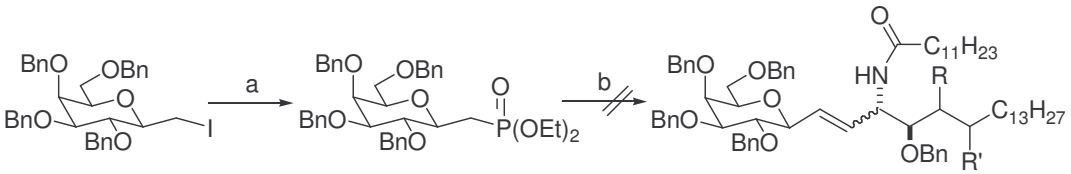

5-11 **5-22** **5-15** R,R' = CH=CH
5-18 R = (*R*)OH R' = H

Reagents and conditions: a) $P(OEt)_3$, toluene, reflux (89%); b) **5-14** or **5-17**, *n*BuLi, hexafluoroisopropanol, DME, -14°C (no reaction).

Scheme 5.4. Attempted HWE Reaction with Phosphonate **5-22**.

with phosphonate **5-22** under the described conditions (e.g., *n*BuLi, excess hexafluoroisopropanol, DME, -14°C). Unfortunately the reaction did not occur, nor when *n*BuLi was used to directly deprotonate phosphonate **5-22** (Scheme 5.4).

Because of these difficulties and the urgency that *C*-glycoside **5-3** was needed for inhibitory analysis, attention was turned toward known, longer routes of synthesis. Dondoni's method of generating the *C*-glycoside[22] was chosen over that of Chaulagain et al.[21] due to the shorter path, greater familiarity with the described synthetic methodology, and because it directly led to the sphingosine product. Iodide **5-12** underwent Wittig coupling with the enantiomer of Garner's aldehyde (**5-23**), which was made in four steps from D-serine,[28] to install the critical *S* configuration at the C3 stereocenter. The resulting mixture of alkenes (**5-24**) was saturated using diimide generated in situ from *p*-tosylhydrazide and sodium acetate to provide compound **5-25**.[29] To add the remainder of the sphingoid base, the acetonide protecting group was selectively removed by acid hydrolysis and the free alcohol (**5-26**) was oxidized using the TPAP catalyst (Scheme 5.5).

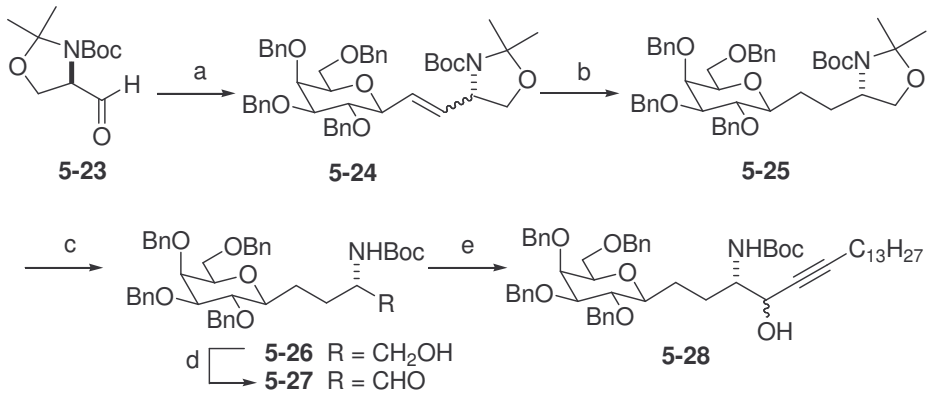

Reagents and conditions: a) **5-12**, *n*BuLi, 4A MS, HMPA, THF, -40°C (60% *Z*+*E*); b) $TsNHNH_2$, 1 M NaOAc (aq.), DME, reflux (85%); c) 4:1 HOAc:H_2O (57%); d) TPAP (8 mol%), NMO, 3A MS, CH_2Cl_2 (58%); e) 1-pentadecyne, *n*BuLi, 4A MS THF, -78°C (34% syn, 20% anti).

Scheme 5.5. Preparation of *C*-Galactoside Intermediate **5-28**.

The sphingosine tail of the ceramide was added to aldehyde **5-27** in a fashion similar to the synthesis of sphingosine as described by Garner et al.,[30] which was a familiar procedure in the Savage research group. 1-Pentadecyne was lithiated using *n*BuLi in THF and introduced to the α-amino aldehyde. Unlike the synthesis of sphingosine, the stereocenter vicinal to the carbonyl group was not as effective at controlling the stereoselectivity of acetylide addition to **5-27**. Instead of primarily affording the *R* configuration at C4, the undesired *S* isomer was the main product (3*S*,4*S*:3*S*,4*R* 1.7:1). The reason for the reversal in selectivity is likely due to the lack of rigidity of the singly-protected amine. Using the Felkin-Anh model of nucleophilic addition to a carbonyl, the inflexible oxazolidine ring of Garner's aldehyde (**3-5**) allows nucleophilic attack preferentially from the re face of the aldehyde, while the si face is blocked by the large butoxycarbonyl and acetonide protecting groups.[30] Thus, acetylide addition proceeds in high selectivity (8:1 re:si attack). In compound **5-27**, the substrate-controlled mechanism of selectivity is much weaker due to the relative equivalence in steric bulk of the HNBoc and *C*-glycosylethyl groups, thus the anti:syn product ratio was eroded (Figure 5.3).

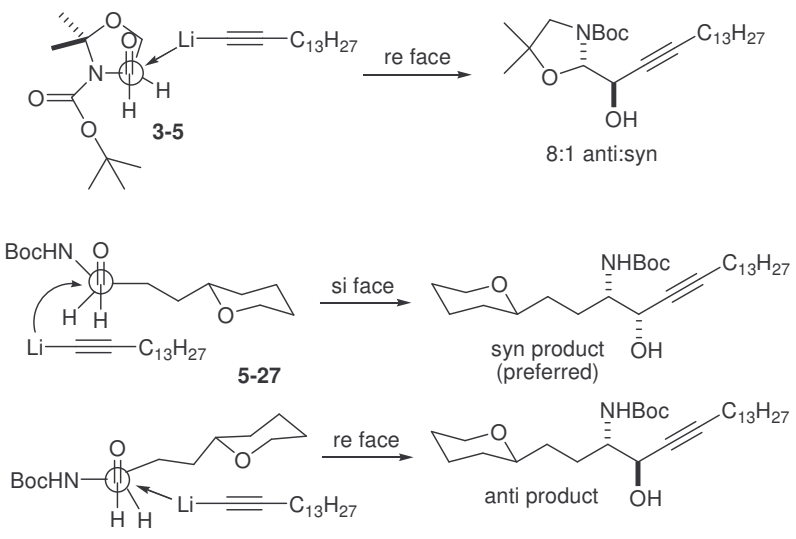

Figure 5.2. Felkin-Anh Models of Acetylide Addition in Aldehyde **5-27**.

To recover the syn product, the diastereomeric mixture of **5-28** was oxidized with TPAP

and the resulting ketone (**5-29**) was selectively reduced to the anti-propargyl alcohol **5-30** using L-selectride by a method described by Dondoni et al (Scheme 5.6).[22]

The structure of the final compound (**5-3**) was completed by deprotecting the amine with hydrogen chloride in a solution of *p*-dioxane then acylating with dodecanoic (lauric) acid using the HBTU coupling agent (**5-31**). Deprotection of the saccharide alcohols and reduction of the alkyne to the *E*-alkene was performed concomitantly using Benkeser's conditions (i.e., Li^o, $EtNH_2$) as described by Garner et al.[30]

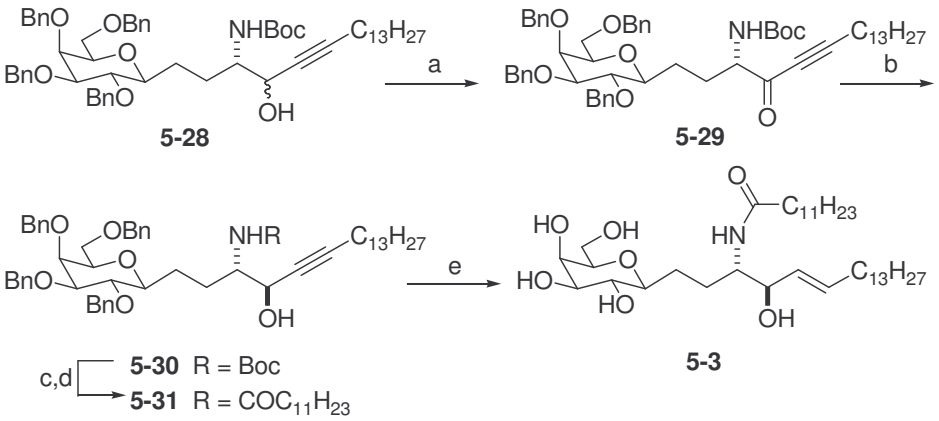

Reagents and conditions: a) TPAP (8 mol%), NMO, 3A MS, CH_2Cl_2 (61%); b) L-Selectride, THF, -78°C (87%); c) 4M HCl in *p*-dioxane, 35°C (61%); d) $HO_2CC_{11}H_{23}$, HBTU, 2:1 CH_2Cl_2:*p*-dioxane, Et_3N (86%); e) Li^o, $EtNH_2$, THF, -78°C (39%).

Scheme 5.6. Preparation of β-*C*-Glycosphingolipid **5-3**.

β-*C*-Glycoside **5-3** was assayed for inhibitory properties of NKT cells by the Strober research group. Compound **5-3** was injected into the peritoneal cavity of mice at different concentrations and blood was drawn to measure levels of IFN-γ and IL-4 cytokines. Up to an injection of 50 μg of compound per mouse, no decrease was seen in the serum concentrations of IFN-γ or IL-4. Additionally, downregulation of the expression of Vα14i NKT cell receptors did not occur, unlike the result when compound **5-4** was administered.

Subsequent analysis of **5-2** demonstrates that the difference in activity between **5-3** and **5-4** is likely due to the *C*-galactoside alteration. GSL **5-2** is very difficult to solubilize for immunological studies, even when formulated with detergent as is typically done for GSLs, such as **5-1** or its surrogate **4-3** (see Chapter 4). Due to this solubility issue, there was concern that **5-2** may be aggregating and not readily available for loading onto CD1d for NKT cell stimulation. To verify this, fluorophore-appended CD1d

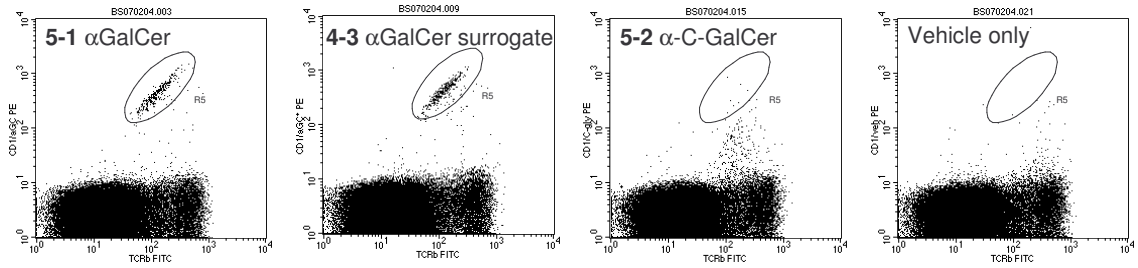

Figure 5.3. Flow Cytometric Analysis of GSL-CD1d Tetramer Staining of Thymic NKT Cells by *C*-Galactoside **5-2** Compared with **5-1** and **4-3** at a 1:400 ratio of CD1d:GSL.[32]

molecules were incubated with aliquots of **5-2** and associated with NKT cells for staining.[31] Only those cells that were associated with CD1d-restricted glycosphingolipids, and thus were marked with a fluorophore, were sorted by fluorescence-activated cell sorting. As seen in the oval gates in Figures 5.3 and 5.4, *O*-glycosides **5-1** and **4-3** were equivalent in detecting those thymic and splenic cells that were able to bind to CD1d-GSL tetramers (i.e., NKT cells), respectively. However, *C*-glycoside **5-2** was found to be ineffective at loading onto CD1d and yielded signals only

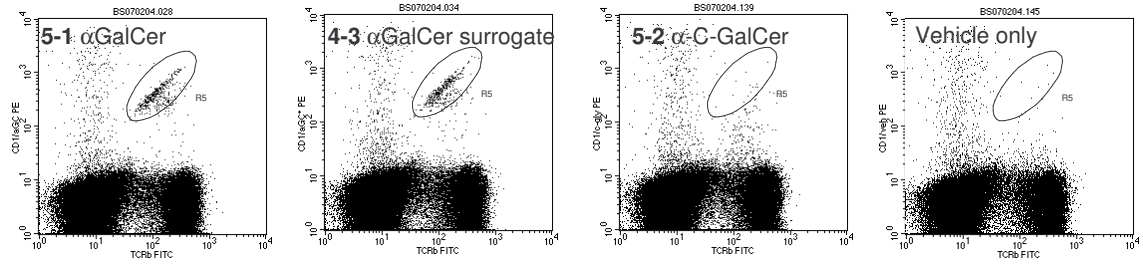

Figure 5.4. Flow Cytometric Analysis of GSL-CD1d Tetramer Staining of Splenic NKT Cells by *C*-Galactoside **5-2** Compared with **5-1** and **4-3** at a 1:400 ratio of CD1d:GSL.[32]

slightly better than vehicle (no GSL) alone.[32] Varying the concentration of GSL with respect to CD1d demonstrated that **5-2** is significantly less effective at forming stable complexes than *O*-glycosides and that higher concentrations must be used (>0.01 μg/mL) to stain NKT cells to a consequential amount (Figure 5.5).[32] It is possible that **5-3** suffers from the same CD1d binding issues as that of **5-2**, making it a poor inhibitor, though there is a possibility that **5-3** may have slightly better solubility due to its sphingosine base. Therefore, a successful synthesis of **5-5** for further inhibitory studies does not hold as much value as it did due to the likelihood that it too will be unable to load onto CD1d and stain NKT cells.

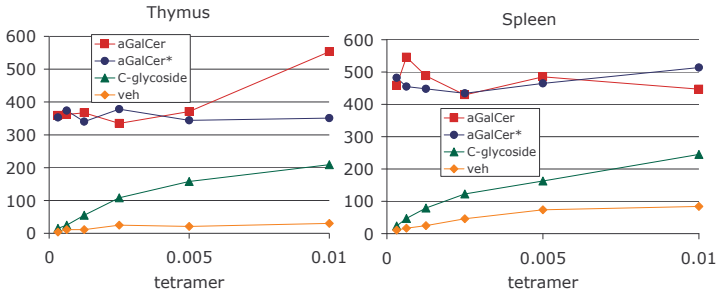

Figure 5.5. Number of NKT Cells Stained at Various Concentrations of GSL-CD1d Tetramers (μg/mL).[32]
aGalCer = **5-1**, aGalCer* = **4-3**, C-glycoside = **5-2**, veh = vehicle

5.3 Conclusions

Glycosphingolipid **5-3** was synthesized to aid in understanding how inhibition of NKT cells could help ameliorate disorders brought about by their unbalanced or uncontrolled activity in the immune system. To increase the potency of known β-galactosylceramide suppressors of NKT cell activity, a *C*-glycosidic bond was installed in a GSL that would be resistant to in vivo degradation. Attempts to couple a *C*-glycoside to formyl ceramides using the Wittig and Horner-Wadsworth-Emmons reactions failed to produce compound **5-3** or its sphingoid analog **5-5** in a minimal number of steps. Instead, an adduct was generated through apparent elimination of the sphingoid alkyl

group, migration of the amide moiety, and apparent reduction of one of the benzyl protecting groups.

The total synthesis of **5-3** was finally accomplished in fourteen steps from 2,3,4,6-tetra-*O*-benzylgalactonolactone with an overall yield of 0.2% via modification of a procedure by Dondoni et al.[21] Immunological assays to evaluate the efficacy of **5-3** as a suppressor of NKT cell activity found no appreciable decrease of cytokines or downregulation of NKT cell receptor expression in mice. From data demonstrating the inability of α-C-GalCer compound **5-2** to load CD1d tetamers and cause subsequent binding to NKT cells, it is possible that the inactivity of **5-3** is due to the same deficiency and that use of the *C*-glycosidic bond is the cause of the abrogated response. Further structure-activity work using *S*- or *N*-glycosidic GSLs may help to elucidate tolerance of CD1d-substrate association and may lead to the design of more effective NKT cell inhibitors

5.4 Experimental Section

Materials and General Methods. Mass spectrometric data were obtained on either a JEOL SX 102A spectrometer for fast atom bombardment (FAB; thioglycerol/Na^+ matrix) or an Agilent Technologies LC/MSD TOF spectrometer for electrospray ionization (ESI; 3500 eV, positive ion mode). ^1H and ^{13}C NMR spectra were obtained on a Varian Unity 500 MHz instrument using 99.8% $CDCl_3$ with 0.05% v/v TMS or 99.96% DMSO-d_6 in ampoules. Methanol, methylene chloride, toluene, and tetrahydrofuran were dried using columns of activated alumina. Flash chromatography was performed using 230-400 mesh silica gel. Thin layer chromatography was performed on aluminum-backed, 254 nm UV-active plates with a silica gel particle size of 250 μm. Reagents were obtained

from Aldrich or Fluka, unless otherwise specified, and were used as received. Note: see Ref. 22 for the experimental procedure for compound **5-9** and Ref. 23 for compounds **5-11**, **5-12**, and **5-24**.

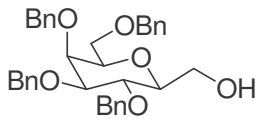

5-10

5-10. 2,3,4,6-tetra-*O*-benzyl-1-ethenyl-β-galactose (1.23 g, 2.23 mmol) was dissolved in anhydrous CH_2Cl_2 (40 mL), cooled to -78°C, and exposed to a stream of ozone until there was a persistence of blue color in the solution (15 m). After flushing with oxygen then nitrogen gas for 15 m each, a methanolic solution of sodium borohydride (1.85 *M*, 12 mL, 22.2 mmol) was added slowly over 5 m at 0°C. After 1 h, another aliquot of the reducing solution (12 mL) along with deionized water (5 mL) were added to complete the reduction (2 h total). The solvent was removed in vacuo after warming slowly to room temperature. The crude solid was dissolved in methanol and adsorbed onto silica gel prior to column chromatography (SiO_2, EtOAc:Hex 1:2) to yield the alcohol as a colorless oil (911 mg, 73%, R_f = 0.32 EtOAc:Hex 1:2). ^{1}H NMR ($CDCl_3$, 500 MHz) δ 7.37-7.27 (m, 20 H), 4.94 ('t,' *J* = 11.7 Hz, 2 H), 4.76 (d, *J* = 11.7 Hz, 1 H), 4.70 (d, *J* = 11.7 Hz, 1 H), 4.65 (d, *J* = 11.7 Hz, 1 H), 4.60 (d, *J* = 11.7 Hz, 1 H), 4.76 (d, *J* = 11.7 Hz, 1 H), 4.41 (d, *J* = 11.7 Hz, 1 H), 3.97 (d, *J* = 2.9 Hz, 1 H), 3.93 (t, *J* = 9.3 Hz, 1 H), 3.85 (d, *J* = 10.7 Hz, 1 H), 3.70 (dd, *J* = 10.7, 4.6 Hz, 1 H), 3.63 (dd, *J* = 9.3, 2.4 Hz, 1 H), 3.61-3.55 (m, 2 H), 3.54-3.50 (m, 1 H), 3.35 (m, 1 H); ^{13}C NMR ($CDCl_3$, 125 MHz) δ 138.79, 138.46, 138.39, 137.95, 128.64, 128.44, 128.35, 128.30, 128.14, 128.03, 127.99, 127.86, 127.80, 127.70, 84.77, 79.77, 77.16, 75.53, 75.36, 74.73,

73.90, 73.70, 72.47, 69.08, 62.68; HRMS (ESI) *m/z* for $C_{35}H_{38}NaO_6$ ($[M+Na]^+$) 577.25623 (100%), calc. 577.25606.

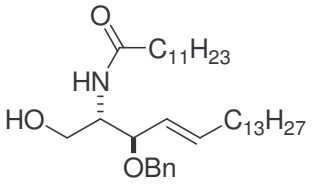

5-13

5-13. The ceramide precursor was acylated and silylated in the same fashion as compound **3-19** (see Chapter 3, section 3.4) but using dodecanoic acid instead. The primary silane (404 mg, 0.678 mmol) was dissolved in anhydrous DMF (45 mL) under N_2 and cooled to 0°C. Sodium hydride (60% emulsion in mineral oil, 109 mg) and tetrabenzylammonium iodide (75 mg, 0.20 mmol) were then added with vigorous stirring followed by dropwise introduction of benzyl bromide (160 μL, 1.35 mmol). The reaction was allowed to warm to room temperature over 12 h, the solvent was removed, and CH_2Cl_2 (75 mL) was added. The organic solvent was washed with deionized water (3 x 20 mL), the aqueous layer was backextracted with CH_2Cl_2 (3 x 25 mL), and dried with Na_2SO_4. Removal of the solvent in vacuo provided the crude product as a colorless oil that was desilylated by dissolving in THF (15 mL) and aqueous HF (3 mL). Aqueous workup was done with sodium bicarbonate quench (2 x 5 mL), extraction with EtOAc (3 x 10 mL), brine wash (5 mL), and drying with excess Na_2SO_4. Flash chromatography (SiO_2, EtOAc:Hex 1:1) of the crude product yielded the purified material as a white solid (159 mg, 41%, R_f = 0.51 EtOAc:Hex 1:1). ^{1}H NMR ($CDCl_3$, 500 MHz) δ 7.36-7.27 (m, 5 H), 6.19 (d, *J* = 6.8 Hz, 1 H), 5.79 (m, 1 H), 5.43 (dd, *J* = 15.1, 7.8 Hz, 1 H), 4.62 (d, *J* = 11.7 Hz, 1 H), 4.26 (d, *J* = 11.7 Hz, 1 H), 4.02 (dd, *J* = 7.3, 3.9 Hz, 1 H), 4.00-3.92 (m, 2 H), 3.60 (m, 1 H), 3.05 (d, *J* = 8.3 Hz, 1 H), 2.16-2.07 (m, 4 H), 1.63-1.52 (m, 2 H),

1.26 (br s, 38 Hz), 0.88 (t, J = 6.8 Hz, 6 H); ^{13}C NMR ($CDCl_3$, 125 MHz) δ 173.52, 137.26, 128.80, 128.11, 126.42, 81.98, 70.91, 62.50, 53.88, 37.06, 32.59, 32.17, 29.94, 29.90, 29.76, 29.73, 29.62, 29.54, 29.45, 29.34, 25.95, 22.95, 14.39; HRMS (ESI) *m/z* for $C_{37}H_{66}NO_3$ ($[M+H]^+$) 572.50275 (100%), calc. 572.50372.

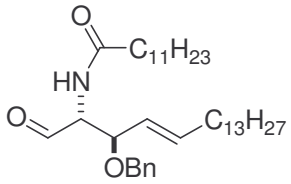

5-14

5-14. Ceramide **5-13** (77 mg, 0.13 mmol) and NMO (25 mg, 0.21 mmol) were dissolved in anhydrous CH_2Cl_2 (4 mL). Whole 3A molecular sieves were added and the mixture was stirred for 15 m before addition of TPAP (2 mg, 0.007 mmol). After 20 m, the reaction was found to be complete by TLC (R_f = 0.50 EtOAc:Hex 1:4). Quenching was done with 5% Na_2SO_3 in brine, followed by a brine wash, a saturated aqueous $CuSO_4$ wash, and drying by Na_2SO_4. The black oil was vacuum filtered to remove particulates and purified by column chromatography (SiO_2, EtOAc:Hex 1:5) yielding the aldehyde as a white, waxy solid (25 mg, 34%). ^{1}H NMR ($CDCl_3$, 500 MHz) δ 9.76 (s, 1 H), 7.35-7.24 (m, 5 H), 6.16 (d, J = 7.3 Hz, 1 H), 5.87 (m, 1 H), 5.60 (dd, J = 15.1, 7.8 Hz, 1 H), 4.66 (dd, J = 7.3, 4.4 Hz, 1 H), 4.61 (d, J = 11.7 Hz, 1 H), 4.29 (d, J = 11.7 Hz, 1 H), 4.14 (dd, J = 7.8, 4.4 Hz, 1 H), 2.19-2.10 (m, 4 H), 1.57 (m, 2 H), 1.41 (m, 2 H), 1.26 (br s, 36 H), 0.88 (t, J = 6.8 Hz, 6 H); ^{13}C NMR ($CDCl_3$, 125 MHz) δ 198.64, 173.26, 137.74, 128.65, 127.93, 125.63, 80.30, 70.70, 62.31, 36.64, 32.51, 32.12, 29.89, 29.84, 29.67, 29.56, 29.44, 29.41, 29.20, 25.74, 22.90, 14.34; HRMS (ESI) *m/z* for $C_{37}H_{64}NO_3$ ($[M+H]^+$) 570.48765 (100%), calc. 570.48807.

Attempted Wittig coupling between **5-12** and **5-14** (representative procedure): Triphenylphosphonium iodide **5-12** (47 mg, 0.051 mmol) was dissolved in anhydrous THF (5 mL) and HMPA (100 μL) under N_2. Freshly crushed 4A molecular sieves (100 mg) were added and the mixture was cooled to -78°C before adding *n*BuLi (1.6 M, 25 μL, 0.040 mmol) dropwise. The reaction mixture was allowed to warm to -40°C over 1 h before cooling back to -78°C. Aldehyde **5-14** (25 mg, 0.044 mmol) was dissolved in anhydrous THF (1 mL) added dropwise over 10 m to the ylide mixture. The temperature was maintained at -78°C for 90 m, before warming slowly to 0°C. The reaction was quenched with NH_4Cl (3 mL), diluted with Et_2O (7 mL), filtered through Celite, washed with PBS at 7 pH (2 mL), and dried with Na_2SO_4. Purification by column chromatography (SiO_2, EtOAc:Hex 1:4) yielded a colorless oil (7 mg, 15% based on theoretical yield of expected product, R_f = 0.47 EtOAc:Hex 1:4). ^{1}H NMR ($CDCl_3$, 500 MHz) δ 7.37-7.26 (m, 20 H), 7.18 (d, *J* = 2.4 Hz, 1 H), 7.17 (d, *J* = 1.4 Hz, 1 H), 5.88 (ddd, *J* = 7.8, 2.4 Hz, 1 H), 5.35 (d, J = 17.6 Hz, 1 H), 5.32 (d, *J* = 10.3 Hz, 1 H), 4.77 (s, 2 H), 4.66 (d, *J* = 12.2 Hz, 1 H), 4.50 (d, *J* = 12.2 Hz, 1 H), 4.42 (d, *J* = 11.2 Hz, 1 H), 4.41 (d, *J* = 12.2 Hz, 1 H), 4.37 (d, *J* = 11.2 Hz, 1 H), 3.46 (d, *J* = 11.7 Hz, 1 H), 4.13 (m, 1 H), 4.08 (dd, *J* = 7.8, 4.4 Hz, 1 H), 3.83-3.79 (m, 2 H), 3.51 (qd, *J* = 9.3, 6.3 Hz, 2 H), 3.04 (d, *J* = 5.4 Hz, 1 H), 1.60 (br s, 2 H), 1.26 (br s, 22 H), 0.89 (t, *J* = 7.3 Hz, 3 H); ^{13}C NMR ($CDCl_3$, 125 MHz) δ 138.41, 138.35, 138.17, 135.90, 129.26, 128.95, 128.72, 128.51, 128.29, 128.20, 127.93, 127.90, 127.87, 127.78, 127.64, 127.48, 126.43, 119.43, 82.23, 80.89, 76.71, 75.43, 73.32, 73.28, 71.37, 70.46, 69.84, 56.04, 43.69, 39.99, 32.12, 29.90, 29.87, 29.75, 29.62, 29.56, 29.17, 28.98, 22.89, 14.33.

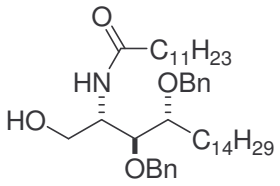

5-16

5-16. Same procedure as synthesis of 5-13 (32%). ^{1}H NMR ($CDCl_3$, 500 MHz) δ 7.36-7.23 (m, 10 H), 5.92 (d, *J* = 8.8 Hz, 1 H), 4.68-4.66 (m, 2 H), 4.49-4.47 (m, 2 H), 4.38 (td, *J* = 10.6, 3.4 Hz, 1 H), 3.75-3.72 (m, 1 H), 3.67 (dd, *J* = 9.3, 3.9 Hz, 1 H), 3.62 (dd, *J* = 9.3, 5.4 Hz, 1 H), 3.51 (m, 1 H), 3.03 (br s, 1 H), 2.02 (m, 2 H), 1.60-1.51 (m, 4 H), 1.26 (br s, 40 H), 0.88 (m, 6 H); ^{13}C NMR ($CDCl_3$, 125 MHz) δ 173.11, 138.38, 137.66, 128.66, 128.60, 128.50, 128.10, 128.02, 127.98, 127.81, 82.04, 73.33 71.76, 69.00, 49.17, 36.92, 33.40, 32.06, 30.06, 29.85, 29.81, 29.65, 29.51, 29.42, 26.38, 25.77, 22.83, 14.27; HRMS (ESI) *m/z* for $C_{44}H_{73}NNaO_4$ ($[M+Na]^+$) 702.54350 (100%), calc. 702.54318.

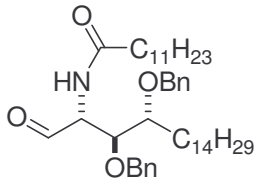

5-17

5-17. Same procedure as synthesis of **5-14** (64%). ^{1}H NMR ($CDCl_3$, 500 MHz) δ 7.34-7.21 (m, 10 H), 5.81 (d, *J* = 9.2 Hz, 1 H), 4.59 (d, *J* = 11.7 Hz, 1 H), 4.51 (m, 1 H), 4.42 (d, *J* = 11.7 Hz, 1 H), 4.35 (d, *J* = 11.7 Hz, 1 H), 4.32 (d, *J* = 11.7 Hz, 1 H), 3.68-3.65 (m, 1 H), 3.45 (dd, *J* = 9.3, 5.4 Hz, 1 H), 2.04 (m, 2 H), 1.56-1.44 (m, 4 H), 1.25 (br s, 40 H), 0.88 (t, *J* = 6.8 Hz, 6 H); ^{13}C NMR ($CDCl_3$, 125 MHz) δ 211.04, 172.75, 137.79, 137.21, 128.63, 128.53, 128.46, 128.26, 127.97, 127.87, 83.35, 73.22, 73.13, 68.07, 49.56, 38.04, 36.68, 32.03, 29.81, 29.76, 29.61, 29.48, 29.32, 25.68, 23.07, 22.80,

14.25; HRMS (ESI) *m/z* for $C_{44}H_{71}NNaO_4$ ($[M+Na]^+$) 700.52717 (100%), calc. 700.52753.

Attempted Wittig coupling between **5-12** and **5-17**: Same procedure as attempted synthesis between **5-12** and **5-14** (35%). ^1H and ^{13}C NMR were obtained in the same manner with equivalent product spectra.

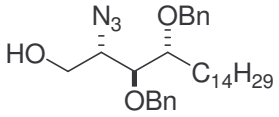

5-19

5-19. 2-Azidophytosphingosine (**4-9**; 950 mg, 2.77 mmol) was dissolved in anhydrous THF (50 mL) and warmed to 60°C. TBSCl (1.23 g, 8.16 mmol) and imidazole (566 mg, 8.31 mmol) were added and the reaction quenched slowly with water (20 mL) after 20 m. The aquesous layer was extracted with EtOAc (3 x 30 mL), the organic fractions combined and washed with 5% HCl (10 mL) and brine (20 mL), and the solution dried with Na_2SO_4. Concentration of the dry solvent yielded the crude silane as a colorless oil (1.31 g, R_f = 0.73 EtOAc:Hex 1:2). The secondary alcohols were benzylated followed by desilylation of the primary alcohol using the same procedure as **5-13** to provide the crude product that was purified by column chromatography (SiO_2, EtOAc:Hex 1:5) yielding a colorless oil (268 mg, 18% from starting material, R_f = 0.60 EtOAc:Hex 1:4). ^1H NMR ($CDCl_3$, 500 MHz) δ 7.37-7.29 (m, 10 H), 4.67 (d, *J* = 11.2, 1 H), 4.59 (d, *J* = 11.2, 1 H), 4.57 (s, 2 H), 3.89 (dd, *J* = 9.8, 3.9 Hz, 1 H), 3.83 (m, 1 H), 3.77-3.71 (m, 2 H), 3.50 (t, *J* = 5.4 Hz, 1 H), 2.10 (d, *J* = 3.9 Hz, 1 H), 1.52-1.38 (m, 2 H), 1.26 (br s, 24 H), 0.88 (t, *J* = 6.8 Hz, 1 H); ^{13}C NMR ($CDCl_3$, 125 MHz) δ 137.95, 137.80, 128.68, 128.18, 128.15, 128.03, 127.92, 82.00, 74.16, 73.67, 71.76, 69.81, 61.84,

32.88, 32.14, 29.88, 29.79, 29.57, 26.04, 22.90, 14.35; HRMS (ESI) *m/z* for $C_{32}H_{50}N_3O_3$ ($[M+H]^+$) 524.38485 (100%), calc. 524.38467.

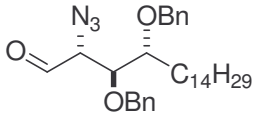

5-20

5-20. Same procedure as synthesis of **5-14** (63%). ^{1}H NMR ($CDCl_3$, 500 MHz) δ 7.39-7.30 (m, 10 H), 4.62 (d, *J* = 11.7, 1 H), 4.58 (d, *J* = 11.7, 1 H), 4.53 (s, 2 H), 3.94 (m, 1 H), 3.72, (dd, *J* = 10.3, 4.9 Hz, 1 H), 3.66 (dd, *J* = 10.3, 6.8 Hz, 1 H), 2.54 (dt, *J* = 7.3, 6.8 Hz, 2 H), 1.51 (m, 2 H), 1.27 (br s, 22 H), 0.90 (t, *J* = 6.8 Hz, 3 H); ^{13}C NMR ($CDCl_3$, 125 MHz) δ 210.38, 137.68, 137.03, 128.76, 128.64, 128.40, 128.23, 128.02, 127.89, 83.47, 73.59, 68.83, 62.17, 39.65, 32.13, 29.90, 29.87, 29.68, 29.64, 29.57, 29.35, 23.09, 22.91, 14.35; HRMS (ESI) *m/z* for $C_{32}H_{51}N_4O_3$ ($[M+NH_4]^+$) 539.39552 (100%), calc. 539.39557.

Attempted Wittig coupling between **5-12** and **5-20**: Same procedure as attempted synthesis between **5-12** and **5-14** (16%). ^{1}H NMR ($CDCl_3$, 500 MHz) δ 7.35-7.24 (m, 20 H), 7.17 (s, 1 H), 7.16 (d, 1 H), 5.87 (ddd, *J* = 8.3, 1.5 Hz, 1 H), 5.34 (d, J = 16.6 Hz, 1 H), 5.30 (d, *J* = 10.3 Hz, 1 H), 4.76 (s, 2 H), 4.65 (d, *J* = 11.7 Hz, 1 H), 4.48 (d, *J* = 12.2 Hz, 1 H), 4.41 (d, *J* = 11.2 Hz, 1 H), 4.39 (d, *J* = 11.2 Hz, 1 H), 4.36 (d, *J* = 11.7 Hz, 1 H), 3.44 (d, *J* = 11.7 Hz, 1 H), 4.12 (m, 1 H), 4.08 (dd, *J* = 7.8, 4.4 Hz, 1 H), 3.82-3.79 (m, 2 H), 3.50 (qd, *J* = 9.3, 6.3 Hz, 2 H), 3.05 (br s, 1 H); ^{13}C NMR ($CDCl_3$, 125 MHz) δ 138.38, 138.32, 138.28, 138.15, 135.88, 128.47, 128.26, 128.17, 127.90, 127.87, 127.78, 127.75, 119.40, 82.2, 80.86, 76.68, 75.40, 73.29, 73.25, 71.34, 70.44, 69.81.

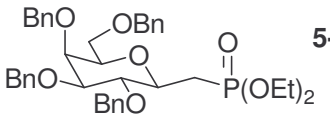

5-22

5-22. Iodide **5-11** (660 mg, 0.993 mmol) was dissolved in anhydrous toluene (10 mL) under N_2 along with ethyl phosphite (1.7 mL, 9.8 mmol) and the reaction was heated to reflux. After 3 h, ESI-MS showed evidence of the formation of the phosphonate product ($[M+H]^+$ = 675.31 m/z). The reaction was periodically monitored in this manner until there was no longer a noticeable change in the ratio of product-to-starting material signals (appx. 7 d). The solvent was removed in vacuo and the residue purified by column chromatography (SiO_2, MeOH:CH_2Cl_2 2:98) to yield a colorless oil (594 mg, 89%, R_f = 0.20 MeOH:CH_2Cl_2 2:98). ^{1}H NMR ($CDCl_3$, 500 MHz) δ 7.36-7.27 (m, 20 H), 4.97 (d, *J* = 11.2, 1 H), 4.94 (d, *J* = 11.7, 1 H), 4.74 (d, *J* = 11.7, 1 H), 4.66 (d, *J* = 11.2, 1 H), 4.65 (d, *J* = 11.2, 1 H), 4.61 (d, *J* = 11.7, 1 H), 4.43 (d, *J* = 11.7, 1 H), 4.39 (d, *J* = 11.7, 1 H), 4.05-3.98 (m, 5 H), 3.68 (q, *J* = 9.3, 1 H), 3.63 (m, 1 H), 3.60 (dd, *J* = 9.3, 2.9 Hz, 2 H), 3.54 (dd, *J* = 6.3, <1 Hz, 2 H), 2.30 (ddd, *J* = 20.0, 15.6, 1.9 Hz, 1 H), 1.93 (td, *J* = 15.6, 9.8 Hz, 1 H), 1.23 (t, *J* = 7.3 Hz, 3 H), 1.20 (t, *J* = 6.8 Hz, 3 H); ^{13}C NMR ($CDCl_3$, 125 MHz) δ 138.88, 138.48, 138.37, 138.02, 128.65, 128.61, 128.57, 128.44, 128.39, 128.15, 128.09, 127.99, 127.88, 127.82, 127.77, 84.76, 78.78, 78.67, 77.16, 75.39, 74.86, 73.98, 73.63, 72,40, 68.85, 61.89, 61.55, 29.41, 28.28, 16.56; HRMS (ESI) *m/z* for $C_{39}H_{47}NaO_8P$ ($[M+Na]^+$) 697.29029 (100%), calc. 697.29008.

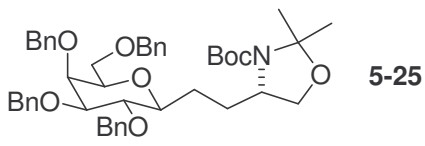

5-25

5-25. Alkene **5-24** (250 mg, 0.333 mmol) and p-toluenesulfonhydrizide (680 mg, 3.65 mmol) were dissolved in 1,2-dimethoxyethane (10 mL) and heated to reflux.

Aliquots of aqueous sodium acetate (1 *M*, 1 mL, 1 mmol) were added to the refluxing solution every 30 m for 150 m total. The reaction was allowed to stir for an additional 2 h at reflux before cooling and stirring for 12 h. The solution was diluted with deionized water (10 mL), extracted with CH_2Cl_2 (4 x 10 mL) and dried with Na_2SO_4. Purification was done by flash chromatography (SiO_2, EtOAc:Hex 1:5) to yield the saturated compound as a colorless oil (212 g, 85%, R_f = 0.36 EtOAc:Hex 1:5). ^{1}H NMR ($CDCl_3$, 500 MHz) δ 7.40-7.21 (m, 20 H), 4.94 (d, *J* = 11.7 Hz, 2 H), 4.74 (d, *J* = 11.7 Hz, 1 H), 4.67 (d, *J* = 11.7 Hz, 1 H), 4.64 (d, *J* = 11.7 Hz, 1 H), 4.61 (d, *J* = 11.7 Hz, 1 H), 4.45 (d, *J* = 11.7 Hz, 1 H), 4.40 (d, *J* = 11.7 Hz, 1 H), 3.97 (br s, 1 H), 3.87-3.81 (m, 2 H), 3.71 (d, *J* = 7.8 Hz, 1 H), 3.65 (t, *J* = 9.3 Hz, 1 H), 3.58-3.50 (m, 5 H), 3.25-3.13 (m, 1 H), 1.89 (br s, 1 H), 1.96-1.82 (m, 2 H), 1.66-1.40 (m, 19 H); ^{13}C NMR ($CDCl_3$, 125 MHz) δ 156.65, 139.01, 138.60, 137.98, 128.69, 128.60, 128.39, 128.21, 128.02, 127.81, 127.74, 127.69, 93.81, 85.08, 80.20, 79.17, 77.15, 75.73, 74.66, 73.70, 72.41, 69.35, 67.11, 57.51, 30.39, 29.92, 28.74, 28.34, 26.95, 23.58, 23.52; HRMS (FAB) *m/z* for $C_{46}H_{57}NNaO_8$ ($[M+Na]^+$) 774.3990 (100%), calc. 774.3976.

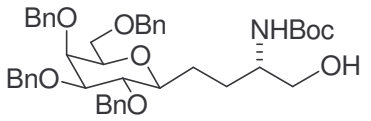

5-26

5-26. Acetonide **5-25** (212 g, 0.282 mmol) was dissolved in acetic acid (2 mL) and water (500 μL) and stirred for 8 h. The solvent was removed in vacuo and the column was purified by an eluent gradient on column chromatography (SiO_2, EtOAc:Hex 1:2 to 1:1) to produce a colorless oil that crystallized to a white powder after total solvent removal (115 mg, 57%, R_f = 0.19 EtOAc:Hex 1:2). ^{1}H NMR ($CDCl_3$, 500 MHz) δ 7.37-7.27 (m, 20 H), 4.93 (d, *J* = 11.7 Hz, 2 H), 4.80 (d, *J* = 5.9 Hz, 1 H), 4.74 (d, *J* = 11.7 Hz,

1 H), 4.67 (d, *J* = 11.7 Hz, 1 H), 4.63 (d, *J* = 11.7 Hz, 1 H), 4.61 (d, *J* = 11.7 Hz, 1 H), 4.45 (d, *J* = 11.7 Hz, 1 H), 4.40 (d, *J* = 11.7 Hz, 1 H), 3.95 (d, *J* = 2.4 Hz, 1 H), 3.66 (t, *J* = 9.3 Hz, 1 H), 3.59-3.53 (m, 4 H), 3.51-3.46 (m, 3 H), 3.20 (t, *J* = 8.3 Hz, 1 H), 2.76 (br s, 1 H), 1.89 (br s, 1 H), 1.62-1.49 (m, 3 H), 1.42 (s, 9 H); ^{13}C NMR ($CDCl_3$, 125 MHz) δ 156.99, 138.80, 138.46, 138.03, 128.63, 128.47, 128.43, 128.11, 128.01, 127.86, 127.82, 127.73, 84.98, 79.48, 78.86, 77.31, 75.66, 74.62, 73.76, 73.67, 72.44, 69.31, 66.72, 53.21, 29.90, 28.58, 28.09, 27.26; HRMS (FAB) *m/z* for $C_{43}H_{53}NNaO_8$ ($[M+Na]^+$) 734.3680 (100%), calc. 734.3663.

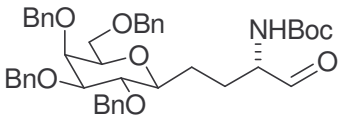

5-27

5-27. Alcohol **5-26** (115 mg, 0.162 mmol) was dissolved in anhydrous CH_2Cl_2 (3 mL) along with NMO (28 mg, 0.24 mmol). Whole 3A molecular sieves were added and allowed to stir at room temperature for 10 m before adding TPAP catalyst (5.0 mg, 0.014 mmol). The reaction was allowed to proceed for 1 h before quenching with 5% Na_2SO_3 in brine, followed by a brine wash, a saturated aqueous $CuSO_4$ wash, and drying by Na_2SO_4. Purification of the black oil by column chromatography (SiO_2, EtOAc:Hex 1:2) yielded the aldehyde as a colorless oil (67 mg, 58%, R_f = 0.50 EtOAc:Hex 1:2). ^{1}H NMR ($CDCl_3$, 500 MHz) δ 9.46 (s, 1 H), 7.37-7.27 (m, 20 H), 5.52 (d, *J* = 6.8 Hz, 1 H), 4.93 (d, *J* = 11.7 Hz, 2 H), 4.74 (d, *J* = 11.7 Hz, 1 H), 4.67 (d, *J* = 11.7 Hz, 1 H), 4.63 (d, *J* = 11.7 Hz, 1 H), 4.60 (d, *J* = 11.7 Hz, 1 H), 4.46 (d, *J* = 11.7 Hz, 1 H), 4.41 (d, *J* = 11.7 Hz, 1 H), 3.94 (d, *J* = 2.0 Hz, 1 H), 3.63 (t, *J* = 9.3 Hz, 1 H), 3.58-3.53 (m, 3 H), 3.50-3.46 (m, 3 H), 3.18 (td, *J* = 9.0, 1.9 Hz, 1 H), 1.98-1.86 (m, 2 H), 1.84-1.72 (m, 1 H), 1.44 (s, 9 H); ^{13}C NMR ($CDCl_3$, 125 MHz) δ 200.71, 155.89, 138.87, 138.35, 138.00, 128.58,

128.40, 128.05, 127.98, 127.84, 127.71, 84.81, 79.29, 78.58, 77.07, 75.59, 74.61, 73.73, 73.63, 72.41, 69.30, 59.71, 28.47, 27.23, 25.23; HRMS (ESI) *m/z* for $C_{43}H_{51}NNaO_8$ ($[M+Na]^+$) 732.35069 (100%), calc. 732.34992.

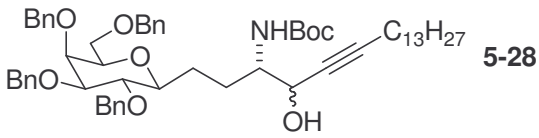

5-28

5-28. 1-Pentadecyne (99 mg, 0.48 mmol) and freshly crushed 4A molecular sieves were put under N_2 then mixed with anhydrous THF (2 mL). The reaction mixture was cooled to -5°C and a solution of *n*BuLi (1.6 *M*, 0.28 mL, 0.45 mmol) was introduced dropwise. After stirring for 30 m, the white suspension was cooled to -78°C and a solution of aldehyde **5-27** (63 mg, 0.089 mmol) in anhydrous THF (500 μL) was added dropwise, turning the color of the precipitate to pink. After stirring for 2 additional h, the reaction was quenched with pH 7.0 PBS buffer, extracted with EtOAc (3 x 5 mL), and dried with Na_2SO_4. Column chromatography (SiO_2, EtOAc:Hex 1:2) resolved the mixture of diastereomeric propargyl alcohols to a 64:36 ratio of colorless oils (major product: 28 mg, 34%, R_f = 0.33 EtOAc:Hex 1:2; minor product: 16 mg, 20%, R_f = 0.29 EtOAc:Hex 1:2). Major product (*syn*): ^{1}H NMR ($CDCl_3$, 500 MHz) δ 7.39-7.28 (m, 20 H), 4.95 (d, *J* = 11.7 Hz, 1 H), 4.94 (d, *J* = 11.7 Hz, 1 H), 4.76 (d, *J* = 11.7 Hz, 2 H), 4.69 (d, *J* = 11.7 Hz, 1 H), 4.65 (d, *J* = 11.7 Hz, 1 H), 4.48 (d, *J* = 11.7 Hz, 1 H), 4.42 (d, *J* = 11.7 Hz, 1 H), 4.30 (br s, 1 H), 3.98 (d, *J* = 2.9 Hz, 1 H), 3.70-3.63 (m, 2 H), 3.61-3.57 (m, 2 H), 3.55-3.49 (m, 3 H), 3.18 (td, *J* = 9.3, 2.4 Hz, 1 H), 2.83 (br s, 1 H), 2.16 (t, *J* = 7.3 Hz, 2 H), 2.01-1.90 (m, 1 H), 1.88-1.78 (m, 1 H), 1.77-1.55 (m, 4 H), 1.45 (s, 9 H), 1.27 (br s, 20 H), 0.90 (t, *J* = 6.8 Hz, 3 H); ^{13}C NMR ($CDCl_3$, 125 MHz) δ 156.77, 138.82, 138.48, 138.05, 128.62, 128.46, 128.42, 128.12, 127.98, 127.82, 127.72, 86.81,

84.97, 79.60, 79.51, 79.18, 78.89, 77.23, 75.69, 74.61, 73.76, 73.68, 72.45, 69.27, 55.64, 32.12, 29.87, 29.74, 29.56, 29.34, 29.14, 28.84, 28.55, 22.89, 18.92, 14.34; HRMS (FAB) *m/z* for $C_{58}H_{79}NNaO_8$ ($[M+Na]^+$) 940.5705 (100%), calc. 940.5698.

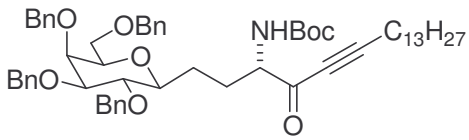

5-29

5-29. Propargyl alcohols **5-28** were combined (44 mg, 0.048 mmol) and dissolved in anhydrous CH_2Cl_2 (2 mL) along with NMO (8 mg, 0.07 mmol). Whole 3A molecular sieves were added and the mixture was stirred at room temperature for 10 m before adding the TPAP oxidant (1 mg, 0.003 mmol). Stirred for 90 m before removing the solvent in vacuo and purifying by column chromatography (SiO_2, EtOAc:Hex 1:5), which provided the pure ketone as a colorless oil (27 mg, 61%, R_f = 0.38 EtOAc:Hex 1:5). ^{1}H NMR ($CDCl_3$, 500 MHz) δ 7.41-7.25 (m, 20 H), 5.12 (d, *J* = 8.3 Hz, 1 H), 4.93 (d, *J* = 11.7 Hz, 1 H), 4.92 (d, *J* = 11.7 Hz, 1 H), 4.75 (d, *J* = 11.7 Hz, 1 H), 4.67 (d, *J* = 11.7 Hz, 1 H), 4.64 (d, *J* = 11.7 Hz, 1 H), 4.62 (d, *J* = 11.7 Hz, 1 H), 4.45 (d, *J* = 11.7 Hz, 1 H), 4.41 (d, *J* = 11.7 Hz, 1 H), 3.98 (d, *J* = 2.4 Hz, 1 H), 3.64 (t, *J* = 9.3 Hz, 1 H), 3.57 (dd, *J* = 9.3, 2.4 Hz, 1 H), 3.55-3.49 (m, 3 H), 3.12 (td, *J* = 9.7, 2.0 Hz, 1 H), 2.29 (t, *J* = 7.3 Hz, 2 H), 2.04-1.90 (m, 2 H), 1.84-1.75 (m, 1 H), 1.55-1.49 (m, 4 H), 1.43 (s, 9 H), 1.25 (br s, 20 H), 0.88 (t, *J* = 6.8 Hz, 3 H); ^{13}C NMR ($CDCl_3$, 125 MHz) δ 187.30, 155.65, 138.85, 138.48, 138.37, 138.08, 128.64, 128.53, 128.44, 128.08, 128.04, 128.00, 127.85, 127.81, 127.73, 98.17, 84.92, 79.36, 78.96, 77.22, 75.74, 74.68, 73.71, 72.41, 69.08, 61.29, 32.12, 29.88, 29.85, 29.64, 29.56, 29.23, 29.12, 28.54, 27.84, 22.90, 19.30, 14.34; HRMS (FAB) *m/z* for $C_{58}H_{77}NNaO_8$ ($[M+Na]^+$) 938.5552 (100%), calc. 938.5541.

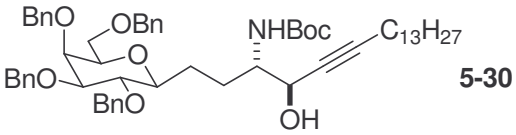

5-30

5-30. Ketone **5-29** (27 mg, 0.029 mmol) was dissolved in anhydrous THF (2 mL) under N_2 and cooled to -78°C. A THF solution of L-Selectride (1.0 M, 58 µL, 0.058 mmol) was added and the reaction was allowed to proceed for 50 m before quenching with MeOH (500 µL). The solution was concentrated and added to a silica gel column for purification (EtOAc:Hex 1:3), yielding the anti-propargyl alcohol diastereomer as a colorless oil (23 mg, 87%, R_f = 0.41 EtOAc:Hex 1:3). ^{1}H NMR ($CDCl_3$, 500 MHz) δ 7.40-7.28 (m, 20 H), 4.93 (d, *J* = 11.7 Hz, 2 H), 4.76 (d, *J* = 6.8 Hz, 1 H), 4.74 (d, *J* = 11.7 Hz, 1 H), 4.67 (d, *J* = 11.7 Hz, 1 H), 4.64 (d, *J* = 11.7 Hz, 1 H), 4.62 (d, *J* = 11.7 Hz, 1 H), 4.46 (d, *J* = 11.7 Hz, 1 H), 4.42-4.39 (m, 2 H), 3.96 (d, *J* = 2.9 Hz, 1 H), 3.65 (t, *J* = 9.3 Hz, 1 H), 3.58 (dd, *J* = 9.3, 2.4 Hz, 1 H), 3.54-3.48 (m, 4 H), 3.21 (td, *J* = 9.3, 2.0 Hz, 1 H), 3.10 (d, *J* = 6.3 Hz, 1 H), 2.29 (td, *J* = 7.3, 1.4 Hz, 2 H), 2.00-1.90 (m, 1 H), 1.78-1.50 (m, 5 H), 1.43 (s, 9 H), 1.25 (br s, 20 H), 0.88 (t, *J* = 6.8 Hz, 3 H); ^{13}C NMR ($CDCl_3$, 125 MHz) δ 157.09, 138.83, 138.50, 138.07, 128.64, 128.50, 128.44, 128.11, 127.99, 127.82, 127.75, 87.33, 85.97, 79.63, 79.28, 77.90, 77.23, 75.76, 74.65, 7376, 73.69, 72.45, 69.26, 66.62, 56.02, 32.14, 29.88, 29.76, 29.57, 29.36, 29.15, 28.86, 28.57, 27.43, 22.90, 18.92, 14.35; HRMS (ESI) *m/z* for $C_{58}H_{80}NO_8$ ($[M+H]^+$) 918.58840 (100%), calc. 918.58784.

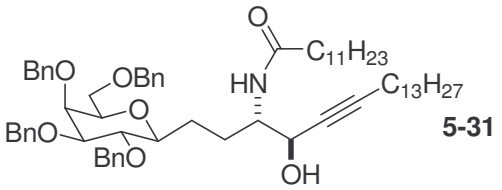

5-31. Propargyl alcohol **5-30** (23 mg, 0.025 mmol) was dissolved in a solution of *p*-dioxane in HCl (4 *M*, 700 µL, 2.8 mmol) and warmed to 35°C. After 3 h, the solvent was removed in vacuo and the crude product was purified by flash chromatography (SiO_2, MeOH:CH_2Cl_2:NH_4OH 10:89:1) to yield a colorless syrup (13 mg, 61%, R_f = 0.29 MeOH:CH_2Cl_2:NH_4OH 5:94:1). HRMS (ESI) *m/z* for $C_{53}H_{71}NNaO_6$ ($[M+Na]^+$) 840.51716 (100%), calc. 840.51736. A solution of dodecanoic (lauric) acid (4 mg, 0.020 mmol) and HBTU (7 mg, 0.018 mmol) was prepared in CH_2Cl_2:*p*-dioxane 2:1 (600 µL) and Et_3N (50 µL) and allowed to stir for 30 m. The free amine was then added to the activated acid in a solution of CH_2Cl_2 (500 µL) and Et_3N (50 µL). After stirring for 12 h, the solvent was removed in vacuo and the residue purified by column chromatography (SiO_2, EtOAc:Hex 1:2). The amide was formed as a white, waxy solid (14 mg, 86%, R_f = 0.45 EtOAc:Hex 1:2). ^{1}H NMR ($CDCl_3$, 500 MHz) δ 7.38-7.26 (m, 20 H), 5.91 (d, *J* = 7.8 Hz, 1 H), 4.95-4.91 (m, 2 H), 4.75 (d, *J* = 6.8 Hz, 1 H), 4.68 (d, *J* = 11.7 Hz, 1 H), 4.62 (d, *J* = 11.7 Hz, 1 H), 4.61 (d, *J* = 11.7 Hz, 1 H), 4.47 (d, *J* = 11.7 Hz, 1 H), 4.43-4.39 (m, 2 H), 3.94 (d, *J* = 2.9 Hz, 1 H), 3.90 (m, 1 H), 3.66-3.62 (m, 1 H), 3.59-3.55 (m, 2 H), 3.53-3.50 (m, 1 H), 3.49-3.44 (m, 1 H), 3.42-3.39 (m, 1 H), 3.26-3.21 (m, 1 H), 2.15-2.10 (m, 4 H), 2.00-1.84 (m, 2 H), 1.74-1.62 (m, 2 H), 1.61-1.52 (m, 2 H), 1.50-1.40 (m, 2 H), 1.25 (br s, 36 H), 0.88 (t, *J* = 6.8 Hz, 6 H); ^{13}C NMR ($CDCl_3$, 125 MHz) δ 171.32, 138.78, 138.46, 137.94, 128.65, 128.44, 128.36, 128.13, 128.07, 127.95, 127.87, 127.75, 84.99, 79.68, 79.29, 79.11, 75.66, 74.67, 73.87, 73.73, 72.56, 69.38, 67.08, 65.97,

60.58, 55.58, 55.07, 36.95, 32.12, 29.88, 29.77, 29.56, 29.37, 29.19, 28.91, 28.53, 26.02, 22.89, 21.23, 18.95, 14.39, 14.32; HRMS (ESI) *m/z* for $C_{65}H_{93}NNaO_7$ ($[M+Na]^+$) 1022.68561 (80%), calc. 1022.68443.

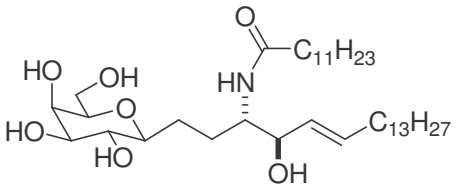

5-3

5-3. Lithium wire (9 mg, 1.2 mmol) was dissolved in $EtNH_2$ at -78°C over a period of 45 m in inert atmosphere (N_2). Amide **5-31** (14 mg, 0.014 mmol) in anhydrous THF (500 µL) was added slowly to the blue solution and allowed to stir for 4 h before warming to room temperature and evaporating the solvent under a stream of nitrogen. The crude solid was suspended in MeOH:$CHCl_3$ and purified by column chromatography (SiO_2, MeOH:$CHCl_3$ 15:85). The alkene was then lyophilized to yield a fluffy white solid (3.5 mg, 39% R_f = 0.42 MeOH:$CHCl_3$ 15:85). ^{1}H NMR (DMSO-d_6, 500 MHz) δ 7.24 (d, *J* = 9.3 Hz, 1 H), 5.50 (m, 1 H), 5.34 (dd, *J* = 15.6, 5.4 Hz, 1 H), 3.67 (br s, 2 H), 3.60-3.34 (m, 4 H), 3.26-3.12 (m, 2 H), 2.89 (t, J = 7.3 Hz, 1 H), 2.14-1.99 (m, 4 H), 1.98-1.90 (m, 1 H), 1.53-1.40 (m, 7 H), 1.23 (br s, 36 H), 0.85 (t, J = 6.8 Hz, 6 H); ^{13}C NMR (DMSO-d_6, 125 MHz) δ 171.86, 131.00, 130.02, 79.82, 78.71, 74.86, 70.71, 68.54, 60.63, 35.55, 35.43, 31.30, 31.27, 29.06, 28.73, 28.68, 25.59, 22.09, 13.92; HRMS (ESI) *m/z* for $C_{37}H_{72}NO_7$ ($[M+H]^+$) 642.53033 (100%), calc. 642.53033.

5.5 References

1) Godfrey, D. I.; Kronenberg, M. *J. Clin. Invest*. **2004**, *114*, 1379.

2) Campos, R. A.; Szczepanik, M.; Itakura, A.; Akahira-Azuma, M.; Sidobre, S.; Kronenberg, M.; Askenase, P. W. *J. Exp. Med*. **2003**, *198*, 1785.

3) Lisbonne, M.; Diem, S.; de Castro Keller, A.; Lefort, J.; Araujo, L. M.; Hachem, P.; Fourneau, J.-M.; Sidobre, S.; Kronenberg, M.; Taniguchi, M.; Van Endert, P.; Dy, M.; Askenase, P.; Russo, M.; Vargaftig, B. B.; Herbelin, A.; Leite-de-Moraes, M. C. *J. Immunol*. **2003**, *171*, 1637.

4) Miyamoto, K.; Miyake, S.; Yamamura, T. *Nature* **2001**, *413*, 531.

5) Goff, R. D.; Gao, Y.; Mattner, J.; Zhou, D.; Yin, N.; Cantu, C., III; Teyton, L.; Bendelac, A.; Savage, P. B. *J. Am. Chem. Soc*. **2004**, *126*, 13602.

6) Zeng, D.; Lee, M.-K.; Tung, J.; Brendolan, A.; Strober S. *J. Immunol*. **2000**, *164*, 5000.

7) Brigl, M.; Brenner, M. B. *Annu. Rev. Immunol*. **2004**, *22*, 817.

8) (a) Motoki, K.; Morita, M.; Kobayashi, E.; Uchida, T.; Akimoto, K.; Fukushima, H.; Koezuka, Y. *Biol. Pharm. Bull.* **1995**, *18*, 1487. (b) Spada, F. M.; Koezuka, Y.; Porcelli, S. A. *J. Exp. Med*. **1998**, *188*, 1529.

9) Naidenko, O. V.; Maher, J. K.; Ernst, Y.; Sakai, T.; Modlin, R. L.; Kronenberg, M. *J. Exp. Med*. **1999**, *190*, 1069.

10) Bertozzi, C. R.; Bednarski, M. D. Synthesis of *C*-Glycosides: Stable Mimics of *O*-Glycosidic Linkages. In *Modern Methods in Carbohydrate Synthesis*. Khan, S. H.; O'Neill, R. A., Eds.; Harwood Academic Publishers, London, England, 1996; pp 316-351.

11) Lin, C.-H.; Lin, H.-C.; Yang, W.-B. *Curr. Top. Med. Chem*. **2005**, *5*, 1431.

12) (a) Sandhoff, K.; Kolter, T. *Trends Cell Biol*. **1996**, *6*, 98. (b) Sandhoff, K.; Kolter, T.; Van Echten-Deckert, G. *Ann. NY Acad. Sci*. **1998**, *845*, 139.

13) Schmieg, J.; Yang, G.; Franck, R. W.; Tsuji, M. *J. Exp. Med*. **2003**, *198*, 1631.

14) Strober, S.; Meyer, E. H.; Umetsu, D. T. Methods Using Glycolipids for Inhibition of NKT Cells and Therapeutic Use. U.S. Pat. Appl. Publ. 2006116332, Jun 1, 2006.

15) Stick, R. V. *Carbohydrates: The Sweet Molecules of Life*; Academic Press: New York, NY, 2001.

16) Dondoni, A.; Marra, A.; Massi, A. *Chem. Commun*. **1998**, 1741.

17) Yang, G.; Schnieg, J.; Tsuji, M.; Franck, R. W. *Angew. Chem. Int. Ed*. **2004**, *43*, 3818.

18) (a) Kraus, G. A.; Molina, M. T. *J. Org. Chem*. **1988**, *53*, 752. (b) Dondoni, A.; Scherrmann, M.-C. *J. Org. Chem*. **1994**, *59*, 6404. (c) Dondoni, A.; Marra, A.; Pasti, C. *Tetrahedron: Asymmetry*, **2000**, *11*, 305. (d) Dondoni, A.; Giovannini, P. P.; Marra, A. J. *Chem. Soc., Perkin Trans. 1* **2001**, 2380.

19) Dondoni, A.; Marra, A. *Chem. Rev*. **2000**, *100*, 4395.

20) (a) McGarvey, G. J.; Benedum, T. E.; Schmidtmann, F. W. *Org. Lett*. **2002**, *4*, 3591. (b) Godin, G.; Compain, P.; Martin, O. R. *Org. Lett*. **2003**, *5*, 3269. (c) Chen, G.; Schmieg, J.; Tsuji, M.; Franck, R. W. *Org. Lett*. **2004**, *6*, 4077. (d) Nolen, E. G.; Kurish, A. J.; Potter, J. M.; Donahue, L. A.; Orlando, M. D. *Org. Lett*. **2005**, *7*, 3383.

21) Chaulagain, M. R.; Postema, M. H. D.; Valeriote, F.; Pietraszkewicz, H. T*etrahedron Lett*. **2004**, *45*, 7791.

22) Dondoni, A.; Perrone, D.; Turturici E. *J. Org. Chem*. **1999**, *64*, 5557.

23) Xie, J.; Durrat, F.; Valery, J.-M. *J. Org. Chem*. **2003**, *68*, 7896.

24) Dondoni, A.; Marra, A.; Massi, A. *Tetrahedron* **1998**, *54*, 2827.

25) Gryko, D.; Chalko, J.; Jurczak, J. Chirality **2003**, *15*, 514.

26) Carey, F. A.; Sundberg, R. J. In *Advanced Organic Chemistry Part B*, 3rd Ed.; Plenum Press: New York, NY, 1990.

27) Blasdel, L. K.; Myers, A. G. *Org. Lett*. **2005**, *7*, 4281.

28) Campbell, A. D.; Raynham, T. M.; Taylor, R. J. K. *Synthesis* **1988**, *8*, 1707.

29) Bertozzi, C. R.; Hoeprich, P. D.; Bednarski, M. D. *J. Org. Chem*. **1992**, *57*, 6092.

30) Garner, P.; Park, J. M.; Malecki, E. *J. Org. Chem*. **1988**, *53*, 4395.

31) Benlagha, K.; Weiss, A.; Beavis, A.; Teyton, L.; Bendelac, A. *J. Exp. Med*. **2000**, *191*, 1895.

32) Sullivan, B. A. The La Jolla Institute for Allergy and Immunology, San Diego, CA 92121; *unpublished observations*, 2006.

CHAPTER 6.

PREPARATION OF GLYCOSPHINGOLIPIDS FROM *SPHINGOMONAS* ALPHA-PROTEOBACTERIA AND THEIR NKT CELL-STIMULATORY ACTIVITY

6.1 Introduction

A challenging aspect of research on structure-activity relationship (SAR) studies between natural killer T cells and their ligands is discovering compounds that act as exogenous or endogenous antigens via restriction by the CD1d protein. Glycosphingolipids are widely found in eukaryotic cells and are critical for the health of the host organism. They have roles as cell growth regulators, cell surface receptors, modulators of cellular events (e.g., proliferation and apoptosis), and form lipid rafts to aid in signal transduction.[1] One of their main functions is in the nervous system where they act as cerebral lipids and insulation in the myelin sheaths of nerve cells.[2] While GSLs are ubiquitous in eukaryotes, especially in mammals, extensive research has been required to sift through this class of ligands to find those that act as stimulants of NKT cells via CD1d-restriction and that may be useful tools in the development of therapeutic agents.

Examination of the pool of known glycosphingolipids has identified only a few compounds that can induce stimulatory activity in NKT cells (Figure 6.1). In endogenous mammalian GSLs, the native β-anomeric linkage between saccharide and ceramide has been found to typically delete the stimulatory effects of otherwise potentially active compounds with a few exceptions. Zhou et al. found that the β-Cer-linked trisaccharide isoglobotrihexosylceramide (iGb3) has the ability to activate

mVα14i and hVα24i cells to a level similar to that of the model compound αGalCer and is likely to be the endogenous ligand responsible for the positive selection of NKT cells in the thymus.[3] Various other natural β-GSLs (e.g., globosides, isoglobosides, lactosylceramide, gangliosides) were found to lack stimulatory activity,[3,4] though it has been reported that some synthetic analogs of sulfatide can induce cytokine release in non-Vα14i/Vα24i NKT cells.[4,5]

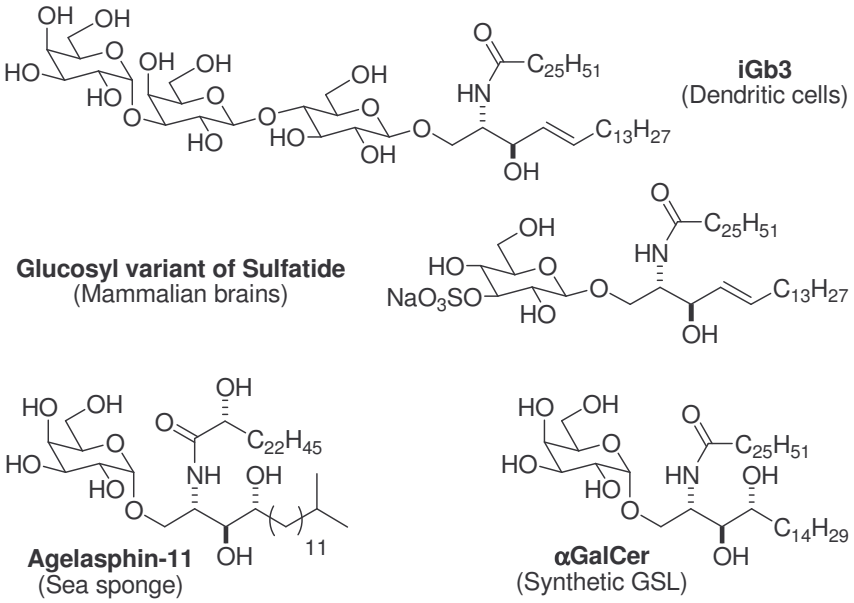

Figure 6.1. Known Glycosphingolipid Antigens of NKT Cells.

The other main source of GSL-based antigens has been the agelasphins, compounds isolated from sea sponge fragments in the 1990s.[6] These compounds differ greatly from mammalian glycolipids in that they are composed of α-anomers, use phytosphingosine rather than mammalian sphingosine, contain solely monopyranoses as the glycon, and often have α-hydroxy amides. These compounds universally prompt noticeable antitumor activity in mice;[7] behavior that led to the optimization of the general agelasphin structure and ultimate synthesis of αGalCer, the model compound that other

NKT cell agonists are often compared to.[8] Although αGalCer has inspired the creation and immunological investigation of other glycosphingolipids (e.g., C6"-appended αGalCer,[9] truncated ceramides,[10,11] GSLs with unsaturation[12]) only one natural ligand of NKT cells had been identified: iGb3. This has hindered researchers from fully understanding the structure-activity relationship between ligand, binding protein, and TCR.

Research by Kawahara and Zahringer led to the discovery of another natural source of glycosphingolipids, the Sphingomonadaceae family of Gram-negative alpha-proteobacteria. In an attempt to extract the Lipid A endotoxin lipopolysaccharide (LPS) from the outer membrane of *Sphingomonas paucimobilis*, they found the presence of a shorter 2-hydroxymyristamide instead of the typical 3-hydroxy long chain fatty acid esters that are present in LPS.[13] Derivatization of the acid-hydrolyzed fragments and subsequent characterization identified three distinct membrane-bound glycosphingolipids: a monosaccharide denoted as GSL-1A[14a] and three tetrasaccharides designated herein as GSL-4A, GSL-4B, and GSL-4C that are differentiated by varying sphinganine structures (Figure 6.2).[14] Like the agelasphins, these bacterial glycolipids are α-anomers, but they contrast from the majority of other known GSLs in that they contain the sphinganine (dihydrosphingosine) long chain base rather than the mammalian sphingosine or plant-based phytosphingosine. The proximal carbohydrate moiety is a glucuronoside (GlcA) instead of galactose. This type of glycolipid differs greatly from the LPS antigen found ubiquitously in Gram-negative bacteria.

Several other similar GSLs have been isolated from the four genera of the Sphingomonadaceae family (i.e., *Sphingomonas*, *Sphingobium*, *Novosphingobium*, and

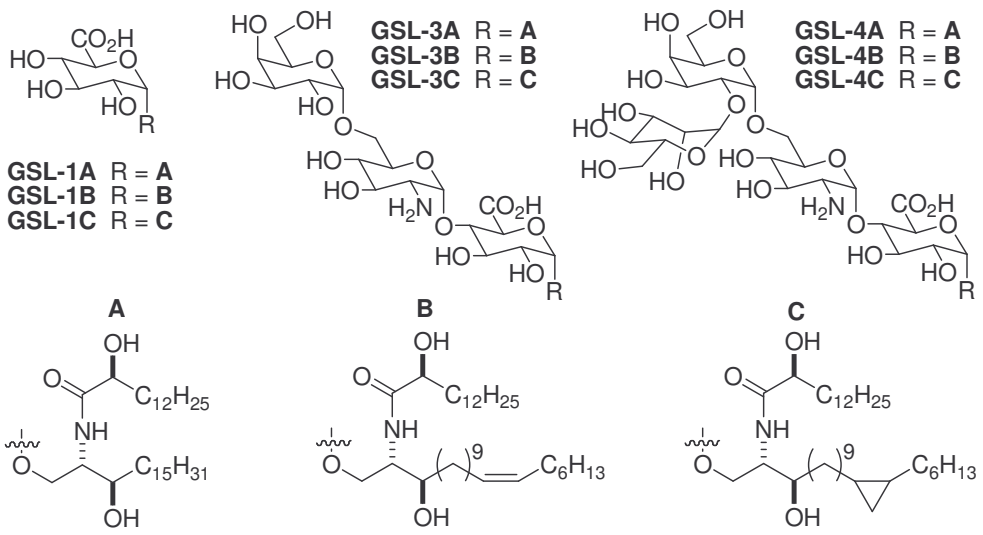

Figure 6.2. Glycosphingolipids from *S. capsulata* and *S. paucimobilis*.[14,17]

Sphingopyxis). In *Sphingomonas yanoikuyae*, galacturonic- (GalA) and GlcA-containing compounds were identified, each with either a C20 unsaturated sphinganine (B in Figure 6.2) or C21 cyclopropylsphinganine base (C; 20 carbon length), yet all four permutations had 2-hydroxymyristic acid in the ceramide.[15] *S. wittichii* has a similar complement of GalA and GlcA glycolipids, both with different combinations of sphinganine (A; 18 carbon length), and C21 cyclopropylsphinganine, coupled to myristic acid either with or without C2-hydroxylation.[16]

In what is considered to be a significant paper covering the isolation of bacterial GSLs, Zahringer and coworkers reported their discovery of six glycolipids from the outer membrane of *Sphingomonas capsulata* (ATCC 14666 as *Novosphingobium capsulatum*).[17] They describe finding the same compound from *S. paucimobilis*, GSL-1A, in *S. capsulata* but with the two variant sphinganines with either the C20 unsaturated (GSL-1B) or C21 cyclopropyl base (GSL-1C) as in the *S. yanoikuyae* glycolipids. A trisaccharide, GSL-3A, of analogous composition to GSL-4A, was also identified but lacking the distal α-mannoside. Interestingly, GSL-3 was also present in two other

permutations, GSL-3B and GSL-3C, with the same ceramides found in *S. paucimobilis* GSL-4B and GSL-4C (Figure 6.2).

The ubiquity of the aforementioned compounds in this bacterial family is remarkable because the various species are found in diverse environments, yet they share this uncommon trait of glycosphingolipid expression in the outer membrane. *S. wittichii* and *yanoikuyae* are often found in soil, though *S. wittichii* has been isolated from the Elbe River and has been identified as a dioxin-degrading microbe.[18] *S. paucimobilis* and other species have been isolated from the ears of rice and other grassy plants from the family Gramineae.[19] Cavicchioli et al. reported the discovery of several species of *Sphingomonas* in ocean water and sediment from climes as varied as Hawaii and Antarctica. They are said to be well-suited to these oligotrophic surroundings due to their ability to thrive, despite the lack of abundant nutrients, through the uptake of various substrates.[20] Research by Giovannoni and coworkers has brought to light a new clade of ocean-dwelling alpha-proteobacteria, SAR11, that may be the most prevalent organisms on the planet. From what little is known of their taxonomy, the SAR11 clade has been located vicinal to the Sphingomonadales order in the phylogenetic tree of alpha-proteobacteria. Therefore, the possibility of finding GSLs in this clade is good.[21]

Sphingomonas have also been linked to pathogenesis in coral reefs and other plant-like organisms. This finding is of particular interest because the agelasphin GSLs were originally culled from sea sponge isolates and it has been known that marine bacteria often infect aquatic plant life. One example of this phenomenon is the recent isolation from Pacific sea sponges of multiple species of *Pseudomonas*,[22] the genus that *S. paucimobilis* was formerly characterized under before being reclassified.[23]

Sphingomonas is an infective agent in humans and like *Pseudomonas*, *S. paucimobilis* has been found to be a hospital-borne pathogen in catheter-using patients and can cause sepsis.[24] Another species, *Novosphingobium aromaticivorans*, has been found to be a causative agent of primary biliary cirrhosis (PBC), an autoimmune disease of the liver that destroys interhepatic bile ducts.[25] These medical diagnoses are relevant to research in the field of innate immunity involving natural killer T cells because a connection has been made between the activity of GSL-bearing *N. aromaticivorans* in PBC and an imbalance of T_H cytokines in infected patients. In the majority of a pool of PBC-infected individuals, mRNA for the T_H1-type cytokine IFN-γ was detected in high levels in liver biopsies. However, mRNA for T_H2 cytokines (e.g., IL-4, IL-5) was not expressed in the same tissue samples.[26] Such an imbalance has been found in other autoimmune disorders (see Chapter 3, section 3.1).

To probe if these responses were related to natural killer T cell behavior, Kronenberg and coworkers used αGalCer-CD1d tetramers to identify any lymphocytes that were participating in autoimmune behavior. Human subjects either with or without PBC were monitored for NKT cell populations in tissue samples. In noninfected individuals, there was a similar concentration of Vα24i cells in blood and the liver. In those people with the disease, the concentration of Vα24i cells was much greater in the liver than the blood and significantly higher than in livers of healthy individuals.[27] The increase in NKT cell concentration due to this disease would suggest a causal relationship exists between *Sphingomonas* microbes and these lymphocytes that are activated by GSL antigens. As was explained by Kronenberg, the population of NKT cells can be as much as 30% of the total group of lymphocytes in the liver. Therefore it is likely that *Sphingomonas* is

causing Vα24i cell activity as witnessed by the biased IFN-γ release during PBC infection.[28]

Before they were found to be active in primary biliary cirrhosis patients, studies had been performed to determine if NKT cells played a role in host defense against microbes and antiinfectious behavior. There is evidence that NKT cells participate in the immune response against infective agents such as bacteria, parasites, fungi, and viruses. There are several cited instances (see Table 6.1) where mice and other animals deficient in either CD1d or classical NKT cell populations (e.g., mVα14i cells) cannot clear communicable organisms, such as *Pseudomonas aeruginosa* (pulmonary tract infection), *Plasmodium berghei* (cerebral malaria), and the encephalomyocarditis virus (encephalitis), that could otherwise be eliminated through innate immune bolstering of the adaptive immune system.[29] In some cases where infected individuals have normal populations of CD1d-restricted T cells, αGalCer has had an adjuvant effect when coadministered with vaccines.[28a]

Infectious agent	Type	αGalCer Activation	Mechanism
Borrelia burgdorferi	Bacteria	Not required	Unknown
Cryptococcus neoformans	Fungus	Not required	IFN-γ
Cytomegalovirus	Virus	Required	IFN-γ, perforin
Encephalomyocarditis virus	Virus	Required	IFN-γ
Hepatitis B virus	Virus	Required	IFN-γ and IFN-α/β
Leishmania major	Parasite	Not required	IFN-γ
Mycobacteria tuberculosis	Bacteria	Required	Modulation of adaptive response
N. aromaticivorans	Bacteria	Not required	IFN-γ
Plasmodium spp.	Parasite	Required	IFN-γ
Trypanosoma cruzi	Parasite	Not required	IFN-γ

Table 6.1. αGalCer-Mediated Host Defense Immune Response.[29]

It was speculated that CD1d-restricted NKT cells could respond to microbial infection either directly by killing infected cells or indirectly by modulating the immune response via cytokine-mediated activation and recruitment of adaptive and innate

immune cells.[29a] An indirect response could likely occur through a Toll-like Receptor (TLR) mechanism such as the one used by a host to identify LPS in Gram-negative bacteria like *E. coli*. In this pathway, bacteria or bacterial components are bound to the membranous CD14 protein of antigen presenting cells and displayed to the TLR, forming a homodimer. This results in the recruitment of several accessory molecules, such as MyD88, that will result in the release of IL-12 to bolster the response of NKT cells that have been activated by CD1d-restricted antigens. The cytokines released by NKT cells elicit activation of lymphocytes and bone-marrow derived cells like macrophages, kill diseased macrophages, recruit granulocytes, and cause maturation of naïve dendritic cells (Figure 6.3).[29a,30]

Besides the question of how NKT cells could be activated in the absence of an administered external stimulant, like αGalCer, it was not known if

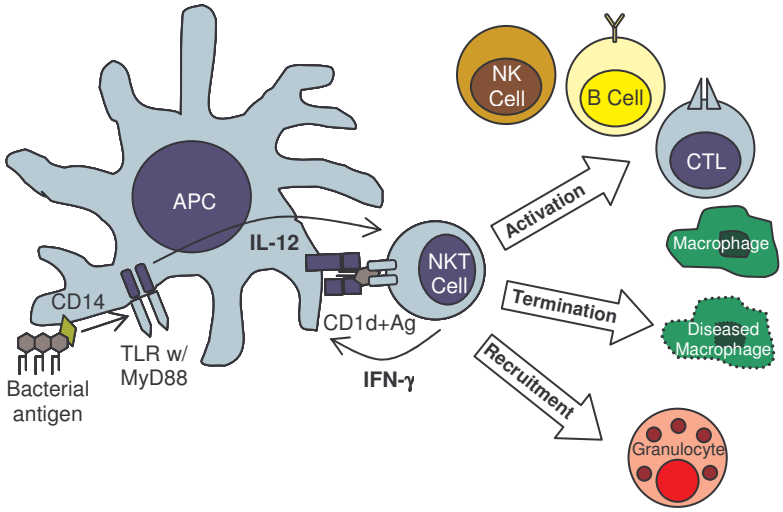

Figure 6.3. NKT Cell-Mediated Host Defense.[29a,30]

CD1d-restricted T cells could be directly activated by exogenous microbial antigens, such as those displayed by *Sphingomonas*. Because *Sphingomonas* lack lipopolysaccharide, the portion of Lipid A used by hosts to recognize invading Gram-negative bacteria, it has been theorized that these bacterial GSLs act in a similar manner, but using CD1d for recognition by the host rather than TLRs. Two significant questions in the research of NKT cell function have been pondered: 1) What is (are) the natural ligand(s) of these

cells and 2) are they endogenous, exogenous, or both? It was believed that the study of *Sphingomonas* GSLs could help provide an answer.

To investigate this matter, glycosphingolipids from *Sphingomonas capsulata* were synthesized (**6-1a** and **6-1b**) along with several structural variants (**6-2**–**6-6**; Figure 6.4)[31] and their ability to interact in vivo and in vitro with CD1d and NKT cells were measured. To aid in the identification of genes involved in glycosphingolipid biosynthesis by *S. capsulata*, an unprotected *Sphingomonas* GSL ceramide was also prepared. LPS-negative *S. capsulata* and LPS-positive *Salmonella*, both Gram-negative microbes, were monitored for NKT cell stimulatory activity to understand the differing mechanisms and requirements in host defense against GSL- or LPS-bearing bacteria.[32]

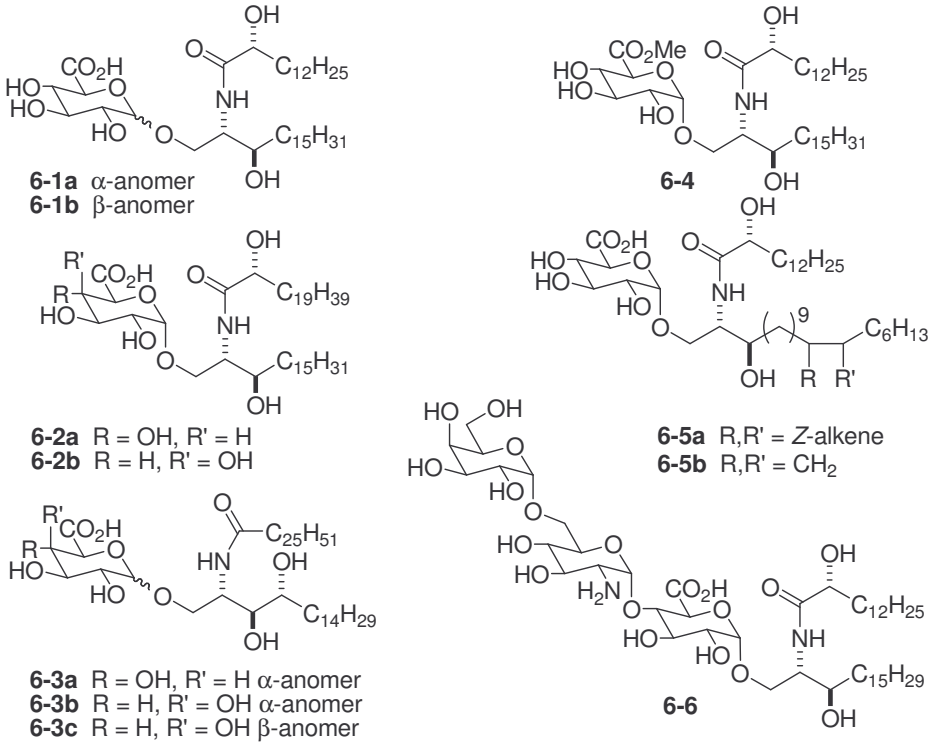

Figure 6.4. Synthetic Glycospingolipids from *Sphingomonas* Bacteria.

6.2 Results and Discussion

Unlike the syntheses of glycosphingolipids described in previous chapters, *Sphingomonas*-derived compounds needed to have the α-hydroxycarboxylic acids created in the lab due to the lack of inexpensive and readily-available materials. (*R*)-Glycidol was used as the chiral building block for the (2*R*)-hydroxymyristamide portion of the *Sphingomonas* ceramide. The tritylated oxirane (**6-7**)[33] was subjected to a Grignard reagent made from 1-bromoundecane, which opened up the less-hindered side of the three-membered ring. Alcohol **6-8** was pivoylated, rather than acetylated, to discourage acyl migration to free alcohols in subsequent steps. Concomitant removal of the trityl protecting group and oxidation of the primary alcohol of **6-9** to a carboxylic acid was achieved under Jones oxidation conditions (i.e., CrO_3, H_2SO_4) with sonication to yield **6-10** (Scheme 6.1). This method was also used to make an unnatural length (C19) for GSL analogs.[31]

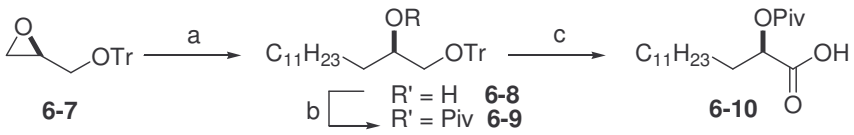

Reagents and conditions: a) $n$$C_{11}H_{23}Br$, Mg, 1,2-dibromoethane, CuI, THF, -30°C (83%); b) PivCl, DMAP, Et_3N, CH_2Cl_2 (87%); c) CrO_3, H_2SO_4, H_2O, acetone (69%).

Scheme 6.1. Preparation of (2*R*)-*O*-Pivaloylmyristic Acid **6-10**.

Construction of the sphinganine base was previously reported by other research groups. Hoffman and Tao described a seven-step scheme from the methyl ester of *N*-Boc-L serine using an 1,3-ketoester intermediate to add the appropriate alkyl tail.[34] So et al. published a slightly more efficient five-step process starting with L-serine and elaborating the structure via nucleophilic attack with an excess of metalloalkanes on the corresponding *N*-Boc Weinreb amide.[35] Since ample sphingosine (**6-11**) was available

from previous synthetic work, and that it could be transformed to sphinganine by simple saturation of the *E*-alkene, it was utilized directly instead of making sphinganine by known methods.

As was done in creating other ceramides, the α-hydroxy acid (**6-10**) was first activated with NHS and DCC and then coupled to sphingosine. Unlike nonhydroxylated acids, coupling with **6-11** did not require a lengthy reaction time (12 h) but instead was complete in a total of 4 h. The yield was also greatly improved (90%) over those from making saturated and unsaturated analogs under the same conditions (50% avg.; see Chapters 3 and 4). The ceramide (**6-12**) was protected in the same manner as other sphingosine ceramides, to provide **6-13**, before subjecting to hydrogenolysis. The protected sphinganine ceramide (**6-14**) was then desilylated at the primary alcohol using aqueous hydrogen fluoride to produce glycuronosyl acceptor **6-15** in seven steps with an overall yield of 12% (Scheme 6.2).

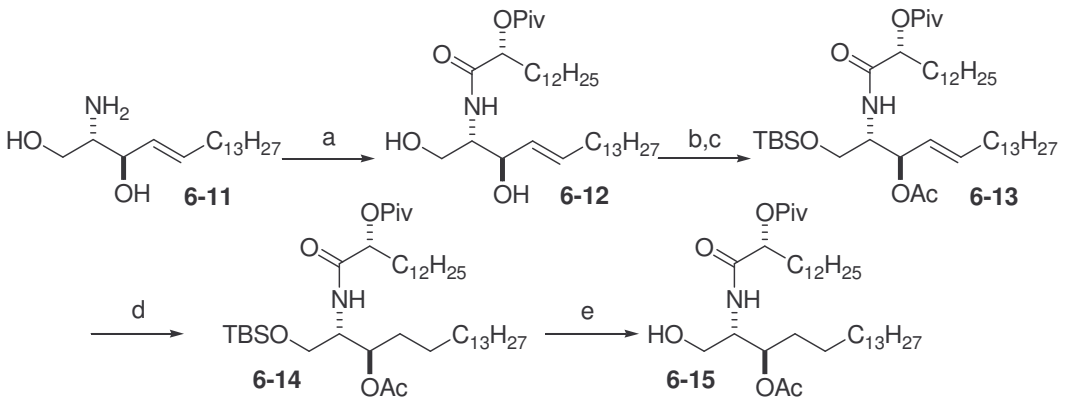

Reagents and conditions: a) **6-10**, NHS, DCC, Et_3N, THF, 80°C, (90%); b) TBSCl, imidazole, THF, 60°C; c) Ac_2O, Et_3N, DMAP, THF (53% over two steps); d) Pd/C (10%), H_2 (200 psi), THF, 20 h (quant.); e) HF (aq.), THF (52%).

Scheme 6.2. Preparation of Sphinganine-Based Ceramide Acceptor **6-15**.

The ceramide was coupled using Koenigs-Knorr-type chemistry[36] to a tribenzylated glucuronosyl bromide donor (**6-16**; Scheme 6.3). Unlike similar couplings involving the

typical glycosyl bromide (**3-15**) with a 2-*O*-benzyl group, the α-anomeric selectivity was eroded, almost providing an equimolar mixture of α- and β-anomers (**6-17a** and **6-17b**). There are few published examples in literature using these types of methyl glycuronosides as donors, but they universally suffer from a lack of selectivity with both "armed" (OBn)[37a] and "disarmed" (OAc)[37b] variants. Switching to a different donor (i.e., thioglycoside) may provide slightly improved biasing to the α-product,[38] yet work making **6-1a** analogs **6-5a** and **6-5b** using 1-ethylthiol armed donors also suffered from lack of anomeric selectivity.[39] It is likely that the abrogated biasing is due to the sluggish nature of the donor, imparted by the carboxyl electron-withdrawing group.[38]

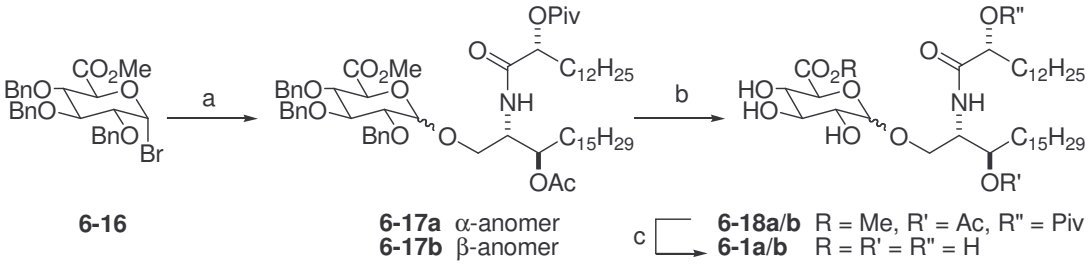

6-16 **6-17a** α-anomer **6-17b** β-anomer **6-18a/b** R = Me, R' = Ac, R" = Piv **6-1a/b** R = R' = R" = H

Reagents and conditions: a) **6-15**, AgOTf, 4A MS, CH_2Cl_2, 0°C (51%, 1:1 α:β-anomers); b) Pd/C (10%), H_2 (300 psi), THF, MeOH (61% avg.); c) NaOMe, MeOH, H_2O (79% avg.).

Scheme 6.3. Preparation of *Sphingomonas* Glycosphingolipids **6-1a** and **6-1b**.

Fortunately, the anomeric mixture could be readily separated by simple column chromatography and the relatively large quantity of β-diastereomer (**6-17b**) produced in this reaction was useful in making unnatural compound **6-1b**. Both **6-17a** and **6-17b** underwent subsequent deprotection to remove the benzyl ethers, the ester groups, and to demethylate the glucuronoside to provide **6-1a** and **6-1b**. Gratifyingly, the final step to remove the acetyl and pivaloyl ester and methyl group in an aqueous methanolic solution of sodium methoxide caused the deprotected glycolipids to precipitate out of solution, as had been done previously (see Chapter 3, section 3.2), without the need for column

chromatography. These two compounds were prepared in a total of eleven steps from (*R*)-*O*-tritylglycidol (**6-7**) and donor **6-16** with an average yield of 1.5%, though in hindsight could have been performed in ten steps by omitting the superfluous hydrogenation of the ceramide.

After the total synthesis of **6-1a** and **6-1b**, there was concern about the actual configuration of the α-hydroxylated myristamide in the *S. capsulata* compounds. Because of ambiguity in the graphical representation of GSL-1,-3, and -4A, which juxtaposed the configurations of the known stereocenters at C2 and C3, it was believed that the stereocenter at C2' was also erroneously reversed to the (*R*)-isomer (see Ref. 17, Fig. 7). This seemed to be logical because many structural analogs of these GSLs, such as the agelasphins[6,7] and the plakosides,[40] also display the (*R*)-configuration at this stereocenter.

To verify the exact configuration of the GSL amide, glycosphingolipids from *S. capsulata* were extracted (see Section 6.4), purified, and hydrolyzed using concentrated HCl. The free acid was methylated, using an aliquot of diazomethane generated in situ, and purified. Methylation was performed in the same way on synthetic acid **6-10** and, after hydrolysis of the Piv group, the two compounds were characterized. Both had the same ^{1}H NMR spectra, as expected (see Section 6.4), but the synthetic (*R*)-enantiomer had an optical rotation of -8.6^{o} and the natural compound was measured at +3.0^{o}, thus demonstrating that the reported (*S*)-configuration was correct.[17]

Preliminary testing on the activity of these compounds as NKT cell stimulants shows that the stereocenter at C2' has little to do with the overall effect of these *Sphingomonas* compounds. An assay of CD1d-restricted IFN-γ production on **6-1a**, its C19' variant **6-**

2a, and several other *S. capulata*-derived α-galactosylceramides[31] found that they generally have similar activity to each other and to αGalCer (Figure 6.5), a finding that was corroborated by Wu et al.[5] Interestingly, the gluco- and galacturonoside analogs of αGalCer that lack the C2' hydroxide (**6-3a** and **6-3b**, respectively) induced slightly greater quantities of secreted IFN-γ than the variant GSL-1 compound (**6-1a**). This particular analysis also suggests that the remote functional groups present in the sphingoids of synthetic GSL-1B (**6-5a**) and GSL-1C (**6-5b**) do not have significant influence on NKT activity. The lone exception in this group is trisaccharide GSL-3 (**6-6**), which did not stimulate. This finding is harmonious with studies on globoside stimulation of NKT cells, where the proximal sugar of oligosaccharide GSLs was inactive if substituted at the C4 position.[3]

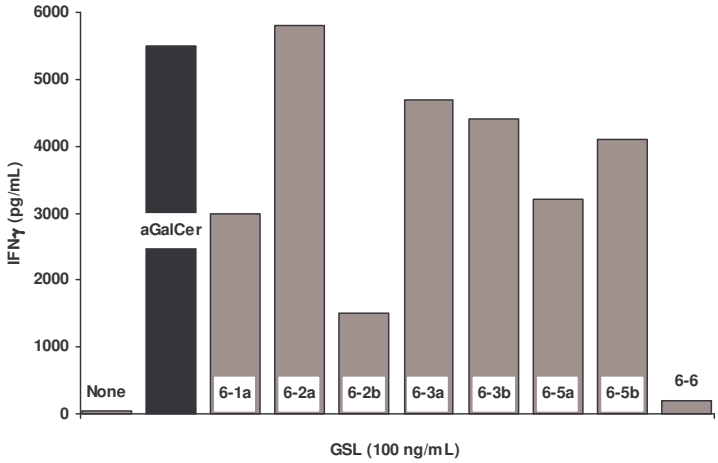

Figure 6.5. IFN-γ Secretion by Murine B6 Spleen Cells with Antigenic αGalCer and *Sphingomonas* GSLs.

To better understand how the overall structure of these α-hydroxysphinganoid glycuronosides corresponded to natural killer T cell stimulation, the eleven synthetic variants of *S. capsulata* GSLs (see Figure 6.4)[31] were tested for murine CD1d-dependent IFN-γ and IL-4 cytokine secretion at varying concentrations (Figure 6.6). From these data, compound **6-2a** had the highest activity of the group, inducing comparable amounts of cytokines as αGalCer. This could be due to the combination of the free (non-esterified) glucuronoside, longer acyl chain (C19), α-anomeric linkage, α-hydroxylated

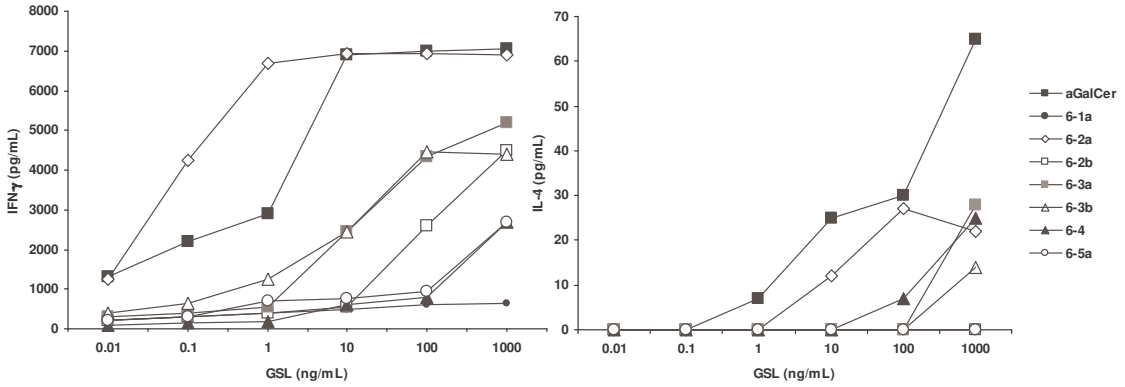

Figure 6.6. Cytokine Release Profiles of αGalCer and *Sphingomonas* GSLs on Murine B6 Spleen Cells.

amide, and sphinganine base because alteration of any one of these traits greatly diminished the activity present in **6-2a** at lower concentrations (<1 μg/mL). It was found that β-anomers (**6-1b**, **6-3c**) have virtually no ability to stimulate NKT cells, along with trisaccharide **6-6**, but making slight changes in the α-anomeric glycons (e.g., GalA vs. GlcA, free acid vs. methyl ester, sphinganine vs. phytosphingosine), other than in **6-2a**, had little influence on overall activity. This demonstrated that the structural features of **6-2a** have a synergistic effect, perhaps allowing it to make a more stable complex in the CD1d-GSL-TCR ternary partnership. From these stimulatory results, it was concluded that the various α-monosaccharide bacterial and bacterial-like glycosphingolipids are antigenic and can cause NKT cell activity.

Species-dependent assays were performed to further gauge the efficacy of **6-2a** as an NKT cell antigen compared to αGalCer. GSL **6-2a** and αGalCer were both able to stain comparable quantities of fresh human Vα24-Jα18 NKT cells, as did β-anomer control **6-1b**. In murine spleen cells, **6-2a** was not able to stain as large a population of NKT cells as αGalCer while the control had a much smaller signal (Figure 6.7). However, in clonal assays using 16 different mVα14 NKT cell hybridomas, there was an equivalent response

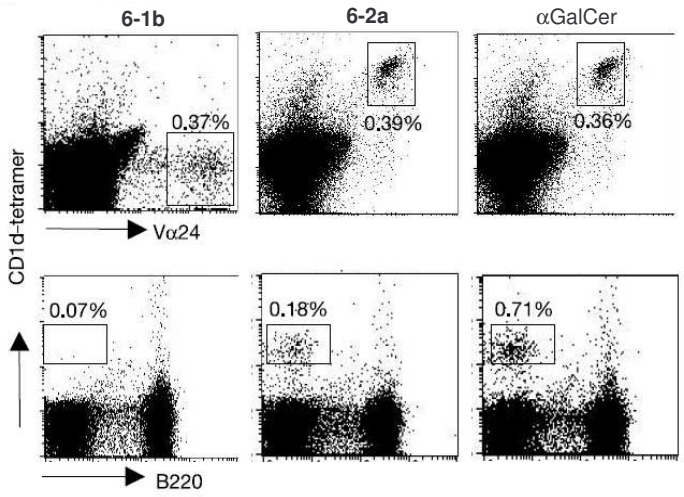

Figure 6.7. NKT Cell Staining by GSL-CD1d Tetramers of Human Vα24i (Upper Row) and Murine (Lower Row) Spleen Cells.[32]

to **6-1b**, **6-2a**, and αGalCer, suggesting that cell staining using tetramers underestimated the actual number of ternary complexes between ligand, protein, and TCR.[32] A second concentration-dependent assay to measure IFN-γ production from synthetic *Sphingomonas* compounds showed that **6-2a** was able to stimulate murine and human NKT cells to the same extent as αGalCer (Figure 6.8).[32]

Although these analyses demonstrate that *Sphingomonas* glycosphingolipids are antigenic to NKT cells, additional data was collected that conclusively indicates that NKT cells directly recognize these GSL ligands. When bone marrow-derived dendritic cells (BMDC) and NKT cells from mice and humans were cocultured in the presence of heat-killed bacteria (i.e., *S. capsulata*, *Ehrlichia muris*, another Gram-negative, LPS-negative alpha-proteobacteria,[41] or LPS-positive *Salmonella typhimurium* at $5x10^6$ counts) or αGalCer (100 ng/mL) there was an appreciable amount of IFN-γ production. When these same bacteria were used with $CD1d^{-/-}$

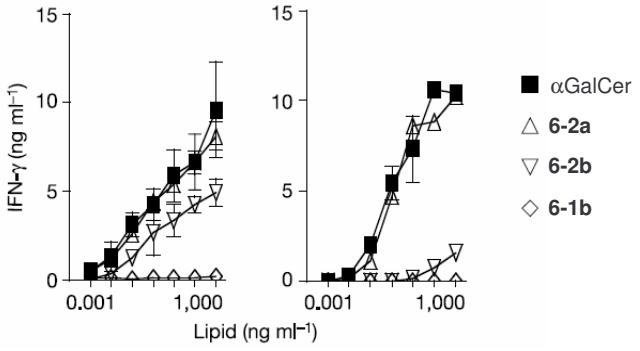

Figure 6.8. IFN-γ Secretion Due to GSL Stimulation of Murine NKT (Left) and Human Vα24i Cells (Right).[32]

murine BMDCs or when anti-CD1d antibodies were administered, there was extreme diminishment of activity (Figure 6.9). Whole spleen cell cultures from B6 mice were also exposed to either bacteria or αGalCer (same concentrations as above) and were found to cause an increasing amount of proliferation of CD1d-αGalCer^{+} NKT cells over a six-day period (Figure 6.10).[32]

To identify differential requirements between the activity of LPS^{+} and LPS^{-} bacteria, IFN-γ output was measured from NKT cells that were cocultured with DCs that either possessed or lacked the gene for the TLR 4 protein MyD88 that is required for LPS recognition. In MyD88$^{+/+}$ DCs, all three bacteria were able to induce stimulation in NKT cells. In MyD88$^{-/-}$ DCs, however, only *Salmonella* could not induce an NKT cell response (Figure 6.11, left). This demonstrates that host identification of LPS^{-} *Sphingomonas* and *Ehrlichia* is not dependent on Toll-like receptors, unlike *Salmonella*.[32]

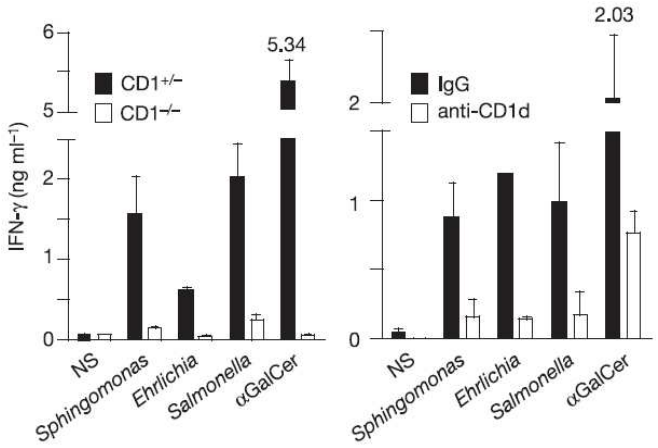

Figure 6.9. CD1d-Restricted Stimulatory Effects of Bacteria on NKT Cells Using Vα14i (Left) or Vα24i Cells (Right).[32]

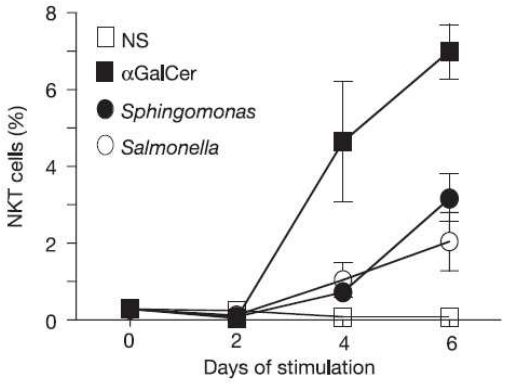

Figure 6.10. B6 Mouse Splenic NKT Cell Stimulation by Heat-Killed Bacteria or Antigenic αGalCer.[32]

Globoside iGb3 was recently identified as a natural endogenous ligand of NKT cells and is

responsible for their maturation in the thymus.[3] In individuals that do not express the β-hexosaminidase gene, which is required to remove the terminal GalNAc sugar from the iGb4 precursor, Hexb$^{-/-}$ DCs are unable to provoke sufficient quantities of NKT cells to fight infection because iGb3 is able to cause NKT cell stimulation but not iGb4. When both Hexb$^{+/-}$ and Hexb$^{-/-}$ DCs were exposed to heat-killed bacteria and purified murine NKT cells, the stimulatory effects from *Sphingomonas* and *Ehrlichia* were comparable.

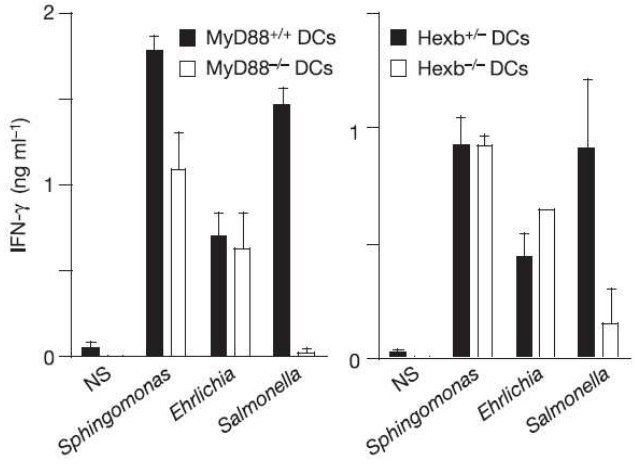

Figure 6.11. Differential Requirements of NKT Cell Stimulation by LPS$^+$ and LPS$^-$ Bacteria using MyD88 and HexB Deficient Mice.[32]

However, stimulation from *Salmonella* did not occur (Figure 6.11, right).[32] Similar results were found when the lectin IB4, a specific binding agent for the Galα(1,3)Gal epitope that is found in iGb3, was administered to a coculture of bacteria or GSL along with DCs and NKT cells. IFN-γ was released by human NKT cells during exposure to *Sphingomonas*, *Ehrlichia*, and αGalCer but was diminished with *Salmonella* and iGb3 (Figure 6.12). It has also been reported that direct replacement of *Salmonella* with LPS in similar assays yield the same results.[42] This information indicates that host defense to *Salmonella* using NKT cells is dependent on iGb3 for activation due to the lack of GSL antigen in LPS$^+$ bacteria. Since GSLs are present in *Sphingomonas*, and likely to be expressed by *Ehrlichia*, NKT cells are not wholly dependent on iGb3 for stimulation.

These data reveal that two different approaches are taken by NKT cells to identify microbes. As with unnatural exogenous antigens, such as αGalCer, bacterial glycosphingolipids were directly recognized by NKT cells through restriction by the CD1d protein expressed by dendritic cells. Therefore, it is likely that in patients with *Sphingomonas*-induced primary biliary cirrhosis, the imbalance from T_H1 over T_H2 cytokines is due to NKT cell activity. Although NKT cells play a factor in fighting infectious behavior against GSL-negative, LPS-positive *Salmonella*, they were not directly being activated by TLR 4. Instead, LPS was identified by a Toll-like receptor on dendritic cells and the innate immune system was activated. Downstream of this event, iGb3 induced the maturation of NKT cells, which fought infection alongside NK cells that had been activated through the TLR 4 pathway.

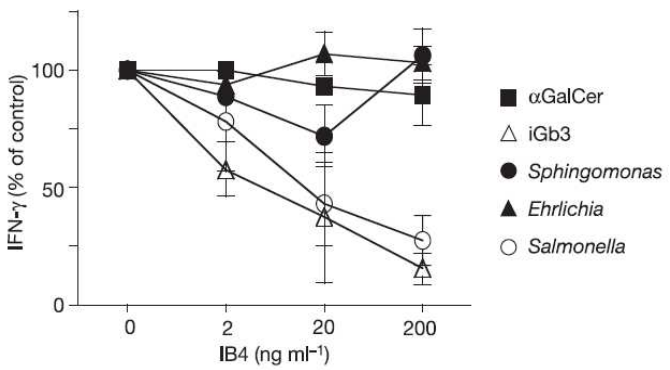

Figure 6.12. Effect of the iGb3-Blocking Lectin IB4 on Antigenic Material and Resulting NKT Cell Activity via CD1d-Restriction.[32]

Interest in the biomechanism of the synthesis of compounds such as GSL-1, has prompted researchers to locate the genes or gene cluster responsible for the assembly of glycosphingolipids in *Sphingomonas*.[43] Based on genetic comparisons both within and without the Sphingomonadaceae family, a group of genes believed to be the glycosyltransferases for GSL biosynthesis has tentatively been identified. One method to ascertain the specific function for each of these genes would be to translate their encoded enzymes individually, through the use of a plasmid, in the presence of GSL components and search for any resulting glycosylated material. To assist the Bendelac group in this

endeavor, the unprotected *S. capsulata* ceramide (**6-19**) was synthesized and with UDP-GlcA (**6-20**) was exposed to enzymes made from the aforemention group of genes (Figure 6.13).

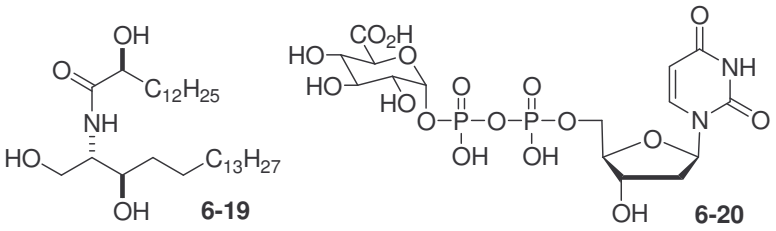

Figure 6.13. Components for Biosynthesis of *S. capsulata* GSL-1.

The natural, (*S*)-enantiomer of 2-*O*-pivaloyhydroxymyristoic acid (**6-21**) was coupled to sphingosine (**6-11**) conveniently with the HBTU coupling agent instead of using the corresponding *N*-hydroxysuccinimidyl ester. This proved to be advantageous due to the quantitative yield of ceramide formation (**6-22**). The *E*-alkene was saturated using a palladium-on-carbon catalyst under hydrogen and then diacetylated to aid in purification. The triester (**6-23**) was deprotected as had been previously done with other glycolipids by exposure to sodium methoxide. The deprotected ceramide (**6-19**) was precipitated from the methanolic solution, lyophilized, and characterized (Scheme 6.4). Research on the identification of the glycosyltransferase responsible for GSL-1A formation using fragments **6-19** and **6-20** has begun and will be reported in due course.[44]

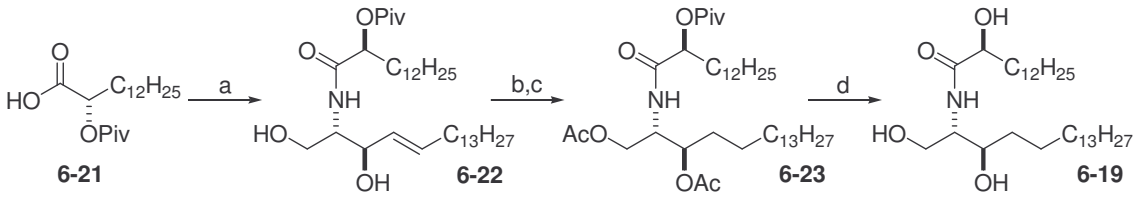

Reagents and conditions: a) **6-11**, HBTU, Et_3N, 2:1 CH_2Cl_2:*p*-dioxane (quant. yield); b) Pd/C (10%), H_2 (200 psi), THF, MeOH; c) Ac_2O, Et_3N, DMAP, THF (75% over two steps); d) NaOMe, MeOH, 40°C (84%).

Scheme 6.4. Preparation of *S. capsulata* GSL Ceramide **6-19**.

6.3 Conclusions

The identification and study of glycosphingolipids from *Sphingomonas capsulata* and other Sphingomonadaceae represent a significant leap forward in research on stimulatory activity of natural killer T cells. Although studies of unnatural antigens derived from αGalCer have helped to elucidate some structure-activity relationships between antigen and response, this natural class of GSLs has allowed immunologists to uncover more information about how NKT cells function in host defense against microbe-borne disease.

The *Sphingomonas* compounds have also given synthetic chemists another challenge in making new groups of biologically-active glycolipids. Glucuronosides **6-1a** and **6-1b**, along with several other analogs, were synthesized according to procedures that had been established making several other types of glycosphingolipids (see Chapters 2–4). Use of the methyl glucuronosyl bromide donor **6-16** was found to be helpful in making both anomers of GSL-1A, yet no α-selectivity was gained by using a benzyl ether at the C2 saccharide position. Further research into making a more active and selective donor for ceramide coupling should facilitate the synthesis of α-glycuronosides in the future. Confirmation of the (*S*)-configuration of the 2-hydroxymyristoyl stereocenter in *Sphingomonas* compounds was achieved via derivatization of the isolated bacterial acid and comparison to its synthetic equivalent. The synthesis of unprotected ceramide **6-19** was also accomplished to aid in the identification of the glycosyltranferase gene of GSL-1A biosynthesis in *S. capsulata*.

Compounds **6-1**–**6-6** were assayed for stimulatory activity and found to be natural exogenous ligands of natural killer T cells. Correlations between structure and activity via CD1d-restriction were identified. These include:

1) α-Anomers typically have significant activity. β-Anomers (**6-1b** and **6-3c**) are completely inactive.

2) Trisaccharide **6-6** has no activity. This is likely due to the lack of an appropriate glycosidase in DCs to cleave the distal sugar(s) that is (are) inhibiting recognition by the NKT cell receptor.

3) There is no significant difference in the activity of GlcACers and GalACers.

4) The C6" acid functional group does not impart nor necessarily detract from overall activity. Methyl esters (**6-4**) and hydroxyl analogs (αGalCer) stimulated IFN-γ secretion to the same extent.

5) As was seen in assays between phytosphingoid **3-3b** and its sphingosine analog **3-4**, there was no apparent advantage of the use of one sphingoid base over another, although a different research collaboration has suggested that there is some diminished response in sphinganine-containing GSLs.[45]

6) Neither the stereocenter configuration of ceramidyl α-hydroxymyristamide nor the hydroxyl group itself appears to impart enhanced or diminished NKT cell activity.

7) GSL **6-2a** induced a greater overall stimulatory response than other bacterial ligands. This is perhaps due to enhanced stability that this particular glycolipid can impart to the protein-antigen-TCR ternary complex.

Comparison of the stimulatory effects of heat-killed LPS$^-$ *S. capsulata* and *E. muris*, versus GSL$^-$/LPS$^+$ *S. typhimurium*, has shown that both types of Gram-negative bacteria promote activation of natural killer T cells through two distinct pathways. Although *Salmonella* recruits NKT cells through general provocation of the innate immune system

via the TLR 4 receptor, they are activated by the endogenous iGb3 ligand and not by LPS itself. Membranous glycosphingolipids of *Sphingomonas*, and possibly *Ehrlichia*, are directly stimulatory towards NKT cells via restriction by CD1d. Thus the first exogenous group of target glycolipid antigens of these lymphocytes has been identified.

6.4 Experimental Section

Materials and General Methods. Mass spectrometric data were obtained on a JEOL SX 102A spectrometer for fast atom bombardment (FAB; thioglycerol/Na^+ matrix) or an Agilent Technologies TC/MSD TOF spectrometer for electrospray ionization (ESI; 3500 eV, positive ion mode). ^1H and ^{13}C NMR spectra were obtained on either a Varian Unity 300 or 500 MHz instrument using 99.8% $CDCl_3$ with 0.05% v/v TMS, 99.8% CD_3OD with 0.05% v/v TMS, or 99.5% pyridine-d_5 or 99.96% DMSO-d_6 in ampoules. Methanol, methylene chloride, and tetrahydrofuran were dried using columns of activated alumina. Flash chromatography was performed using 230-400 mesh silica gel. Thin layer chromatography was performed on aluminum-backed, 254 nm UV-active plates with a silica gel particle size of 250 μm. Reagents were obtained from Aldrich or Fluka, unless otherwise specified, and were used as received.

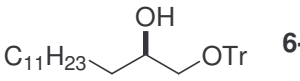

6-8

6-8. 1-Bromoundecane (3.6 mL, 16.1 mmol) in anhydrous ether (65 mL) was added to magnesium turnings (576 mg, 23.7 mmol) under N_2 followed by five drops of 1,2-dibromoethane with stirring. After the solution turned a grey-green color, anhydrous THF (90 mL) was added. After 30 m, most of the magnesium was consumed. The temperature was lowered to -30°C and CuI (310 mg, 1.63 mmol) was added. After an additional 30 m, **6-7** (2.5 g, 7.9 mmol) in anhydrous THF (15 mL) was added dropwise to

the gray suspension. The reaction was allowed to warm to 0°C and stirred for 3 h before quenching with deionized water (50 mL). The mixture was extracted with Et_2O:Hex (1:2, 3 x 75 mL), washed with brine, dried over $MgSO_4$, and concentrated in vacuo. Purification by flash chromatography (SiO_2, hexanes then EtOAc:Hex 1:9) yielded a colorless oil that slowly evolved to a white solid (3.11 g, 83%) under vacuum. ^{1}H NMR ($CDCl_3$, 300 MHz) δ 7.44 (m, 6 H), 7.26 (m, 9 H), 3.75 (m, 1 H), 3.16 (dd, *J* = 9.3, 3.2 Hz, 1 H), 3.03 (dd, *J* = 9.3, 7.6 Hz, 1 H), 2.40 (br s, 1 H), 1.45-1.20 (m, 22 H), 0.88 (t, *J* = 6.8 Hz, 3 H); ^{13}C NMR ($CDCl_3$, 75 MHz) δ 144.08, 128.82, 127.98, 127.21, 86.78, 71.10, 67.96, 33.52, 32.08, 29.83, 29.82, 29.78, 29.75, 29.71, 29.52, 25.65, 22.86, 14.29; HRMS (FAB) *m/z* for $C_{33}H_{44}NaO_2$ ([M+Na]$^+$) 495.3226 (100%), calc. 495.3239.

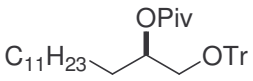

6-9

6-9. Monoprotected diol **6-8** (1.3 g, 2.8 mmol) was dissolved in anhydrous CH_2Cl_2 (10 mL) along with DMAP (409 mg, 335 mmol) and Et_3N (0.5 mL, 3.6 mmol) under N_2. Pivaloyl chloride (0.40 ml, 3.3 mmol) was added dropwise and the reaction was allowed to proceed for 14 h before quenching with deionized water (10 mL). The mixture was extracted with hexanes (3 x 20 mL), washed with brine, dried over $MgSO_4$, and concentrated in vacuo. Flash chromatography (SiO_2, hexanes then EtOAc:Hex 5:95) yielded a colorless oil that slowly transformed to a white solid (1.34 g, 87%, R_f = 0.41 EtOAc:Hex 5:95) under vacuum. ^{1}H NMR ($CDCl_3$, 300 MHz) δ 7.43 (m, 6 H), 7.26 (m, 9 H), 5.07 (m, 1 H), 3.11 (m, 2 H), 1.55 (m, 2 H), 1.35-1.10 (m, 29 H), 0.88 (t, *J* = 6.8 Hz, 3 H); ^{13}C NMR ($CDCl_3$, 75 MHz) δ 178.34, 144.20, 128.90, 127.96, 127.15, 86.40, 73.08, 64.95, 39.09, 32.14, 31.13, 29.88, 29.85, 29.83, 29.72, 29.67, 29.63, 29.57, 27.53,

25.25, 22.91, 14.34; HRMS (FAB) *m/z* for $C_{38}H_{52}NaO_3$ ([M+Na]$^+$) 579.3811 (100%), calc. 579.3814.

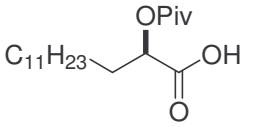

6-10

6-10. The fully-protected diol **6-9** (1.34 g, 2.40 mmol) was dissolved in acetone (80 mL) and oxidized by sonicating in the presence of Jones reagent (1.8 mL; 3 g CrO_3, 22 ml H_2O, 2.5 mL H_2SO_4) at 40^{o}C for 1 h. Additional aliquots of the oxidant (7 x 1.8 mL) were added every 3 h until TLC (EtOAc:Hex 1:9, $R_{f\ S.M.}$ = 0.68) showed no change in starting material consumption. Isopropanol (5 mL) was then added to quench the reaction. The solution was decanted, the solid remnant was washed with acetone (3 x 15 mL), and any residual acid was neutralized with $NH_3 \cdot H_2O$ (10 mL; 28% solution). The resulting blue precipitate was filtered and washed leaving a colorless solution. After concentration, the crude product was purified by flash chromatography (SiO_2, EtOAc:Hex 1:4 with 1% HOAc), yielding a colorless oil (546 mg, 69%). $[\alpha]^{25}_D$ +13.8^o (c 1.2, $CHCl_3$); ^{1}H NMR ($CDCl_3$, 300 MHz) δ 4.96 (t, *J* = 6.5 Hz, 1 H), 1.88 (m, 2 H), 1.45-1.35 (m, 2 H), 1.34-1.16 (m, 27 H), 0.88 (t, *J* = 6.8 Hz, 3 H); ^{13}C NMR ($CDCl_3$, 75 MHz) δ 178.30, 176.52, 71.82, 38.89, 32.14, 31.12, 29.86, 29.82, 29.73, 29.56, 29.27, 27.21, 25.35, 22.91, 14.34; HRMS (FAB) *m/z* for $C_{19}H_{36}NaO_4$ ([M+Na]$^+$) 351.2497 (100%), calc. 351.2511.

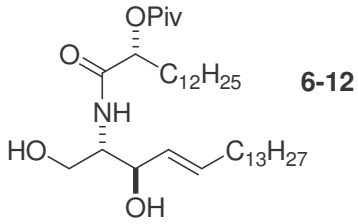

6-12

6-12. Pivaloyl-protected acid **6-10** (274 mg, 0.834 mmol) was dissolved in anhydrous THF (10 mL) and warmed to 60°C. *N*-Hydroxysuccinimide (112 mg, 0.973 mmol) and DCC (190 mg, 0.921 mmol) were added and the reaction was warmed to reflux. After 1 h, a solution of sphingosine (**6-11**; 245 mg, 0.818 mmol) in anhydrous THF (3 mL) and Et_3N (1 mL) was added. The reaction was allowed to reflux for an additional 3 h when no observable change was seen by TLC (5% MeOH in CH_2Cl_2, $R_{f\ pdt}$ = 0.39). The solvent was removed in vacuo and the residue was dissolved in MeOH and CH_2Cl_2 then adsorbed onto silica gel. Purification of the mixture by flash chromatography (SiO_2, MeOH:CH_2Cl_2 5:95) provided a white powder (450 mg, 90%, R_f = 0.39 MeOH:CH_2Cl_2 5:95). ^{1}H NMR ($CDCl_3$:CD_3OD 99:1, 300 MHz) δ 7.08 (d, *J* = 9.5 Hz, 1 H), 5.75 (m, 1 H), 5.50 (dd, *J* = 15.1, 6.8 Hz, 1 H), 5.07 (m, 1H), 4.17 (t, *J* = 6.0 Hz, 1 H), 3.83 (m, 2 H), 3.60 (dd, J = 12.2, 5.4 Hz, 1 H), 2.05 (m, 2 H), 1.91-1.76 (m, 4 H), 1.52-1.16 (m, 51 H), 0.88 (t, *J* = 6.8 Hz, 6 H); ^{13}C NMR ($CDCl_3$ and three drops CD_3OD, 75 MHz) δ 178.25, 171.81, 134.49, 129.99, 74.53, 73.03, 61.34, 55.33, 39.48, 34.38, 33.05, 32.63, 30.40, 30.36, 30.26, 30.06, 29.93, 29.89, 27.44, 26.32, 25.62, 23.35, 14.49; HRMS (FAB) *m/e* for $C_{37}H_{71}NNaO_5$ ($[M+Na]^+$) 632.5222 (100%), calc. 632.5230.

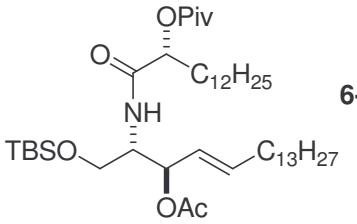

6-13

6-13. Ceramide diol **6-12** (450 mg, 0.738 mmol) was dissolved in anhydrous THF (10 mL) at 60°C. TBSCl (167 mg, 1.11 mmol) and imidazole (75 mg, 1.11 mmol) were added and the reaction was allowed to proceed for 5 m before TLC (5% MeOH in CH_2Cl_2) showed the disappearance of all starting material. Water was used to quench the reaction, which was extracted with EtOAc (3 x 10 mL). The organic layer was washed with 5% HCl solution and brine, and dried over $MgSO_4$. The compound was concentrated in vacuo, dissolved in anhydrous THF (10 mL) and acetylated with acetic anhydride (1 mL), Et_3N (1 mL), and DMAP (50 mg, 0.41 mmol) without further purification. The reaction was mixed for 10 m and was quenched with ice. The protected diol was extracted with EtOAc (3 x 10 mL), washed with sat. aq. $NaHCO_3$ (2 x 10 mL), brine, 5% HCl solution (2 x 10 mL), brine, and dried over $MgSO_4$. After adsorbing the crude compound onto silica gel, it was purified by flash chromatography (SiO_2, EtOAc:Hex 1:8) yielding a colorless oil (298 mg, 53%, R_f = 0.44 EtOAc:Hex 1:8). ^1H NMR ($CDCl_3$, 300 MHz) δ 6.30 (d, *J* = 9.5 Hz, 1 H), 5.78 (m, 1 H), 5.37 (dd, *J* = 15.5, 6.8 Hz, 1 H), 5.29 (m, 1H), 5.18 (dd, *J* = 6.7, 4.7 Hz, 1 H), 4.20 (m, 1 H), 3.74 (dd, *J* = 10.5, 2.9 Hz, 1 H), 3.54 (dd, J = 10.5, 4.2 Hz, 1 H), 2.00 (s, 3 H), 1.97 (m, 2 H), 1.84-1.64 (m, 2 H), 1.38-1.10 (br s, 51 H), 0.85 (m, 15 H), 0.00 (s, 3 H), -0.01 (s, 3 H); ^{13}C NMR ($CDCl_3$, 75 MHz) δ 176.75, 169.75, 169.72, 137.25, 124.80, 73.79, 73.30, 61.79, 51.89, 38.97, 32.49, 32.06, 29.84, 29.81, 29.77, 29.71, 29.65, 29.58, 29.50, 29.45, 28.99,

27.28, 26.03, 24.65, 22.82, 21.31, 18.40, 14.24, -5.51, -5.45; HRMS (FAB) *m/z* for $C_{45}H_{87}NNaO_6Si$ ($[M+Na]^+$) 788.6211 (100%), calc. 788.6200.

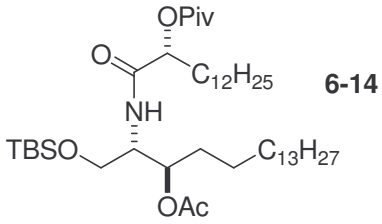

6-14

6-14. Unsaturated ceramide **6-13** (298 mg, 0.389 mmol) was dissolved in anhydrous THF (8 mL), mixed with a palladium catalyst (10% on carbon; 60 mg, 20% w/w), and exposed to H_2 gas (200 psi). After reacting for 20 h, H_2 was evacuated and the mixture was filtered through a Celite plug with THF. TLC showed that all starting material was gone with the appearance of a single product spot (R_f = 0.52 EtOAc:Hex 1:8). A pure colorless oil (299 mg, quantitative yield) was obtained following column chromatography purification (SiO_2, EtOAc:Hex 1:8). ^{1}H NMR ($CDCl_3$, 500 MHz) δ 6.45 (d, *J* = 9.8 Hz, 1 H), 5.17 (t, *J* = 5.6 Hz, 1 H), 4.92 (m, 1 H), 4.19 (m, 1H), 3.71 (dd, *J* = 10.3, 2.9 Hz, 1 H), 3.56 (dd, *J* = 10.3, 3.9, 1 H), 2.01 (s, 3 H), 1.82 (m, 2 H), 1.32-1.18 (m, 57 H), 0.85 (m, 15 H), 0.01 (s, 3 H), -0.01 (s, 3 H); ^{13}C NMR ($CDCl_3$, 125 MHz) δ 176.96, 170.58, 169.75, 73.83, 73.49, 61.99, 51.61, 38.90, 32.07, 31.90, 30.96, 30.45, 29.86, 29.82, 29.69, 29.60, 29.52, 29.43, 27.29, 26.04, 25.29, 24.62, 22.84, 21.20, 18.45, 14.26, -5.50, -5.45; HRMS (FAB) *m/z* for $C_{45}H_{90}NO_6Si$ ($[M+H]^+$) 768.6538 (100%), calc. 768.6537.

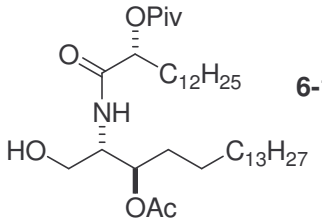

6-15

6-15. Sphinganine-based ceramide **6-14** (150 mg, 0.229 mmol) was dissolved in THF (3 mL) and aqueous HF (1 mL). After 4 m, TLC showed complete deprotection of the silyl group (EtOAc:Hex 1:2. $R_{f\ pdt}$ = 0.37). The reaction was quenched with saturated $NaHCO_3$ (10 mL), extracted with EtOAc (1 x 10 mL), and washed with more $NaHCO_3$. The aqueous layers were combined and extracted with EtOAc (5 mL) followed by drying over $MgSO_4$. The solution was concentrated in vacuo and purified by flash chromatography (SiO_2, EtOAc:Hex 1:2) yielding a colorless oil (67 mg, 52%, R_f = 0.48 EtOAc:Hex 1:2). ^{1}H NMR ($CDCl_3$, 500 MHz) δ 6.72 (d, *J* = 8.8 Hz, 1 H), 5.15 (dd, *J* = 6.6, 5.2 Hz, 1 H), 4.85 (m, 1 H), 4.02 (m, 1 H), 3.61 (dt, *J* = 12.2, 3.4 Hz, 1 H), 3.52 (dd, *J* = 9.3, 2.9, 1 H), 2.81 (br s, 1 H), 2.12 (s, 3 H), 1.90-1.80 (m, 2 H), 1.68-1.56 (m, 2 H), 1.42-1.36 (br s, 55 H), 0.88 (t, *J* = 6.8 Hz, 6 H); ^{13}C NMR ($CDCl_3$, 125 MHz) δ 177.37, 172.42, 170.53, 74.03, 73.80, 61.41, 52.75, 39.07, 32.11, 31.95, 31.38, 29.90, 29.86, 29.74, 29.68, 29.65, 29.56, 29.53, 29.43, 27.43, 25.72, 24.90, 22.89, 21.19, 14.32; HRMS (FAB) *m/z* for $C_{39}H_{75}NNaO_6$ ([M+Na]$^+$) 676.5482 (100%), calc. 676.5492.

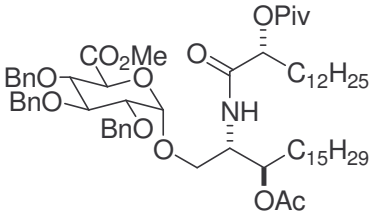

6-17a

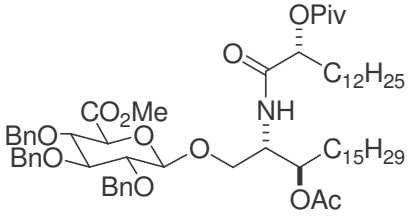

6-17b

6-17a and **6-17b**. Bromide donor **6-16** (30 mg, 0.06 mmol) and ceramide acceptor **6-15** (18 mg, 0.03 mmol) were dissolved in anhydrous CH_2Cl_2 (10 mL). The solution was

cooled to 0°C and freshly powdered 4A molecular sieves were added. After stirring for 10 m, AgOTf (18 mg, 0.09 mmol) was added in the dark and the reaction vessel was covered with foil to exclude light. After 2 h, the reaction was filtered through Celite with an EtOAc rinse, the filtrate was concentrated, and the crude oil was purified by column chromatography (SiO_2, EtOAc:Hex 1:6) to yield α-anomer **6-17a** (16 mg, 26%, R_f = 0.48 EtOAc:Hex 1:4) and β-anomer **6-17b** (14 mg, 25%, R_f = 0.34 EtOAc:Hex 1:4) as colorless oils. **6-17a**: ^{1}H NMR ($CDCl_3$, 500 MHz) δ 7.39-7.24 (m, 15 H), 6.33 (d, *J* = 3.5 Hz, 1 H), 5.43 (t, *J* = 6.0 Hz, 1 H), 5.33-5.30 (m, 1 H), 4.79 (d, *J* = 3.5 Hz, 1 H), 4.72 (d, *J* = 11.7 Hz, 1 H), 4.70 (d, *J* = 11.7 Hz, 1 H), 4.69 (d, *J* = 11.7 Hz, 1 H), 4.63 (d, *J* = 11.7 Hz, 1 H), 4.55 (d, *J* = 11.7 Hz, 1 H), 4.50 (d, *J* = 11.7 Hz, 1 H), 4.13 (d, *J* = 10.5 Hz, 1 H), 3.77-3.73 (m, 2 H), 3.79-3.68 (m, 2 H), 3.65 (m, 1 H), 3.62 (s, 3 H), 3.48 (dd, J = 9.5, 3.5 Hz, 1 H), 2.05 (s, 3 H), 1.88-1.85 (br s, 2 H), 1.61-1.49 (m, 4 H), 1.30-1.05 (m, 53 H), 0.88 (t, *J* = 6.8 Hz, 6 H); ^{13}C NMR ($CDCl_3$, 125 MHz) δ 177.34, 170.82, 169.98, 169.10, 138.75, 138.59, 138.02, 128.69, 128.70, 128.08, 127.99, 127.95, 127.87, 127.74, 103.79, 84.22, 81.70, 79.44, 75.89, 75.20, 75.18, 74.60, 74.11, 73.73, 68.49, 51.99, 50.87, 39.31, 32.64, 31.80, 31.45, 29.98, 29.87, 29.75, 29.71, 29.50, 29.01, 28.79, 27.84, 25.50, 25.34, 22.90, 21.47, 14.39; HRMS (FAB) *m/z* for $C_{67}H_{103}NNaO_{12}$ ($[M+Na]^+$) 1136.7388 (100%), calc. 1136.7372. **6-17b**: ^{1}H NMR ($CDCl_3$, 500 MHz) δ 7.36-7.21 (m, 15 H), 6.27 (d, *J* = 9.5 Hz, 1 H), 5.02 (t, *J* = 10.5 Hz, 1 H), 4.99-4.98 (m, 1 H), 4.90 (d, *J* = 10.5 Hz, 1 H), 4.84 (d, *J* = 11.0 Hz, 1 H), 4.79 (d, *J* = 11.5 Hz, 1 H), 4.78 (d, *J* = 11.0 Hz, 1 H), 4.71 (d, *J* = 11.0 Hz, 1 H), 4.58 (d, *J* = 11.5 Hz, 1 H), 4.40 (d, *J* = 7.5 Hz, 1 H), 4.38-3.34 (m, 1 H), 3.91 (dd, *J* = 10.0, 7.0 Hz, 1 H), 3.80 (t, *J* = 9.0 Hz, 1 H), 3.73 (s, 3 H), 3.66-3.60 (m, 2 H), 3.45 (t, *J* = 8.0 Hz, 1 H), 2.06 (s, 3 H), 1.88-1.78 (m, 2 H), 1.62-1.50

(m, 4 H), 1.30-1.21 (m, 53 H), 0.89 (t, J = 6.8 Hz, 3 H), 0.88 (t, J = 6.8 Hz, 3 H); ^{13}C NMR ($CDCl_3$, 125 MHz) δ 177.32, 170.81, 170.08, 169.10, 138.48, 138.30, 138.00, 128.69, 128.65, 128.31, 128.21, 128.07, 127.96, 103.99, 84.01, 81.77, 79.43, 75.94, 75.34, 75.32, 74.56, 73.96, 73.67, 68.40, 52.68, 50.83, 39.04, 32.18, 31.80, 31.34, 29.96, 29.78, 29.61, 29.55, 27.31, 25.51, 24.94, 22.94, 21.25, 14.38; HRMS (FAB) *m/z* for $C_{67}H_{103}NNaO_{12}$ ([M+Na]$^+$) 1136.7382 (100%), calc. 1136.7372.

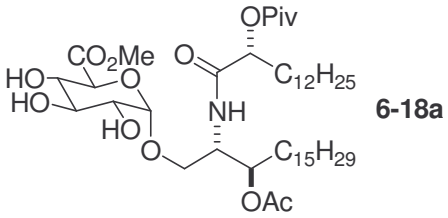

6-18a

6-18a. Glycolipid **6-17a** (12 mg, 0.011 mmol) was dissolved in anhydrous THF (5 mL) and MeOH (5 mL) and placed inside a hydrogenation vessel. Palladium on carbon (10%, 20 mg) was added slowly and the container filled with H_2 (300 psi). After 12 h, the vessel was evacuated and the suspension was filtered through a Celite plug using EtOAc as a diluent. After concentration in vacuo, the compound was purified by column chromatography (SiO_2, MeOH:CH_2Cl_2 5:95) to yield the α-anomer as a colorless oil (5 mg, 60%). ^{1}H NMR ($CDCl_3$, 500 MHz) δ 6.59 (d, J = 9.8 Hz, 1 H), 5.21 (dd, J = 8.8, 1.9 Hz, 1 H), 4.92-4.89 (m, 2 H), 4.44 (s, 1 H), 4.40-4.35 (m, 2 H), 3.92-3.85 (m, 1 H), 3.84 (s, 3 H), 3.76 (dd, J = 10.7, 2.9 Hz, 1 H), 3.53 (dd, J = 10.7, 3.4 Hz, 1 H), 3.42 (br s, 1 H), 2.96 (br s, 3 H), 2.03 (s, 3 H), 1.90-1.82 (m, 2 H), 1.67-1.56 (m, 4 H), 1.36-1.21 (m, 53 H), 0.88 (t, J = 6.8 Hz, 6 H); ^{13}C NMR ($CDCl_3$, 125 MHz) δ 178.22, 171.57, 170.58, 170.57, 99.62, 74.53, 73.97, 73.81, 71.84, 71.14, 67.75, 53.02, 51.15, 39.21, 32.16, 31.82, 31.67, 29.90, 29.67, 29.60, 29.44, 27.28, 25.57, 25.06, 22.93, 21.35, 14.36; HRMS (FAB) *m/z* for $C_{46}H_{85}NNaO_{12}$ ([M+Na]$^+$) 866.5952 (100%), calc. 866.5964.

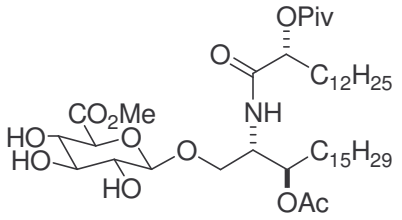

6-18b

6-18b. Same procedure as synthesis of **6-18a** (61%). ^{1}H NMR ($CDCl_3$, 500 MHz) δ 6.62 (d, *J* = 9.8 Hz, 1 H), 5.07 (m, 1 H), 4.89-4.86 (m, 1 H), 4.35-4.28 (m, 2 H), 4.09 (br s, 1 H), 3.87 (d, *J* = 10.0 Hz, 1 H), 3.82 (s, 3 H), 3.77-3.71 (m, 2 H), 3.59 (t, J = 9.0 Hz, 1 H), 3.34 (t, *J* = 7.5 Hz, 1 H), 2.06 (s, 3 H), 1.88-1.80 (m, 2 H), 1.62-1.54 (m, 4 H), 1.38-1.23 (m, 53 H), 0.88 (t, *J* = 6.8 Hz, 6 H); ^{13}C NMR ($CDCl_3$, 125 MHz) δ 178.98, 171.23, 170.45, 170.15, 103.55, 75.84, 75.80, 74.57, 74.21, 73.00, 71.56, 68.38, 52.56, 51.19, 39.20, 32.16, 31.81, 29.94, 29.60, 27.30, 27.21, 25.55, 25.00, 22.93, 21.26, 14.43; HRMS (FAB) *m/z* for $C_{46}H_{85}NNaO_{12}$ ($[M+Na]^+$) 866.5963 (100%), calc. 866.5964.

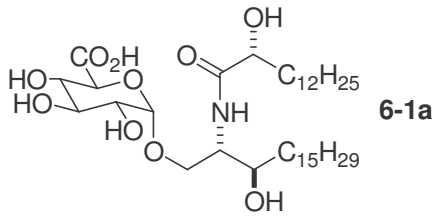

6-1a

6-1a. Compound **6-18a** (5 mg, 0.007 mmol) was dissolved in MeOH (3 mL) followed by sodium methylate (1 mg, 0.015 mmol) and deionized water (5 μL). The mixture was stirred at room temperature and the product allowed to precipitate over a 12 h period. The suspension was transferred to a tube, centrifuged (2500 rpm, 10 m), and washed with MeOH (3 mL). After repeating this process, the compound was dissolved in DMSO (1 mL) and lyophilized to yield a fluffy white powder (3 mg, 80%). ^{1}H NMR (pyridine-d_5, 500 MHz) δ 8.45 (d, *J* = 9.3 Hz, 1 H), 5.56 (d, *J* = 3.9 Hz, 1 H), 5.08 (d, *J* = 9.8 Hz, 1 H), 4.74 (m, 1 H), 4.71 (t, *J* = 9.3 Hz, 1 H), 4.66 (dd, *J* = 7.8, 3.9 Hz, 1 H), 4.62

(t, *J* = 9.8 Hz, 1 H), 4.55 (dd, *J* = 10.3, 3.9 Hz, 1 H), 4.42 (dd, *J* = 10.3, 4.9, 1 H), 4.30-4.25 (m, 2 H), 2.28-2.20 (m, 1 H), 2.16-2.04 (m, 1 H), 1.94-1.50 (m, 4 H), 1.27 (br s, 44 H), 0.88 (t, *J* = 6.8 Hz, 6 H); ^{13}C NMR (DMSO-d_6, 125 MHz) δ 171.69, 169.89, 99.35, 73.35, 70.68, 70.40, 70.19, 70.00, 69.10, 67.77, 67.23, 49.88, 35.35, 31.12, 28.92, 28.81, 28.53, 25.24, 25.16, 21.87, 13.56; HRMS (FAB) *m/z* for $C_{38}H_{73}NNaO_{10}$ ([M+Na]$^+$) 726.5140 (100%), calc. 726.5127.

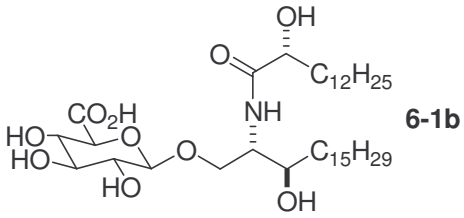

6-1b

6-1b. Same procedure as synthesis of **6-1a** (77%). ^{1}H NMR (DMSO-d_6, 500 MHz) δ 7.36 (d, *J* = 10.0 Hz, 1 H), 6.36 (br s, 1 H), 5.32 (d, *J* = 6.5 Hz, 1 H), 4.93 (d, *J* = 4.5 Hz, 1 H), 4.82 (d, *J* = 4.5 Hz, 1 H), 4.12 (d, *J* = 7.5 Hz, 1 H), 3.87 (dd, *J* = 10.3, 4.5 Hz, 1 H), 3.82 (dt, *J* = 5.5, 5.0 Hz, 1 H), 3.66 (dd, *J* = 10.5, 3.0 Hz, 1 H), 3.63-3.59 (m, 1 H), 3.46 (m, 1 H), 3.18 (d, *J* = 9.5 Hz, 1 H), 3.13-3.04 (m, 1 H), 2.95 (td, *J* = 8.0, 4.5 Hz, 1 H), 1.60-1.46 (m, 2 H), 1.44-1.32 (m, 2 H), 1.23 (br s, 46 H), 0.85 (t, J = 6.8 Hz, 6 H); ^{13}C NMR (DMSO-d_6, 125 MHz) δ 172.27, 169.86, 99.41, 72.70, 70.52, 70.40, 70.24, 70.06, 69.55, 67.97, 67.82, 49.82, 35.33, 33.64, 31.15, 28.82, 28.56, 25.22, 24.40, 21.90, 13.66; HRMS (FAB) *m/z* for $C_{38}H_{73}NNaO_{10}$ ([M+Na]$^+$) 726.5146 (100%), calc. 726.5127.

Isolation of *Sphingomonas* glycosphingolipids GSL-1A/C and GSL-3A/C. *Sphingomonas capsulata* (ATCC 14666) was grown in 3 L of nutrient broth at 26°C for 72 h before being centrifuged (5000 rpm, 10 m) and washed with deionized water three times to remove the broth material. The bacterial pellet was lyophilized to yield 650 mg

of dry cellular material. Following an established procedure,[17] the cell solids were suspended in a solution of 2:1 $CHCl_3$:MeOH (15 mL) and sonicated for 10 minutes to remove the more lipophilic compounds. The mixture was centrifuged (5000 rpm, 5 m), the supernatant removed and the solids were again sonicated and isolated in the same fashion. The extracted cellular solid material was suspended in 1:3 $CHCl_3$:MeOH (13 mL) and refluxed for 1 h at 80°C. After cooling, centrifugation (5000 rpm, 5 m), and supernatant removal, the process was repeated. The combined refluxed extracts were concentrated and examined by TLC ($CHCl_3$:MeOH:H_2O 65:25:4). Five distinct spots were visible at R_f = 0.65, 0.60, 0.51, 0.30, and 0.16 using *p*-anisaldehyde stain. The crude mixture was then purified by microcolumn chromatography (SiO_2, $CHCl_3$:MeOH:H_2O 65:25:4), to yield the upper three spots as a mixture and the bottom two spots separately with the purified R_f values of 0.46 (0.84 mg) and 0.23 (1.33 mg) in the same solvent. The upper of these two fractions was identified as a mixture of GSL-1A and GSL-1C. ^{1}H NMR (DMSO-d_6, 500 MHz) data was thesame as reported in the literature[17] and similar to that of **6-1a**; GSL-1A: HRMS (ESI) *m/z* for $C_{38}H_{73}NNaO_{10}$ ($[M+Na]^+$) 726.51212 (100%), calc. 726.51267; GSL-1C: HRMS (ESI) *m/z* for $C_{41}H_{77}NNaO_{10}$ ($[M+Na]^+$) 744.56110 (100%), calc. 744.56202. The lower of the two fractions was identified as a mixture of GSL-3A and GSL-3C. ^{1}H NMR (DMSO-d_6, 500 MHz) data was the same as reported in the literature[17] and similar to that in Ref. 38 for **6-6**; GSL-3A: HRMS (ESI) *m/z* for $C_{50}H_{94}N_2NaO_{19}$ ($[M+Na]^+$) 1049.63300 (100%), calc. 1049.63430; GSL-3C: HRMS (ESI) *m/z* for $C_{53}H_{98}N_2NaO_{19}$ ($[M+Na]^+$) 1067.68280 (100%), calc. 1067.68366.

Isolation and characterization of (2*S*)-hydroxymyristic acid from *S. capsulata* and comparison to synthetic (2*R)*-hydroxymyristic acid. Combined fractions of isolated *S. capsulata* glycosphingolipids GSL-1 and GSL-3 (5 mg) were refluxed in HCl (4 *M*, 2 mL) at 100°C for 2 h. Three drops of concentrated HCl were added to the cooled reaction and the solution was stored for 12 h at 0°C. An equal volume of MeOH was added (2 mL) and the reaction mixture was extracted with $CHCl_3$ (5 x 2 mL). Diazomethane reagent (2 mL; made in situ using 1-methyl-3-nitro-1-nitrosoguanidine in Et_2O and 40% aqueous KOH) was added and the reaction quenched immediately with aqueous HOAc (2 mL). The aqueous layer was extracted with $CHCl_3$ (3 x 2 mL) and the organic layers were combined, concentrated, and purified by column chromatography (SiO_2, EtOAc:Hex 1:4) to yield a white solid (1 mg, R_f = 0.42 EtOAc:Hex 1:4). $[\alpha]^{25}_D$ +3.0° (c 1.0, $CHCl_3$); ^{1}H NMR ($CDCl_3$, 500 MHz) δ 4.19 (m, 1 H), 3.79 (s, 3 H), 2.68 (d, *J* = 5.9 Hz, 1 H), 1.82-1.74 (m, 1 H), 1.67-1.59 (m, 1 H), 1.26 (br s, 20 H), 0.88 (t, *J* = 6.8 Hz, 3 H); HRMS (FAB) *m/z* for $C_{15}H_{28}NaO_3$ ($[M+Na]^+$) 279.1937 (100%), calc. 279.1931. Protected acid **6-10** (100 mg, 0.304 mmol) was depivoylated by dissolving in MeOH (5 mL) and adding sodium methylate (25 mg, 0.46 mmol). Rapid precipitation of the free α-hydroxyacid occurred. The mixture was neutralized with 5% aqueous HCl (1 mL) and extracted with $CHCl_3$ (5 x 3 mL) followed by methyl ester formation using diazomethane (2 mL; same as above). A similar workup and purification followed providing methyl 2*R*-hydroxymyristoate (44 mg, 52%, R_f = 0.42 EtOAc:Hex 1:4). $[\alpha]^{25}_D$ -8.6° (c 2.9, $CHCl_3$); ^{1}H NMR ($CDCl_3$, 500 MHz) δ 4.19 (dd, *J* = 7.3, 4.4 Hz, 1 H), 3.79 (s, 3 H), 2.68 (br s, 1 H), 1.82-1.75 (m, 1 H), 1.67-1.60 (m, 1 H), 1.26 (br s, 20 H), 0.88 (t, *J* = 6.8 Hz, 3 H); ^{13}C NMR ($CDCl_3$, 500 MHz) δ 176.07, 70.65, 52.63, 34.59, 32.10, 29.85, 29.83,

29.74, 29.65, 29.54, 29.49, 24.93, 22.88, 14.30; HRMS (FAB) *m/z* for $C_{15}H_{28}NaO_3$ ($[M+Na]^+$) 279.1935 (100%), calc. 279.1931.

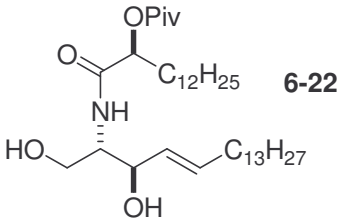

6-22

6-22. (2*S*)-*O*-Pivaloylhydroxymyristic acid (**6-21**; 78 mg, 0.24 mmol) was dissolved in anhydrous CH_2Cl_2 (5 mL) and *p*-dioxane (2.5 mL) along with Et_3N (50 µL, 0.35 mmol) and HBTU (100 mg, 0.26 mmol). The acid was allowed to activate for 20 m before addition of sphingosine (78 mg, 0.26 mmol) in a solution of anhydrous CH_2Cl_2 (2 mL), *p*-dioxane (1 mL), and Et_3N (50 µL, 0.35 mmol), which helped to dissolve the cloudy reaction mixture. After stirring for 12 h, the solvent was removed in vacuo and the crude residue was purified by column chromatography (SiO_2, MeOH:CH_2Cl_2 5:95) to yield a colorless oil (158 mg, quantitative yield, R_f = 0.42 MeOH:CH_2Cl_2 5:95). ^{1}H NMR ($CDCl_3$, 500 MHz) δ 6.92 (d, *J* = 8.3 Hz, 1 H), 5.75 (m, 1 H), 5.50 (dd, *J* = 15.1, 6.3 Hz, 1 H), 5.13 (dd, *J* = 7.8, 4.4 Hz, 1 H), 4.26 (d, *J* = 3.5 Hz, 1 H), 3.98 (dd, *J* = 9.8, 3.4 Hz, 1 H), 3.88-3.82 (m, 2 H), 3.70-3.65 (m, 2 H), 2.03 (dt, *J* = 7.3, 6.8 Hz, 2 H), 1.91-1.78 (m, 2 H), 1.48-1.21 (m, 51 H), 0.88 (t, *J* = 6.8 Hz, 6 H); ^{13}C NMR ($CDCl_3$, 125 MHz) δ 177.38, 170.74, 133.85, 128.89, 74.07, 73.87, 62.05, 54.02, 38.95, 38.71, 32.41, 32.03, 29.81, 29.77, 29.75, 29.64, 29.51, 29.47, 29.38, 29.30, 29.25, 27.16, 24.96, 22.79, 14.23; HRMS (ESI) *m/z* for $C_{37}H_{71}NNaO_5$ ($[M+Na]^+$) 632.51852 (100%), calc. 632.52245.

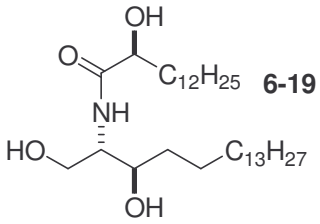

6-19. Ceramide **6-22** (158 mg, 0.259 mmol) was dissolved in anhydrous THF (4 mL) and MeOH (100 μL) and placed inside a hydrogenation vessel. Palladium on carbon (10%, 32 mg) was added slowly and the container filled with H_2 (200 psi). After 5 h, the vessel was evacuated and the reaction checked by TLC ($R_{f\ alkane}$ = 0.46, $R_{f\ alkene}$ = 0.39, MeOH:CH_2Cl_2 5:95) and the suspension was filtered through a Celite plug using EtOAc as a diluent. After concentration in vacuo, the crude alkane was peracetylated by dissolving in THF (5 mL) and adding excess Ac_2O (1 mL), Et_3N (1 mL), and DMAP (25 mg). After stirring for 12 h, the solvent was removed in vacuo and the residue was purified by flash chromatography (SiO_2, EtOAc:Hex 1:4) to yield the product (**6-23**) as a colorless oil that eventually solidified to a waxy, white solid under vacuum (132 mg, 75%, R_f = 0.48 EtOAc:Hex 1:4). ^{1}H NMR ($CDCl_3$, 500 MHz) δ 6.43 (d, *J* = 9.3 Hz, 1 H), 5.14 (d, *J* = 6.8, 4.9 Hz, 1 H), 4.85 (m, 1 H), 4.41 (ddd, *J* = 6.3, 5.4, 3.9 Hz, 1 H), 4.26 (dd, *J* = 11.7, 6.3 Hz, 1 H), 4.07 (dd, *J* = 11.7, 3.9 Hz, 1 H), 2.06 (s, 3 H), 2.05 (s, 3 H), 1.88-1.78 (m, 2 H), 1.62-1.53 (m, 2 H), 1.40-1.20 (m, 55 H), 0.88 (t, *J* = 6.8 Hz, 6 H); ^{13}C NMR ($CDCl_3$, 125 MHz) δ 177.08, 171.01, 170.78, 170.15, 73.83, 62.57, 50.09, 39.03, 32.09, 31.84, 31.44, 29.86, 29.83, 29.79, 29.70, 29.60, 29.56, 29.51, 29.37, 29.21, 25.42, 24.80, 24.72, 22.86, 21.10, 20.91, 14.29; HRMS (ESI) *m/z* for $C_{41}H_{80}N_2O_6$ ($[M+NH_4]^+$) 696.65041 (100%), calc. 696.60109. Triester **6-23** (132 mg, 0.226 mmol) was taken up into anhydrous MeOH (1.5 mL) and a solution of NaOMe (1 *M*, 700 μL, 0.700 mmol) was added. The reaction was warmed slightly (40°C) to aid hydrolysis of

the pivaloyl ester. After 10 m, the fully deprotected product precipitated out of solution as a white solid. After stirring for a total of 30 m, the mixture was centrifuged (3800 rpm, 5 m), the supernatant was removed, and the solid was washed with MeOH (2 mL). After repeating, the solid was dissolved in 1:1 DMSO:H_2O (1 mL) and lyophilized to a white fluffy power (87 mg, 84%). ^{1}H NMR ($CDCl_3$:DMSO-d_6 1:1, 500 MHz) δ 4.03 (br s, 1 H), 3.91 (d, J = 8.3 Hz, 1 H), 3.78 (br s, 1 H), 3.68 (br s, 1 H), 3.62 (d, J = 9.8 Hz, 1 H), 3.37 (s, 1 H), 2.59 (br s, 1 H), 1.79 (br s, 1 H), 1.70-1.15 (m, 50 H), 0.88 (m, 6 H); ^{13}C NMR ($CDCl_3$:DMSO-d_6 1:1, 125 MHz) δ 174.52, 77.42, 72.08, 71.48, 61.28, 53.61, 34.18, 33.79, 33.59, 31.43, 29.20, 29.07, 28.87, 25.67, 24.77, 22.21, 13.74; HRMS (ESI) *m/z* for $C_{32}H_{65}NNaO_4$ ([M+Na]$^+$) 550.48006 (100%), calc. 550.48058.

6.5 References

1) Hanada, K. *Jpn. J. Infect. Dis*. **2005**, *58*, 131.

2) Kundu, S. K. In *Glycoconjugates: Composition, Structure, and Function*; pp. 203-262; Allen, H. J.; Kisailus, E. C., Eds.; Marcel Dekker, Inc.: New York, NY, 1992.

3) Zhou, D.; Mattner, J.; Cantu, C., III; Schrantz, N.; Yin, N.; Gao, Y.; Sagiv, Y.; Hudspeth, K.; Wu, Y.-P.; Yamashita, T.; Teneberg, S.; Wang, D.; Proia, R. L.; Levery, S. B.; Savage, P. B.; Teyton, L.; Bendelac, A. *Science* **2004**, *306*, 1786.

4) Schrantz, N.; Teyton, L. The Scripps Research Institute, Department of Immunology, La Jolla, CA 92037; *unpublished observations*, 2005.

5) Wu, D.; Xing, G.-W.; Poles, M. A.; Horowitz, A.; Kinjo, Y.; Sullivan, B.; Bodmer-Narkevitch, V.; Plettenburg, O.; Kronenberg, M.; Tsuji, M.; Ho, D. D.; Wong, C.-H. *Proc. Nat. Acad. Sci. USA* **2005**, *102*, 1351.

6) (a) Natori, T.; Koezuka Y.; Higa, T. *Tetrahedron Lett*. **1993**, *34*, 5591. (b) Natori, T.; Morita, M.; Akimoto, K.; Koezuka, Y. *Tetrahedron* **1994**, *50*, 2771.

7) Motoki, K.; Kobayashi, E.; Uchida, T.; Fukushima, H.; Koezuka Y. *Bioorg. Med. Chem. Lett*. **1995**, *5*, 705.

8) Morita, M.; Motoki, K.; Akimoto, K.; Natori, T.; Sakai, T.; Sawa, E.; Yamaji, K.; Koezuka, Y.; Kobayashi, E.; Fukushima, H. *J. Med. Chem*. **1995**, *38*, 2176.

9) Zhou, X.-T.; Forestier, C.; Goff, R. D.; Li, C.; Teyton, L.; Bendelac, A.; Savage, P. B. *Org. Lett*. **2002**, *4*, 1267.

10) Miyamoto, K.; Miyake, S.; Yamamura, T. *Nature* **2001**, *413*, 531.

11) Goff, R. D.; Gao, Y.; Mattner, J.; Zhou, D.; Yin, N.; Cantu, C., III; Teyton, L.; Bendelac, A.; Savage, P. B. *J. Am. Chem. Soc*. **2004**, *126*, 13602.

12) Liu, Y.; Goff, R. D.; Zhou, D.; Mattner, J.; Sullivan, B. A.; Khurana, A.; Cantu, C., III; Ravkov, E. V.; Ibegbu, C. C.; Altman, J. D.; Teyton, L. T.; Bendelac, A.; Savage, P. B. *J. Immunol. Methods* **2006**, *312*, 34.

13) Kawahara, K.; Uchida, K.; Aida, K. *Biochim. Biophys. Acta*. **1982**, *712*, 571.

14) (a) Kawahara, K.; Seydel, U.; Matsuura, M.; Danbara, H.; Rietschel, E. T.; Zahringer, U. *FEBS Lett*. **1991**, *292*, 107. (b) Kawasaki, S.; Morigushi, R.; Sekiya, K.; Nakai, T.; Ono, E.; Kume, K.; Kawahara, K. *J. Bacteriol*. **1994**, *176*, 284. (c) Kawahara, K.; Kuraishi, H.; Zahringer, U. *J. Ind. Microbiol. Biotechnol*. **1999**, *23*, 408.

15) Naka, T.; Fujiwara, N.; Yabuuchi, E.; Doe, M.; Kobayashi, K.; Kato, Y.; Yano, I. *J. Bacteriol*. **2000**, *182*, 2660.

16) Kawahara, K.; Kubota, M.; Sato, N.; Tsuge, K.; Seto, Y. *FEMS Microbiol. Lett*. **2002**, *214*, 289.

17) Kawahara, K.; Moll, H.; Knirel, Y. A.; Seydel, U.; Zahringer, U. *Eur. J. Biochem*. **2000**, *267*, 1837.

18) Wittich, R.-M.; Wilkes, H.; Sinnwell, V.; Francke, W.; Fortnagel, P. *Appl. Environ. Microbiol*. **1992**, *58*, 1005.

19) Kawahara, K.; Mizuta, I.; Katabami, W.; Koizumi, M.; Wakayama, S. *Biosci. Biotech. Biochem*. **1994**, *58*, 600.

20) Cavicchioli, R.; Fegatella, F.; Ostrowski, M.; Eguchi, M.; Gottschal, J. *J. Ind. Microbiol. Biotechnol*. **1999**, *23*, 268.

21) (a) Morris, R. A.; Rappe, M. S.; Connon, S. A.; Vergin, K. L.; Siebold, W. A.; Carlson, C. A.; Giovannoni, S. J. *Nature* **2002**, *420*, 806. (b) Giovannoni, S. J.; Tripp, H. J.; Givan, S.; Podar, M.; Vergin, K. L.; Baptista, D.; Bibbs, L.; Eads, J.; Richardson, T. H.; Noordewier, M.; Rappe, M. S.; Short, J. M.; Carrington, J. C.; Mathur, E. J. *Science* **2005**, *309*, 1242.

22) Romanenko, L. A.; Uchino, M.; Falsen, E.; Frolova, G. M.; Zhukova, N. V.; Mikhailov, V. V. *Int. J. System. Evolution. Microbiol*. **2005**, *55*, 919.

23) Yabuuchi, E.; Yano, I.; Oyaizu, H.; Hashimoto, Y.; Ezaki, T.; Yamamoto, H. *Microbiol. Immunol*. **1990**, *34*, 99.

24) Hsueh, P. R.; Teng, L. J.; Yang, P. C.; Chen, Y. C.; Pan, H. J.; Ho, S. W.; Luh, K. T. *Clin. Infect. Dis*. **1998**, *26*, 676.

25) Selmi, C.; Balkwill, D. L.; Invernizzi, P.; Ansari, A. A.; Coppel, R. L.; Podda, M.; Leung, P. S.; Kenny, T. P.; Van De Water, J.; Nantz, M. H.; Kurth, M. J.; Gershwin, M. E. *Hepatology* **2003**, *38*, 1250-1257.

26) Shindo, M.; Mullin G. E.; Braun-Elwert, L.; Bergasa, N. V.; Jones, E. A.; James, S. P. *Clin. Exp. Immunol*. **1996**, *105*, 254.

27) Kita, H.; Naidenko, O. V.; Kronenberg, M.; Ansari, A. A.; Rogers, P.; He, X.-S.; Koning, F.; Mikayama, T.; Van De Water, J. ; Coppel, R. L.; Kaplan, M.; Gershwin, M. E. *Gastroenterology* **2002**, *123*, 1031.

28) Kinjo, Y.; Wu, D.; Kim, G.; Xing, G.-W.; Poles, M. A.; Ho, D. D.; Tsuji, M.; Kawahara, K.; Wong, C.-H.; Kronenberg, M. *Nature* **2005**, *434*, 520.

29) (a) Brigl, M.; Brenner, M. B. *Annu. Rev. Immunol*. **2004**, *22*, 817. (b) Hayakawa, Y.; Godfrey, D. I.; Smyth, M. J. *Curr. Med. Chem*. **2004** *11*, 241. (c) Kronenberg, M.; Gapin, L. *Nat. Rev. Immunol*. **2002**, *2*, 557.

30) Pier, G. B.; Lyczak, J. B.; Wetzler, L. M., Eds. *Immunology, Infection, and Immunity*; ASM Press: Washington, DC, 2004.

31) Savage, P. B.; Deng, S.; Long, X.; Yin, N.; Gao, Y.; Goff, R. D. Brigham Young University, Department of Chemistry and Biochemistry, Provo, UT 84602; *manuscript in preparation*, 2006.

32) Mattner, J.; DeBord, K. L.; Ismail, N.; Goff, R. D.; Cantu, C., III; Zhou, D.; Saint-Mezard, P.; Wang, V.; Gao, Y.; Yin, N.; Hoebe, K.; Schneewind, O.; Walker, D.; Beutler, B.; Teyton, L.; Bendelac, A.; Savage, P. B. *Nature* **2005**, *343*, 525. Figures 6.7-6.12 are adapted by permission, Copyright 2005 Macmillan Publishers Ltd.

33) Lin, H.-K.; Gelb, M. H. *J. Am. Chem. Soc*. **1993**, *115*, 3932.

34) Hoffman, R. V.; Tao, J. *J. Org. Chem*. **1998**, *63*, 3979.

35) So, R. C.; Ndonye, R.; Izmirian, D. P.; Richardson, S. K.; Guerrera, R. L.; Howell, A. R. *J. Org. Chem*. **2004**, *69*, 3233.

36) Hanessian, S.; Banoub, J. *Methods Carbohydr. Chem*. **1980**, *8*, 247.

37) (a) Van Boeckel, C. A. A.; Beetz, T.; Kock-Van Dalen, A. C.; Van Bekkum, H *Recl. Trav. Chim. Pays-Bas* **1987**, *106*, 596. (b) Schmidt, F.; Monneret, C. *J. Chem. Soc., Perkin Trans. 1* **2002**, *10*, 1302.

38) Garegg, P. J.; Olsson, L.; Oscarson, S. *J. Org. Chem*. **1995**, *60*, 2200.

39) Yin, N. Part II: Synthesis of Glycosphingolipids to Study Natural Killer T Cell Stimulation. Ph.D. Dissertation, Brigham Young University, Provo, UT, 2004.

40) Nicolaou, K. C.; Li, J.; Zenke, G. *Helv. Chim. Acta* **2000**, *83*, 1977.

41) Lin, M.; Rikihisa, Y. *Infect. Immun*. **2003**, *71*, 5324.

42) Brigl, M.; Bry, L.; Kent, S. C.; Gumperz, J. E.; Brenner, M. B. *Nature Immunol*. **2003**, *4*, 1230.

43) Takeuci, M.; Hamana, K.; Hiraishi A. *Int. J. System. Evolution. Microbiol*. **2001**, *51*, 1405.

44) Trivedi, O. A.; Bendelac, A. University of Chicago, Department of Pathology, Chicago, IL 60637; *unpublished observations*, 2006.

45) Wu, D.; Zajonc, D. M.; Fujio, M.; Sullivan, B. A.; Kinjo, Y.; Kronenberg, M.; Wilson, I. A.; Wong, C.-H. *Proc. Nat. Acad. Sci. USA* **2006**, *103*, 3972.

CHAPTER 7.

ISOLATION AND CHARACTERIZATION OF A GLYCOSPHINGOLIPID FROM THE ALPHA-PROTEOBACTERIUM *EHRLICHIA MURIS*

7.1 Introduction

The etiology of disease is a vital segment of medical research because it provides investigators with knowledge of how maladies are originated, whether it be from an external source, such as viruses or parasites, or innately-derived from the affected organism. When exogenous pathogens are involved, it is often more facile to diagnose the cause of disease (e.g., identification of an infectious bacteria) than to discover the root mechanism.[1] In other words, determining the type of communicable organism and recognizing the resulting symptoms may be routine, but understanding the specific means by which the organism causes disease requires a more in-depth analysis. For example, cystic fibrosis patients are notoriously infected with *Pseudomonas aeruginosa* during later stages of the disease. In the early period of research on cystic fibrosis it was found that bacterial infections were often the ultimate cause of death, yet it took several years of research to discover how the bacteria was contributing to the mortality of afflicted individuals.[2]

Likewise, Gram-negative *Sphingomonas* bacteria, a causative agent of primary biliary cirrhosis,[3] had been scrutinized for decades before it was recognized that they do not express the archetypical lipopolysaccharide (LPS) antigen, but rather glycosphingolipids.[4] It even took several years after this discovery to recognize that through these membranous compounds, *Sphingomonas spp*. are able to cause an

inflammatory host defense response directly via CD1d-mediated presentation to natural killer T cells,[5] rather than the typical immune reaction involving LPS binding to Toll-like receptor 4 on antigen presenting cells.[1] The magnitude of this finding is significant because it represents the first identified group of exogenous glycosphingolipids from bacteria that cause direct stimulation of NKT cells through CD1d-restriction. Furthermore, it has been shown that the immune response against *Sphingomonas* is of a high magnitude because these bacterial GSLs induce secretion of the T_H1-type cytokine IFN-γ in quantities equivalent to those when the model synthetic antigen αGalCer is used (see Chapter 6, section 6.2).

Due to the direct antigenic behavior of *Sphingomonas capsulata* on NKT cells, it was desired to identify other bacteria that were involved in the same type of activating mechanism. An initial literature search using other alpha-proteobacteria as the general pool for potential candidates[6] led to the realization that there are a number of similarly classified microbes that do not express LPS[7] and/or that CD1 proteins are involved with host defense response against said organisms.[8] One of the alpha-proteobacterial families that was lacking in LPS and Lipid A expression is Ehrlichiaceae, a member of the class of Rickettsiales. Like many other Rickettsiales, *Ehrlichia spp*. are obligate intracellular bacteria and must grow inside host eukaryotic cells to survive. *Ehrlichia* are the causative organisms for ehrlichiosis, a tick-borne disease that largely affects canines (*E. canis*), cattle (*E. ruminatium*), sheep (*E. ovina*), and horses (*Neorickettsia risticii*). Humans can also be infected by *Ehrlichia chaffeensis* and *Anaplasma phagocytophilum*, the agents responsible for human monocytic ehrlichiosis and human granulocytic ehrlichiosis, respectively.[9] These diseases cause severe flu-like symptoms that often

require hospitalization and may result in death (3% fatality rate, often due to misdiagnosis), but can be treated with tetracycline antibiotics like doxycycline.[7]

Ehrlichia muris is a mildly virulent species that affects rodents and is often used as a model of other *Ehrlichia* due to the widespread availability of knockout (KO) mice. In these KO murine models, immunodeficient individuals are often subject to persistent infection due to their inability to clear the bacteria from infected host cells.[10] As was reported in Chapter 6 (see Figures 6.9, 6.11, and 6.12), the immune response in humans and mice to heat-killed *E. muris* is CD1d-dependent and does not follow the mechanistic pathway used to clear LPS-positive microbes, like *Salmonella typhimurium*.[5] It has been reported that in an animal model of fatal monocytotropic ehrlichiosis, mice with subnormal levels of $CD4^+$ cells, which include T_H1 and NKT cells, have downregulated quantities of IFN-γ in the spleen. Transplantation of IFN-γ-producing cells, however, protected infected subjects from *Ehrlichia*-derived *ixodes ovatus* ticks.[11] Further research into the infectious behavior of *E. muris* found that it causes murine NKT cells to secrete IFN-γ as analyzed by flow cytometry (Figure 7.1A). In KO mice lacking CD1d, *E. muris* is approximately ten times more populous in spleen cells than in $CD1d^{+/-}$ subjects up to seven days after infection, thus demonstrating the dependence on CD1d to activate NKT cells for bacterial clearance of *Ehrlichia*

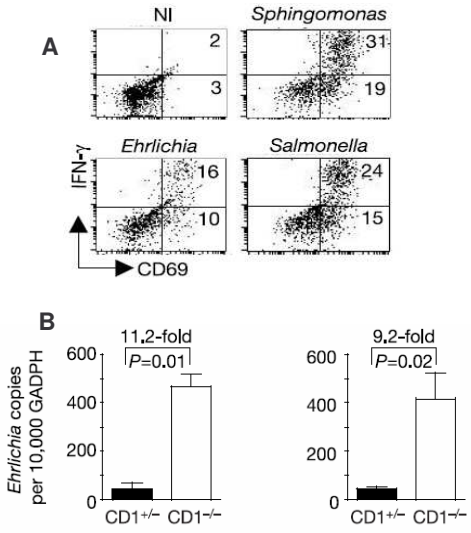

Figure 7.1. **A**. In Vivo Activaton of NKT Cells by Heat-Killed Bacteria.[5] **B**. Bacterial Clearance of *E. muris* at 2 d (Left) and 7 d (Right) in $CD1d^{+/-}$ and $CD1d^{-/-}$ Mice.[5]

(Figure 7.1B).[5] Thus, *E. muris* was deemed to be a likely candidate to display glycosphingolipids due to the CD1d-mediated defense mechanism against it in the immune systems of host organisms.

To probe the extent of glycosphingolipid expression in bacteria, *E. muris* and two other species, *Borrelia burgdorferi* (ATCC 35210) and *Brucella neotomae* (ATCC 23459), were scrutinized due to the following reasons:

1) *E. muris* – The lack of LPS and host-dependence on NKT cells for clearance, as with LPS$^-$ *Sphingomonas spp*., demonstrates that its antigenic activity is likely due to glycosphingolipid expression.

2) *B. burgdorferi* – Like *E. muris*, *B. burgdorferi* is a tick-borne bacterium and is the etiological bacteria of Lyme's disease. It also lacks LPS[12] and has been reported to cause autoimmunity problems in mice lacking CD1d.[8]

3) *B. neotomae* – A non-Rickettsiales alpha-proteobacteria expressing LPS that was used as a control to gauge CD1d-restricted activity.[13]

From this study, evidence of a glycosphingolipid from *E. muris* was obtained and a putative structure has been proposed.

7.2 Results and Discussion

Unlike *E. muris*, *B. burgdorferi* and *B. neotomae* are not obligate intracellular bacteria and do not require incubation inside eukaryotic cells and specialized techniques for purification from host material; they can be grown using fairly simple microbiological techniques. Before extraction of glycosphingolipids was attempted, heat-killed portions of these two bacteria were assayed for stimulatory activity. *B. burgdorferi* ($5x10^6$) was found to lack the ability to cause IL-2 secretion in a murine DN32 hybridoma in the

presence of dendritic cells, though it did induce modest IFN-γ production in human NKT cells (Figure 7.2). *B. neotomae* ($5x10^6$) also was able to influence the same amount of IFN-γ production, yet caused a much greater amount of IL-2 to be made than *B. burgdorferi*. However, in comparison to αGalCer (100 ng/mL), *S. capsulata*, and *E. muris* the quantities of cytokines induced by these two bacteria were significantly lower (see Chapter 6, Figure 6.9).

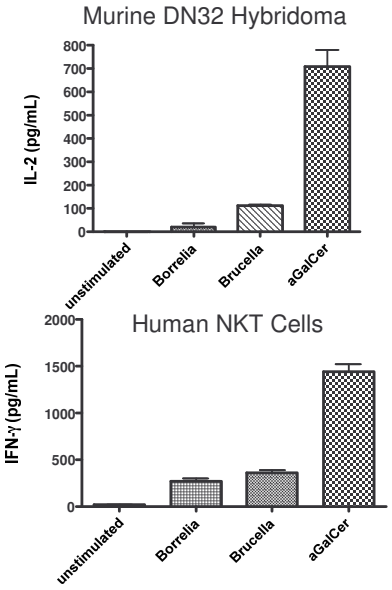

Figure 7.2. Comparison of Heat-Killed Bacteria ($5x10^6$)to αGalCer for NKT Cell Stimulatory Activity.

Because it was more facile to grow than the other two microbes, *B. burgdorferi* was examined initially, although it had a lesser capacity to cause cytokine release in NKT cells. It was originally planned to attempt an extraction of GSLs, but a recent paper reported the discovery of two different glycolipid compounds (**7-1a** and **7-1b**), comprising at least one-third of the total lipid mass of *B. burgdorferi* (Figure 7.3).[14]

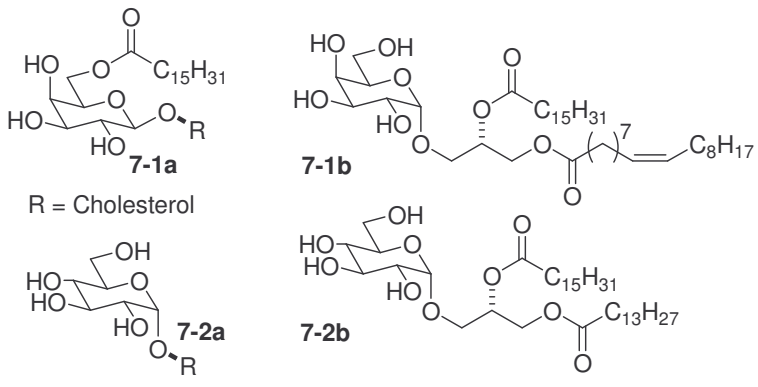

Figure 7.3. Natural (**7-1**) and Synthetic (**7-2**) Glycolipids of *Borrelia burgdorferi*.[14]

Synthetic analogs of **7-1a** (**7-2a**) and **7-1b** (**7-2b**) were devoid of any CD1d-restricted stimulatory activity on both hVα24i and mVα24i cell populations, however. This result,

coupled with the finding that *B. burgdorferi* has scant antigenic activity of NKT cells, prompted research on this species to be halted.

Brucella neotomae was then scrutinized for GSL content. Glycolipid extraction was performed as previously described by Kawahara and Zahringer (see Chapter 6, section 6.4),[15] which yielded five compounds that were separable by silica gel using a Pasteur pipette microcolumn. Following purification, the fractions were analyzed by ^{1}H NMR and appraised for signals representative of glycosphingolipids. Because of the minute quantities of extractable material (approximately 0.25-1 mg from 3 L of inoculated broth), lyophilization was required to remove water, which often obscured the 3-4 ppm region using 99.96% DMSO-d_6 solvent even with peak suppression.

In the spectra of these various unknown compounds, a large peak at 1.26 ppm, representing one or multiple long chain alkyl groups, and a triplet at 0.88 ppm (J = 6.8 Hz), due to one or more alkyl methyl radicals, were typically found. Also, a triplet at 2.16 ppm (J = 7.3 Hz), which is representative of methylene protons proximal to a carbonyl group, is universally seen. Other commonly-found features are peaks near 5.3 ppm and 2.0 ppm that indicate the presence of alkenyl and allyl protons, respectively, though these signals did not integrate to the same ratio as those from the alkyl peaks. Other signals due to sphingoid bases (m, dd, td, or tt, 3-5 ppm) and amide protons (d, 7.4-7.8 ppm) were lacking. There were some peaks in the 3-4 ppm range that could have been due to a saccharide and a doublet of comparable intensity at 5.6 ppm from an anomeric proton, but treatment of the compounds with potassium hydroxide resulted in hydrolysis with one of the resulting fractions appearing to be a long-chain fatty acid. It is likely that the compounds isolated from *B. neotomae* were diacylglycerols, glycolipids

frequently encountered in cellular membranes, or LPS, which is known to be expressed by this organism.[13] An assay of all the isolated bacterial fractions measuring CD1d-restricted cytokine production by NKT cells indicated that CD1d was necessary for an immune response in four of the five *B. neotomae* components, yet this is also seen in LPS-bearing bacteria like *Salmonella* (Figure 7.4).[5] For a more specific response, KO mice lacking the TLR 4 MyD88 protein or Hexb$^{-/-}$ mice could be used to indicate if these compounds are causing stimulation of NKT cells through the indirect LPS pathway (see Chapter 6, section 6.2). However, due to the small stimulatory capability of these fractions and that ^{1}H NMR evidence was not present to support the existence of GSLs in *Brucella neotomae*, further studies of this bacterium were not pursued.

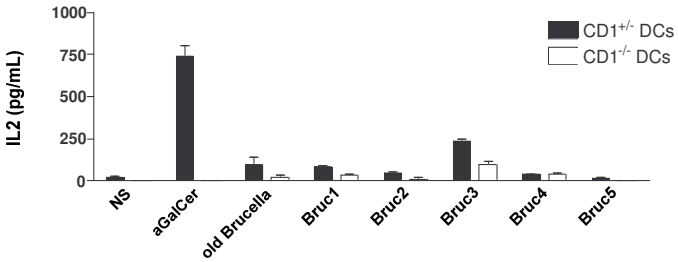

Figure 7.4. CD1d-Restricted Activity of *Brucella neotomae* Fractions on Murine NKT Cells.

Attention was then turned to *Ehrlichia muris*, which was supplied by the Walker research group from the University of Texas Medical Branch.[11] As with previous bacterial samples, *E. muris* was subjected to the same procedure to extract any existing glycosphingolipids. From the crude material, eleven spots were visualized by TLC and after microcolumn chromatography nine separate fractions were able to be isolated with masses generally ranging from 0.2-1.2 mg from the original 200 mg sample of freeze-dried bacterial solids. A comparison of TLCs between *Sphingomonas capsulata* and *Ehrlichia muris* using eluent described by Zahringer and coworkers ($CHCl_3$:MeOH:HOAc:H_2O 25:14:4:2)[15] yielded a match in an R_f value (0.48) between an

E. muris fraction and GSL-1A, a compound isolated from *S. capsulata* (see Chapter 6, section 6.1).

The individual samples were lyophilized to minimize interference from water and analyzed by ^{1}H NMR, as was done with previous bacterial compounds, to locate any potential GSL candidates. In general, the isolated fractions did not have the proper signal integration ratio between alkyl peaks (0.9-2.0 ppm) and downfield proton peaks (3-5 ppm) that are inherent in GSLs. Only one fraction, designated **Em3**, seemed to be a viable contender. Its ^{1}H NMR spectrum contained intense alkyl peaks at 1.46, 1.23, and 0.85 ppm from one or more long chains and also signals indicating the presence of multiple double bonds at 5.32, 2.73, and 2.01 ppm for alkenyl, diallyl, and allyl groups, respectively. Also present in the spectrum were a doublet at 7.60 ppm for an amide proton, a triplet at 2.06 ppm for an α-methylene carbonyl group, and several doublets

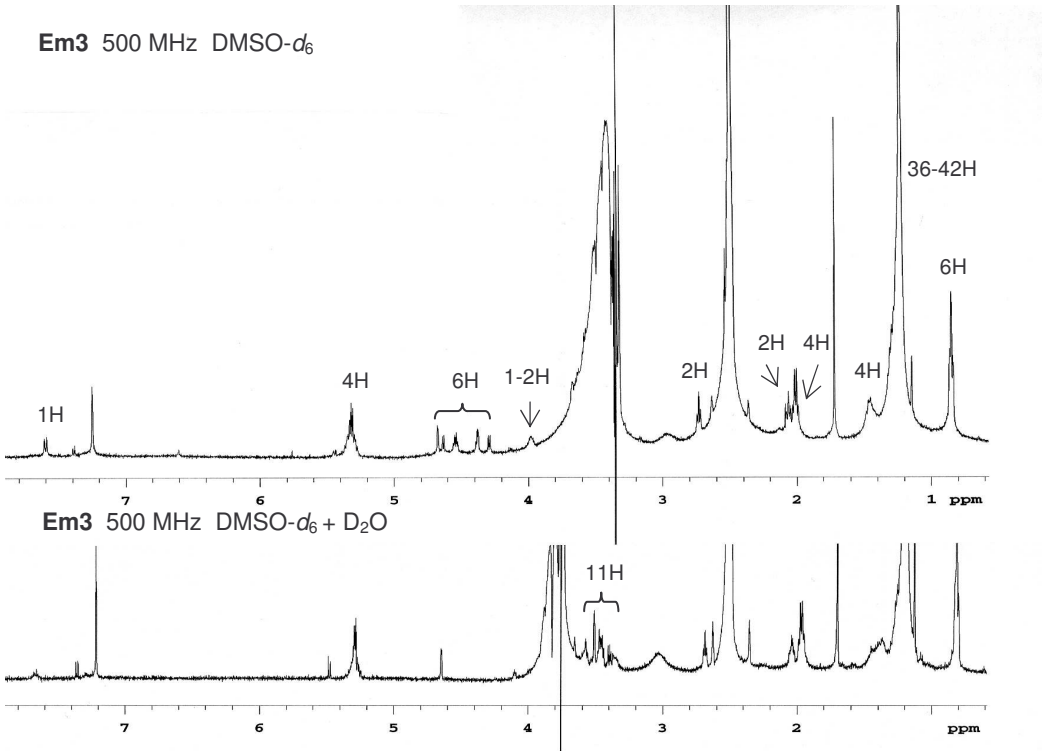

Figure 7.5. ^{1}H NMR Spectral Comparison of **Em3** Before and After Deuterium Exchange.

from 4.3 to 4.7 ppm that are commonly found in nonaggregated NMR samples of GSLs in deuterated pyridine or DMSO (Figure 7.5, top).

Although water suppression was done, there was still an appreciable peak that blocked any signals in the region where non-anomeric saccharide protons would appear (3.3-3.8 ppm). To shift the water peak from that area and uncover any hidden peaks, D_2O was added to the sample. Four groups of multiplets from 3.4-3.6 ppm were made visible that, when compared to the integration of other peaks, had an area equivalent to 11 protons. In addition, the four peaks representing five protons from 4.3 to 4.7 ppm and the amide proton at 7.60 ppm were eliminated due to deuterium exchange (Figure 7.5, bottom). The nonexchangeable polar protons, excluding those arising from an alkene system, totaled twelve, the number expected to be found in a phytosphingosine-containing monoglycosylsphigolipid (Table 7.1). Unfortunately, because of the scant quantity of material (1.29 mg), a useful ^{13}C NMR spectrum could not be obtained.

^1H Type[a]	Chemical shift (ppm)	Splitting pattern (Hz)	Integration[d]	D_2O exchange
Amide	7.60[b]	d, J = 8.7	1	Yes
Alkenyl	5.35-5.29[b]	m	4	No
Anomeric (α)	4.67[b]	d, J = 2.9	1	No
Hydroxyl	4.63[b]	d, J = 6.3	1	Yes
Hydroxyl	4.55-4.53[b]	m	2	Yes
Hydroxyl	4.38[b]	d, J = 3.9	1	Yes
Hydroxyl	4.29[b]	d, J = 7.3	1	Yes
Unknown	3.98[b]	m	1-2	Unknown[e]
Unknown	3.66[c]	br s	1	No
Unknown	3.59-3.54[c]	m	2	No
Unknown	3.53-3.43[c]	m	5	No
Unknown	3.41-3.39[c]	m	2	No
Unknown	3.37-3.34[c]	m	1	No
Diallyl	2.73[b]	t, J = 6.3	2	No
-COCH_2-	2.06[b]	t, J = 7.3	2	No
Allyl	2.01[b]	dt, J = 6.8, 6.3	4	No
Alkyl	1.50-1.40[b]	m	4	No
Alkyl	1.23[b]	br s	36-42	No
Methyl	0.85[b]	m	6	No

[a]As compared with ^1H NMR spectra of characterized synthetic glycosphingolipids.
[b]500 MHz, DMSO-d_6. [c]500 MHz, DMSO-d_6+D_2O.
[d]Integration of alkyl groups were done in a separate ratio due to baseline elevation.
[e]Water peak shift due to D_2O addition obscured this signal.

Table 7.1. Identifiable Signals from *Ehrlichia muris* Compound **Em3**.

The sample of **Em3** was then analyzed by mass spectrometry (MS) to identify the mass peak and attempt to ascertain the molecular formula. A fast atom bombardment (FAB) technique found the base peak to have a mass of 792.5897 m/z. By instructing the MS analysis software to identify candidates with zero or one nitrogen, one to ten oxygens, and zero to two sodium atoms, the two best-fit molecular formulas with the lowest deviation were $C_{51}H_{79}NNaO_4$ (-1.0 mmu) and $C_{44}H_{83}NNaO_9$ (-6.8 mmu). The latter formula was more likely to fit with that of a GSL due to the number of oxygen atoms (nine are found in αGalCer) and the double bond equivalents (thirteen and four, respectively). Using electrospray ionization (ESI) mass spectrometry with a software method to search for a compound of known formula, a measured mass peak at 770.61320 m/z was attributed to a mass of $C_{44}H_{84}NO_9$ ($[M+H]^+$, calc. 770.61406 m/z), which differed by 0.00086 mmu.

From these mass spectrometry and ^1H NMR data, a partial structure was proposed (Figure 7.6). The deuterium-exchangeable peaks at 4.3 to 4.7, representing at least five different protons are likely from a saccharide and sphingoid base. These types of peaks, along with there splitting patterns, have been seen in several synthetic compounds such as αGalCer, **3-3b**, and **3-4**. The doublet at 4.67 ppm appears to be from an anomeric proton and the smaller splitting constant (J = 2.9 Hz) would be expected from an axial-equatorial relationship to the proximal proton, as what is seen in α-anomers of galactosides and glucosides. If seven carbons are assigned to a monosaccharide and eighteen for the typical length of a sphingoid base, then twenty are left for an amide, which is present due to the amide proton at 7.60 ppm, α-methylene

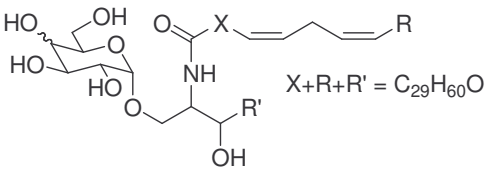

Figure 7.6. Initial Proposed Structure of **Em3.**

group at 2.06 ppm, and odd-numbered molecular formula for one nitrogen atom. The eicosanoids, a group of C20 fatty acids, are common in biological systems and are precursors in the production of prostaglandins, thromboxanes, and leukotrienes.[16] The integration of 4:2:4 (2:1:2) of alkenyl-derived signals at 5.32, 2.73, and 2.01 ppm indicate the presence of a 1,4-diene, something that would be novel if found on a sphingoid base yet is a group seen in the eicosenoic acids, like arachidonic acid. The number of double bond equivalents remaining, if two are used for the diene, is two: one for a saccharide ring and one for a carbonyl pi bond, which also fits with the ^{1}H NMR evidence.

Lacking from this information is evidence showing the type of sphingoid base and saccharide and the location of the double bond in the putative ceramide of **Em3**. It is likely that the mammalian sphingosine base can be disqualified as a potential structure due to the lack of the characteristic splitting pattern arising from the *E*-alkene. From the number of oxygen atoms in the molecular formula, the likelihood of phytosphingosine being present is high, although sphinganine could be in the compound along with a hydroxyl group on the amide chain. This latter possibility is not likely to be the case due to hydroxylation occurring at the C2' position on other natural glycosphingolipids, such as the agelasphins,[17] the plakosides,[18] and the Sphingomonas GSLs,[15] and that the putative C2' carbon has two protons attached to it (triplet at 2.06 ppm).

To help clarify these unknown details, which were largely due to the multiplet nature of the NMR proton signals from 3.3 to 3.7 ppm, a fraction of **Em3** (0.54 mg) was peracetlyated using acetic anhydride, DMAP, and Et_3N. After purification of peracetyl **Em3** (**Em3OAc**), the obtained ^{1}H NMR spectra resolved many of the polar proton peaks from each other for more accurate integration. It was also found that six distinct singlets

around 2.0 ppm were present, indicating six acetate groups or rather six hydroxides in the original **Em3** compound. From this spectrum the apparent anomeric proton doublet was pushed downfield to 5.45 ppm, having a coupling constant of 3.4 Hz. Another doublet with the *J* value of 3.4 Hz at 4.90 ppm was identified.

In the 3-5 ppm region, other peaks with splitting patterns distinctive of glycosphingolipids were seen, so a ^{1}H NMR comparison of several synthetic compounds was performed to aid in peak identification. The molecule with the greatest similarity to **Em3** was **4-2a**, an eicosadieneoyl compound (see Chapter 4). Comparison of the FAB-MS data of **Em3** to **4-2a** ($[M+Na]^+$, 792.5969 m/z) showed that they have the same molecular formula. Their ^{1}H NMR spectra also share many similarities (Figure 7.7). A peracetylated sample of **4-2a** (**7-3**, structure on following page) was compared with that of **Em3OAc** and the signals were correlated according to chemical shift, splitting pattern, and integration (Figure 7.8). From this comparison, more evidence was gleaned to clarify the structure of **Em3** (Table 7.2).

	Chemical shift (ppm)[a]		Splitting pattern (Hz)		Integration	
7-3 Proton	**7-3**	**Em3OAc**	**7-3**	**Em3OAc**	**7-3**	**Em3OAc**
Amide	6.34	6.45	d, *J* = 9.8	br s	1	1
H1”	5.45	5.45	d, *J* = 2.9	d, *J* = 3.4	1	1
Alkenyl	5.41-5.33		m		4	
H2”	5.31	5.38-5.26[b]	m	m[b]	1	6[b]
H3	5.27		dd, *J* = 10.3, 2.4		1	
H3”	5.14	5.14	dd, *J* = 10.7, 3.4	dd, *J* = 10.7, 3.4	1	1
H4”	4.90	4.90	d, *J* = 3.4	d, *J* = 3.4	1	1
H4	4.87	4.87	dt, *J* = 9.3, 2.4	m	1	1
H2	4.37	4.37	tt, *J* = 9.8, 2.4	t, *J* = 9.8	1	1
H5”	4.13-4.09	4.13-4.09	m	m	2	2
H6”	4.05-4.01	4.05-4.01	m	m	1	1
$H1_A$	3.66	3.67-3.62	dd, *J* = 10.7, 2.4	m	1	Unknown[c]
$H1_B$	3.40	3.41-3.39	dd, *J* = 10.7, 2.4	m	1	Unknown[c]
H13’	2.77	2.77	t, *J* = 6.8	t, *J* = 6.3	2	2

[a]500 MHz, $CDCl_3$.
[b]Includes the alkenyl, H2”, and H3 peaks.
[b]These peaks were obscured by a broad peak from 3.78-3.30 ppm.

Table 7.2. Comparison of ^{1}H NMR Signals of **7-3** to **Em3OAc**.

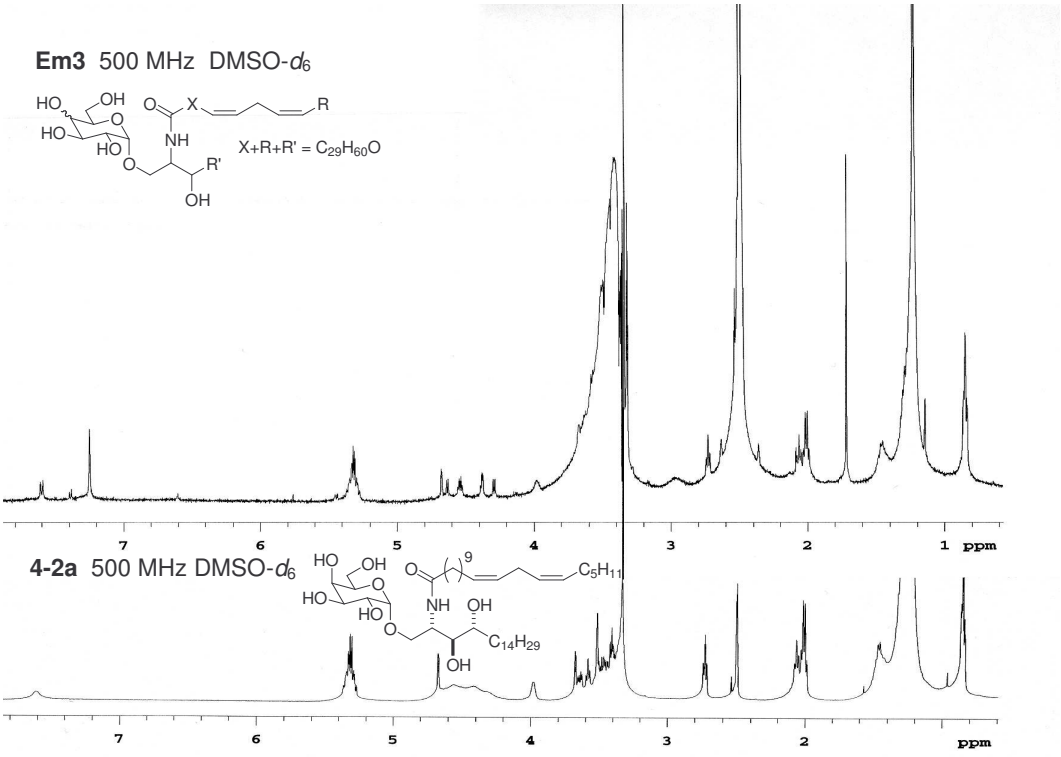

Figure 7.7. ^{1}H NMR Spectral Comparison of **Em3** and Glycosphingolipid **4-2a**.

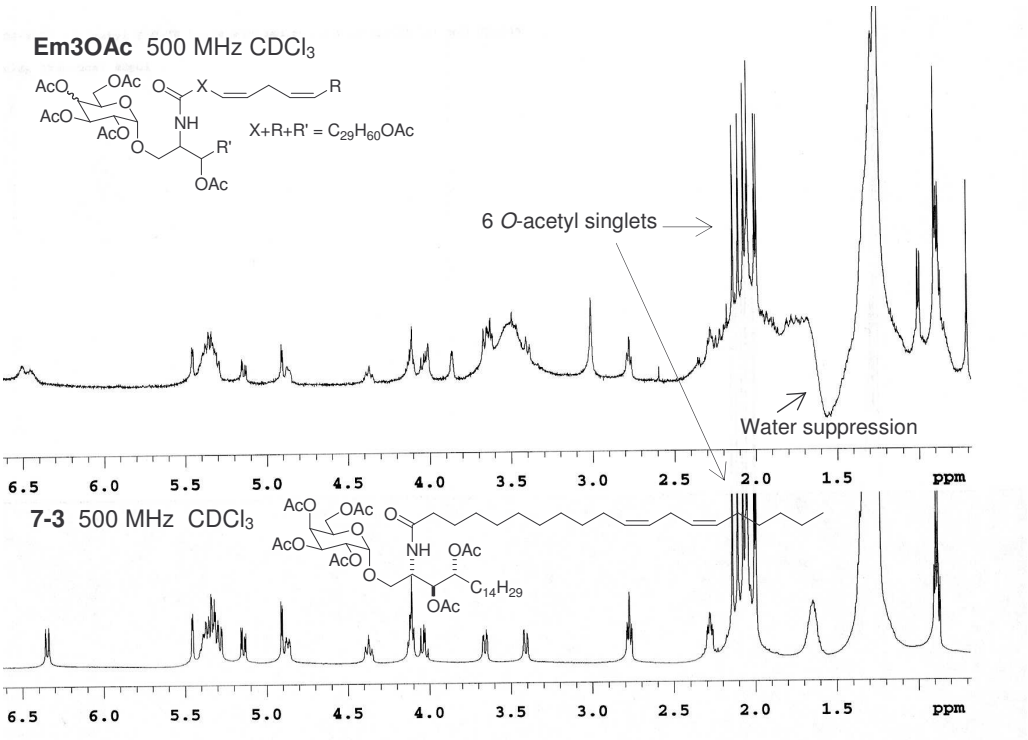

Figure 7.8. ^{1}H NMR Spectral Comparison of Peracetates **Em3OAc** and **7-3**.

The apparent triplet of triplets pattern of the signal at 4.37 ppm is evident in **Em3OAc**, yet only the larger coupling constant can be discerned. This arises from the H2 proton that is split by the amide proton and the diastereotopic protons $H1_A$ and $H1_B$, yet coupling was not observed with H3. The correlation of the peak at 4.87 ppm, which is a doublet of triplets in **7-3** for H4, provides further evidence that the long chain base in **Em3** is phytosphingosine (Figure 7.9).

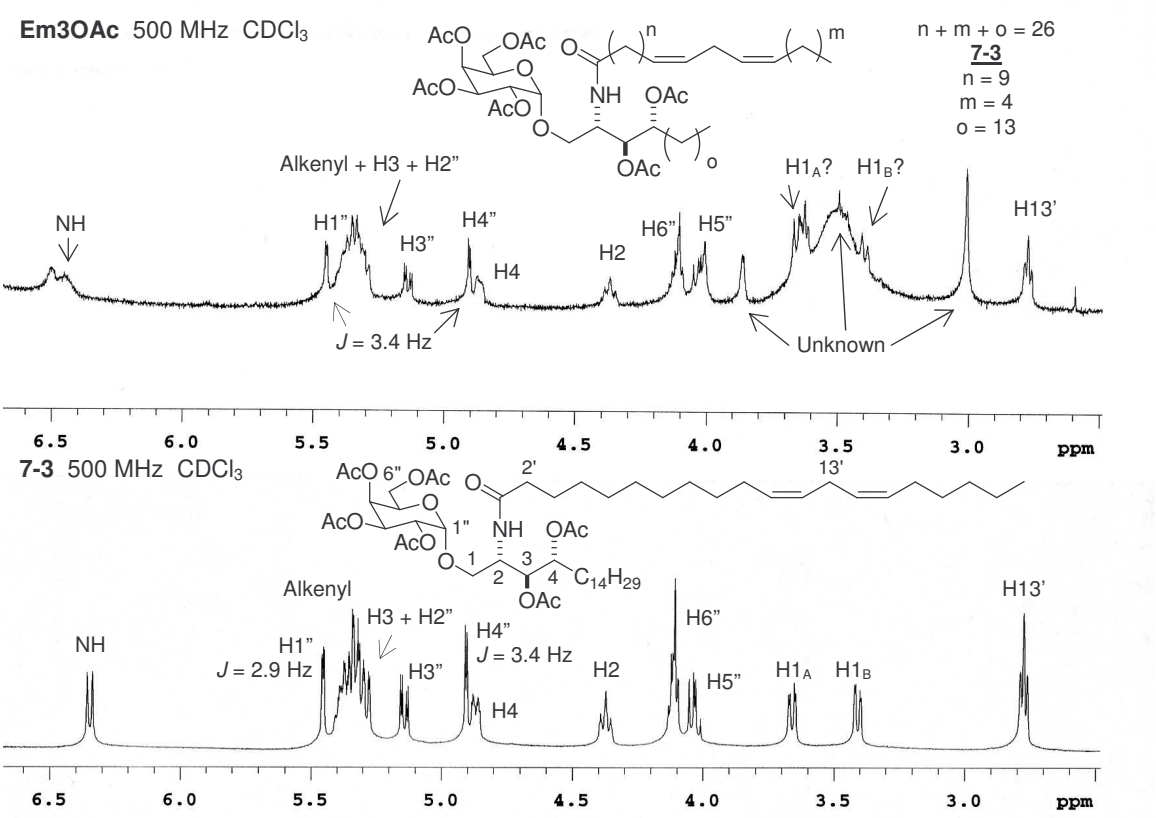

Figure 7.9. Comparison of Downfield ^{1}H NMR Signals of **Em3OAc** and **7-3**.

The saccharide present in **Em3** is likely to be galactose with an α-anomeric bond to the ceramide. The anomeric proton is clearly visible as a doublet at 5.45 ppm, in **Em3OAc**, with the 3.4 Hz coupling value indicating an axial-equatorial relationship to H2". This splitting could be possible with a β-mannoside, but mannosylceramides have been found not to stimulate mVα14i NKT cells[19] and, as will be discussed below, **Em3**

was found to be antigenic to this cell line. The doublet at 4.90 ppm is the H4" proton of the saccharide of **Em3OAc**, as determined by comparison to the analogous signal in the ^{1}H NMR spectrum of **7-3**. Like H1", the *J* value of 3.4 Hz suggests an axial-equatorial relationship with a proximal proton, H3", which occurs in galactose and not glucose.

Non-spectral analysis of these peracetylated derivatives gave further affirmation of the close structural relationship between **Em3** and **4-2a**. Assay by ESI-MS showed that the peracetates both likely share the same molecular formula ($C_{56}H_{95}NO_{15}$), as the intense peaks at 1022.67660 m/z for **Em3OAc** and 1022.67756 m/z for **7-3** (calc. 1022.67745 m/z) are equivalent in mass. A TLC comparison in 1:3 EtOAc:Hexanes showed that they coelute at an R_f value of 0.38.

Although these data establish several correlations that can be used to identify the structure of **Em3**, the location of the 1,4-diene has yet to be determined. It is possible that this functional group is present in the terminus of the sphingoid base, but this seems unlikely as 1,4-diene-containing eicosenoic acids can be found free and unincorporated in mammalian cells[20] and are available for incorporation into cellular membranous compounds of obligate intracellular bacteria, such as *Ehrlichia muris*. Other alpha-proteobacteria (e.g., *Sphingomonas spp*., *Caulobacter spp*.) have been found to change the fatty acid composition of their outer leaflet due to environmental conditions,[21] so it is likely that *E. muris* will do the same to adapt and thrive in its eukaryotic surroundings. Thus, there is a greater probability that the fatty acid portion contains this structural feature.

Unfortunately, due to the small amount of available **Em3** and the difficulty of growing *Ehlrichia muris* in vitro, the quantitiy of material was not sufficient to use for

further structural analysis. Subsequent characterization could be performed using techniques described by Kawahara et al. in the analysis of the *Sphingomonas* GSLs.[15] To verify the location of the diene in **Em3**, basic hydrolysis could easily be performed to separate the amide moiety from the rest of the molecule. Derivatization using diazomethane followed by NMR characterization would be able to verify if the unsaturation is present in the amide or sphingoid base. Determining the exact position of the 1,4-diene in the amide chain could then be accomplished by GCMS or GLCMS analysis using methyl esters of known fatty acids. This procedure should also be able to verify the geometry of the diene, whether it is *Z* or *E*, though by far most natural unsaturated fatty acids have the cis configuration.[22] Likewise, if the alkene was found to be incorporated into the sphingoid base, a nicotinate derivative could be made and fractionated by electron ionization or chemical ionization MS techniques to find the location of the diene.

Aliquots of each of the nine isolated compounds were submitted to collaborators in the Bendelac research group at the University of Chicago. The materials (1 μg each) were coadministered with both $CD1d^{+/-}$ and $CD1d^{-/-}$ dendritic cells to a murine DN32 Vα14i NKT cell hybridoma and the quantity of IL-2 cytokine was measured. In comparison to αGalCer, all nine fractions had less than 50% of the stimulatory capacity, yet **Em3** had the greatest activity by far of the *E. muris* compounds. Another fraction, **Em2**, that was more nonpolar than **Em3** as seen by TLC, also induced a significant amount of IL-2 production over the other compounds (Figure 7.10).

The ^{1}H NMR of **Em2** was reexamined to identify any features that could possibly explain the activity. It was found that like **Em3**, there were signals indicative of a

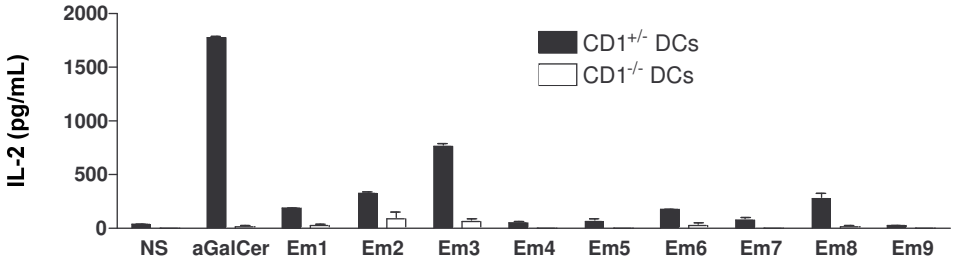

Figure 7.10. CD1d-Restricted Murine NKT Cell Activity of *Ehrlichia muris* Compounds.

polyalkene, such as a 1,4-diene. Three multiplets centered at 5.32, 2.77, and 2.00 ppm had the integration ratio of 2:1:2, the same as the alkenyl:diallyl:allyl proportion from the ^{1}H NMR spectrum of **Em3**. Comparison with the spectrum of (11*Z*,18*Z*)-eicosadienoic acid (**7-4**, structure on following page) shows that **Em2** likely contains the acid component of the ceramide of **Em3**, though the fraction is possibly composed of at least one other lipid compound (Table 7.3). Differences in the integration of the alkenyl peaks to those from the alkyl chain (e.g., 2.18, 1.47, 1.26, 0.85 ppm) can be due to other carboxylic acids, which often run concurrently on TLC plates (Figure 7.11). The presence of this alkenoic acid gives further credence to the premise of the diene being located on the amide chain rather than the sphingoid base of **Em3**.

	Chemical shift (ppm)		Splitting pattern (Hz)		Integration	
7-4 Proton	**7-4**[a]	**Em2**[b]	**7-4**	**Em2**	**7-4**	**Em2**[c]
Alkenyl	5.40-5.32	5.37-5.29	m	m	4	2
Diallyl	2.78	2.82-2.72	t, J = 6.8	m	2	1
-COCH_2-	2.35	2.18	t, J = 7.8	t, J = 7.8	2	---
Allyl	2.05	2.09-1.95	dt, J = 7.3, 6.8	m	2	2
Alkyl	1.63	1.50-1.40	quintet, J = 7.3	m	2	---
Alkyl chain	1.28	1.26	br s	br s	18	---
Methyl	0.89	0.85	t, J = 6.8	t, J = 6.8	3	---

[a]500 MHz, $CDCl_3$. [b]500 MHz, DMSO-d_6.
[c]Alkyl peaks did not have a consistent integration ratio.

Table 7.3. Comparison of ^{1}H NMR Signals of **7-4** to **Em2**.

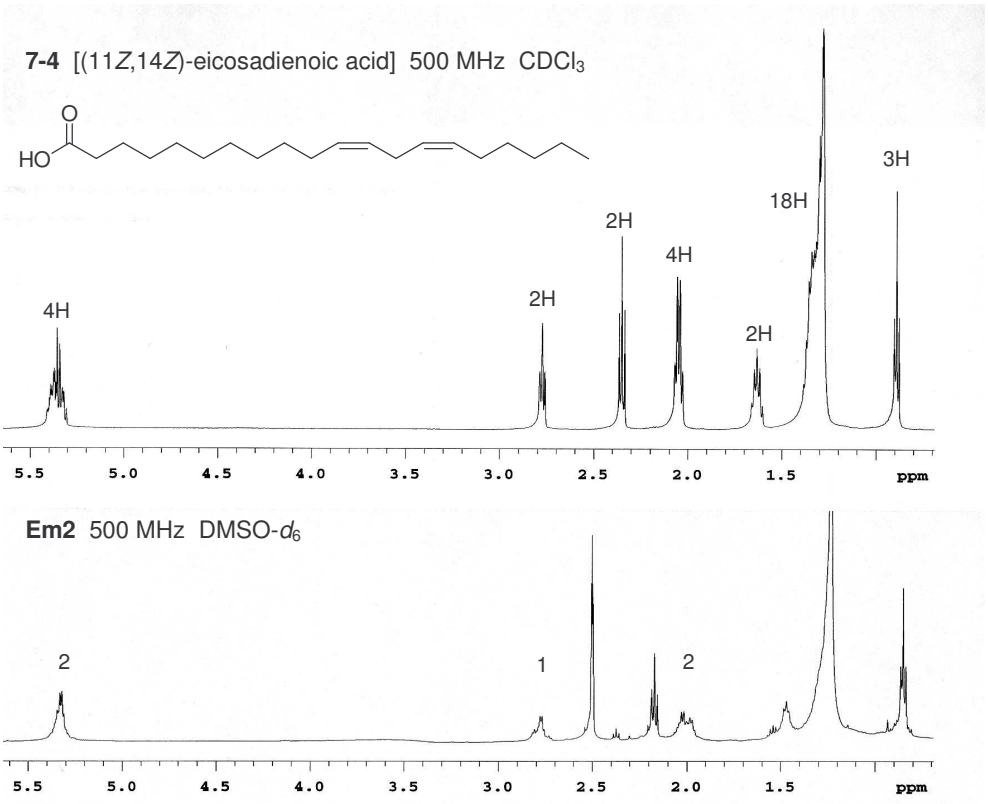

Figure 7.11. ^{1}H NMR Spectral Comparison of **Em2** and Dienoic Acid **7-4**.

The stimulatory activity of **Em2** on NKT cells is interesting, because generally the only ligands that induce activity are glycosphingolipids. Although CD1d is a promiscuous binder, there are relatively few types of compounds that can form a stable complex with the natural killer T cell receptor. There have been no published studies on carboxylic acids as promoters of NKT cell activity, but research has shown that eicosenoids, like arachidonic acid, have regulatory properties in lymphocytes and bone marrow-derived immune cells[23] and that they can cause T_H cells to secrete both T_H1 and T_H2-type cytokines.[24] It is possible that there is a similar occurrence with **Em2** on NKT cells, however, the more likely scenario is that NKT cells are being activated downstream from immune system recognition of **Em2**, as is done when the LPS from *Salmonella* is detected by Toll-like receptors.[5]

The discovery of **Em3** and the alkenyl **Em2** compound from the same lab that produced **Em3**-like **4-2a** prompts the concern that contamination of the bacterial sample happened somewhere during the process of extraction and characterization. Since **4-2a** was synthesized before the isolation of the *E. muris* compounds, there is the possibility that **Em3** and **Em2** could be synthetic compounds that made their way into the biological material. Before the *Sphingomonas* GSLs were extracted (see Chapter 6, section 6.4), there was apprehension that trace amounts of synthetic compounds might end up in the bacterial fractions. To avoid this, separate glassware, solvents, and reaction vessels were used in synthetic and biological work. All glassware used in the extraction of the bacterial glycolipids were purchased specifically for said application and were thoroughly cleansed in a KOH/isopropanol bath before use and reuse. The batch of *E. muris* obtained from the Walker group was subjected to a second round of extractions to remove any residual **Em3**. Only 250 µg were yielded, but the quantity was sufficient for a ^{1}H NMR showing many of the peaks from the first batch of **Em3** (Figure 7.12). This demonstrates that the original sample would have had to be contaminated at the source rather than in the Savage research lab.

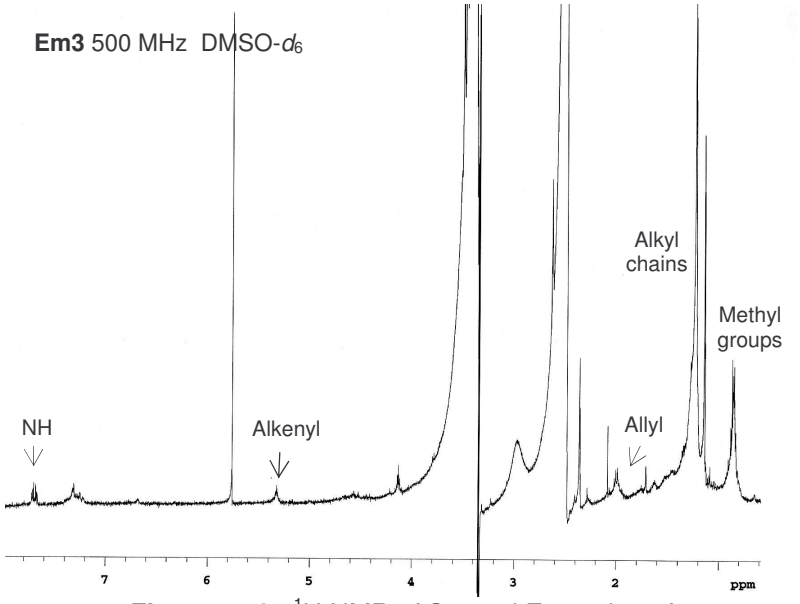

Figure 7.12. ^{1}H NMR of Second Extraction of **Em3** from Original *Ehrlichia muris* Sample.

7.3 Conclusions

Samples from three Gram-negative bacteria, *Borrelia burgdorferi*, *Brucella neotomae*, and *Ehrlichia muris* were examined for NKT cell stimulatory activity. Due to previous assays of LPS-negative, heat-killed *Ehrlichia muris* demonstrating its antigenic behavior towards NKT cells,[5] it was believed that this bacterium displays GSLs on its outer membrane and that through these compounds host defense is activated. *B. burgdorferi*, because of its close taxonomy to *E. muris* and because it also lacks LPS, was thought to contain the same type of glycolipids. Extraction, purification, and characterization of these microbes led to the discovery of only one compound that is a putative GSL: **Em3** from *E. muris*.

Using known synthetic galactosylceramides with similar ^{1}H NMR spectra, a structure of **Em3** has been proposed based on the molecular formula of $C_{44}H_{83}NO_9$, which was obtained by high-resolution mass spectrometric analysis (Figure 7.13). It contains a galactoside with an axial (α) glycosidic bond to a ceramide that is most likely composed of phytosphingosine and a long chain amide. A 1,4-diene is also present in the molecule. The exact location of the alkene has not been determined, but from ^{1}H NMR comparison of **4-2a**, a GSL that possesses the same functional group, it is likely to be incorporated into the amide chain. The identification of **Em2**, which shares the same spectral features as an eicosenoic acid, from the same batch of bacteria provides additional evidence that the amide contains the diene. Due to the lack of material, full characterization could not be performed nor could a ^{13}C NMR be obtained. However, with a greater sample size, hydrolysis of **Em3** followed by derivatization and

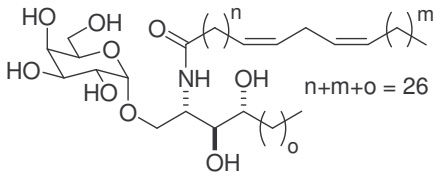

Figure 7.13. Proposed Structure of **Em3.**

GLC-MS analysis should be sufficient to identify the location of the unsaturation and verify the geometry of the double bonds.

Immunological analysis of the nine various fractions from *E. muris* found that **Em2** and **Em3** induce noticeable activity of NKT cells. Although they do not have the same potency as αGalCer, **Em2** and **Em3** were able to cause IL-2 production to a significant degree over the other bacterial compounds. Because it had a much greater capacity for NKT cell stimulation and needed to be bound by CD1d to induce activity, **Em3** is very likely a glycosphingolipid and is the antigenic agent causing host response against the infectious nature of *Ehrlichia muris*.

7.4 Experimental Section

Materials and General Methods. Mass spectrometric data were obtained on a JEOL SX 102A spectrometer for fast atom bombardment (FAB; thioglycerol/Na^+ matrix) or an Agilent Technologies TC/MSD TOF spectrometer for electrospray ionization (ESI; 3500 eV, positive ion mode). ^1H and ^{13}C NMR spectra were obtained on either a Varian Unity 500 MHz instrument using 99.8% $CDCl_3$ with 0.05% v/v TMS or 99.96% DMSO-d_6 in ampoules. Methanol and chloroform used in the extractions were HPLC-grade. Flash chromatography was performed using 230-400 mesh silica gel. Thin layer chromatography was performed on aluminum-backed, 254 nm UV-active plates with a silica gel particle size of 250 μm. Reagents were obtained from Aldrich or Fluka, unless otherwise specified, and were used as received.

Extraction and isolation of membranous compounds from *Brucella neotomae*. *Brucella neotomae* (ATCC 23459) was grown in 3 L of Oxoid Brucella medium base

with 5% heat deactivated horse serum at 37°C for 24 h before being centrifuged (5000 rpm, 10 m) and washed with deionized water three times to remove the broth material. The bacterial pellet was lyophilized to yield 120 mg of dry cellular material. Following an established procedure,[15] the cell solids were suspended in a solution of 2:1 $CHCl_3$:MeOH (15 mL) and sonicated for 10 minutes to remove the more lipophilic compounds. The mixture was centrifuged (5000 rpm, 5 m), the supernatant removed, and the solids were again sonicated and isolated in the same fashion. The extracted cellular solid material was suspended in 1:3 $CHCl_3$:MeOH (8 mL) and refluxed for 1 h at 80°C. After cooling, centrifugation (5000 rpm, 5 m), and supernatant removal, the process was repeated. The combined refluxed extracts were concentrated and examined by TLC ($CHCl_3$:MeOH:H_2O 65:25:4). Three spots were visible at R_f = 0.96, 0.86, and 0.05 using *p*-anisaldehyde stain. The crude mixture was then purified by microcolumn chromatography (SiO_2, $CHCl_3$:MeOH:H_2O 65:25:4), to yield three distinct fractions. Following analysis by ^{1}H NMR (500 MHz, DMSO-d_6), the three fractions were separately dissolved in 1:3 $CHCl_3$:MeOH (2 mL) and saponified with KOH (1 *M*, 1.5 mL) at 40°C for 12 h. The basic solution was neutralized to a pH of 7 with aqueous HCl (6 *M*), extracted with $CHCl_3$ (4 x 2 mL), and dried with Na_2SO_4. TLC analysis ($CHCl_3$:MeOH:H_2O 65:25:4) showed that the three compounds had been hydrolyzed. Following purification by column chromatography (SiO_2, MeOH:$CHCl_3$ 5:95) the three resulting spots (R_f = 0.96, 0.63, 0.41) were examined by ^{1}H NMR. Only the saponified fraction at R_f = 0.41 had a sufficient mass (250 μg) to yield a useful spectrum. Compound at R_f = 0.41: ^{1}H NMR ($CDCl_3$, 500 MHz) δ 5.30 (m, 1[a]), 2.18 (t, *J* = 7.3 Hz,

2^b), 1.97 (m, 2^a), 1.45-1.40 (m, 2^b), 1.26 (br s, 30^b), 0.85 (t, J = 6.8 Hz, 3^b). Note: a and b denote separate integration ratios.

Extraction and isolation of membranous compounds from *Ehrlichia muris*. *Ehrlichia muris* was grown as previously described.[11] The bacterial pellet was lyophilized to yield 191 mg of dry cellular material, which was suspended in a solution of 2:1 $CHCl_3$:MeOH (3 mL) and sonicated for 10 minutes to remove the more lipophilic compounds. The mixture was centrifuged (5000 rpm, 5 m), the supernatant removed, and the solids were again sonicated and isolated in the same fashion. The extracted cellular solid material was suspended in 1:3 $CHCl_3$:MeOH (2 mL) and refluxed for 1 h at 80°C. After cooling, centrifugation (5000 rpm, 5 m), and supernatant removal, the process was repeated. The combined refluxed extracts were concentrated and examined by TLC ($CHCl_3$:MeOH:H_2O 65:25:4), which revealed eleven spots using *p*-anisaldehyde stain. The crude mixture was then purified by microcolumn chromatography (SiO_2, MeOH:$CHCl_3$ 1:4 to 1:2 to 1:1 to 2:1 to 3:1), to yield nine distinct fractions with the R_f values of 0.95 (**Em1**), 0.85 (**Em9**), 0.82 (**Em2**), 0.71 (**Em3**), 0.38 (**Em4**), 0.35 (**Em5**), 0.18 (**Em6**), 0.13 (**Em7**), 0.08 (**Em8**) using the eluent $CHCl_3$:MeOH:H_2O 65:25:4.

Characterization of **Em2**. ^{1}H NMR (DMSO-d_6, 500 MHz) δ 5.37-5.29 (m, 2), 2.82-2.72 (m, 1), 2.18* (t, J = 7.8 Hz), 2.09-1.95 (dt, J = 7.3, 6.8 Hz, 2), 1.50-1.40* (quintet, J = 7.3 Hz), 1.26* (br s), 0.85* (t, J = 6.8 Hz). *Integration unreliable.

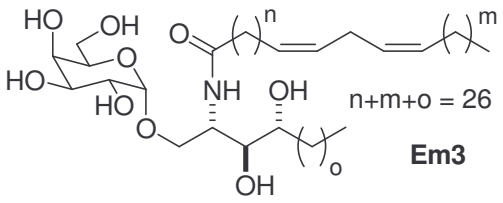

Characterization of **Em3**. ^{1}H NMR (DMSO-d_6, 500 MHz) δ 7.60 (d, J = 8.7 Hz, 1^{a}), 5.35-5.29 (m, 4^{a}), 4.67 (d, J = 2.9 Hz, 1^{a}), 4.63 (d, J = 6.3 Hz, 1^{a}), 4.55-4.53 (m, 2^{a}), 4.38 (d, J = 3.9 Hz, 1^{a}), 4.29 (d, J = 7.3 Hz, 1^{a}), 3.98 (m, 1-2^{a}), 2.73 (t, J = 6.3 Hz, 2^{a}), 2.06 (t, J = 7.3 Hz, 2 H^{a}), 2.01 (dt, J = 6.8, 6.3 Hz, 4^{a}), 1.50-1.40 (m, 4^{b}), 1.23 (br s, 36-42^{b}), 0.85 (m, 6^{b}); ^{1}H NMR (DMSO-d_6:D_2O 25:1, 500 MHz) δ 5.35-5.29 (m, 4^{a}), 4.67 (d, J = 2.9 Hz, 1^{a}), 3.66 (br s, 1^{a}), 3.59-3.54 (m, 2^{a}), 3.53-3.43 (m, 5^{a}), 3.41-3.39 (m, 2^{a}), 3.37-3.34 (m, 1^{a}), 2.73 (t, J = 6.3 Hz, 2^{a}), 2.06 (t, J = 7.3 Hz, 2 H^{a}), 2.01 (dt, J = 6.8, 6.3 Hz, 4^{a}), 1.50-1.40 (m, 4^{b}), 1.23 (br s, 36-42^{b}), 0.85 (m, 6^{b}). Note: a and b denote separate integration ratios. HRMS (FAB) *m/z* for $C_{44}H_{84}NO_9$ ([M+H]$^{+}$) 770.6135 (72.8%), *m/z* for $C_{44}H_{83}NNaO_9$ ([M+Na]$^{+}$) 792.5897 (100%), (ESI) *m/z* for $C_{44}H_{84}NO_9$ ([M+H]$^{+}$) 770.61320 (100%), calc. 770.61406.

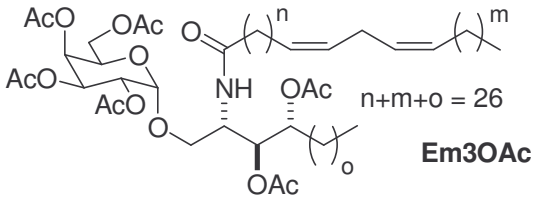

Em3OAc. Bacterial fraction **Em3** (0.54 mg) was dissolved in THF (4 drops) and acetic anhydride (1 drop), Et_3N (1 drop), and DMAP (1 mg, 0.008 mmol) were added. The reaction vessel was sonicated for 90 m, and the reaction monitored for completion by TLC. Using the eluent EtOAc:Hex 1:2, a lone spot at R_f = 0.38 was visualized. The compound was purified by column chromatography (SiO_2, EtOAc:Hex 1:2) to yield a colorless oil (appx. 0.5 mg). ^{1}H NMR ($CDCl_3$, 500 MHz) δ 6.45 (m, 1), 5.45 (d, J = 3.4

Hz, 1), 5.38-5.26 (m, 6), 5.14 (dd, *J* = 10.7, 3.4 Hz, 1), 4.90 (d, *J* = 3.4 Hz, 1), 4.87 (m, 1), 4.37 (t, *J* = 9.8 Hz, 1), 4.13-4.09 (m, 2), 4.05-4.01 (m, 1), 3.67-3.62 (m), 3.41-3.39 (m), 2.77 (t, *J* = 6.3 Hz, 2), 2.14* (s), 2.10* (s), 2.07* (s), 2.05* (s), 2.00* (s), 1.99* (s), 1.26* (br s), 0.90-0.88* (m); HRMS (ESI) *m/z* for $C_{56}H_{95}NO_{15}$ ($[M+H]^+$) 1022.67660 (100%), calc. 1022.67745. *Integration unreliable.

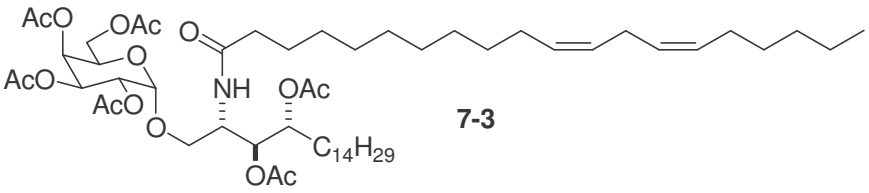

7-3

7-3. Glycosphingolipid **4-2a** (5.0 mg, 0.006 mmol) was dissolved in THF (0.5 mL), and acetic anhydride (250 µL), Et_3N (250 µL), and DMAP (1 mg, 0.008 mmol) were added. The reaction vessel was sonicated for 90 m, and the reaction monitored for completion by TLC. Using the eluent EtOAc:Hex 1:2, a lone spot at R_f = 0.38 was visualized. The compound was purified by column chromatography (SiO_2, EtOAc:Hex 1:2) to yield a colorless oil (5.5 mg, 92%). ^{1}H NMR ($CDCl_3$, 500 MHz) δ 6.34 (d, *J* = 9.8 Hz, 1 H), 5.45 (d, *J* = 2.9 Hz, 1 H), 5.41-5.33 (m, 4 H), 5.31 (m, 1 H), 5.27 (dd, *J* = 10.3, 2.4 Hz, 1 H), 5.14 (dd, *J* = 10.7, 3.4 Hz, 1 H), 4.90 (d, *J* = 3.4 Hz, 1 H), 4.87 (dt, *J* = 9.3, 2.4 Hz, 1 H), 4.37 (tt, *J* = 9.8, 2.4 Hz, 1 H), 4.13-4.09 (m, 2 H), 4.05-4.01 (m, 1 H), 3.66 (dd, *J* = 10.7, 2.4 Hz, 1 H), 3.40 (dd, *J* = 10.7, 2.4 Hz, 1 H), 2.77 (t, *J* = 6.8 Hz, 2 H), 2.28 (dt, *J* = 7.8, 3.4 Hz, 2 H), 2.14 (s, 3 H), 2.10 (s, 3 H), 2.07 (s, 3 H), 2.05 (s, 3 H), 2.00 (s, 3 H), 1.99 (s, 3 H), 1.70-1.58 (m, 4 H), 1.26 (br s, 42 H), 0.88 (m, 6 H); ^{13}C NMR ($CDCl_3$, 125 MHz) δ 173.11, 171.38, 170.92, 170.64, 170.41, 169.93, 130.40, 130.36, 128.14, 97.30, 73.62, 70.57, 68.10, 67.67, 67.40, 66.89, 61.98, 47.92, 36.92, 32.14, 31.73, 29.93, 29.88, 29.83, 29.80, 29.74, 29.57, 29.51, 27.47, 27.39, 25.94, 25.85, 22.91, 22.79,

21.21. 20.96, 20.89, 20.85, 20.80, 14.35, 14.30; HRMS (ESI) *m/z* for $C_{56}H_{95}NO_{15}$ ($[M+H]^+$) 1022.67756 (100%), calc. 1022.67745.

7.5 References

1) Pier, G. B.; Lyczak, J. B.; Wetzler, L. M., Eds. *Immunology, Infection, and Immunity*; ASM Press: Washington, DC, 2004.

2) Lyczak, J. B.; Cannon, C. L.; Pier, G. B. *Clin. Microbiol. Rev*. **2002**, *15*, 194.

3) Selmi, C.; Balkwill, D. L.; Invernizzi, P.; Ansari, A. A.; Coppel, R. L.; Podda, M.; Leung, P. S.; Kenny, T. P.; Van De Water, J.; Nantz, M. H.; Kurth, M. J.; Gershwin, M. E. *Hepatology* **2003**, *38*, 1250.

4) Kosako, Y.; Yabuuchi, E.; Naka, T.; Fujiwara, N.; Kobayashi, K. *Microbiol. Immunol*. **2000**, *44*, 563.

5) Mattner, J.; DeBord, K. L.; Ismail, N.; Goff, R. D.; Cantu, C., III; Zhou, D.; Saint-Mezard, P.; Wang, V.; Gao, Y.; Yin, N.; Hoebe, K.; Schneewind, O.; Walker, D.; Beutler, B.; Teyton, L.; Bendelac, A.; Savage, P. B. *Nature* **2005**, *343*, 525. Figure 7.1 is adapted by permission, Copyright 2005 Macmillan Publishers Ltd.

6) Gupta, R. S. *Crit. Rev. Microbiol*. **2005**, *31*, 101.

7) Lin, M.; Rikihisa, Y. *Infect. Immun*. **2003**, *71*, 5324.

8) Kumar, H.; Belperron, A.; Barthold, S. W.; Bockenstedt, L. K. *J. Immunol*. **2000**, *165*, 4797.

9) *Ehrlichiosis*; The Center for Food Security and Public Health, Iowa State University: Ames, IA, 2005.

10) Feng, H.-M.; Walker, D. H. *Infect. Immun*. **2004**, *72*, 966.

11) Ismail, N.; Soong, L.; McBride, J. W.; Valbuena, G.; Olano, J. P.; Feng, H.-M.; Walker, D. H. *J. Immunol*. **2004**, *172*, 1786.

12) Takayama, N.; Rothenberg, R. J.; Barbour, A. G. *Infect. Immun*. **1987**, *55*, 2311.

13) Lopez-Goni, I.; Moriyon, I., Eds. *Brucella: Molecular and Cellular Biology*; Horizon Bioscience: Wymondham, Norfolk, England, 2004.

14) Ben-Menachem, G.; Kubler-Kielb, J.; Coxon, B.; Yergey, A.; Schneerson, R. *Proc. Natl. Acad. Sci. USA* **2003**, *100*, 7913.

15) Kawahara, K.; Moll, H.; Knirel, Y. A.; Seydel, U.; Zahringer, U. *Eur. J. Biochem*. **2000**, *267*, 1837.

16) Baker, R. R. *Clin. Biochem*. **1990**, *23*, 455.

17) (a) Natori, T.; Koezuka Y.; Higa, T. *Tetrahedron Lett*. **1993**, *34*, 5591. (b) Natori, T.; Morita, M.; Akimoto, K.; Koezuka, Y. *Tetrahedron* **1994**, *50*, 2771. (c) Motoki, K.; Kobayashi, E.; Uchida, T.; Fukushima, H.; Koezuka Y. *Bioorg. Med. Chem. Lett*. **1995**, *5*, 705.

18) Nicolaou, K. C.; Li, J.; Zenke, G. *Helv. Chim. Acta* **2000**, *83*, 1977.

19) Uchimura, A.; Shimizu, T.; Makajima, M.; Ueno, H.; Motoki, K.; Fukushima, H.; Natori, Y.; Koezuka, Y. *Bioorg. Med. Chem*. **1997**, *5*, 1447.

20) Bettazzoli, L.; Zirrolli, J. A.; Reidhead, C. T.; Shahgholi, M.; Murphy, R. C. Incorporation of Arachidonic Acid into Glycerophopholipids of a Murine Bone Marrow Derived Mast Cell. In *Advances in Prostaglandin, Thromboxane, and Leukotriene Research*; Samuelsson, B.; Dahlen, S.-E.; Fritsch, J.; Hedqvist, P., Eds.; Raven Press: New York, NY, 1990; Vol. 20., pp.71-78.

21) Mannisto, M. K.; Puhakka, J. A. *Arch. Microbiol*. **2001**, *177*, 41.

22) Mathews, C. K.; Van Holde, K. E., Eds. *Biochemistry*, 2nd Edition; The Benjamin/Cummings Publishing Company: New York, NY, 1996.

23) Julian, L. *J. Infect*. **2004**, *49*, 88.

24) Lewis, R. A. Interactions of Eicosanoids and Cytokines in Immune Regulation. In *Advances in Prostaglandin, Thromboxane, and Leukotriene Research*; Samuelsson, B.; Dahlen, S.-E.; Fritsch, J.; Hedqvist, P., Eds.; Raven Press: New York, NY, 1990; Vol. 20., pp.170-178.

APPENDIX.

^{1}H AND ^{13}C NMR SPECTRA OF FINAL COMPOUNDS

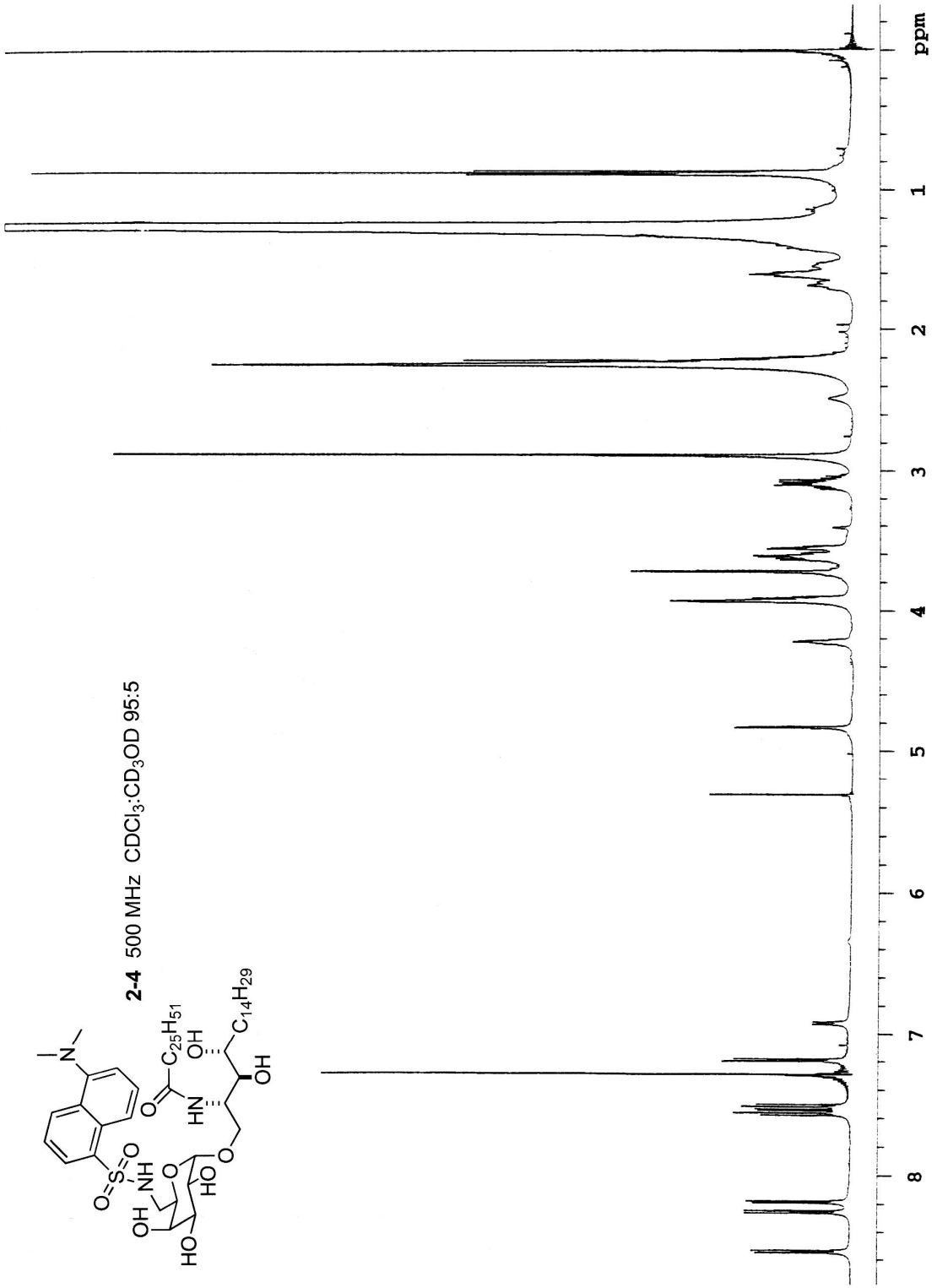

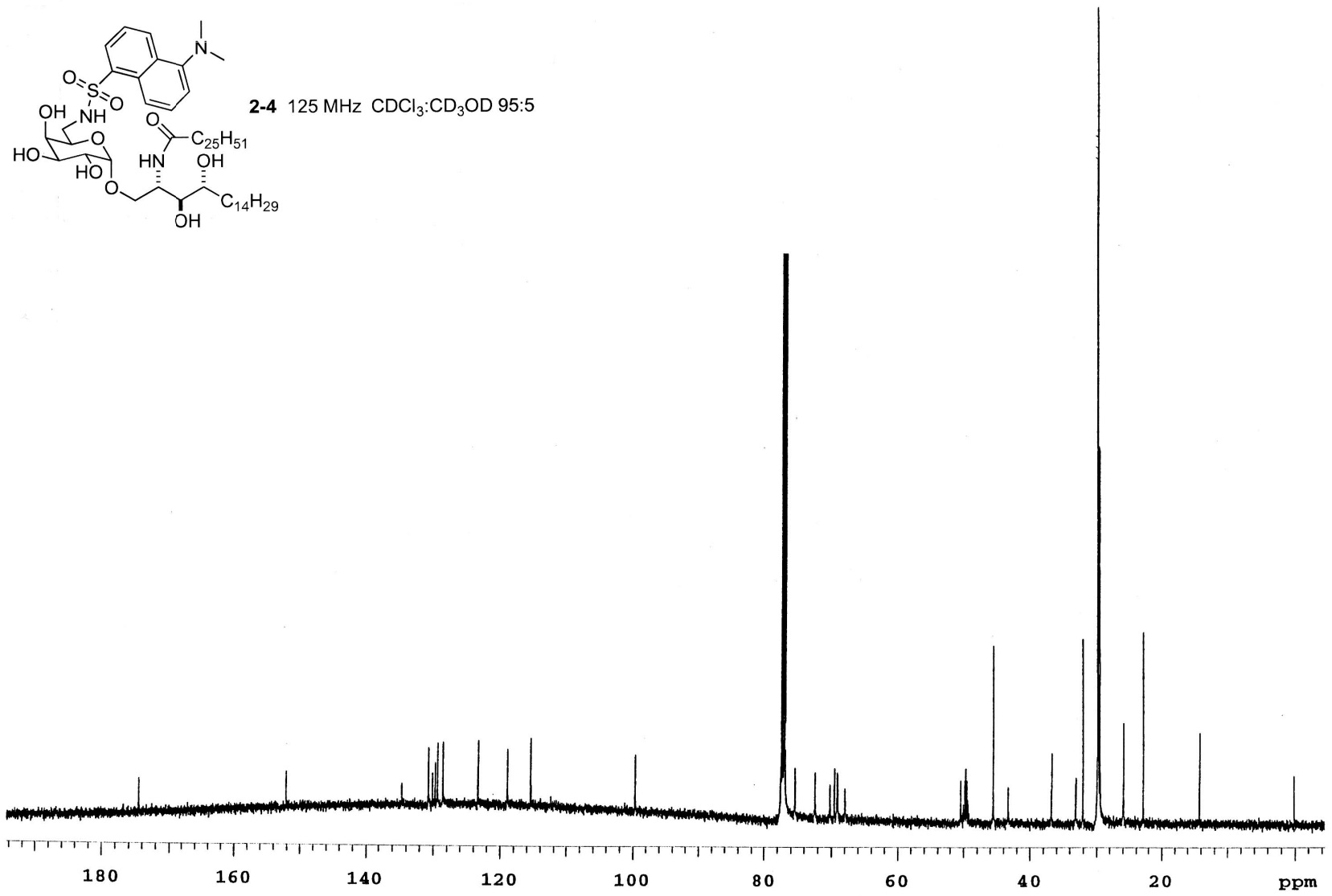

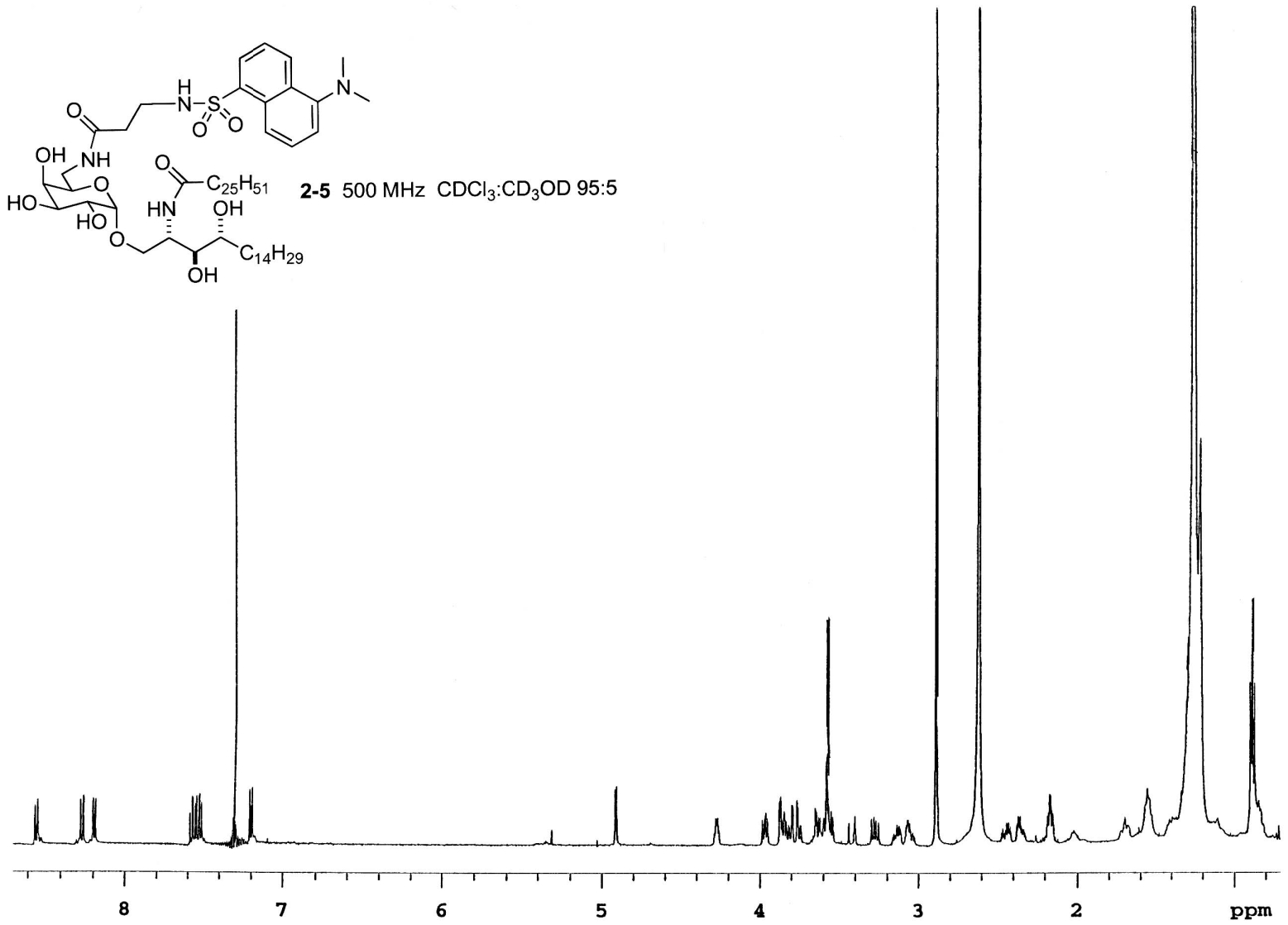

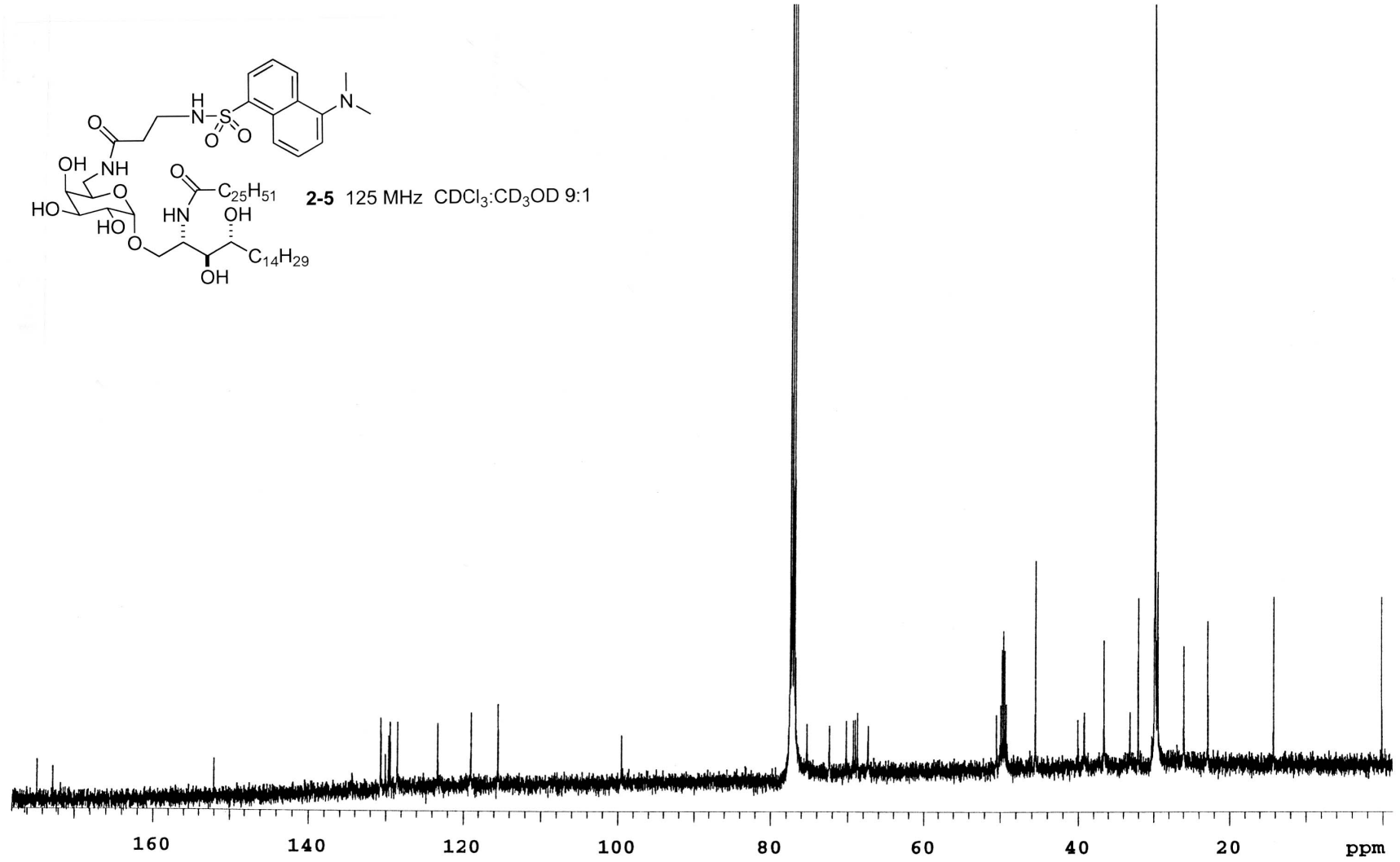

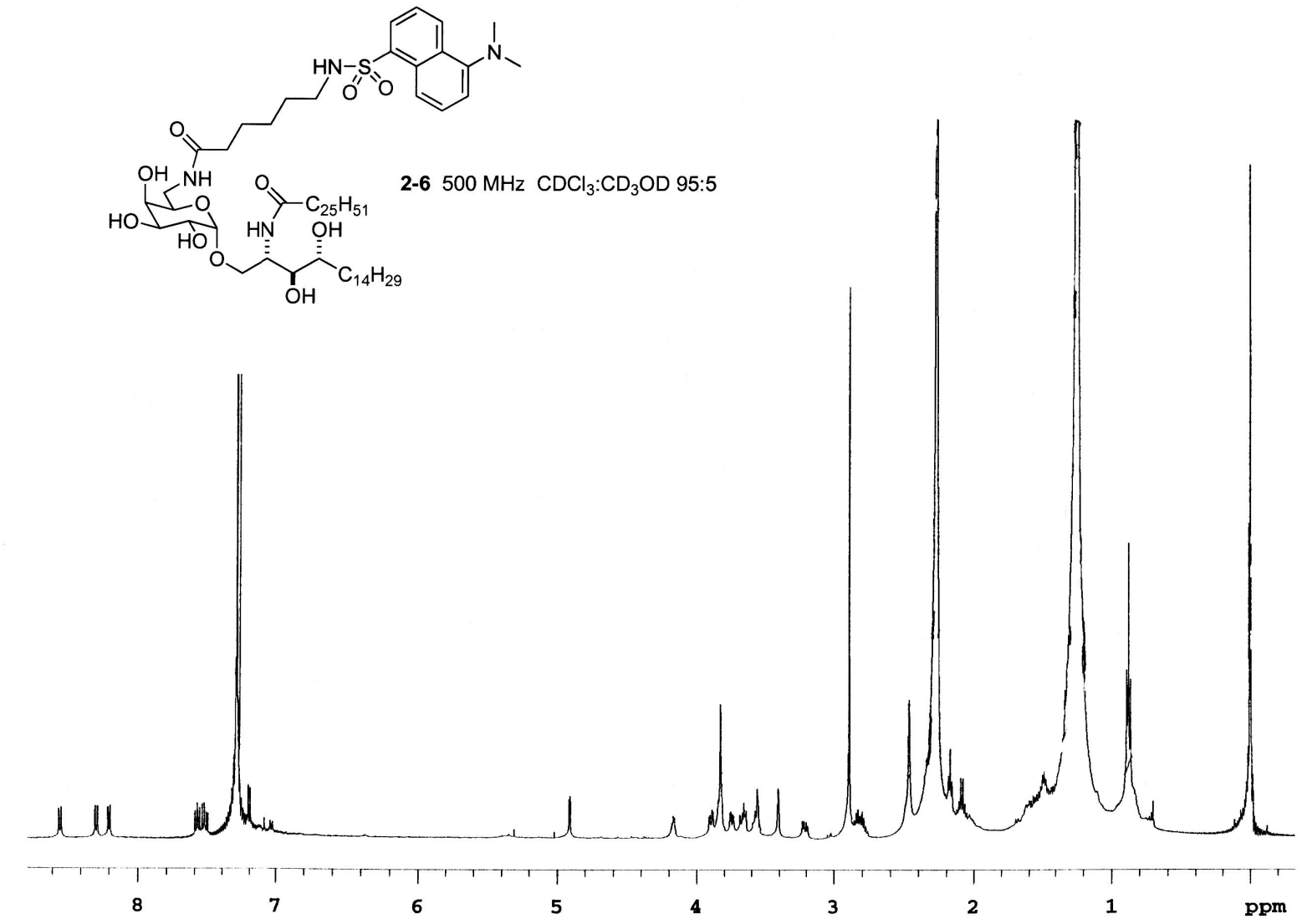

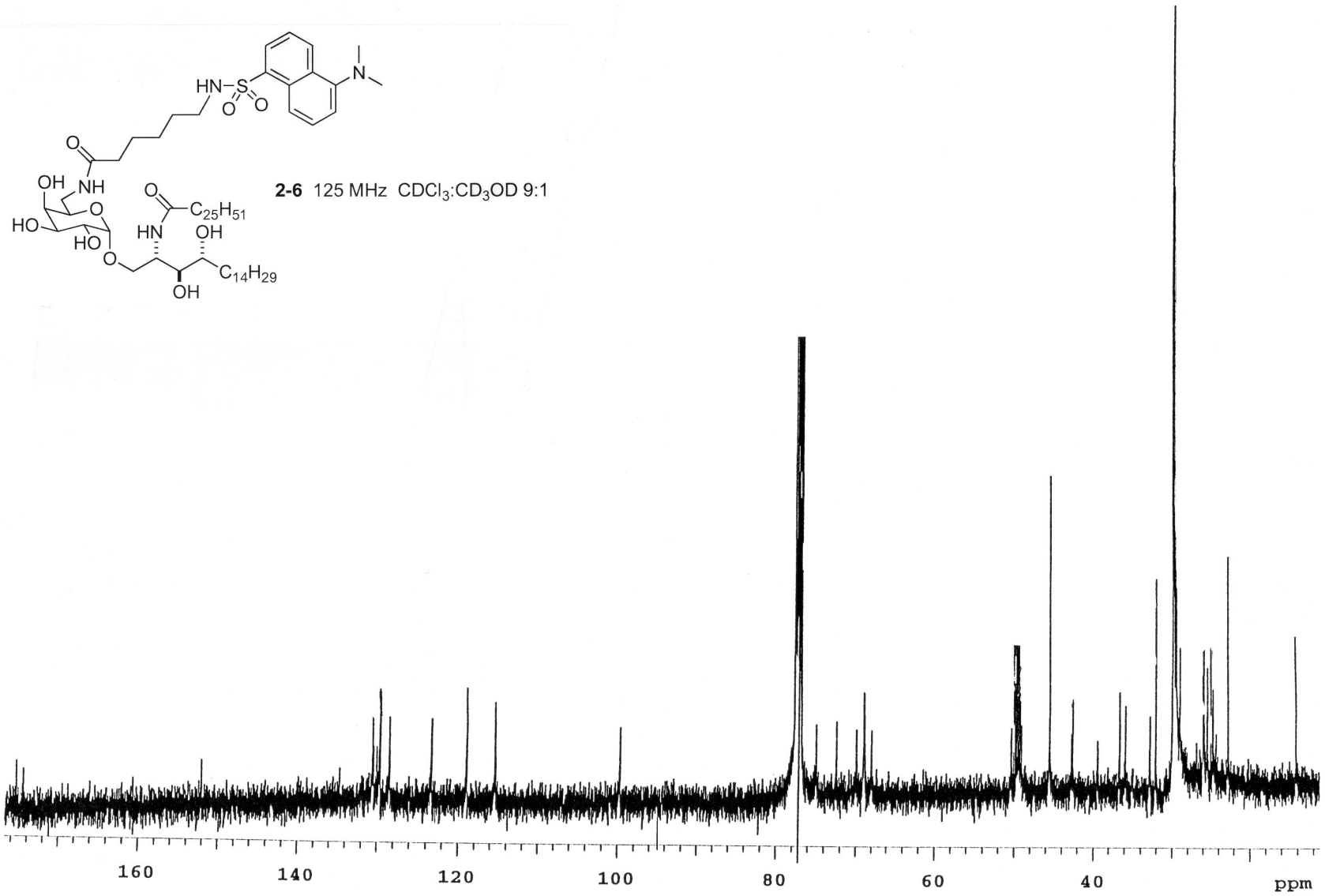

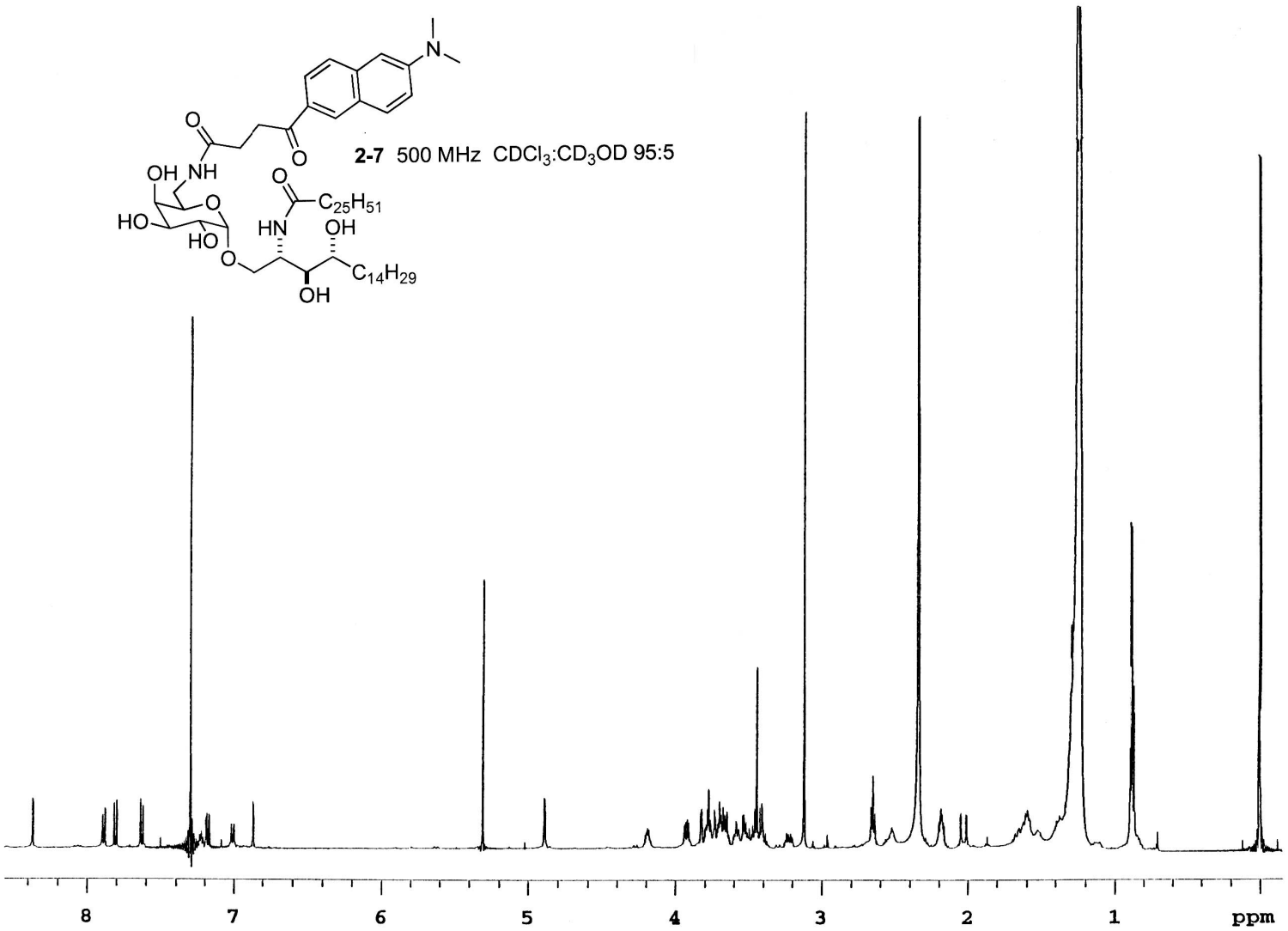

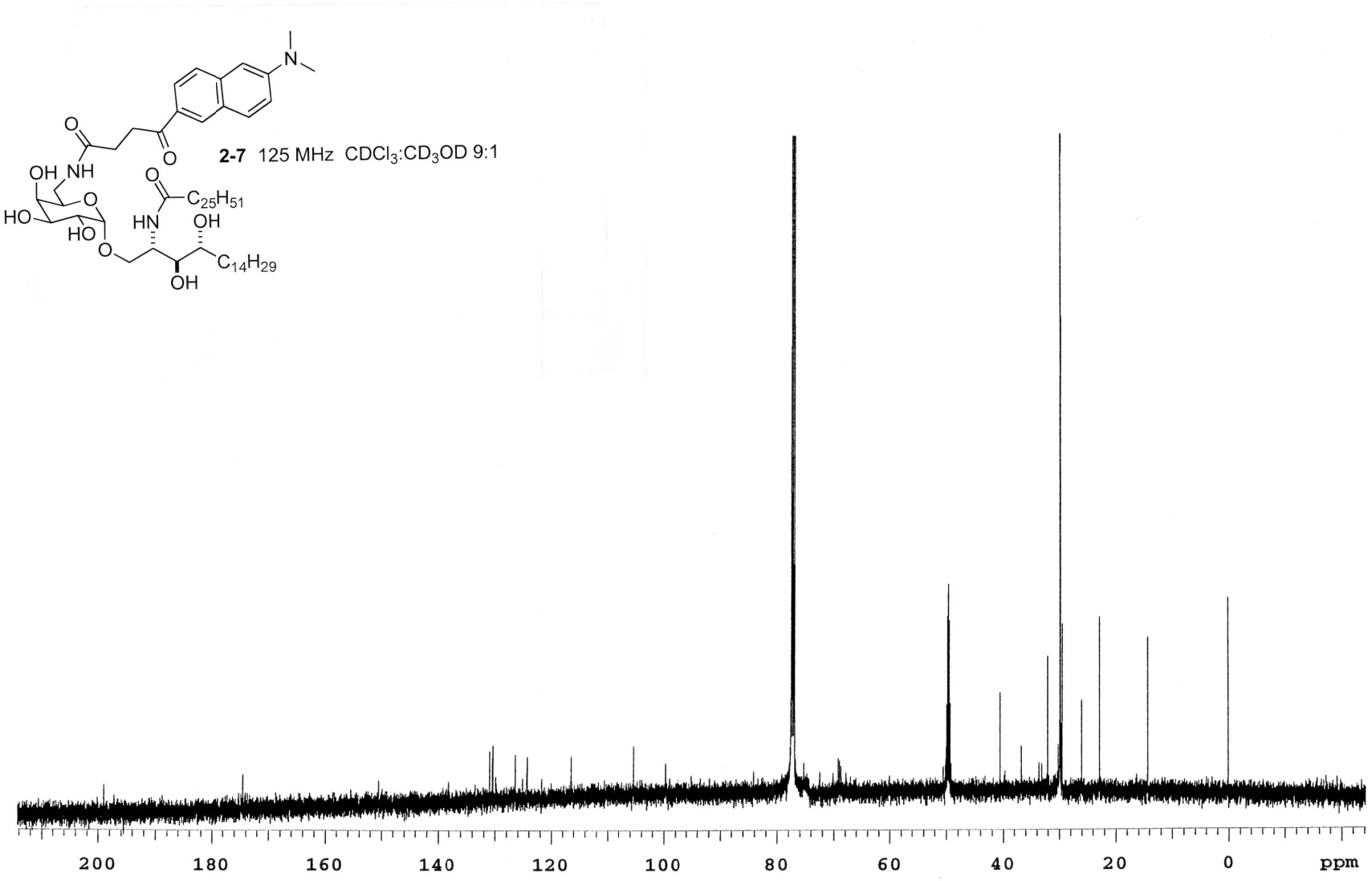

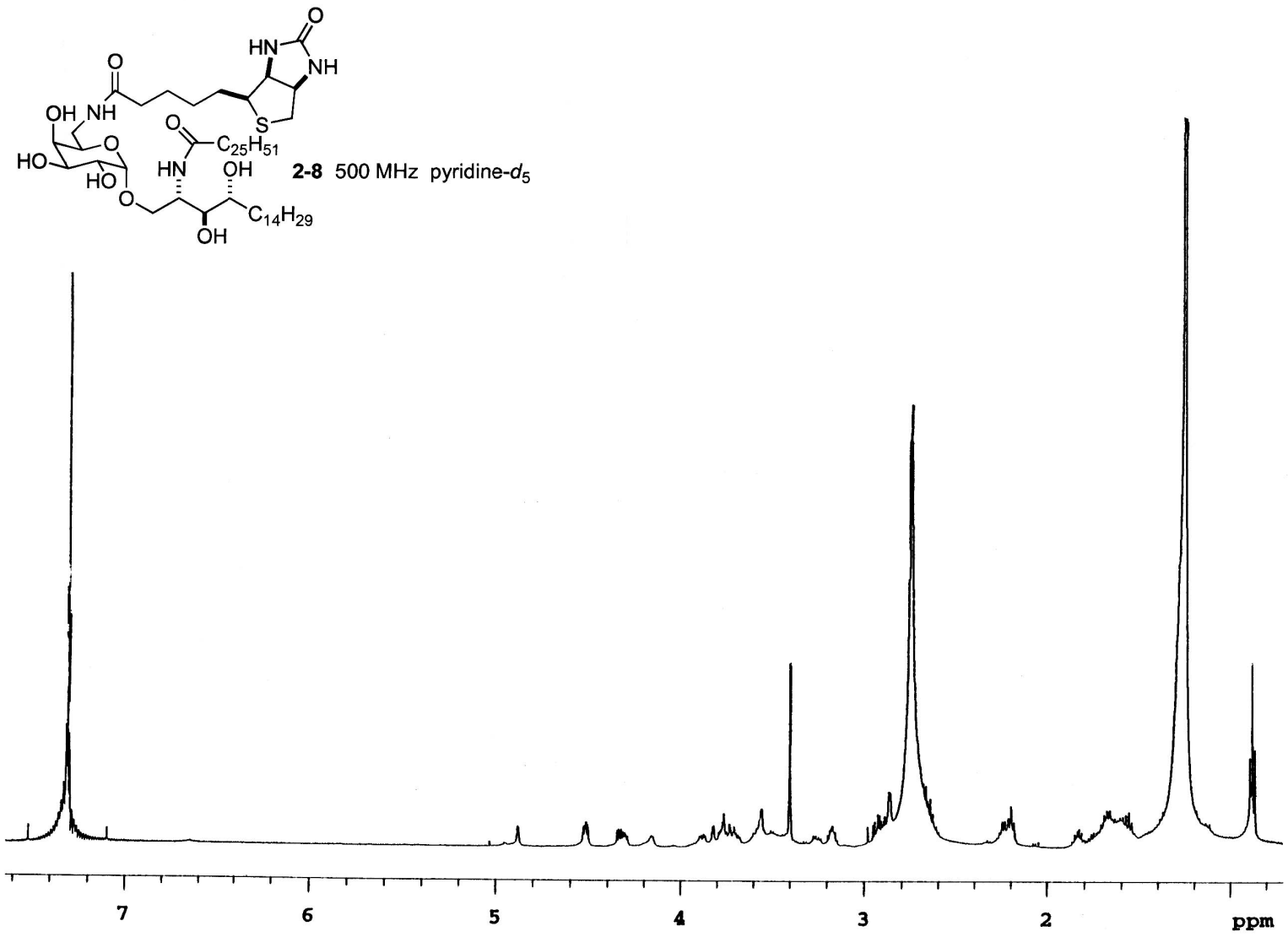

2-8 500 MHz pyridine-d_5

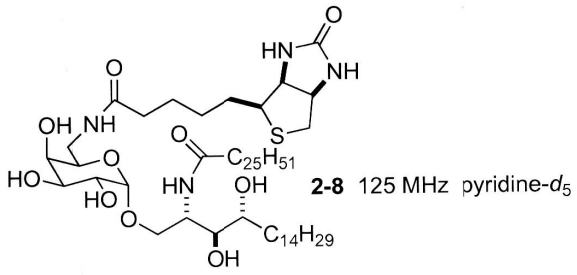

2-8 125 MHz pyridine-d_5

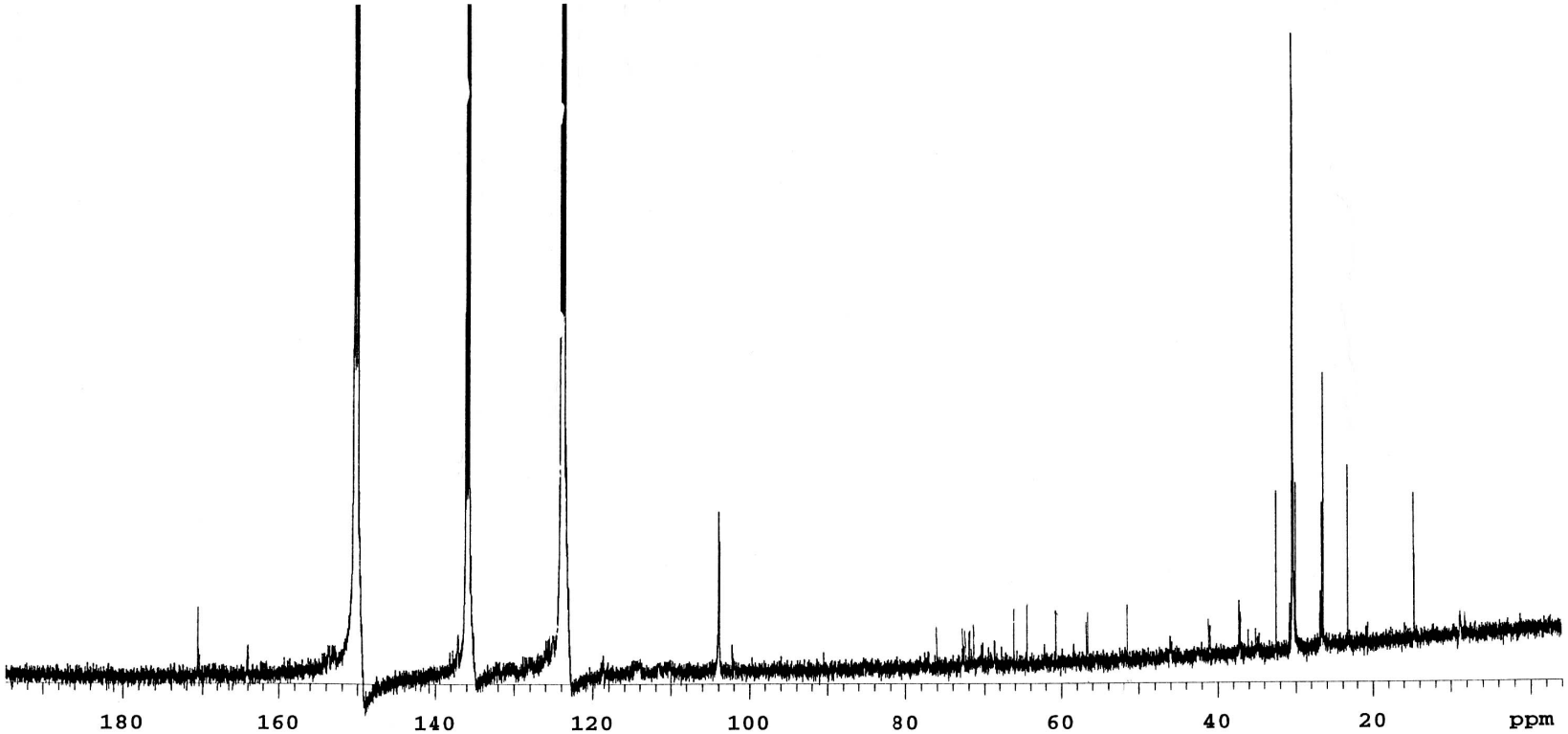

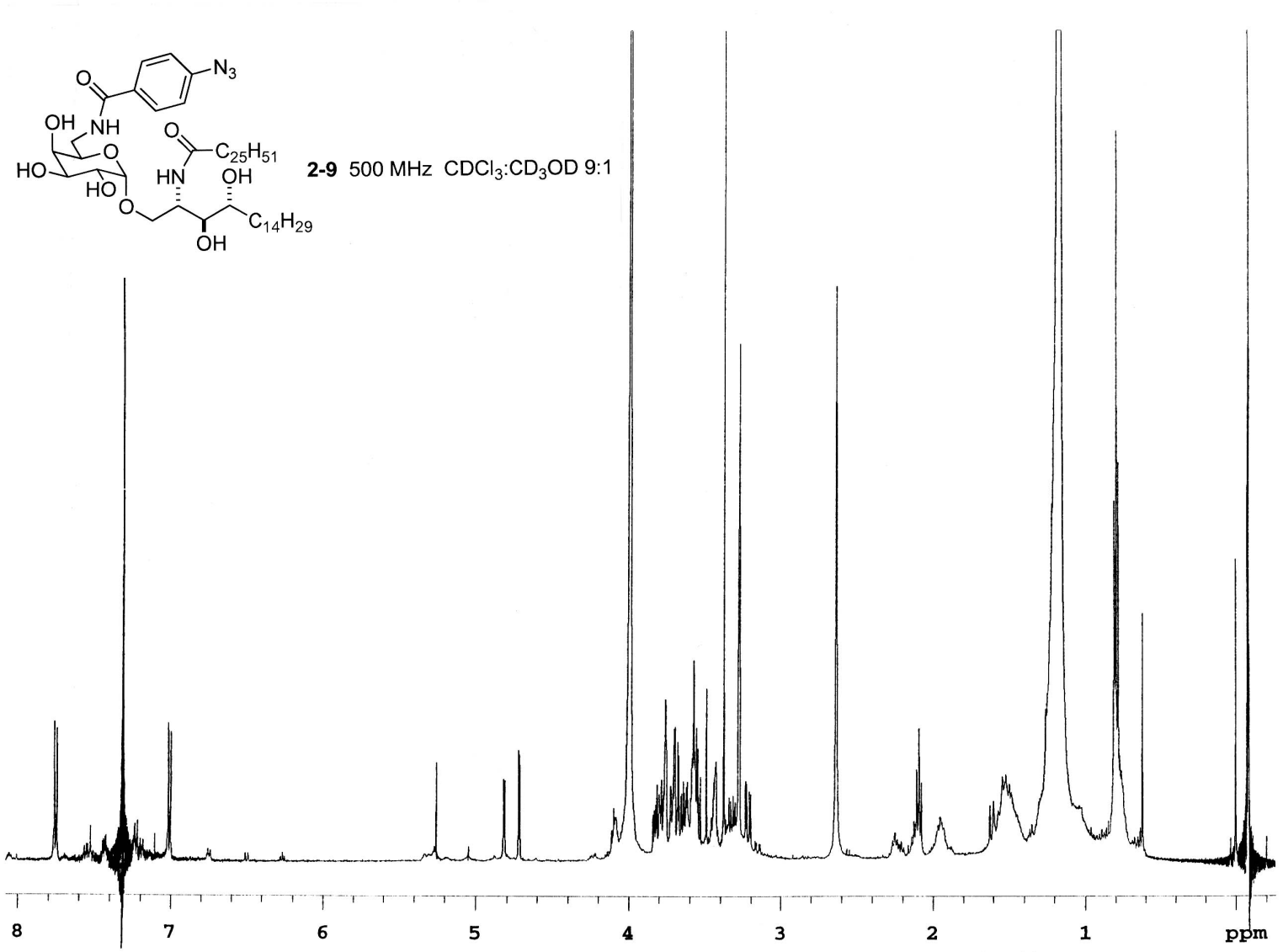

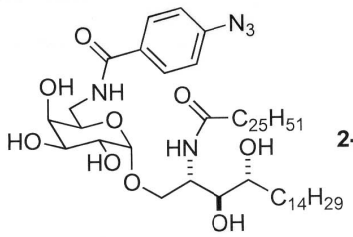

2-9 125 MHz $CDCl_3$:CD_3OD 95:5

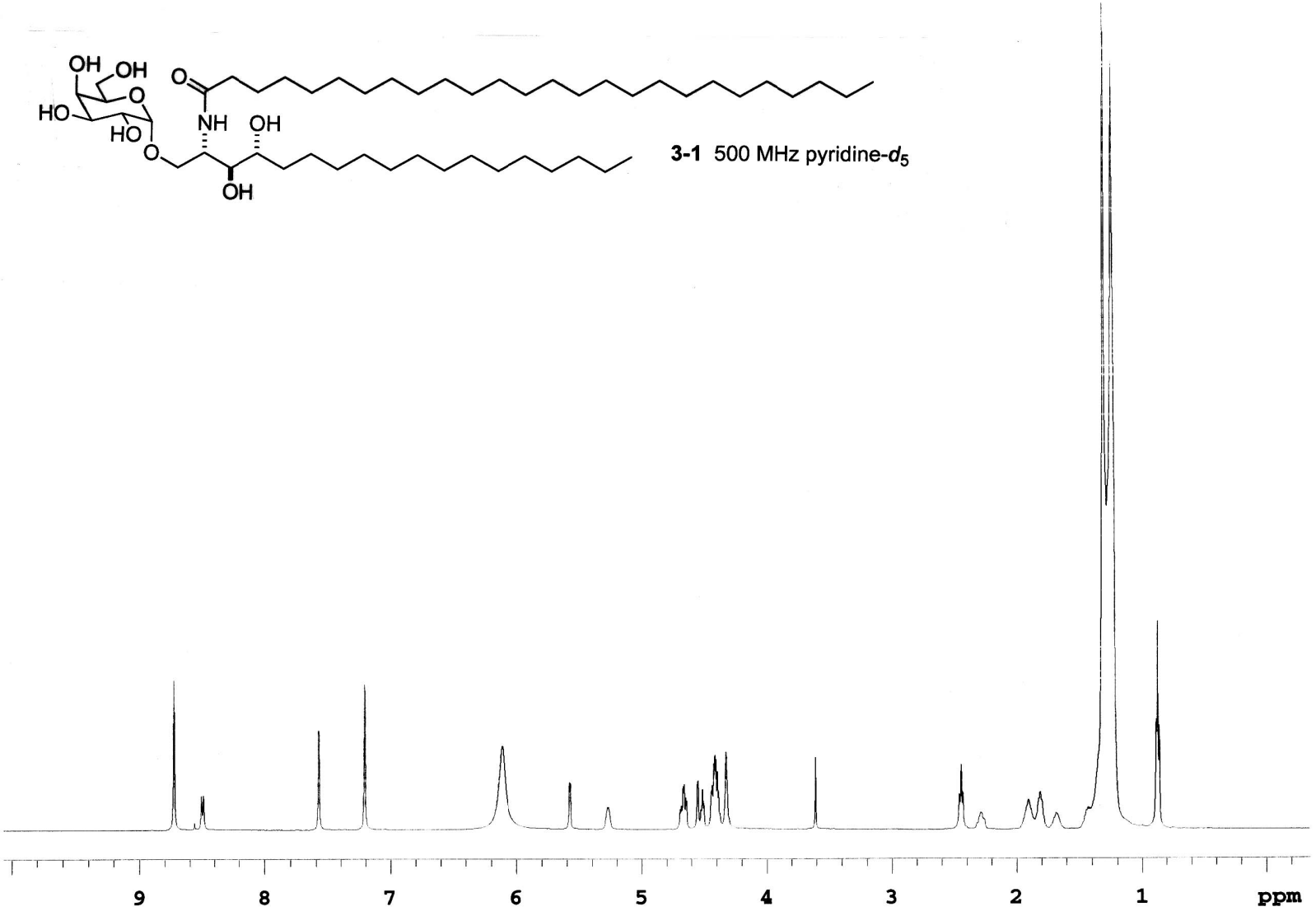

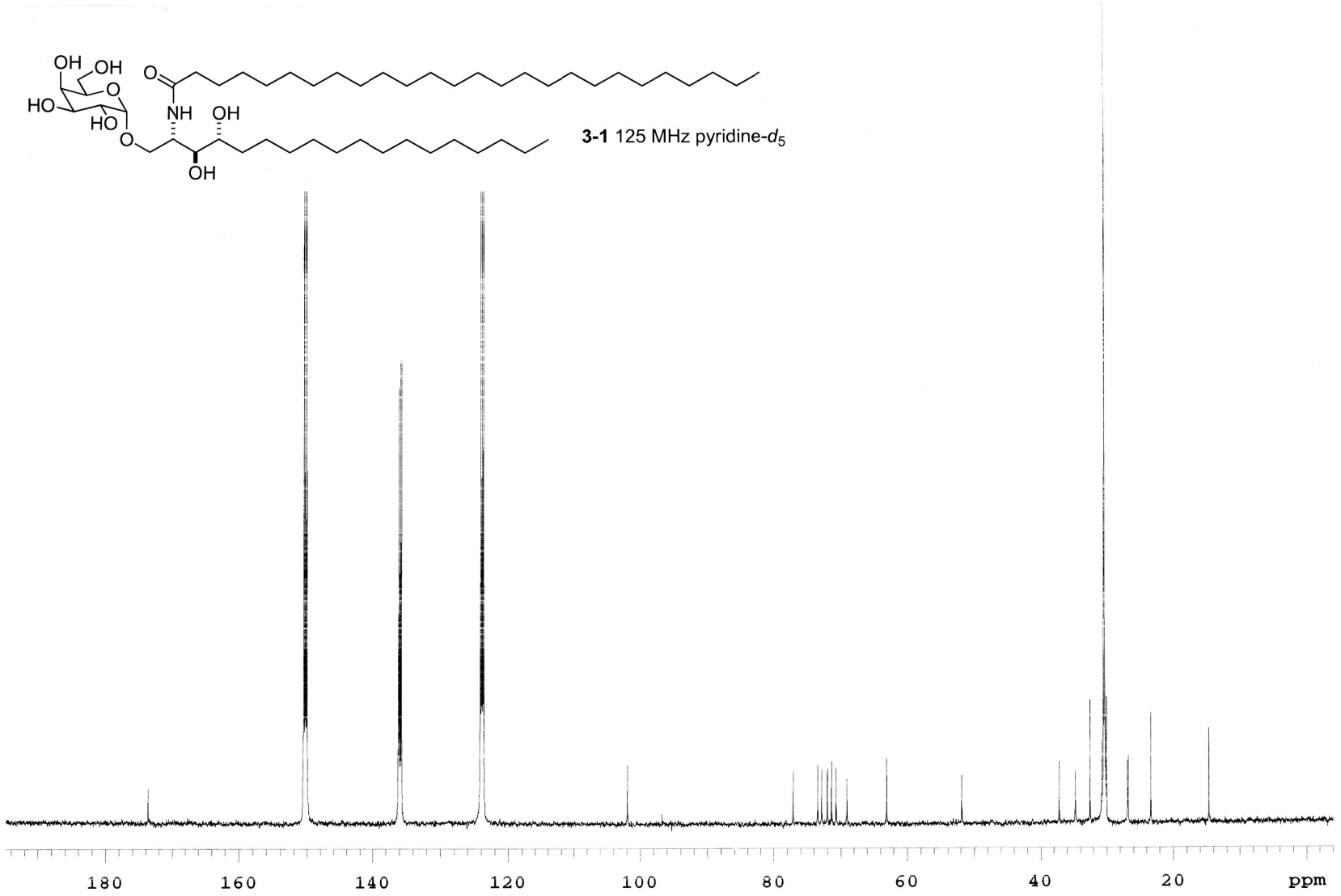

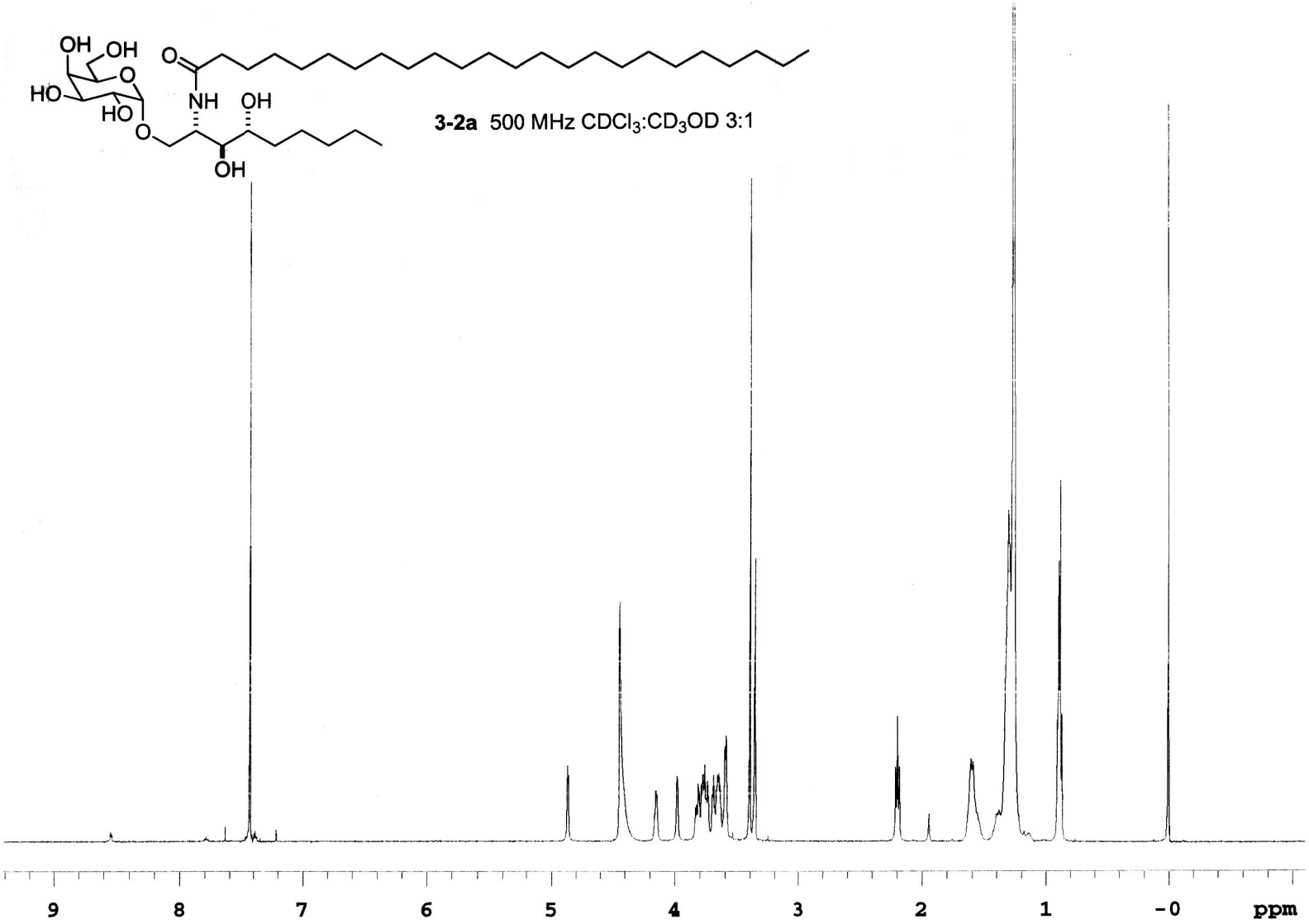

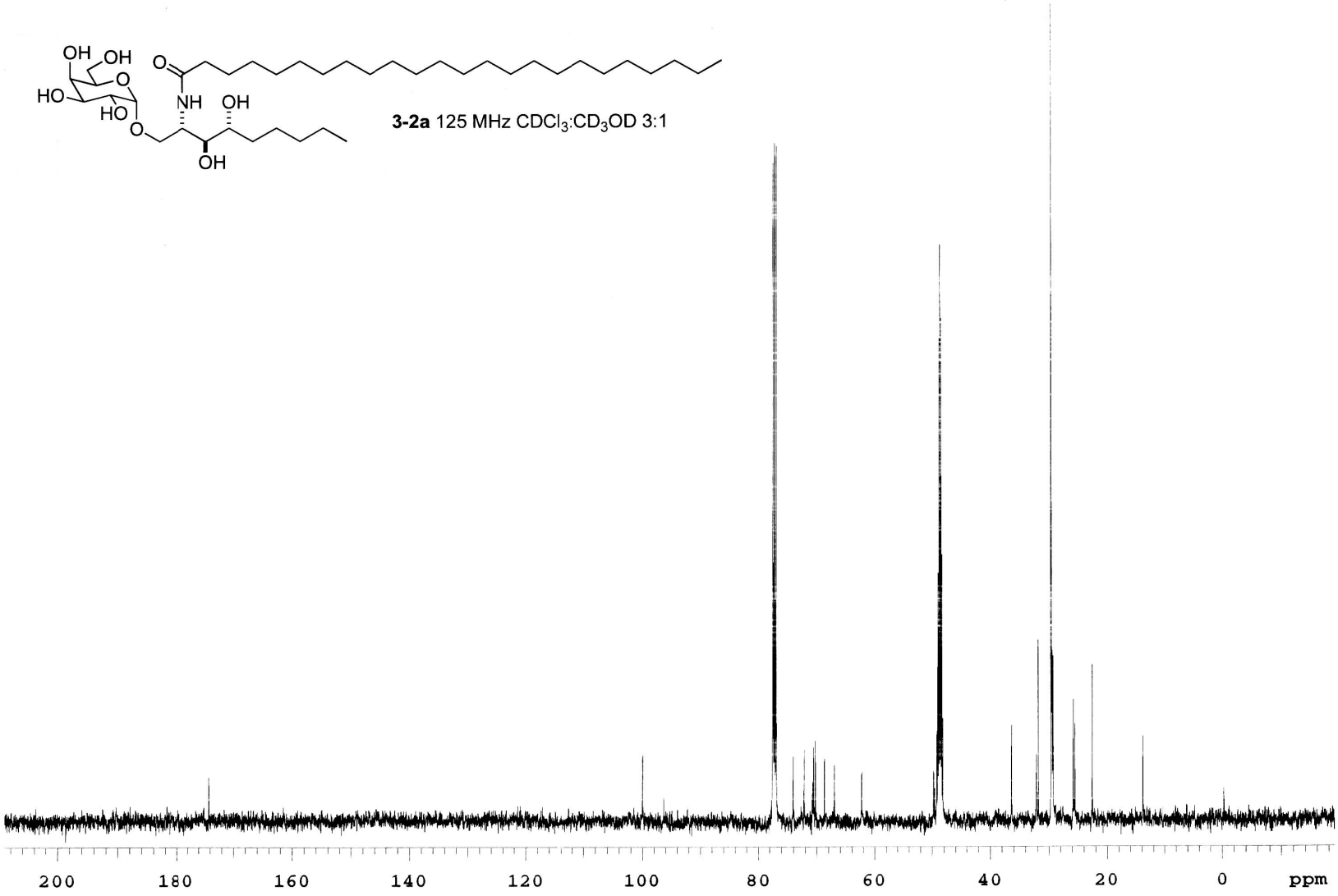

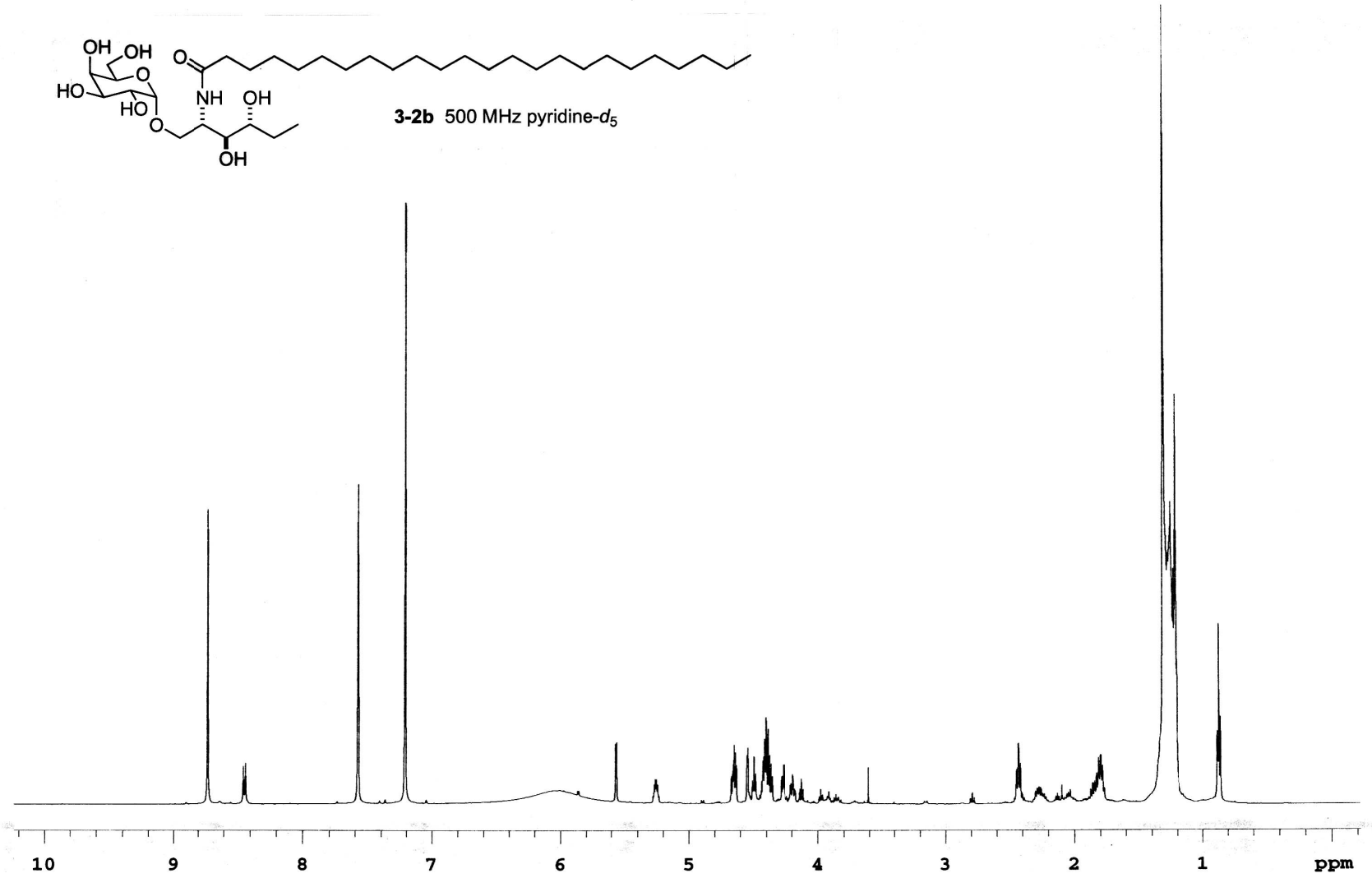

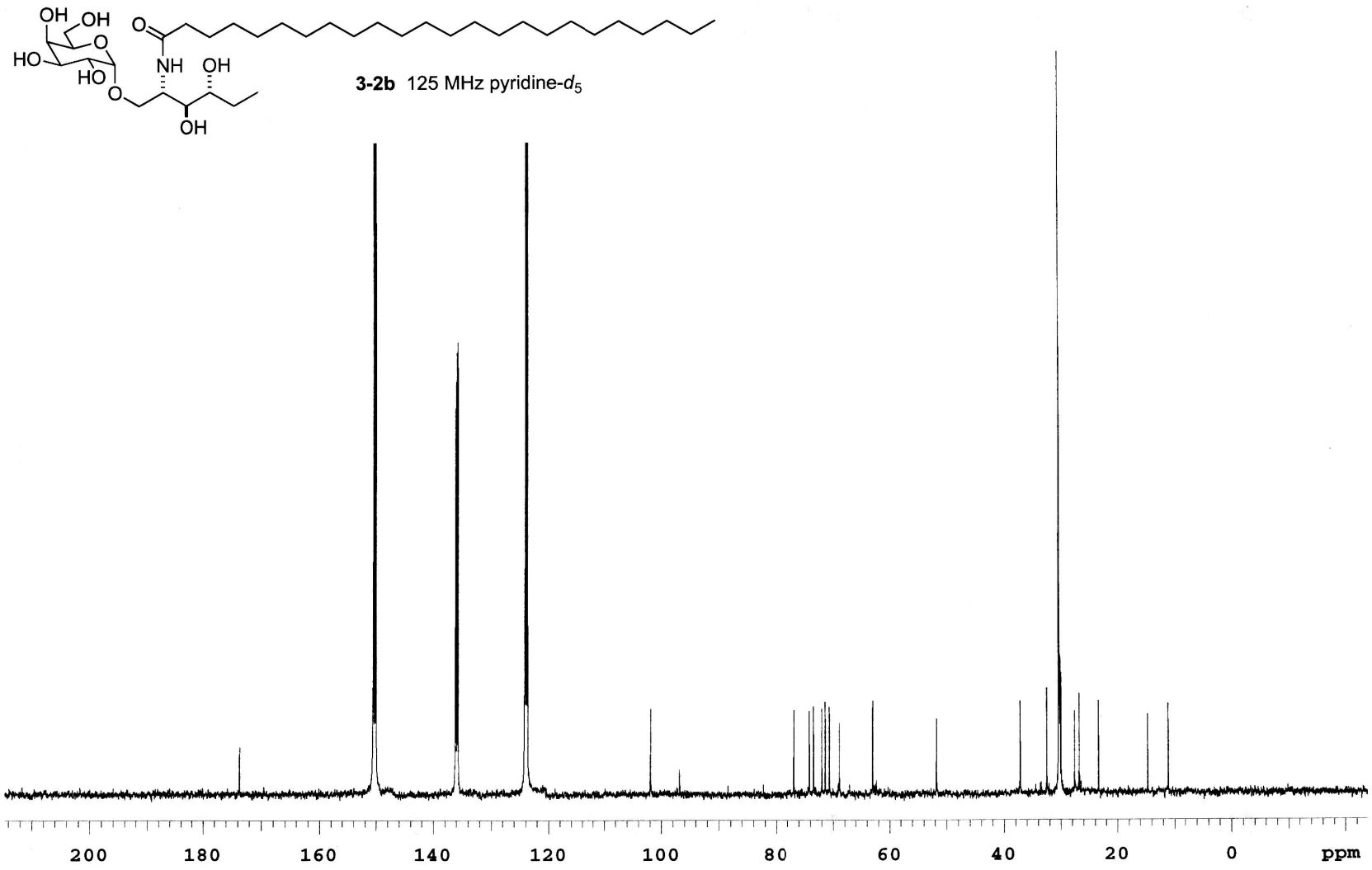

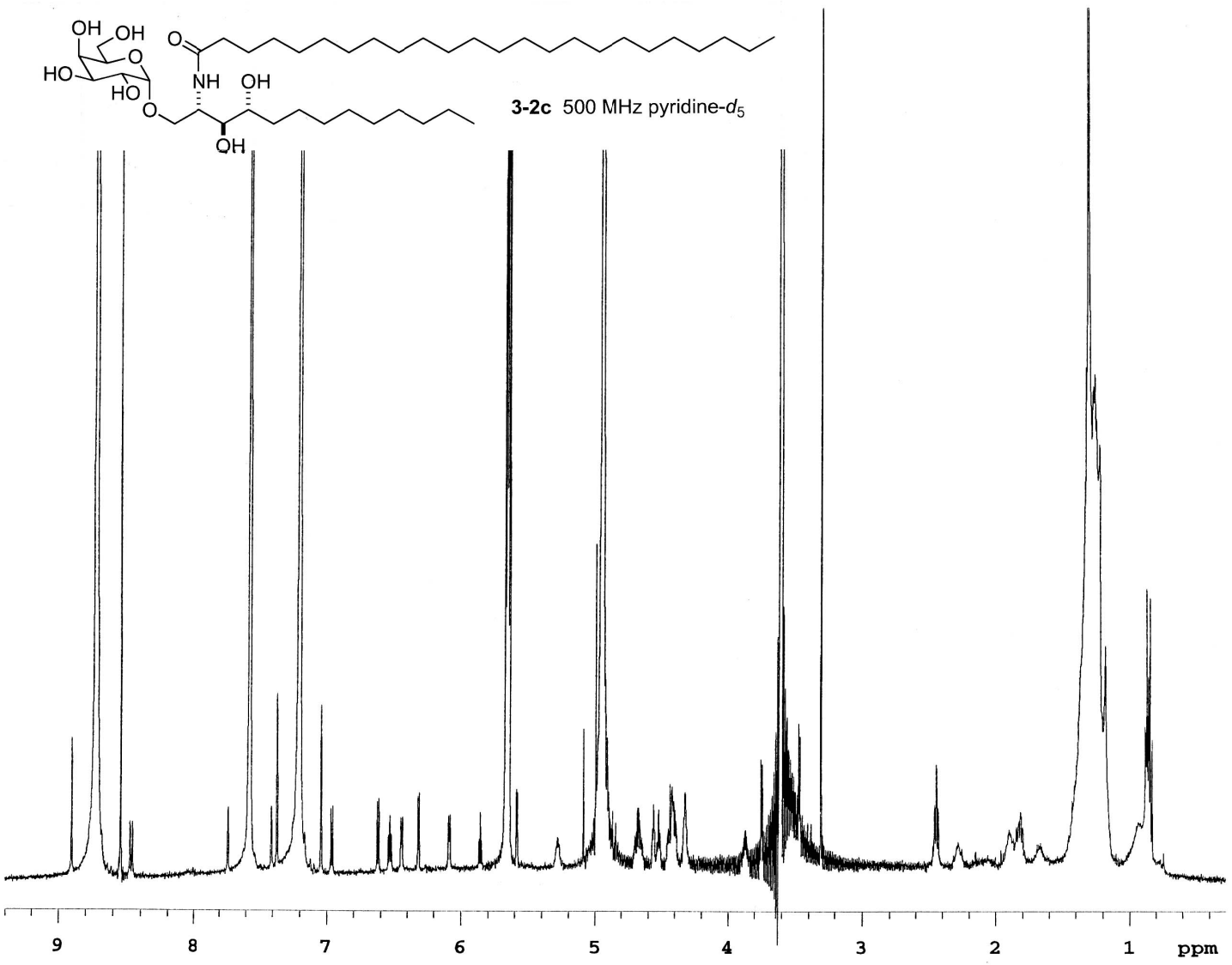

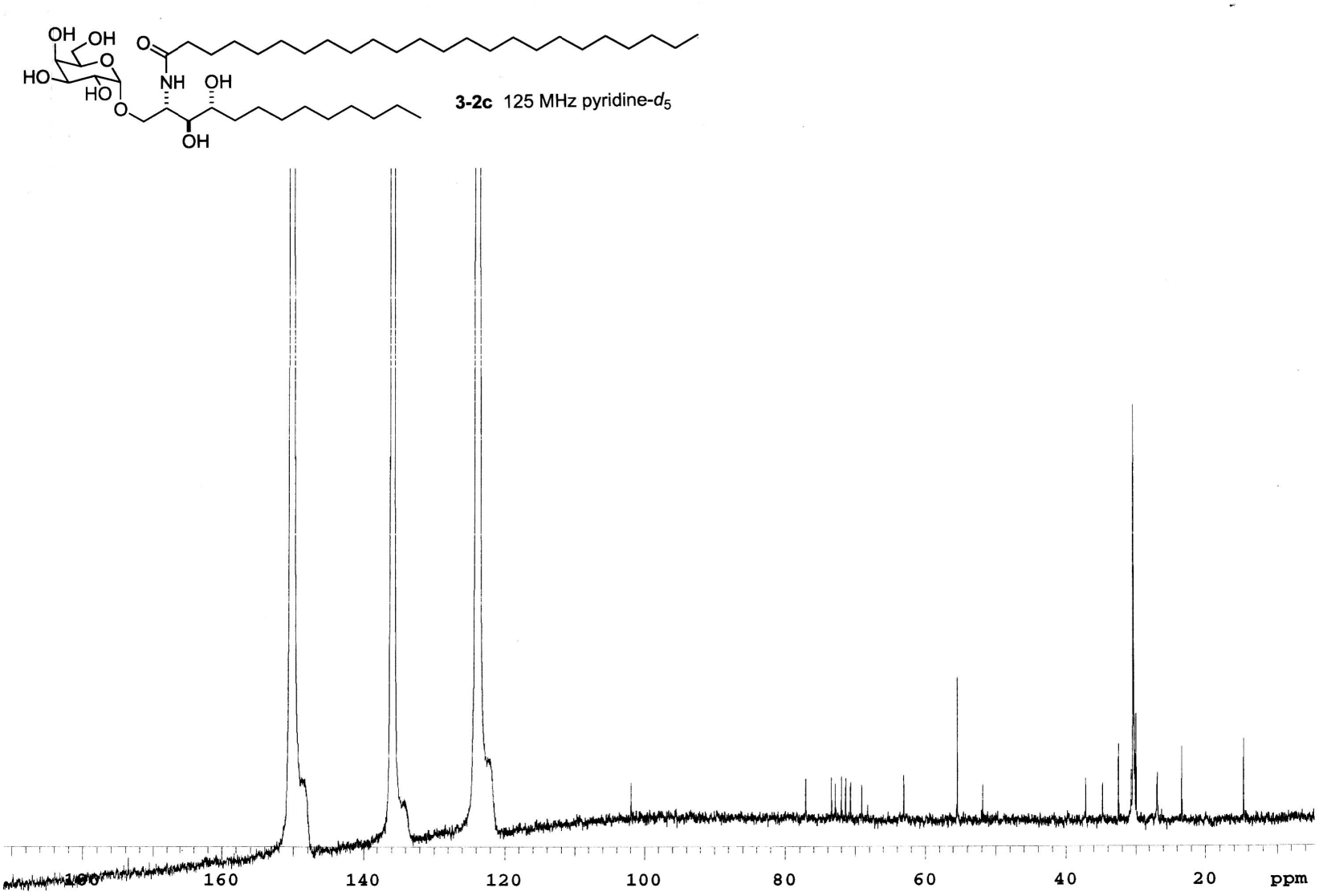

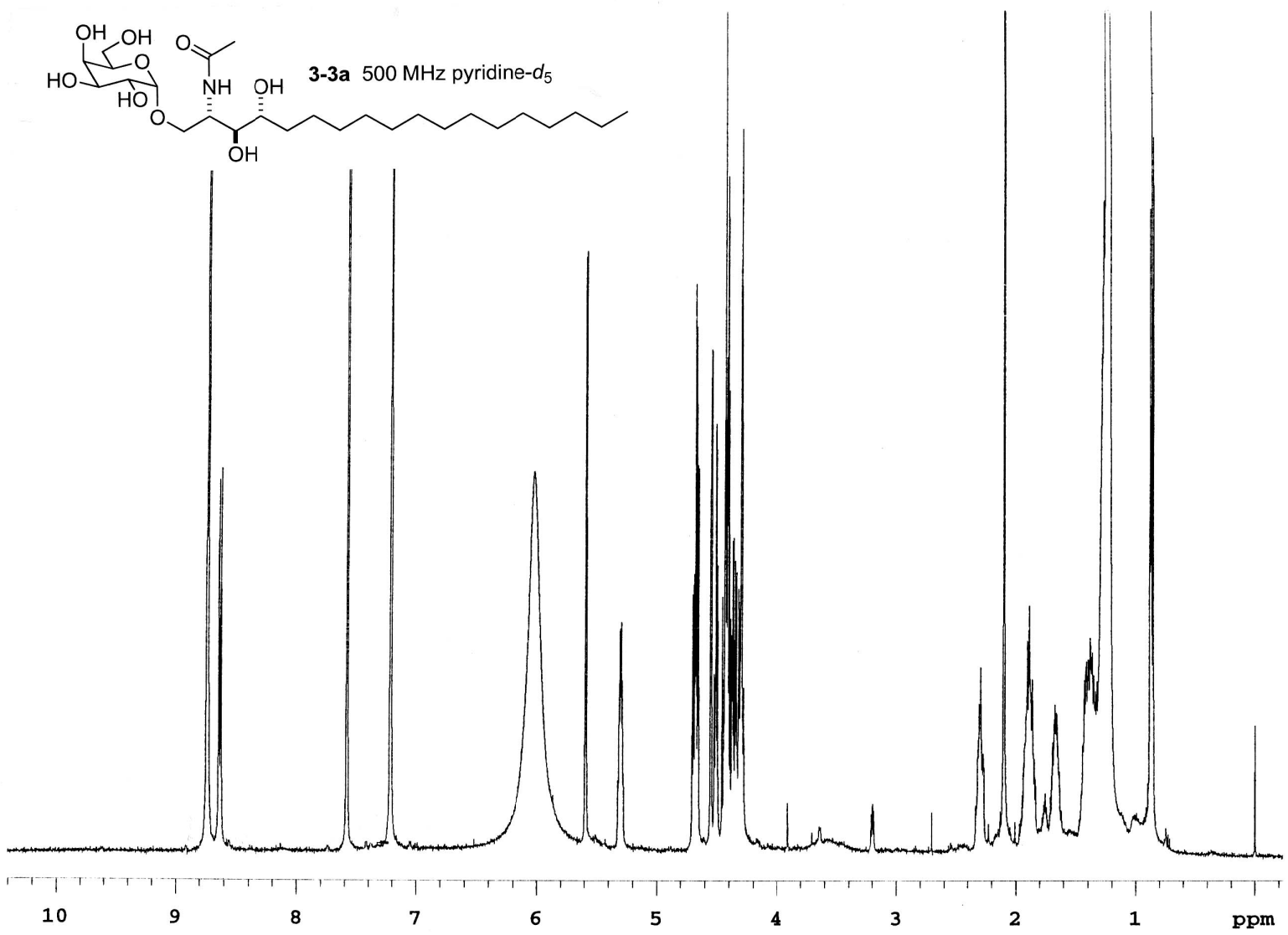

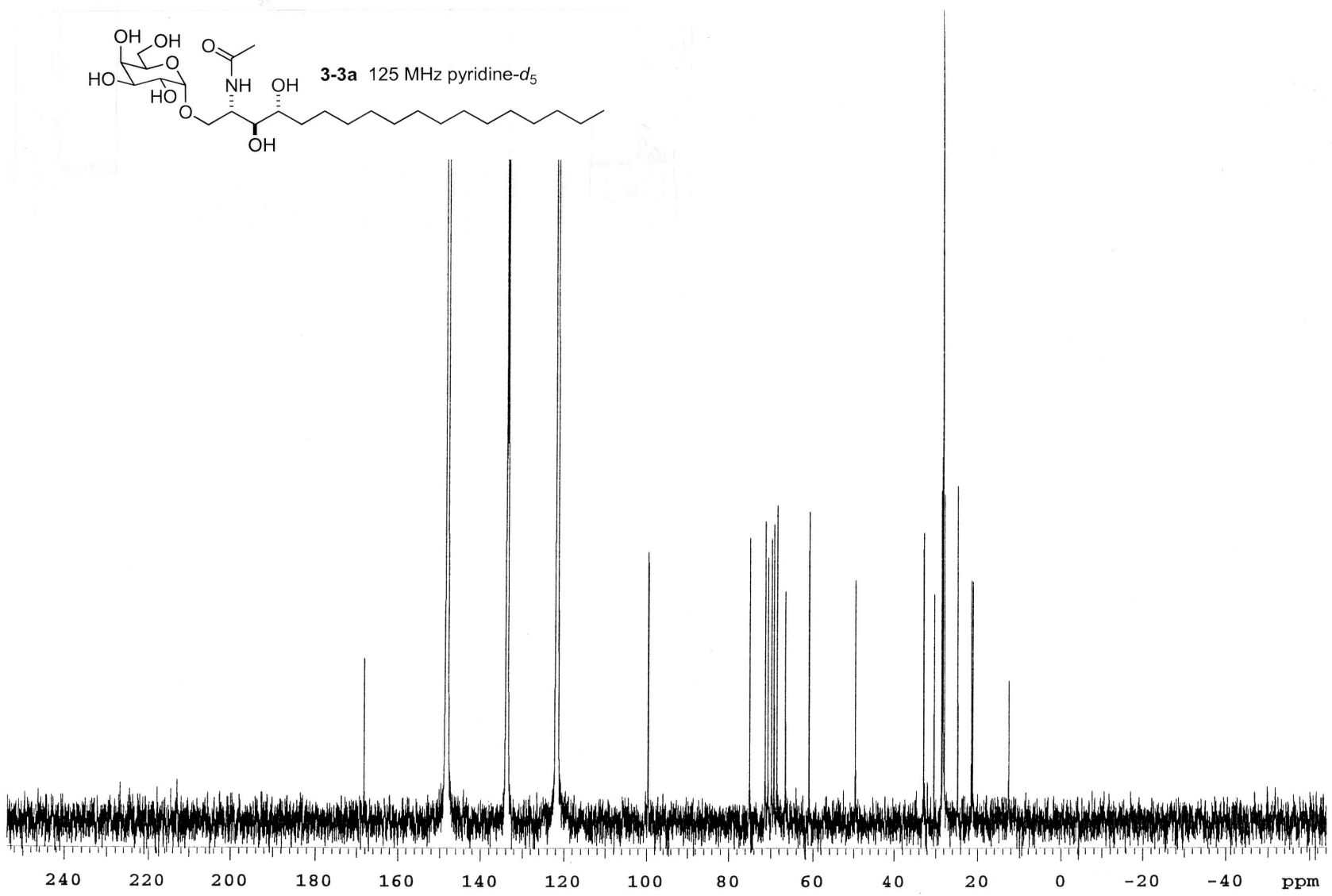

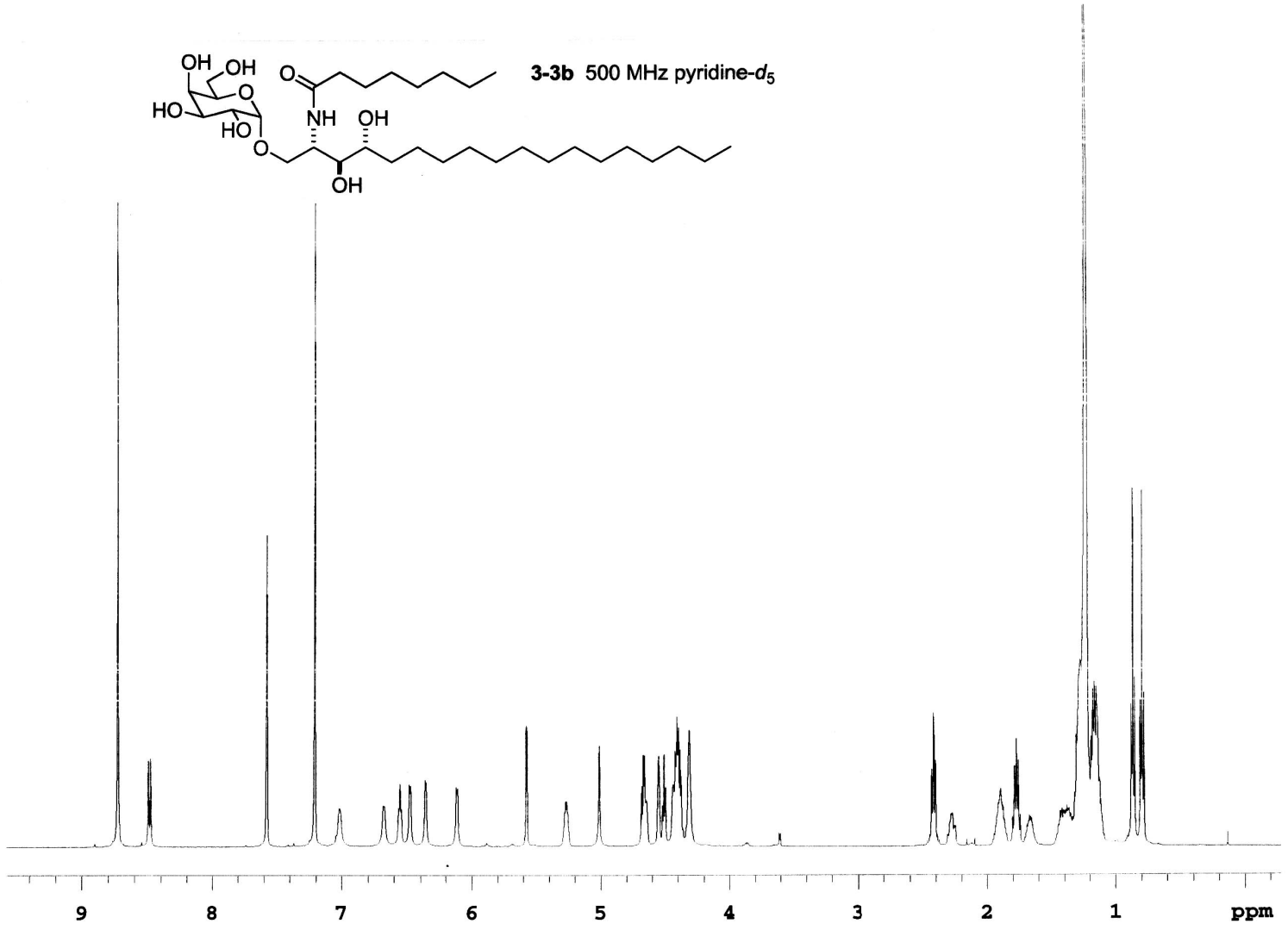

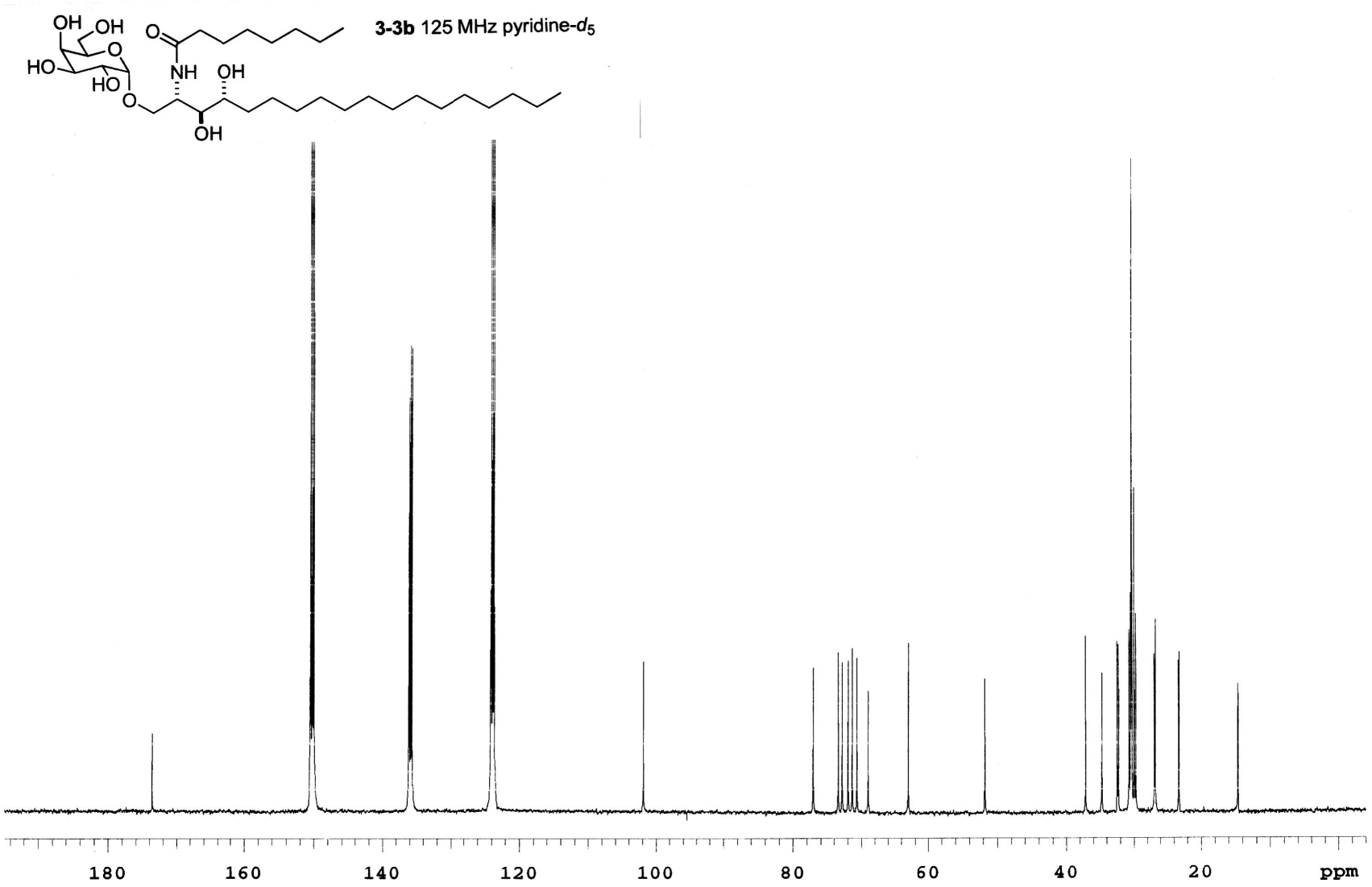

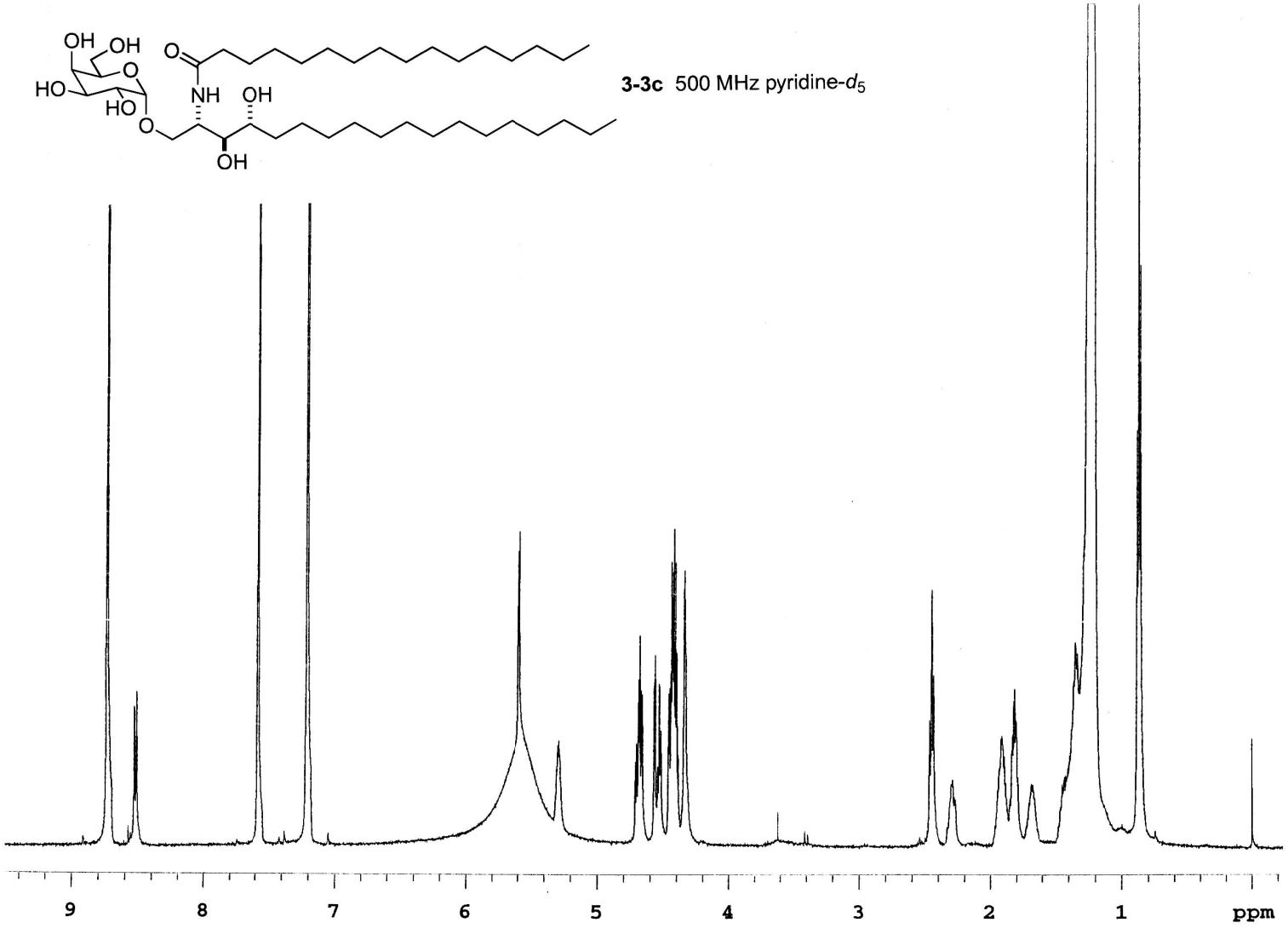

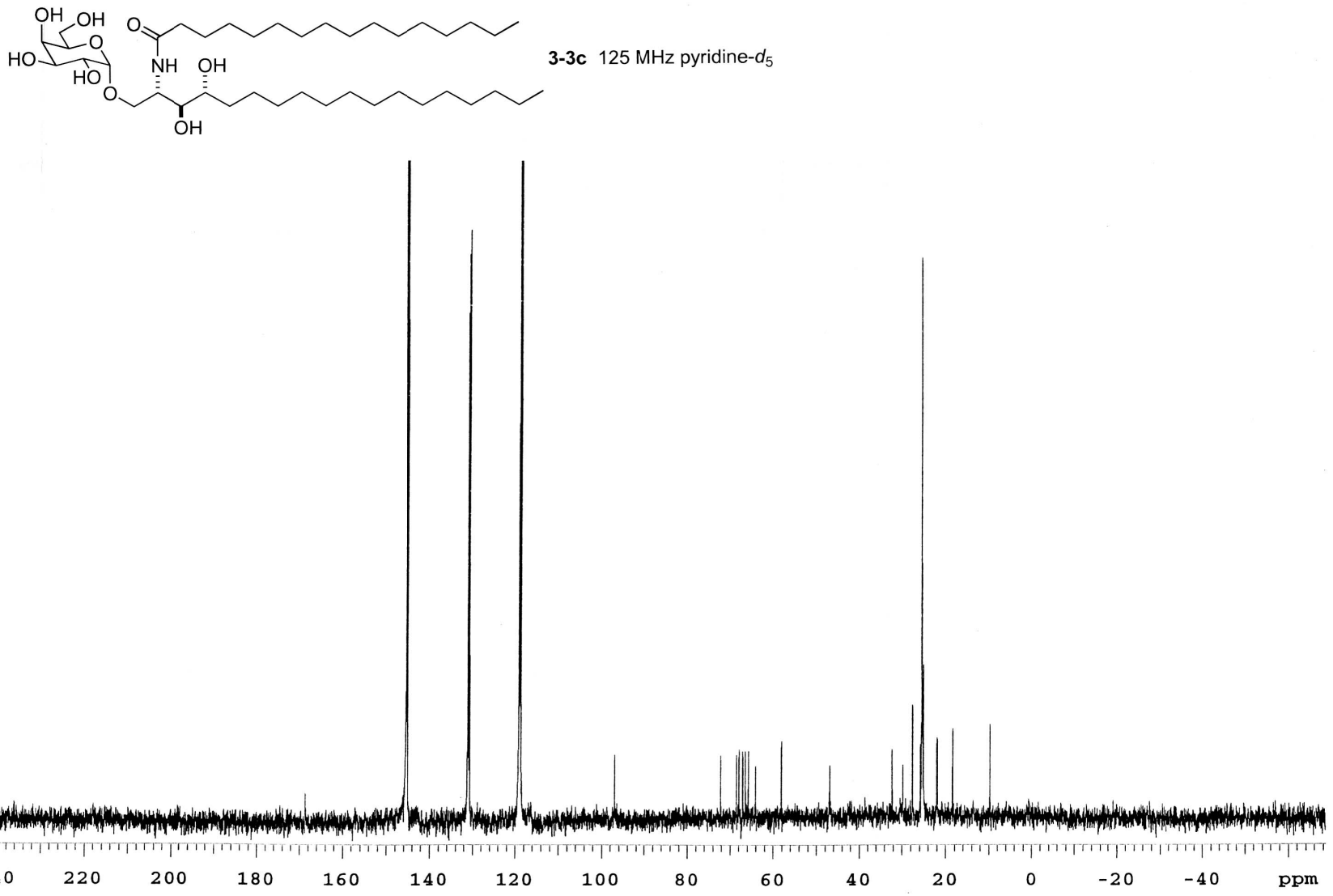

3-3c 125 MHz pyridine-d_5

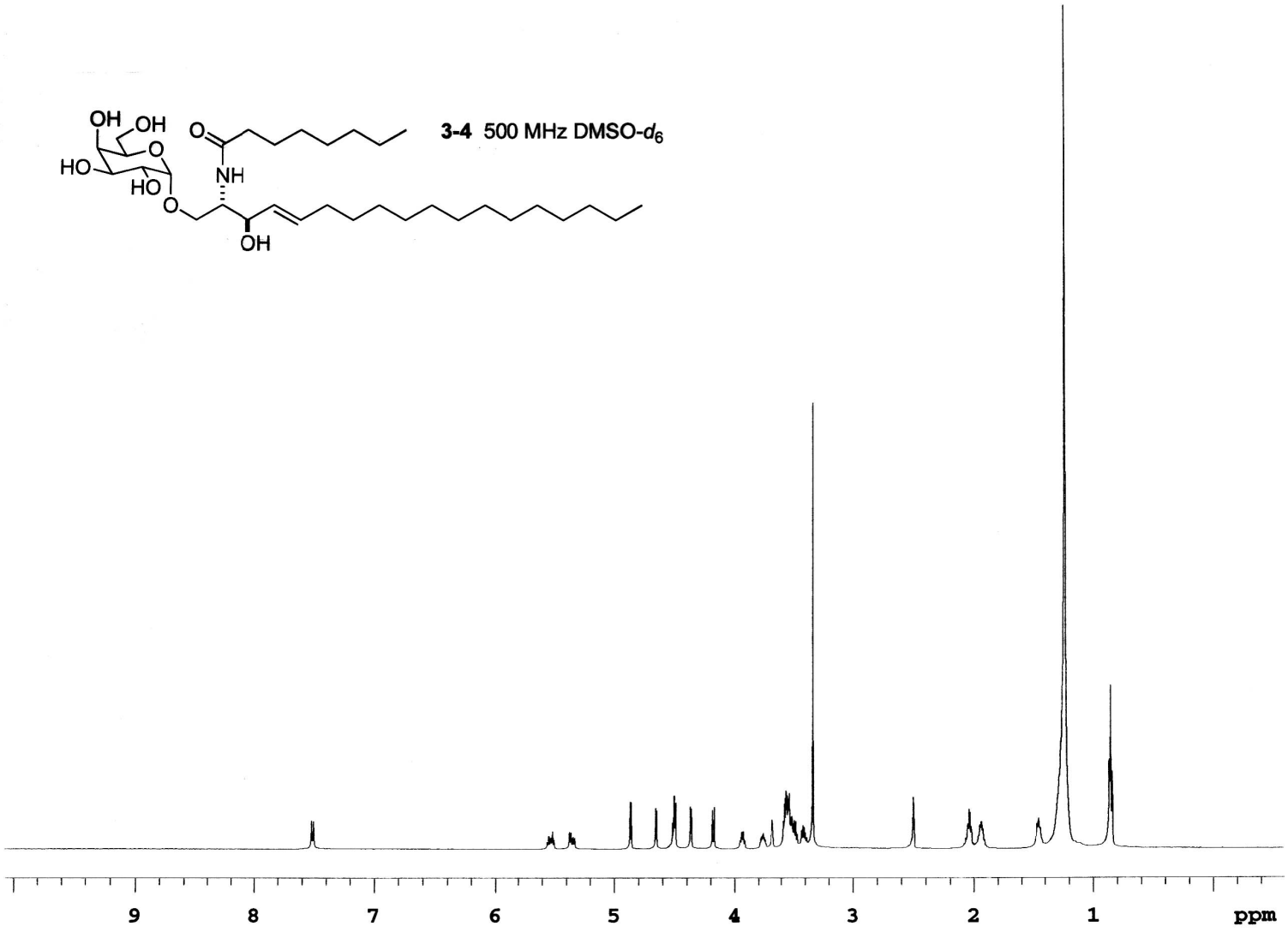

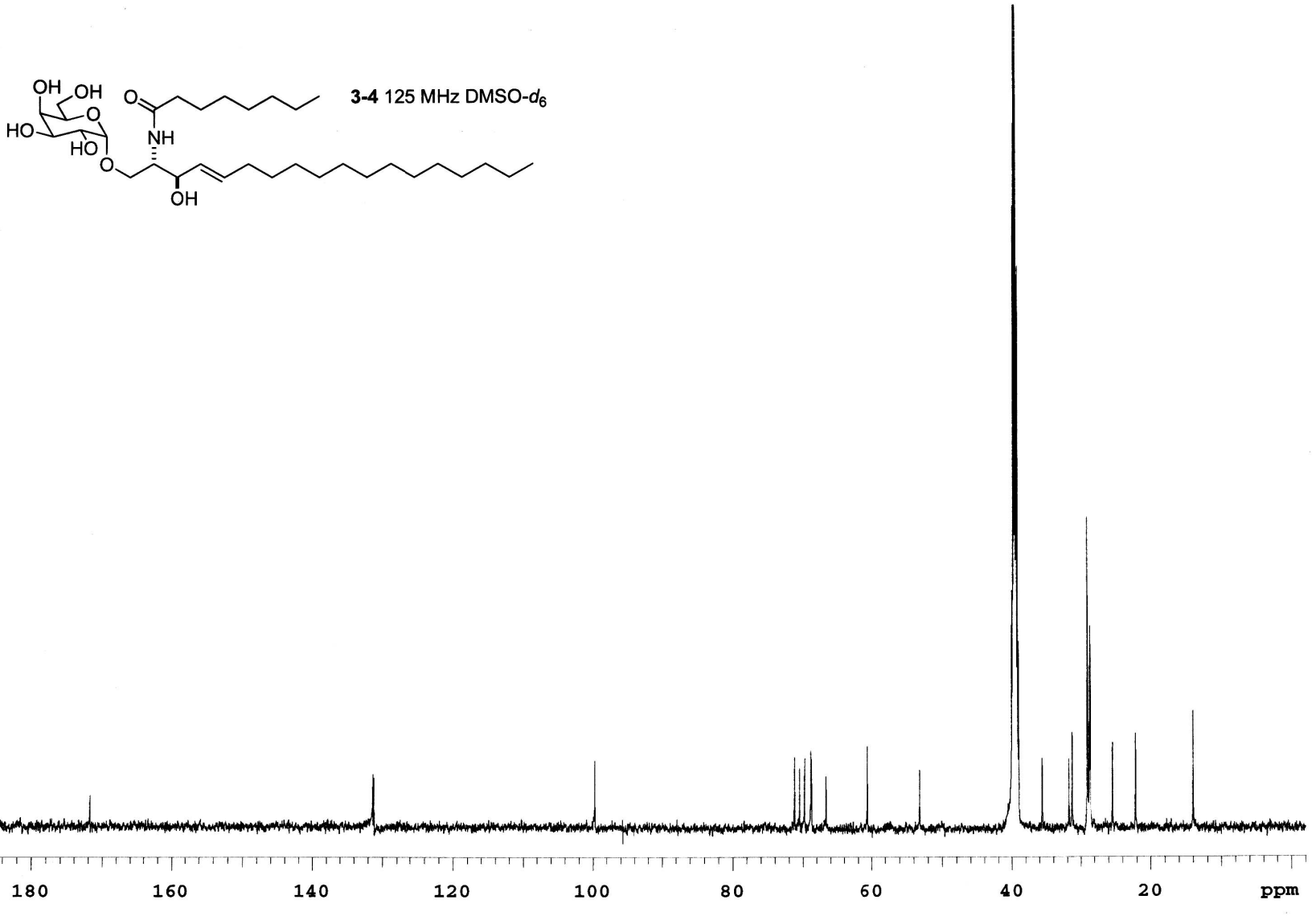

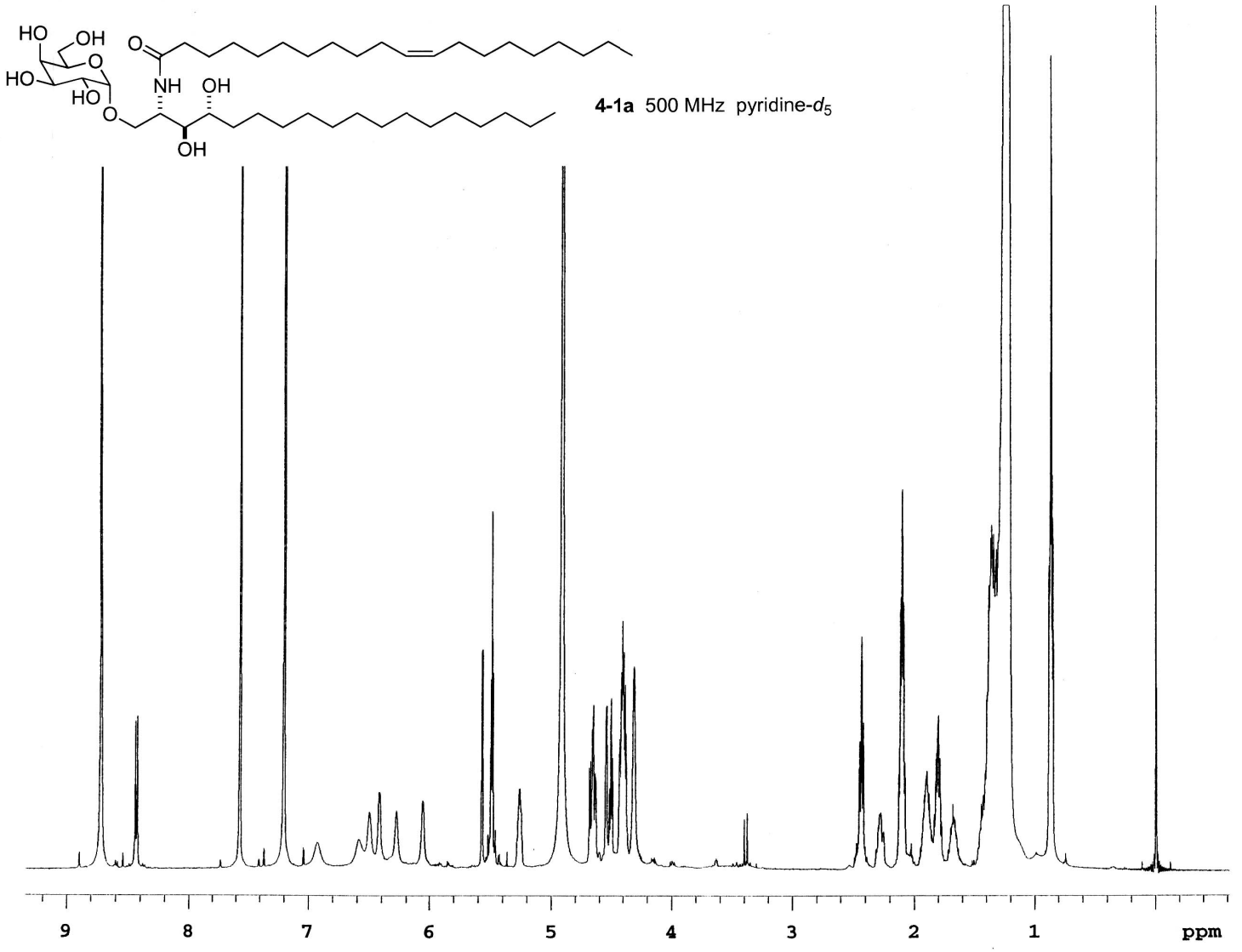

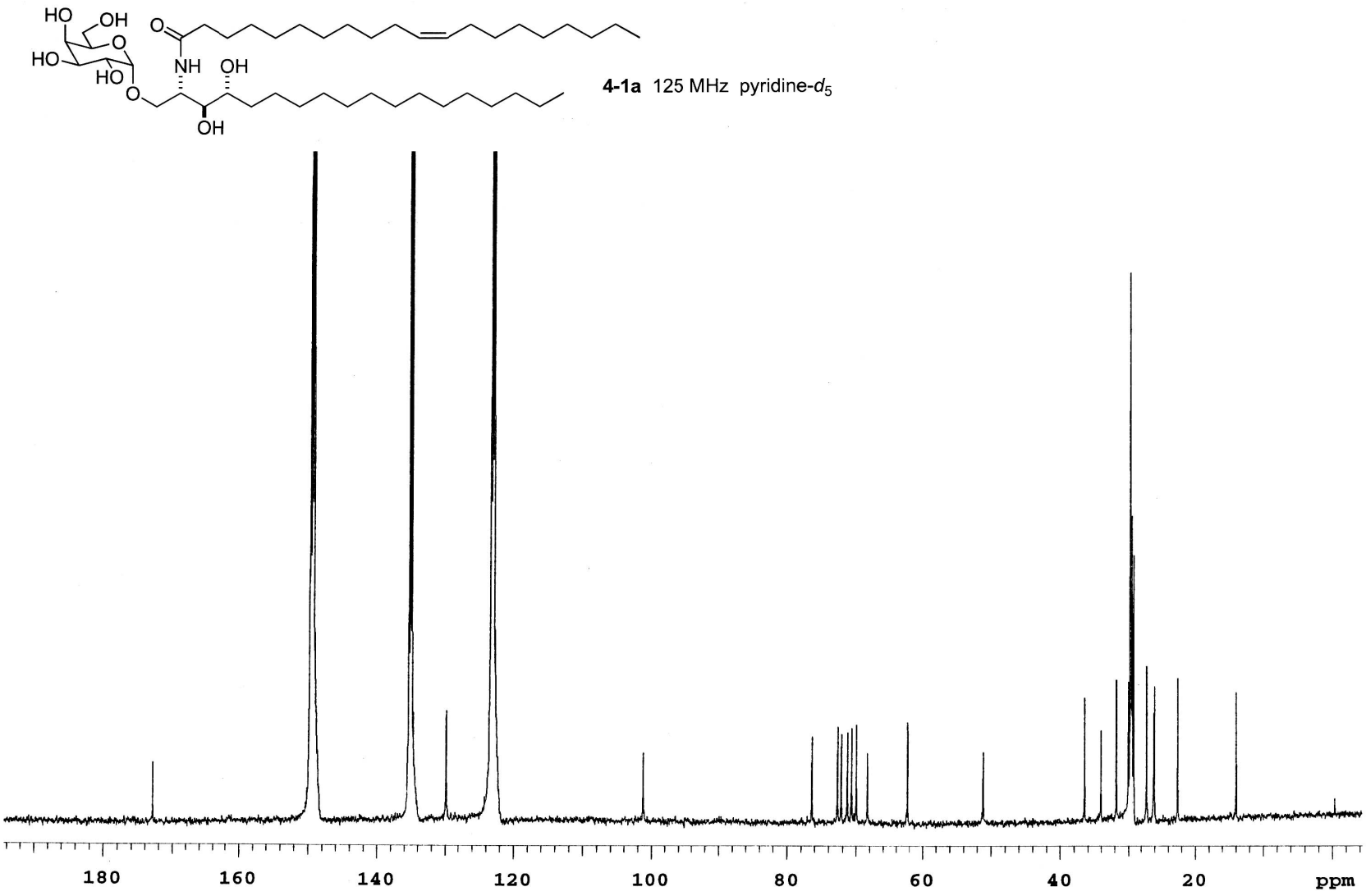

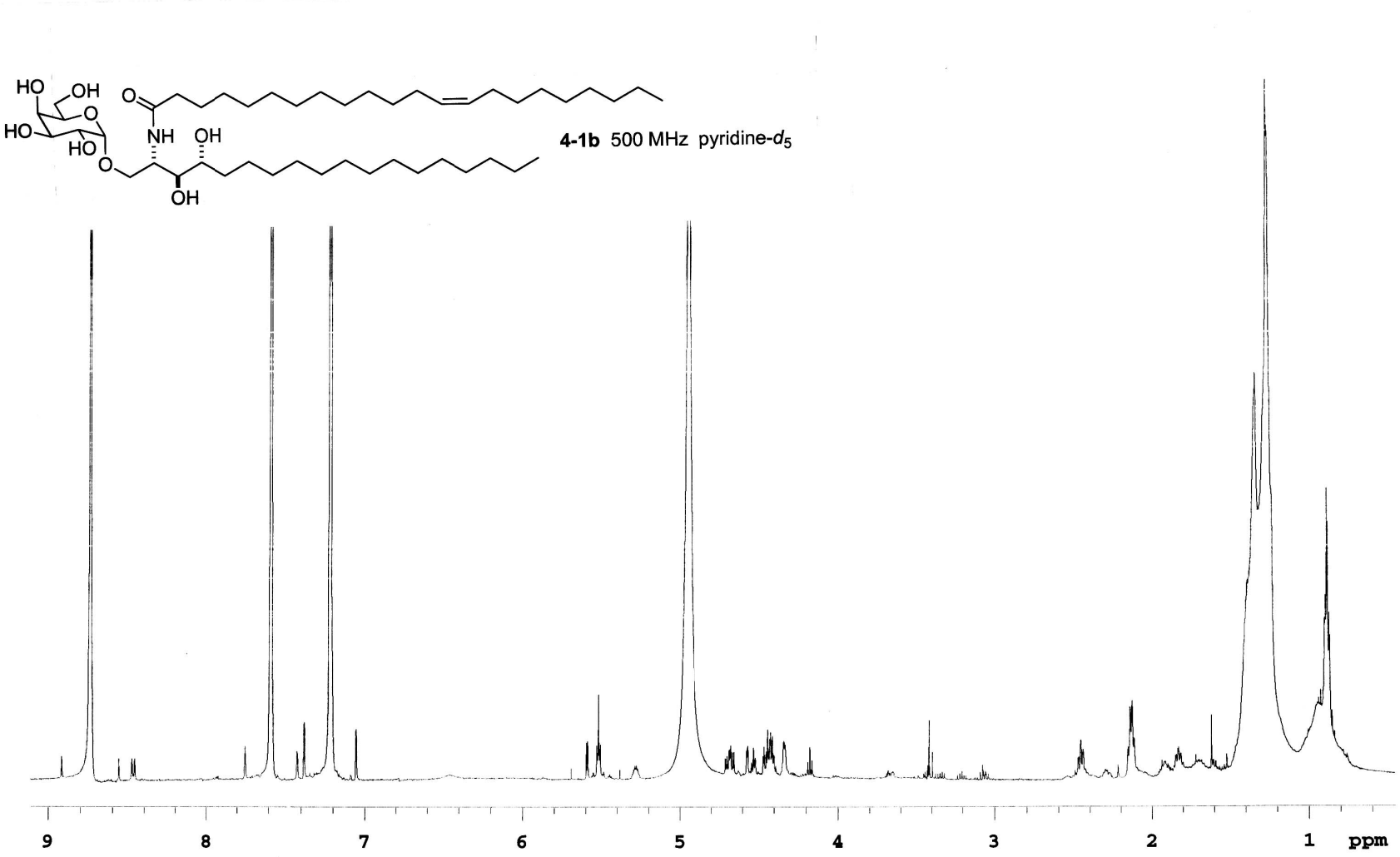

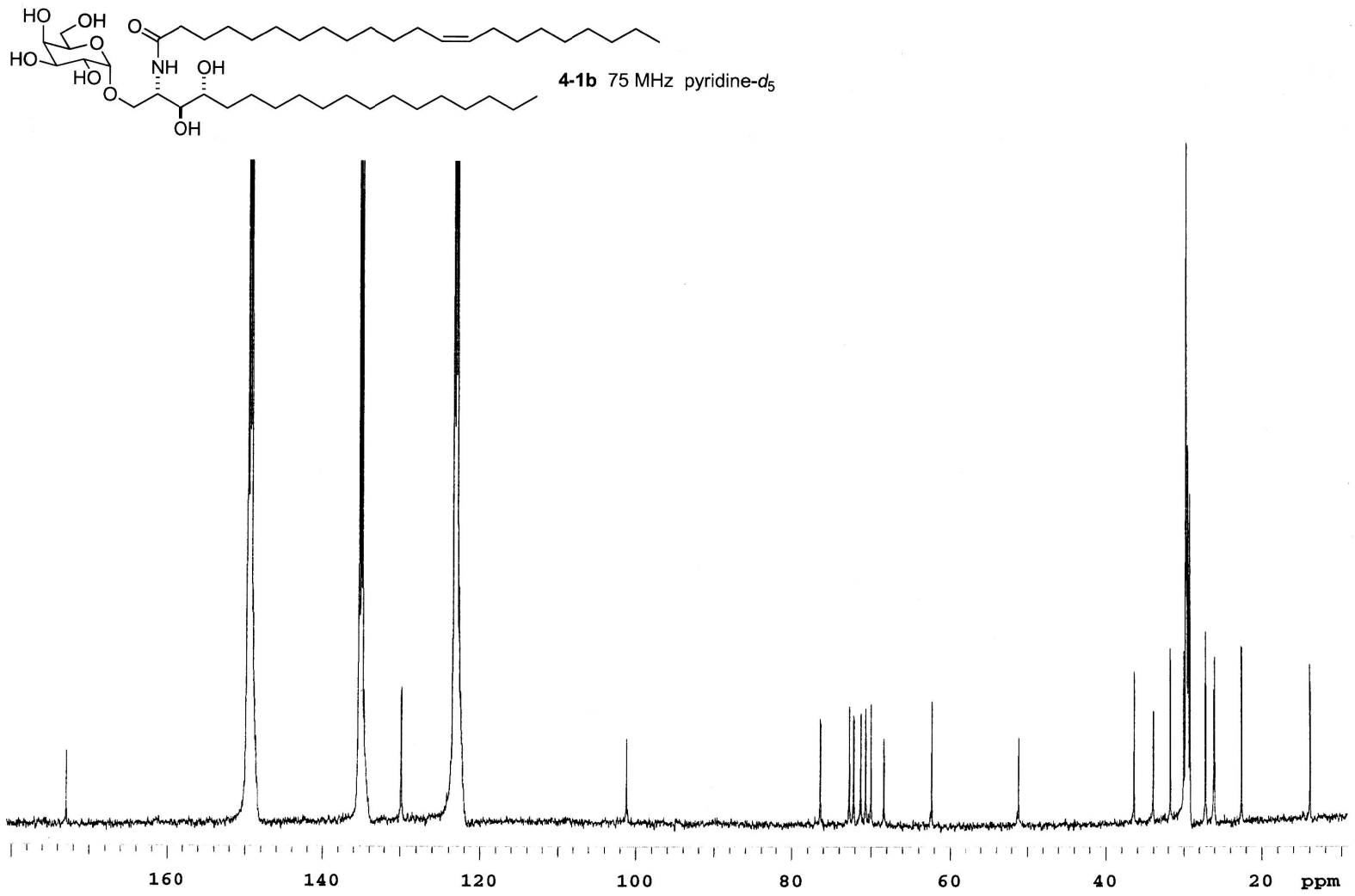

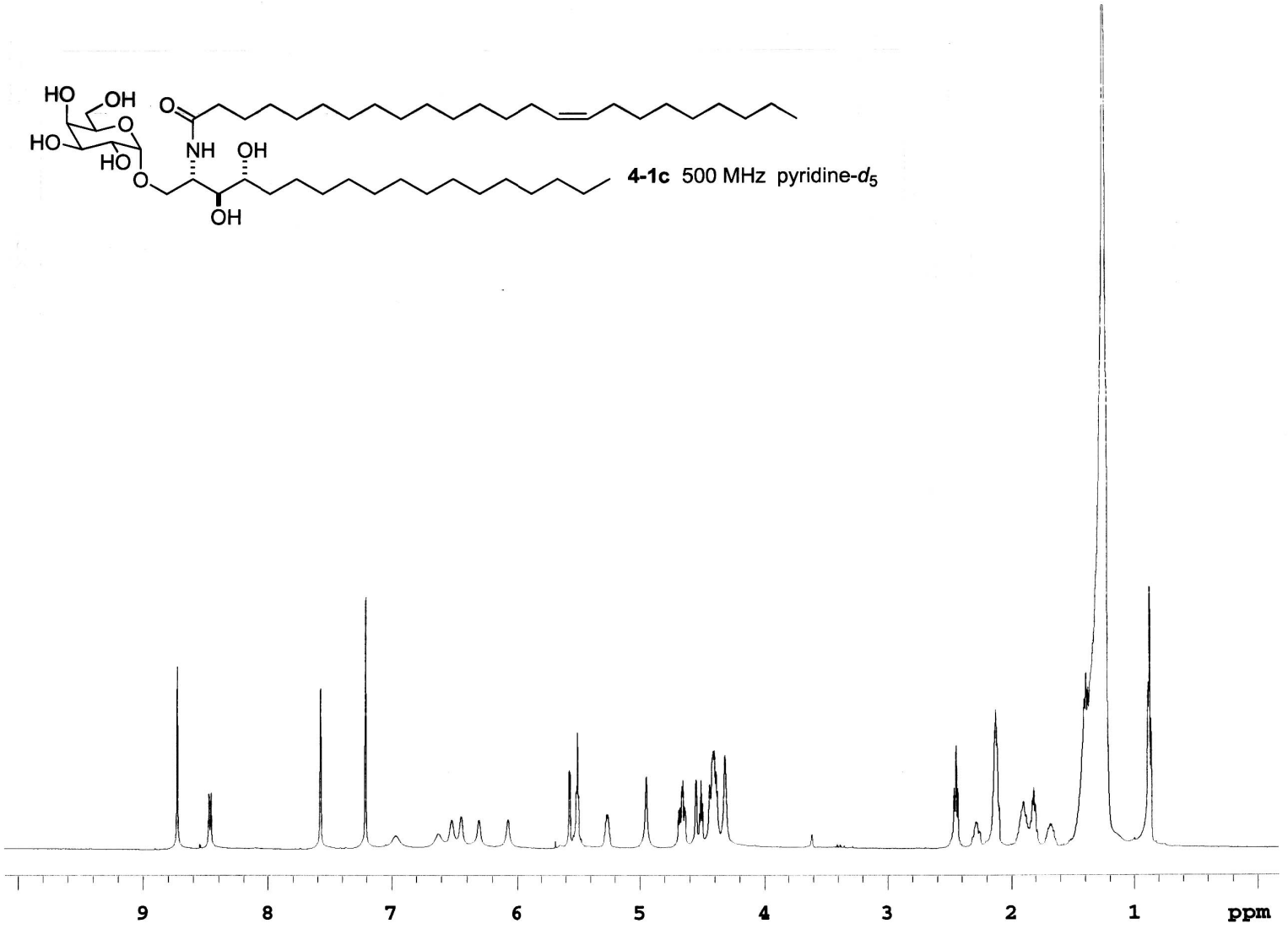

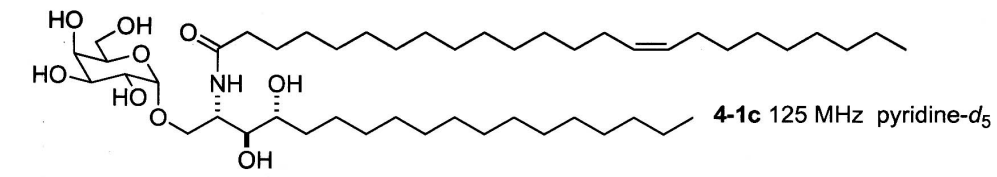

4-1c 125 MHz pyridine-d_5

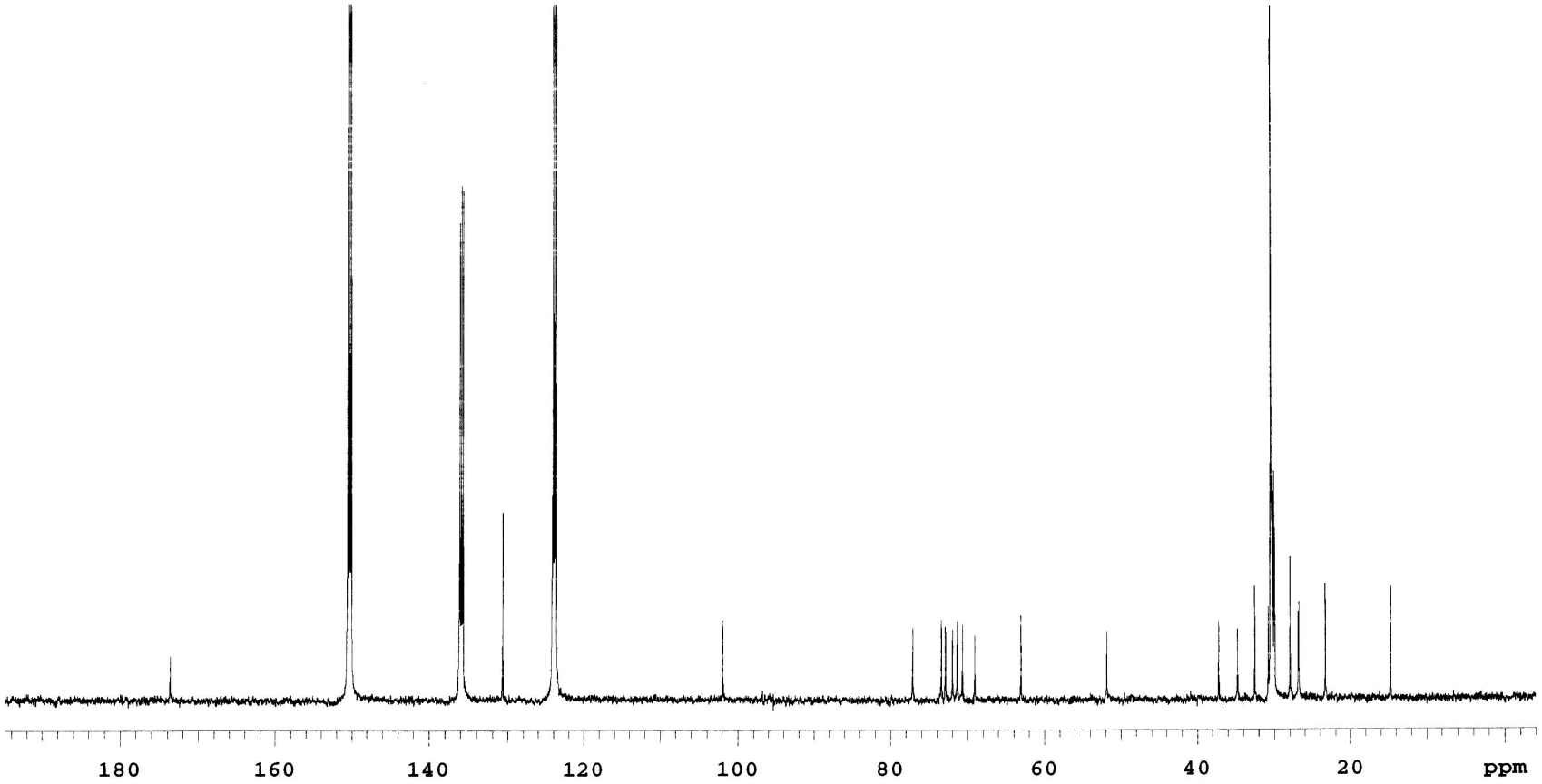

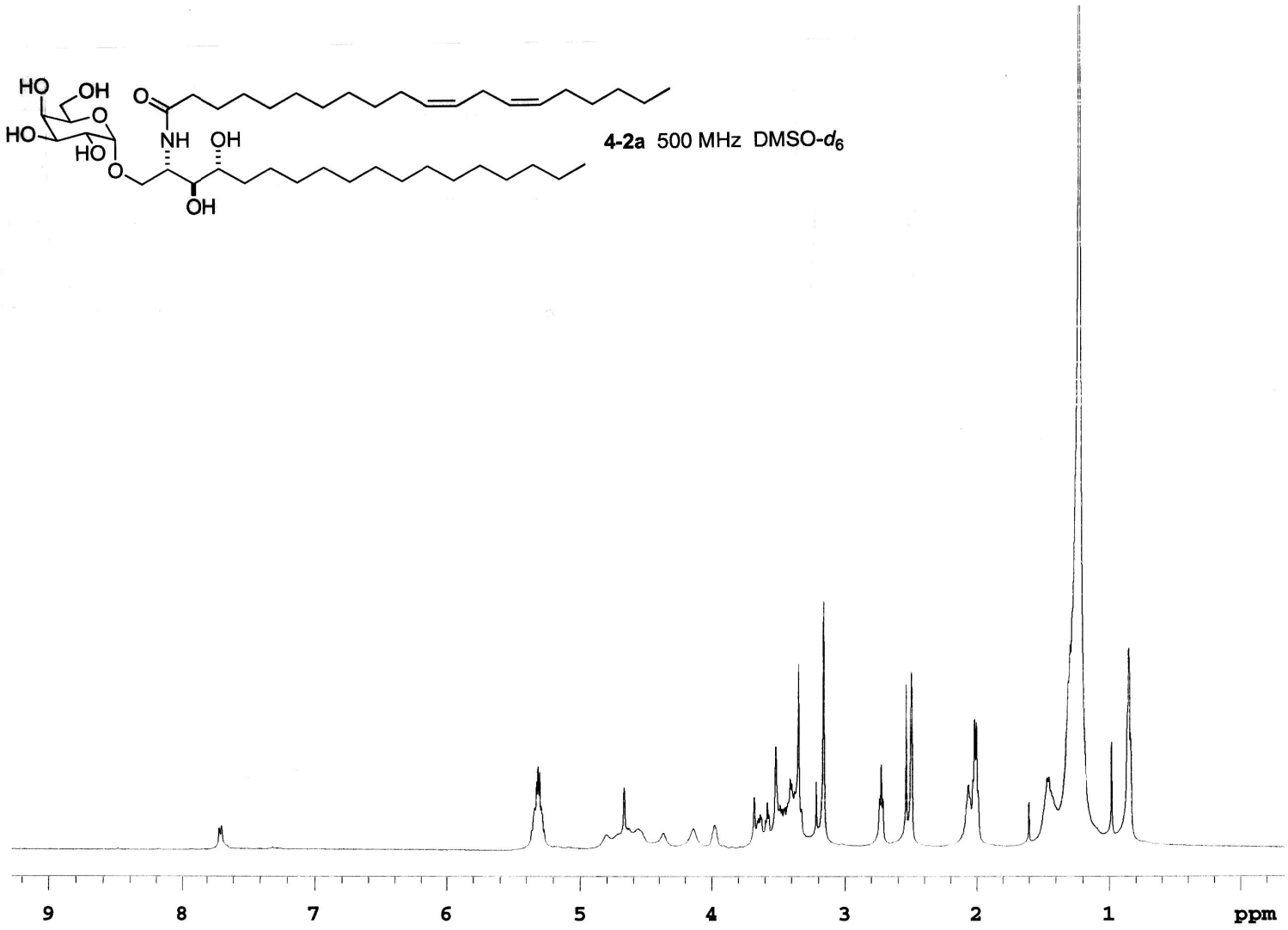

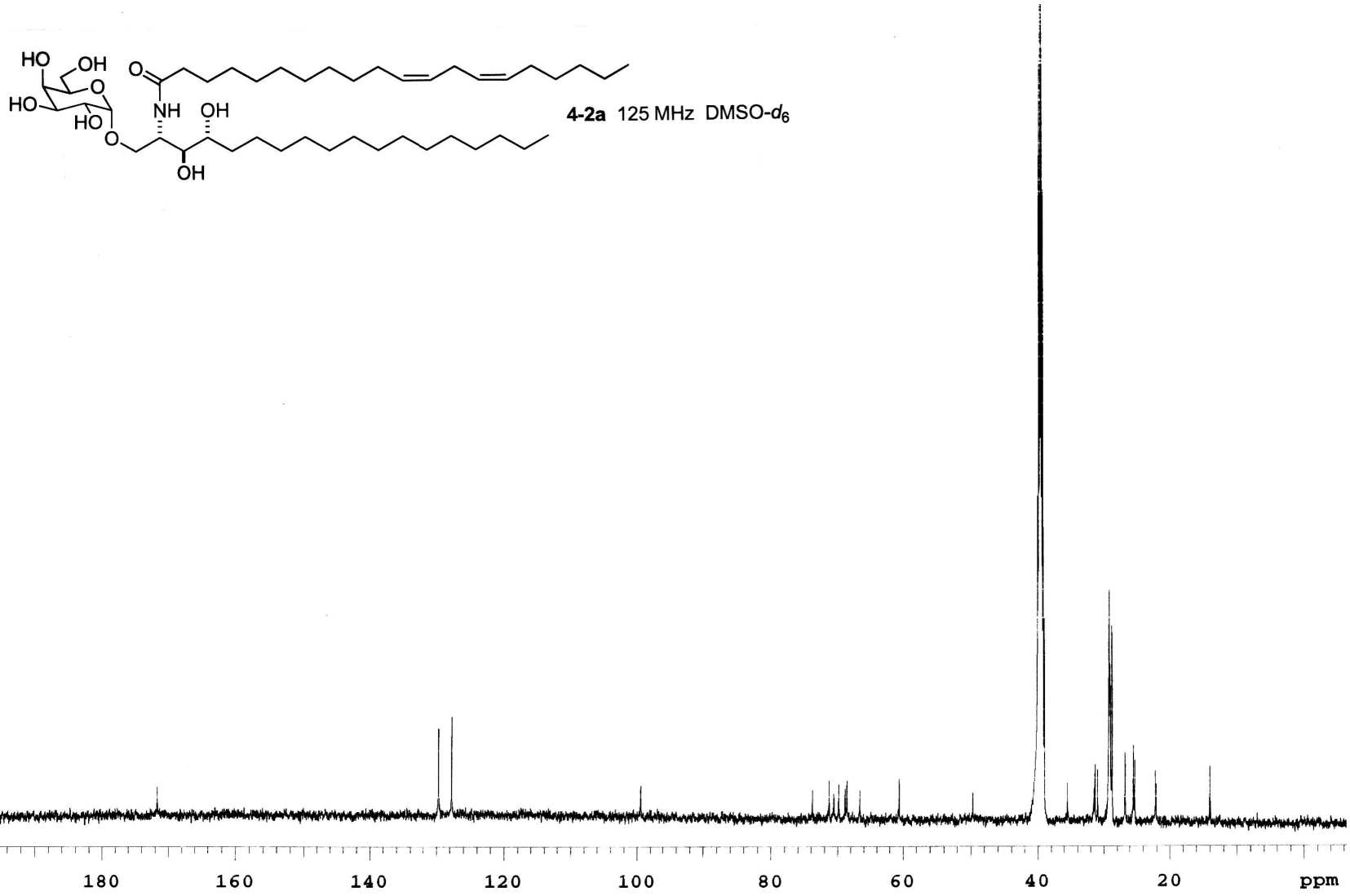

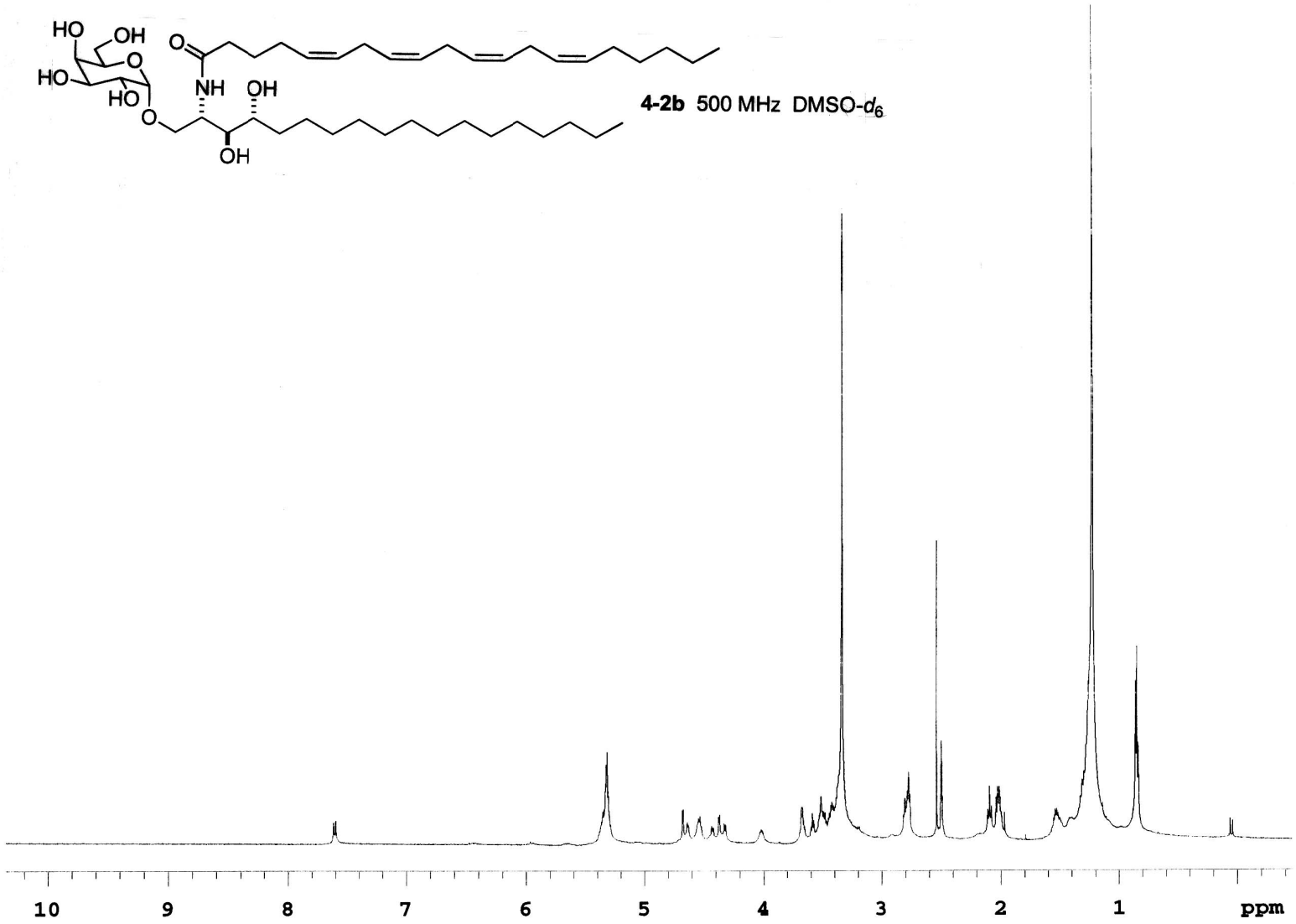

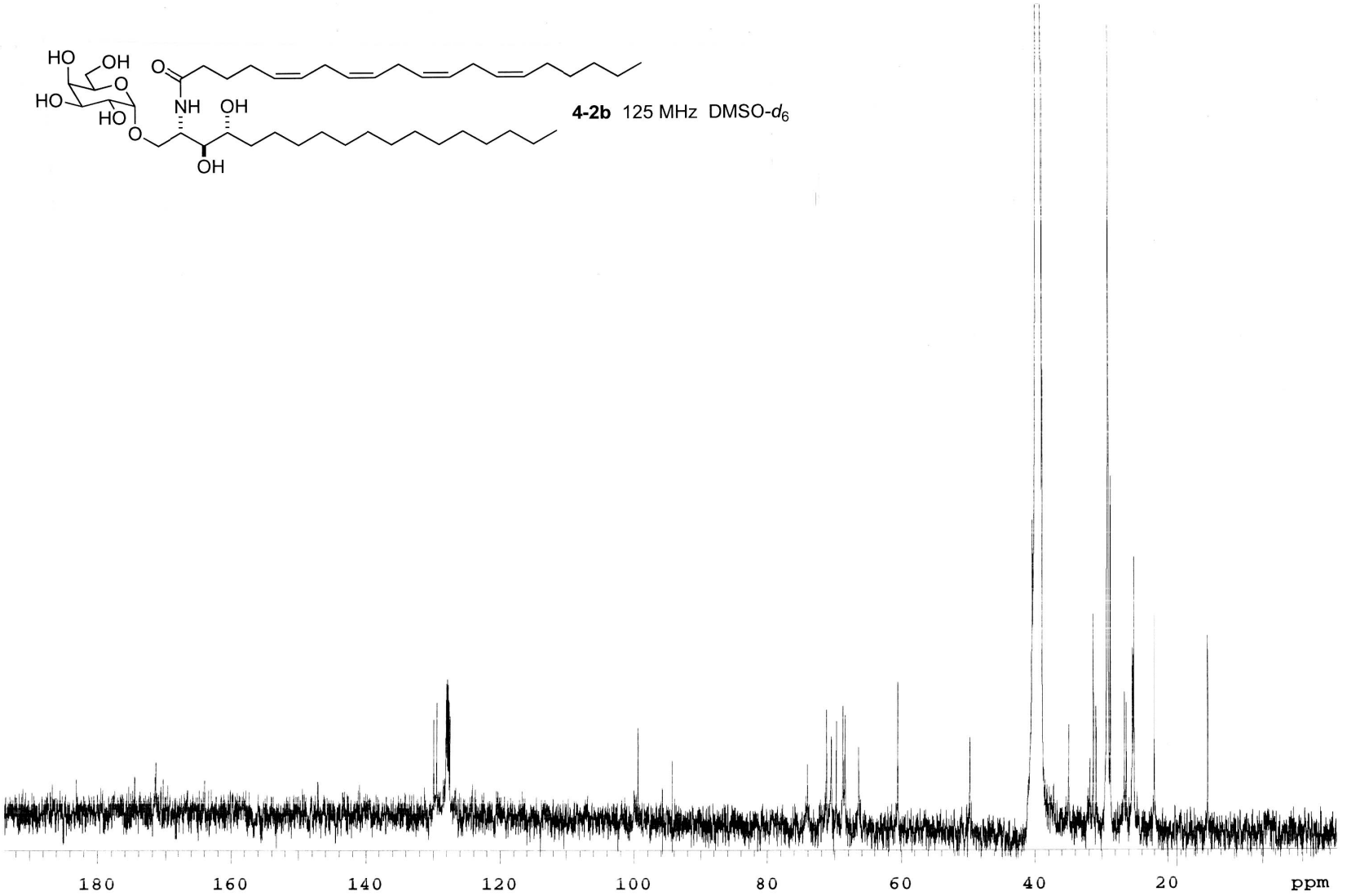

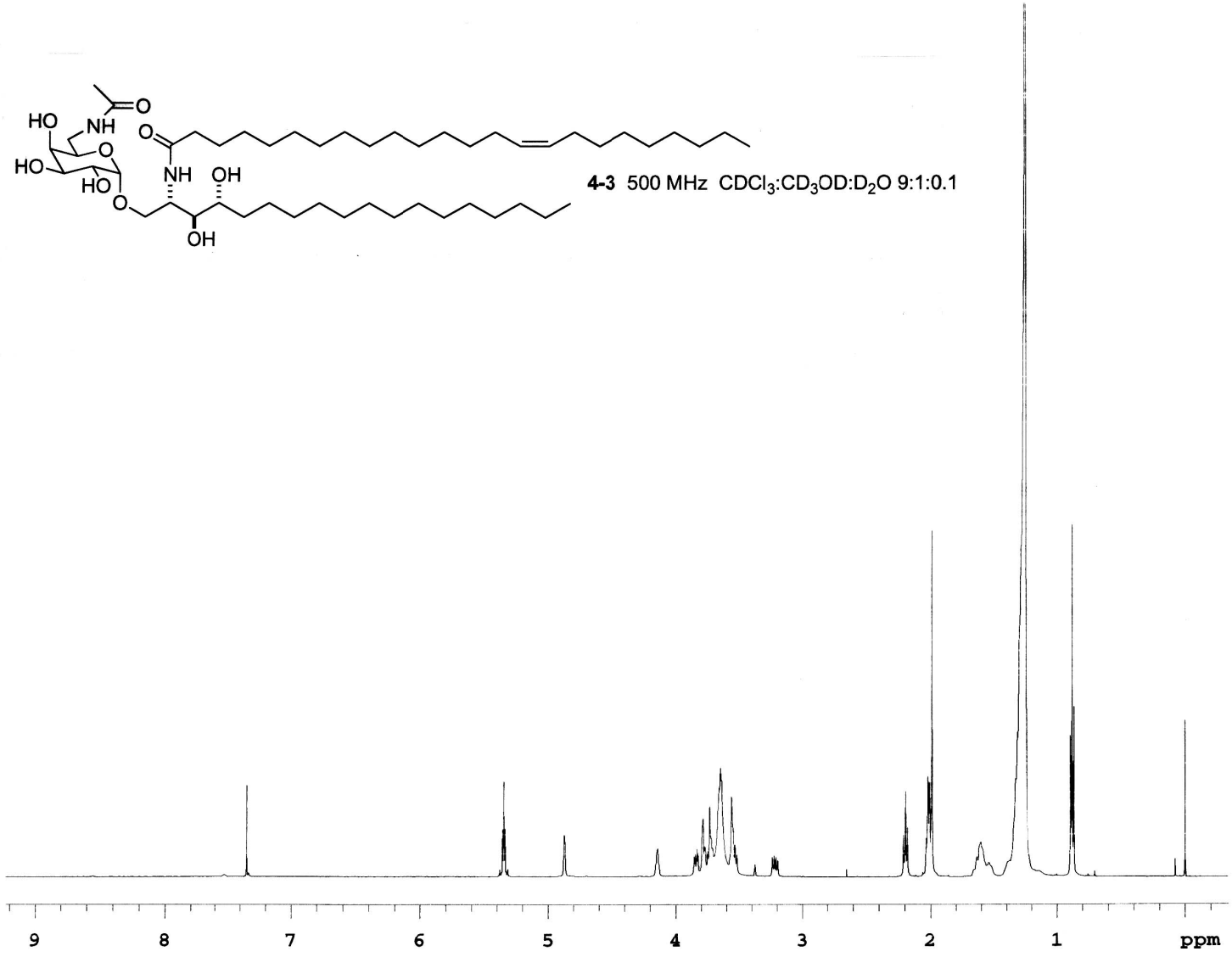

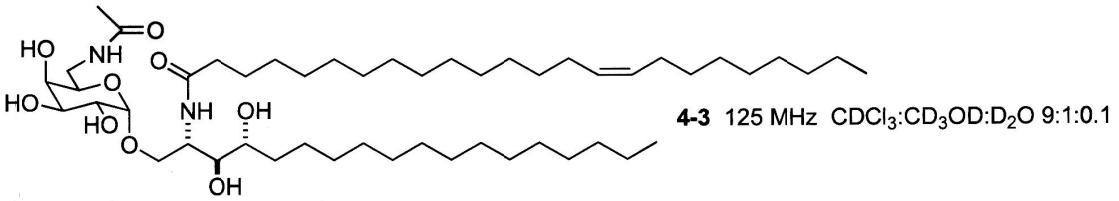

4-3 125 MHz $CDCl_3$:CD_3OD:D_2O 9:1:0.1

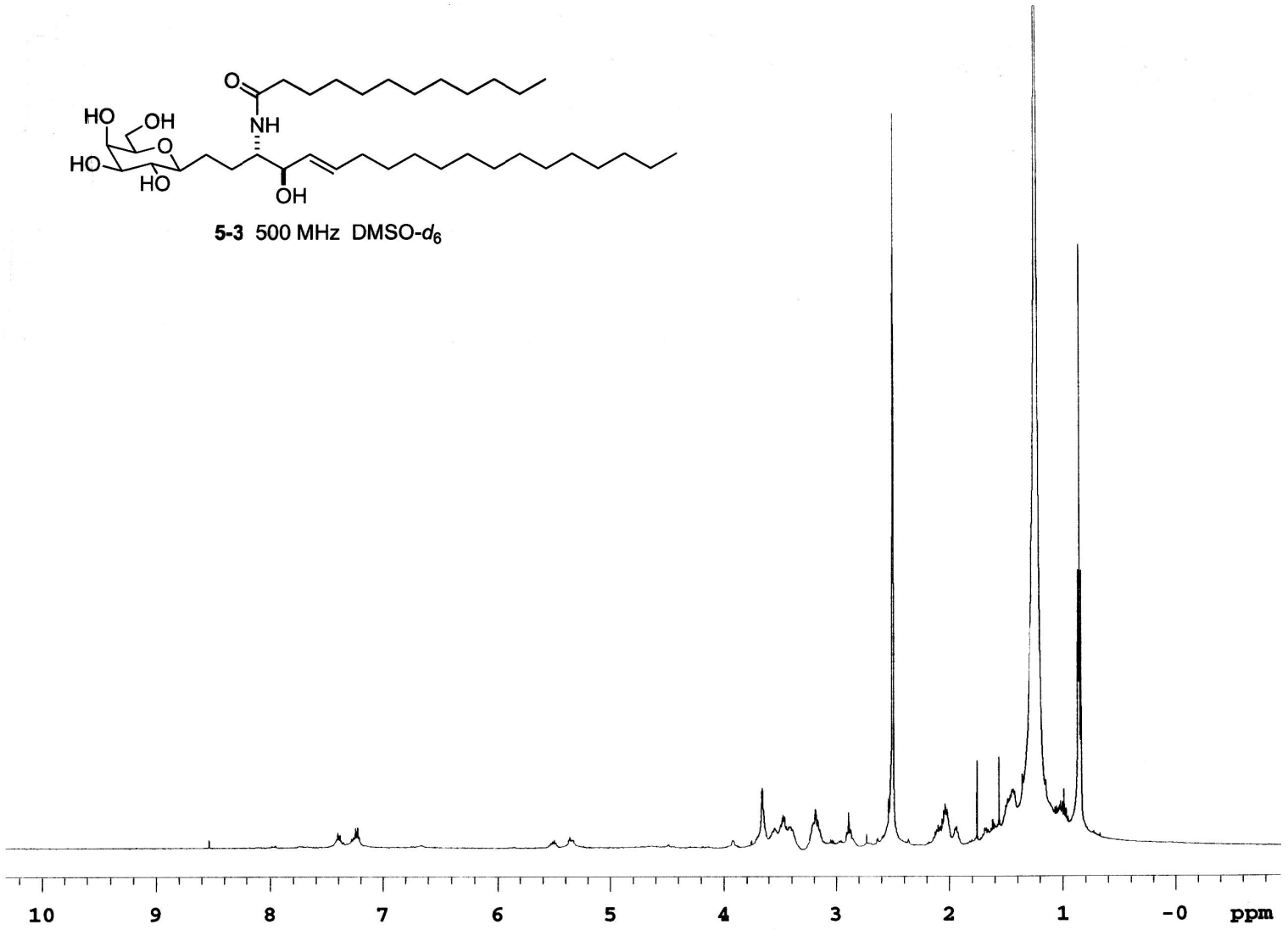

5-3 500 MHz DMSO-d_6

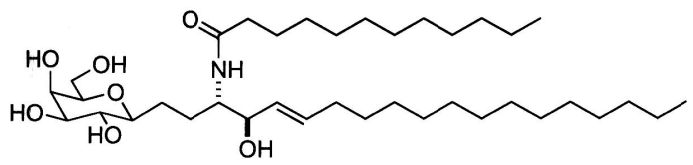

5-3 125 MHz DMSO-d_6